

# UC San Diego

## UC San Diego Electronic Theses and Dissertations

### Title

Anthropogenic particulate source characterization and source apportionment using aerosol time-of-flight mass spectrometry

### Permalink

<https://escholarship.org/uc/item/1qj2486m>

### Author

Toner, Stephen Mark

### Publication Date

2007

Peer reviewed|Thesis/dissertation

UNIVERSITY OF CALIFORNIA, SAN DIEGO

**Anthropogenic Particulate Source Characterization and Source  
Apportionment Using Aerosol Time-of-Flight Mass Spectrometry**

A dissertation submitted in partial satisfaction of the requirements for the degree

Doctor of Philosophy

in

Chemistry

by

Stephen Mark Toner

Committee in charge:

Professor Kimberly A. Prather, Chair  
Professor Seth M. Cohen  
Professor Robert E. Continetti  
Professor John E. Crowell  
Professor Ray F. Weiss

2007

Copyright

Stephen Mark Toner, 2007

All rights reserved

This dissertation of Stephen Mark Toner is approved and  
acceptable in quality and form for publication on microfilm:

---

---

---

---

---

Chair

University of California, San Diego

2007



Dedicated to my father, Luke Toner (1919 – 1993);  
and  
to my mother, Sonja Toner, for all of her love and support.

It is our collective and individual responsibility to protect and nurture the global family,  
to support its weaker members and to preserve and tend to the environment in which we  
all live.

*Dalai Lama*

# Table of Contents

Signature Page .....	iii
Dedication .....	iv
Epigraph.....	v
Table of contents.....	vi
List of figures.....	xii
List of tables.....	xviii
Acknowledgements.....	xx
Vita, publications, and fields of study .....	xxiv
Abstract.....	xxvi
Chapter 1 Introduction .....	1
1.1 Aerosols .....	1
1.2 Sampling Techniques for Aerosol Source Apportionment.....	8
1.2.1 Filter and Impactor Techniques .....	8
1.2.2 Particle Sizing Techniques.....	9
1.2.3 Particle Mass Spectrometry Techniques.....	10
1.3 Aerosol Time-of-Flight Mass Spectrometry .....	13
1.3.1 ATOFMS Particle Inlet Region .....	13
1.3.2 ATOFMS Particle Sizing Region .....	16
1.3.3 ATOFMS Laser Desorption/Ionization Mass Spectrometry Region.....	17
1.4 ATOFMS Data Analysis.....	18

1.4.1 Particle Clustering using Adaptive Resonance Theory-2a (ART-2a).....	19
1.4.2 Classification & Apportionment Using Match-ART-2a with Predefined Clusters .....	21
1.5 Research Objectives and Synopsis.....	22
1.6 References.....	25
Chapter 2 Single particle analysis of a Minuteman SR19 II rocket motor exhaust plume using Aerosol Time-of-Flight Mass Spectrometry .....	
2.1 Synopsis .....	38
2.2 Introduction.....	39
2.3 Experimental .....	41
2.4 Results and Discussion .....	45
2.4.1 Particle size distributions for the SRM wake and soil samples .....	45
2.4.2 SRM exhaust wake particle classes .....	47
2.4.3 Resuspended soil sample particle classes .....	51
2.4.4 Comparison to the results found with PALMS on the Athena II SRM .....	57
2.5 Acknowledgements.....	59
2.6 References.....	60
Chapter 3 Single particle characterization of ultrafine and accumulation mode particles from heavy duty diesel vehicles using aerosol time-of-flight mass spectrometry.....	
3.1 Synopsis .....	64

3.2	Introduction.....	65
3.3	Experimental .....	67
3.4	Results and Discussion .....	73
3.4.1	Description of Particle Types Observed with UF-ATOFMS .....	73
3.4.2	Analysis of Size Segregated Chemical Composition for each HDDV .....	82
3.4.3	Particle Composition as a Function of Driving Cycle & HDDV.....	86
3.4.4	Composition and Reproducibility Over a Larger Size Range .....	90
3.4.5	Prospects for Apportionment .....	92
3.5	Acknowledgements.....	93
3.6	References.....	96
Chapter 4 Using mass spectral source signatures to apportion exhaust particles from gasoline and diesel powered vehicles in a freeway study using UF-ATOFMS.....		
		103
4.1	Synopsis .....	103
4.2	Introduction.....	104
4.3	Experimental .....	106
4.4	Results and discussion .....	109
4.4.1	Creation and Comparison of Particle Seeds From Source Studies.....	109
4.4.2	Particles Detected that Match to HDDV/LDV Source Seeds .....	117
4.4.3	Temporal Trends and Correlations with UF-ATOFMS Data .....	118
4.5	Acknowledgements.....	129

4.6	References.....	131
Chapter 5 Source apportionment of freeway-side PM <sub>2.5</sub> using ATOFMS .....		
5.1	Synopsis .....	136
5.2	Introduction.....	137
5.3	Experimental.....	138
5.4	Results and Discussion .....	140
5.4.1	Quality Assurance of ATOFMS Data.....	140
5.4.2	Comparison with Standard Particle Counts .....	143
5.4.3	Comparison of Particle Phase and Gas Phase Data .....	145
5.4.4	Comparison of Temporal Trends from Peripheral Instruments .....	147
5.4.5	Upwind/Downwind Sampling .....	149
5.4.6	Data Analysis Used for Apportionment.....	158
5.4.7	Source Apportionment Using ART-2a .....	160
5.4.8	Size Resolved Source Apportionment Temporal Series.....	164
5.5	Acknowledgements.....	168
5.6	References.....	169
Chapter 6 Source Apportionment of PM <sub>2.5</sub> in Athens (Greece) and Mexico City		
	Using an ATOFMS Derived Mass Spectral Source Library .....	174
6.1	Synopsis .....	174
6.2	Introduction.....	175
6.3	Experimental .....	177
6.4	Results and Discussion .....	180
6.4.1	Source apportionment of ambient particles in Athens, Greece.....	180

6.4.2	Source Signature Matching for Athens, Greece .....	187
6.4.3	Source apportionment of ambient particles in Mexico City .....	191
6.4.4	Source Signature Matching for Mexico City .....	198
6.4.5	Future implementations .....	203
6.5	Acknowledgements.....	205
6.6	References.....	206
Chapter 7	Conclusion and Future Directions.....	215
7.1	Conclusion .....	215
7.2	Future Directions .....	219
7.3	Final Thought.....	221
7.4	References.....	222
Appendix 1	Development of an ATOFMS Mass Spectral Source Signature	
	Library.....	226
A1.1	Synopsis .....	226
A1.2	Heavy Duty & Light Duty Vehicle Signatures .....	226
A1.3	Additional Source Signatures .....	234
A1.4	References.....	239
Appendix 2	Supporting Information for Chapter 4.....	242
A2.1	Error and Percent Matching as a Function of Vigilance Factor.....	242
A2.2	References.....	246
Appendix 3	Supporting Information for Chapter 6.....	247
A3.1	Variations in the Source Signature Matching Technique .....	247
A3.2	Matching Technique Variation Results for Athens, Greece .....	249

A3.3 Matching Technique Variation Results for Mexico City.....	255
A3.4 References.....	261
Appendix 4 Source Matching Script.....	262
A4.1 Introduction.....	262
A4.2 Source_Matching_Script_06_30_07.....	262



## List of Figures

Figure 1.1	Schematic of an atmospheric aerosol size distribution.....	2
Figure 1.2	A) Calculated deposition of particles in various regions of the respiratory tract for polydisperse Aerosol. B) Schematic diagram of the human respiratory tract.....	4
Figure 1.3	Global annual mean radiative forcing due to various atmospheric agents. ....	6
Figure 1.4	Instrument schematic of the A) ATOFMS and B) UF-ATOFMS.....	14
Figure 2.1	A) Particle size distribution of the Minuteman rocket wake sample. B) Particle size distribution of re-suspended soil samples.....	46
Figure 2.2	Statistical composition of the Minuteman rocket wake based on ART-2a results of ATOFMS data.....	48
Figure 2.3	A) Representative spectrum for the top ART-2a class from the Minuteman rocket wake. B) Representative spectrum for EC/OC containing class from the Minuteman rocket wake .....	50
Figure 2.4	A) Comparison of the re-suspended soil sample statistical compositions based on ART-2a results. B) Average statistical composition of the HAFB re-suspended soil samples .....	52
Figure 2.5	A) Representative spectrum for the top soil particle class based on ART-2a results. B) Representative spectrum of the 2 <sup>nd</sup> soil particle class based on ART-2a results .....	54
Figure 2.6	Representative spectrum of the soil particle class detected	

within the Minuteman rocket wake sample .....	56
Figure 3.1 Sampling set-up used for HDDV dynamometer experiment. ....	71
Figure 3.2 (A – G), Positive and negative ion representative mass spectra for the particle classes sampled in HDDV exhaust. ....	75
Figure 3.3 Statistical breakdown of the scaled particle classes observed from the HDDV exhaust.....	81
Figure 3.4 (A – I), UF-ATOFMS size segregated chemical composition of particles observed for each HDDV for each driving test scaled number to SMPS per gram of CO <sub>2</sub> .....	84
Figure 3.5 Average SMPS size distributions for all HDDVs during the 5-cycle tests.....	87
Figure 3.6 (A – I), UF-ATOFMS particle classes scaled number to SMPS per gram of CO <sub>2</sub> for each HDDV on each test cycle. ....	89
Figure 3.7 Comparison of the top three HDDV particle classes with those observed of the same type in an ambient freeway study with the UF-ATOFMS.....	94
Figure 4.1 Dot product comparisons of the representative area matrices between the general classes from the HDDV and LDV dynamometer experiments using UF-ATOFMS.....	112
Figure 4.2 ART-2a matching error analysis using non-exclusive matching of HDDV and LDV dynamometer particles. ....	114
Figure 4.3 ART-2a matching error analysis using exclusive matching of HDDV and LDV dynamometer particles. ....	116

Figure 4.4	Weight matrices of the top particle types detected during freeway study that match to vehicle study signatures.....	118
Figure 4.5	Temporal plots of A) NO <sub>x</sub> gas data vs. aethalometer data; and B) HDDV video counts vs. aethalometer data.....	121
Figure 4.6	Wind data along with LDV & HDDV traffic counts, and HDDV/LDV/Other ART-2a matching results for UF-ATOFMS fine-mode particles. ....	124
Figure 4.7	SMPS data along with LDV & HDDV traffic counts, and HDDV/LDV/Other ART-2a matching results for UF-ATOFMS ultrafine particles.. ....	126
Figure 4.8	Time series of aethalometer data with HDDV/LDV apportioned particles. ....	128
Figure 5.1	A) QA plot of UF-ATOFMS particle scatters vs. particles scattered that produced a mass spectrum. B) Comparison of the two standard inlet ATOFMS instruments particle detections when running side-by-side at the freeway site. ....	142
Figure 5.2	A) Comparison of sub-100 nm SMPS counts to sub-100 nm particles detected with the UF-ATOFMS at the freeway site. B) Comparison of fine mode particles detected with the APS versus with the standard inlet ATOFMS at the freeway site.....	144
Figure 5.3	A) Comparison of sub-100 nm UF-ATOFMS particles detected with CO measurements. B) Comparison of sub-100 nm UF-ATOFMS particles detected with NO <sub>x</sub> measurements. C) Comparison of CO	

and NO <sub>x</sub> measurements at the freeway site.....	146
Figure 5.4 A) Comparison of aethalometer and NO <sub>x</sub> measurements at the freeway site. B) Comparison of aethalometer and nephelometer measurements at the freeway site. ....	148
Figure 5.5 A) SMPS and APS particle number concentrations at the freeway site from. B) SMPS and APS particle number concentrations at the upwind sampling site. ....	150
Figure 5.6 Particle size distribution data of: A) Standard inlet ATOFMS at the upwind sampling site. B) Standard inlet ATOFMS at the freeway sampling site. C) UF-ATOFMS at the freeway site. ....	152
Figure 5.7 Positive and negative ion mass spectra for the regional background (A) vanadium and (B) EC particle types. (C) The temporal trends of the vanadium particle type. (D) Temporal trends of total background vanadium particles versus the total background EC particles.....	154
Figure 5.8 Hourly HYSPLIT model 24-hour back trajectories at 500 m for each day at the freeway study site.....	156
Figure 5.9 Size resolved source apportionment of the particles detected at the upwind (top) and freeway (bottom) sampling sites. ....	161
Figure 5.10 Time series of the size segregated source apportionment fractions for the freeway site ultrafine and accumulation mode particles detected with the UF-ATOFMS and ATOFMS.....	166
Figure 6.1 Temporal series of the mass spectral source library matching results for Athens, Greece ambient A) submicron particles; and	

B) supermicron particles .....	182
Figure 6.2 Size resolved source apportionment of the ATOFMS detected	
ambient particles for Athens, Greece.....	186
Figure 6.3 The top matching mass spectral source signatures for each source	
for Athens, Greece ATOFMS data .....	189
Figure 6.4 The top matching non-source specific mass spectral signatures for	
each type for Athens, Greece ATOFMS data .....	190
Figure 6.5 Temporal series of the mass spectral source library matching	
results for Mexico City ambient A) submicron particles; and	
B) supermicron particles .....	192
Figure 6.6 Size resolved source apportionment of the ATOFMS detected	
ambient particles for Mexico City .....	196
Figure 6.7 The top matching mass spectral source signatures for each source	
for Mexico City ATOFMS data.....	199
Figure 6.8 The top matching non-source specific mass spectral signatures for	
each type for Mexico City ATOFMS data.....	200
Figure A1.1 Number of particles matched to each HDDV and LDV source	
seed for A) Ultrafine particles (50 – 100 nm); B) Smaller accumulation	
mode (SAM) particles (100 – 140 nm); C) Larger accumulation mode	
(LAM) particles > 140 nm. ....	232
Figure A3.1 Top) Athens, Greece sampling site location; Bottom) Mexico	
City sampling site location.....	248
Figure A3.2 Temporal series of the mass spectral source library matching	

results for Athens, Greece submicron ATOFMS detected particles at different Match-ART-2a parameters.....	250
Figure A3.3 Temporal series of the mass spectral source library matching results for Athens, Greece supermicron ATOFMS detected particles at different Match-ART-2a parameters.....	253
Figure A3.4 Size resolved source apportionment of the ATOFMS detected ambient particles for Athens, Greece at different Match-ART-2a parameters .....	254
Figure A3.5 Temporal series of the mass spectral source library matching results for Mexico City submicron ATOFMS detected particles at different Match-ART-2a parameters.....	256
Figure A3.6 Temporal series of the mass spectral source library matching results for Mexico City supermicron ATOFMS detected particles at different Match-ART-2a parameters.....	259
Figure A3.7 Size resolved source apportionment of the ATOFMS detected ambient particles for Mexico City at different Match-ART-2a parameters .....	260

## List of Tables

Table 2.1	Soil samples collected from Hill Air Force Base, Utah rocket testing area .....	43
Table 3.1	Heavy Duty Diesel Vehicles (HDDVs) tested and driving cycles performed .....	68
Table 3.2	Dilution ratios (DR) for each HDDV and cycle .....	70
Table 4.1	List of instrumentation.....	107
Table 5.1	List of instruments used at the freeway and upwind sampling sites.....	139
Table 6.1	Percent of Athens, Greece particles matched to the mass spectral source library at different match-ART-2a Vigilance Factors (VF) .....	185
Table 6.2	Percent of Mexico City particles matched to the mass spectral source library at different match-ART-2a Vigilance Factors (VF) .....	195
Table A1.1	Structure of the Mass Spectral Source Signature Library for Ultrafine (50 – 100 nm) Particle Matching.....	235
Table A1.2	Structure of the Mass Spectral Source Signature Library for Smaller Accumulation Mode (SAM: 100 – 140 nm) Particle Matching .....	236
Table A1.3	Structure of the Mass Spectral Source Signature Library for Larger Accumulation Mode (LAM: 140 – 1000 nm) & Supermicron (1000 nm +) Particle Matching.....	237
Table A2.1	Percent of particles matched with varying vigilance factor (VF) .....	243
Table A2.2	Percent of particles matched with varying vigilance factor (VF) for vehicle source seeds made at a VF of 0.70 .....	245

Table A3.1	Percent of Athens, Greece particles matched to the mass spectral source library at different match-ART-2a Vigilance Factors (VF) .....	251
Table A3.2	Percent of Mexico City particles matched to the mass spectral source library at different match-ART-2a Vigilance Factors (VF) .....	257



## **Acknowledgements**

My enthusiasm for research in chemistry began at Cal. State Univ. Northridge when I had the privilege of working as an undergraduate researcher for Dr. Omar Zahir. My interest in environmental chemistry complimented well with the work he was doing, and the knowledge I received working and conversing with him always gave me the drive to experiment and seek more answers. Dr. Zahir and a good friend I made in his lab, Dr. Mark Libardoni constantly pushed me to take my knowledge and skills to the next level and are a big part of why I chose to pursue a Ph.D. Sadly, Dr. Zahir passed away prematurely in August of 2005, leaving a large void in the academic community and many hearts.

My desire to pursue my interest in environmental chemistry in graduate school lead me to Dr. Kimberly Prather, who, in 2001, was at UC-Riverside. The research being conducted by the group, developing and using unique instrumentation for analyzing individual atmospheric particles, was exactly what I had been looking for and the graduate students in the group were some of the nicest and most talented I'd ever met. I thank Kim for giving me the opportunity to work in her research group and for helping me expand my knowledge. I also thank Kim for never giving up on me. I have gone through many life experiences during my time in graduate school, and Kim has been very supportive through it all.

During my years in graduate school I've had the privilege of working with and befriending many wonderful people. Specifically, Dr. Georges Khairallah, who was a post-doc in the group when I first joined, took me under his wing and let me help him

totally dismantle, reassemble, and tune one of the ATOFMS instruments in my first week. Because of Georges, I encountered just about everything one could experience with the instrument in the shortest possible time. He was also one of the nicest people anyone could have the privilege to work with. I also have to thank Dr. Ryan Wenzel, who taught me a lot about the instruments, the software, and data analysis while he was with the group, and who became a very close friend to me. There was no other person who could make procrastinating so appealing, but at the same time so educational. Dr. David Sodeman, who was my partner on many field studies and also became a very good friend outside the lab. David and I traveled to such exotic places as Riverside, El Monte, and Utah and worked amazingly well together. I thank him for all he taught me about data analysis and his encouragement over the years. I'd also like to thank Laura Shields for being there for me during the final stages of my graduate career. She has been a great friend and companion, without whom I probably would have lost my mind a few times.

Other group members, past and present, I'd like to acknowledge are Dr. Keith Coffee, Dr. Sergio Guazzotti, Dr. Yongxuan Su, Dr. Thomas Rebotier, Dr. Dave Suess, Dr. Sharon Qin, Dr. Ryan Moffet, Dr. Matt Spencer, Michele Sipin, John Holecek, Kerri Denkenberger, Andy Ault, Lindsay Hatch, Meagan Moore, Ryan Sullivan, Myra Kosak, and Joe Mayer. I have had many scientific discussions and have made good friends with many of these individuals and am happy to have worked with them. I also need to acknowledge Dr. Hiroshi Furutani. Hiroshi joined the Prather group as a post doc a little over a month before me, and had been with the group the entire time I was. He was been a good friend and colleague throughout my graduate career and has always been a great source for advice.

Other scientists outside our group that I have been fortunate to work with include Professor Michael Kleeman, Michael Robert, Chris Jakober, Professor Jamie Schauer, Professor Phil Hopke, Dr. Pentti Paatero, Dr. Manuel Dall'Osto, Dr. Adel Sarofim, Dr. JoAnn Lighty, Professor Douglas Magde, and Dr. Carl Hoeger.

I would also like to thank my doctoral committee Professor Robert Continetti, Professor John Crowell, Professor Seth Cohen and Professor Ray Weiss for their role in helping me obtain this degree.

My Mother and my siblings have always been supportive of me throughout my time in graduate school, despite how often they would ask when I'm going to finish. Their love and support helped me keep going through the hardest times.

Chapter 2 is in preparation for submission to Atmospheric Science and Technology in 2007. Toner, S.M., D.A. Sodeman, and K.A. Prather, Single particle analysis of a Minuteman SR19 II rocket motor exhaust plume using aerosol time-of-flight mass spectrometry. The authors thank Kerry Kelly, and Dave Wagner for their help with collecting the DustTrak data and for helping with the sampling setup. Additionally, we thank Adel Sarofim, JoAnn Lighty from the University of Utah and James (Tom) Callaghan from Hill Air Force Base for their help with coordinating this study. This text is reprinted with permission from Taylor and Francis, Inc.

Chapter 3 has been published in full and is reprinted here with permission from the American Chemical Society. Toner S.M., D.A. Sodeman, and K.A. Prather, Single particle characterization of ultrafine and accumulation mode particles from heavy duty diesel vehicles using aerosol time-of-flight mass spectrometry, Environmental Science & Technology, 40 (12), 3912-3921, 2006.

Chapter 4 has been published in full and is reprinted here with permission from Elsevier. Toner, S.M., L.G. Shields, D.A. Sodeman, and K.A. Prather, Using mass spectral source signatures to apportion exhaust particles from gasoline and diesel powered vehicles in a freeway study using UF-ATOFMS, *Atmospheric Environment*, doi:10.1016/j.atmosenv.2007.08.005, 2007.

Chapter 5 has been submitted for publication in full to *Atmospheric Environment* in 2007. Toner, S.M., L.G. Shields, and K.A. Prather, Source apportionment of freeway-side PM<sub>2.5</sub> using ATOFMS. The authors thank Dan Cayan and Alex Revchuk of the Scripps Institution of Oceanography (SIO) at UCSD for setting up the micro-meteorological stations and providing their data for this study. We also thank UCSD and their facilities management for all their cooperation and help with setting up power to the freeway site. Lastly, we thank Michael Kleeman and Michael Robert from UC-Davis for their collaboration with this study. This text is reprinted with permission from Elsevier.

Chapter 6 is in preparation for submission to *Atmospheric Environment* in 2007. Toner, S.M., Moffet, R.C., Dall'Osto, M., Harrison, R.M., and K.A. Prather, Source apportionment of PM<sub>2.5</sub> in Athens (Greece) and Mexico City using an ATOFMS derived mass spectral source library. The authors thank Laura Shields, Sharon Qin, Thomas Rebotier, and Kerri Denkenberger for their help and input with testing the source signature library. This text is reprinted with permission from Elsevier.

The work in this dissertation was supported by the California Air Resources Board (CARB), Environmental Protection Agency (EPA), the Strategic Environmental Research and Development Program (SERDP), and the Department of Defense (DOD).

## Vita

- 2000            B.S. with honors in Chemistry with an emphasis in Environmental  
Chemistry, California State University, Northridge
- 2000 – 2001   Graduate research assistant, Dept. of Chemistry, California State  
University, Northridge
- 2000 – 2001   Teaching assistant, Dept. of Chemistry, California State University,  
Northridge
- 2001 – 2007   Graduate research assistant, Dept. of Chemistry & Biochemistry,  
University of California, San Diego
- 2001 – 2007   Teaching assistant, Dept. of Chemistry & Biochemistry, University of  
California, San Diego
- 2004            M.S. in Chemistry, University of California, San Diego
- 2007            Ph.D. in Chemistry, University of California, San Diego

## Publications

Toner, S.M., R.C. Moffet, M. Dall'Osto, R.M. Harrison, and K.A. Prather, Source apportionment of PM<sub>2.5</sub> in Athens (Greece) and Mexico City using an ATOFMS derived mass spectral source library, *to be submitted to Atmospheric Environment*, 2007.

Toner, S.M., L.G. Shields, and K.A. Prather, Source apportionment of freeway-side PM<sub>2.5</sub> using ATOFMS, *Atmospheric Environment*, submitted, 2007.

Toner, S.M., D.A. Sodeman, and K.A. Prather, Single particle analysis of a Minuteman SR19 II rocket motor exhaust plume using aerosol time-of-flight mass spectrometry, *to be submitted to Atmospheric Science & Technology*, 2007.

Toner, S.M., L.G. Shields, D.A. Sodeman, and K.A. Prather, Using mass spectral source signatures to apportion exhaust particles from gasoline and diesel powered vehicles in a freeway study using UF-ATOFMS, *Atmospheric Environment*, doi:10.1016/j.atmosenv.2007.08.005, 2007.

Toner, S.M., D.A. Sodeman, and K.A. Prather, Single particle characterization of ultrafine and accumulation mode particles from heavy duty diesel vehicles using aerosol time-of-flight mass spectrometry, *Environmental Science & Technology*, 40 (12), 3912-3921, 2006.

Qin, X., L.G. Shields, S.M. Toner, and K.A. Prather. Single Particle Characterization in Riverside, CA during the SOAR 2005 Campaign – Part 1: Seasonal Comparisons, *manuscript in preparation*, 2007.

Shields, L.G., X. Qin, S.M. Toner, and K.A. Prather. Aging effects on source apportionment from the single particle perspective, *manuscript in preparation*, 2007.

Shields, L.G., X. Qin, S.M. Toner, S.V. Hering, and K.A. Prather. Detection of ambient ultrafine aerosols by single particle techniques during the SOAR 2005 campaign, *manuscript in preparation*, 2007.

Qin, X., L.G. Shields, S.M. Toner, and K.A. Prather. The Effect of APS Scaling Functions on the Quantification of Aerosol Time-of-Flight Mass Spectrometry Measurements, *manuscript in preparation*, 2007.

Shields, L.G., X. Qin, S.M. Toner, and K.A. Prather. Characterization of Trace Metals in Single Urban Particles during the SOAR 2005 Campaign, *manuscript in preparation*, 2007.

Spencer, M. T., L.G. Shields, D.A. Sodeman, S.M. Toner, and K.A. Prather. Comparison of oil and fuel particle chemical signatures with particle emissions from heavy and light duty vehicles. *Atmospheric Environment*, 40, 5224-5235, 2006.

Sodeman, D.A., S.M. Toner, and K.A. Prather, Determination of single particle mass spectral signatures from light duty vehicle emissions, *Environmental Science & Technology*, 39 (12), 4569-4580, 2005.

## **Fields of Study**

Major Field: Chemistry

Studies in Mass Spectrometry & Analytical Chemistry:  
Professor Kimberly A. Prather

Studies in Atmospheric Chemistry:  
Professor Kimberly A. Prather

# **ABSTRACT OF THE DISSERTATION**

## **Anthropogenic Particulate Source Characterization and Source Apportionment Using Aerosol Time-of-Flight Mass Spectrometry**

by

Stephen Mark Toner

Doctor of Philosophy in Chemistry

University of California, San Diego, 2007

Professor Kimberly A. Prather, Chair

Methods of measuring the chemical and physical properties of aerosols as well as proper source apportionment of ambient particles are necessary to provide insight as to the roles they play in the environment and their impact on human health. In addition, the ability to apportion ambient particles quickly and accurately will be very helpful for environmental and health agencies and for monitoring and enforcing emission standards by allowing such agencies to determine the primary source of aerosols in their monitoring areas. The goal of this dissertation is to provide a new approach for aerosol source apportionment using aerosol time-of-flight mass spectrometry (ATOFMS) single particle data. This goal was accomplished by determining unique mass spectral signatures for

specific aerosol sources and by developing these signatures into a source signature library in which ambient ATOFMS data can be matched and apportioned.

The creation of the source signature library (SSL) began with the characterization of specific sources themselves. Heavy duty diesel vehicle (HDDV) emissions were characterized using ATOFMS from a dynamometer study. The particle types detected for HDDVs were compared to those from a previous dynamometer study of gasoline powered light duty vehicles (LDV) to see if HDDV and LDV particles can be distinguished. A SSL was then created for the HDDV and LDV emissions to test the ability to properly apportion between the two sources on ambient ATOFMS data collected next to a major freeway using a SSL matching technique. This work demonstrated that the two sources are readily distinguishable in a fresh emission environment, and that the matching method is a valid means for apportioning ATOFMS data. The SSL was then extended for multiple specific sources as well as for non-source specific particles and was used to apportion the same freeway study particles; showing that the source matching method is able to accurately distinguish different particle sources and that there can be a large contribution from sources other than vehicles near a major freeway. Lastly, the SSL matching method was used to apportion ambient aerosols for two major non-US cities to show that the SSL matching technique is applicable to worldwide ambient ATOFMS data.



# 1 Introduction

## 1.1 Aerosols

Aerosols are defined as a liquid or solid suspended in a gas and range in size from a few nanometers to tens of micrometers; and aerosols can be emitted directly into the atmosphere as primary aerosols or by gas-to-particle conversion processes to form secondary aerosols. Particles in the air can have effects on the global scale, such as with climate and visibility, and can also affect objects as small as biological cells and with the circuitry in microchips [Bao *et al.*, 2007; de la Fuente *et al.*, 2006; Hirata *et al.*, 2005; Kleinman *et al.*, 2003; Liu *et al.*, 2007; Ramanathan *et al.*, 2001; Rosenfeld, 2006]. Figure 1.1 shows a diagram of the different size modes and common methods of generation for atmospheric aerosols [Finlayson-Pitts and Pitts, 1999]. As can be seen, there are three size modes for atmospheric particles, and these will be referred to extensively throughout this dissertation. The mode between 10 and 100 nm is typically referred as the ultrafine mode, and sometimes as the Aitken nuclei range. The mode ranging from 100 – 1000 nm is known as the accumulation, or submicron, mode, while the mode above 1000 nm is referred as the coarse, or supermicron, mode.

One of the major concerns about aerosols is their effect on human health. Recent epidemiological studies have shown that the health effects of aerosol can range from fibrosis and edema of the lungs to cardiopulmonary disease and cancer [Dockery *et al.*, 1993; Elder *et al.*, 2004; Kreyling *et al.*, 2005; Penttinen *et al.*, 2001; Pope, 2000; Pope *et al.*, 2002; Schlesinger and Cassee, 2003; Tager, 2005]. The extent of penetration

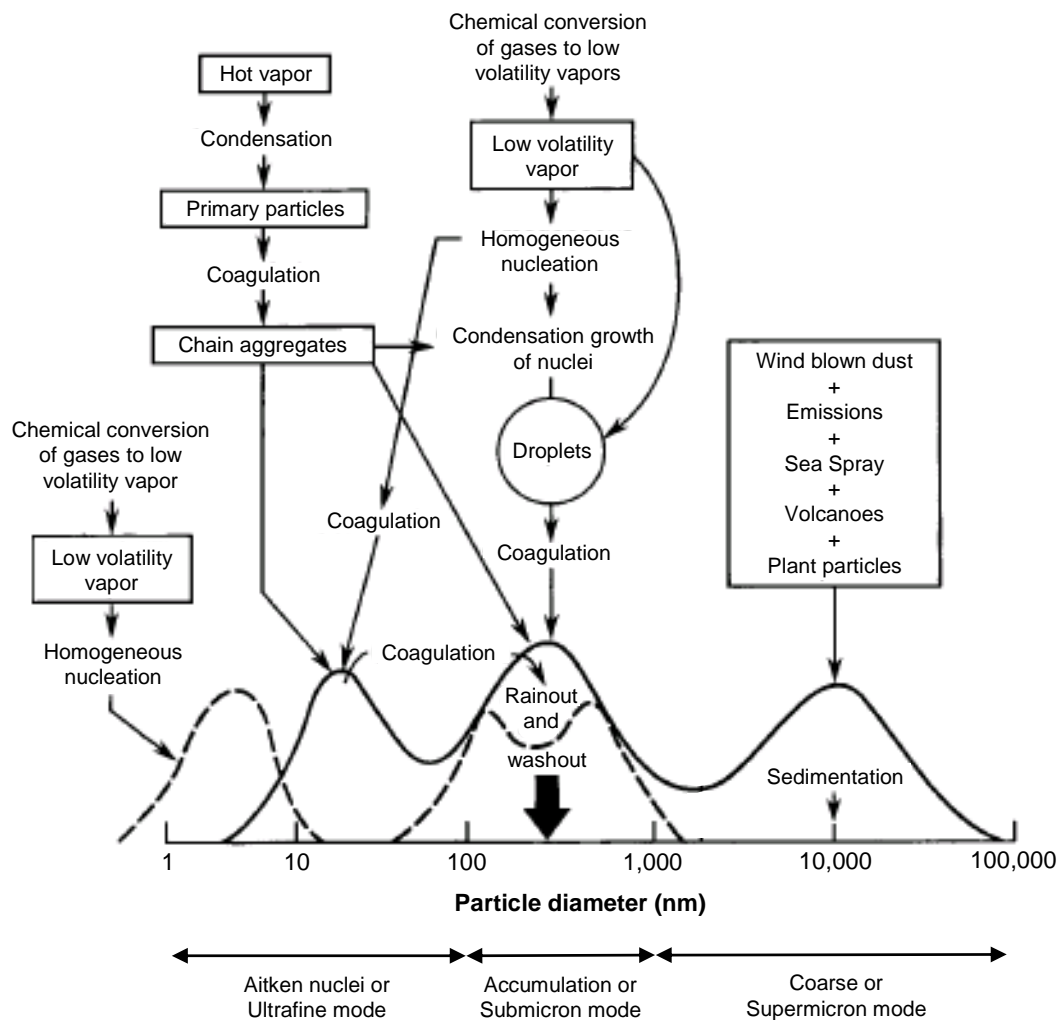


**Figure 1.1** Schematic of an atmospheric aerosol size distribution (adapted with permission from Finlayson-Pitts, B.J., and J.N. Pitts, *Chemistry of the Upper and Lower Atmosphere: Theory, Experiments, and Applications*, p. 355., Academic Press, San Diego, CA. Copyright 1999 Academic Press).

aerosols can have in the human body depends greatly upon their size [Cooney *et al.*, 2004; Lieutier-Colas, 2001; Morawska *et al.*, 2005; Oberdorster *et al.*]. Figure 1.2 shows a diagram of aerosol penetration and deposition through the human airway system [Finlayson-Pitts and Pitts, 1999; Yeh *et al.*, 1996]. As shown in the figure, larger particles ( $> 1000$  nm) deposit in the nasal cavity and the larynx. Smaller particles ( $< 1000$  nm) are able to penetrate deeper into the lungs where they can come in contact with the lung tissue. Ultrafine particles can penetrate to the alveolar region of the lungs where they can be absorbed into the bloodstream. Such particles have been shown to have adverse affects on the cardiopulmonary system and other target organs, such as the liver and the central nervous system [Oberdorster *et al.*, 2005]. The extent of damage or toxicity a particle can have once in the lungs largely depends upon its chemical composition. Particles composed of alumina have been shown to have little toxicological effect but have been shown to cause fibrosis of the lung tissue [Benke *et al.*, 1998; Dinman, 1988; Fritschi *et al.*, 2001]. Particles coated with carcinogenic polycyclic aromatic hydrocarbons (PAHs) can lead to the formation of tumors in the lungs and in other regions of the body if they are able to pass into the bloodstream through the lungs [Chiang and Liao, 2006; Kameda *et al.*, 2005; Lewtas, 1993; Norramit *et al.*, 2005]. Heavy metals, such as chromium, lead, and cadmium, on inhaled particles can be absorbed into the bloodstream and cause toxicological effects on target organs (such as the kidneys, liver, and heart) [Barbier *et al.*, 2005; Davies *et al.*, 1997; Mushtakova *et al.*, 2005; Pritchard *et al.*, 1996; Toscano and Guilarte, 2005].

The negative effects aerosols have on visibility can be seen in many cities and

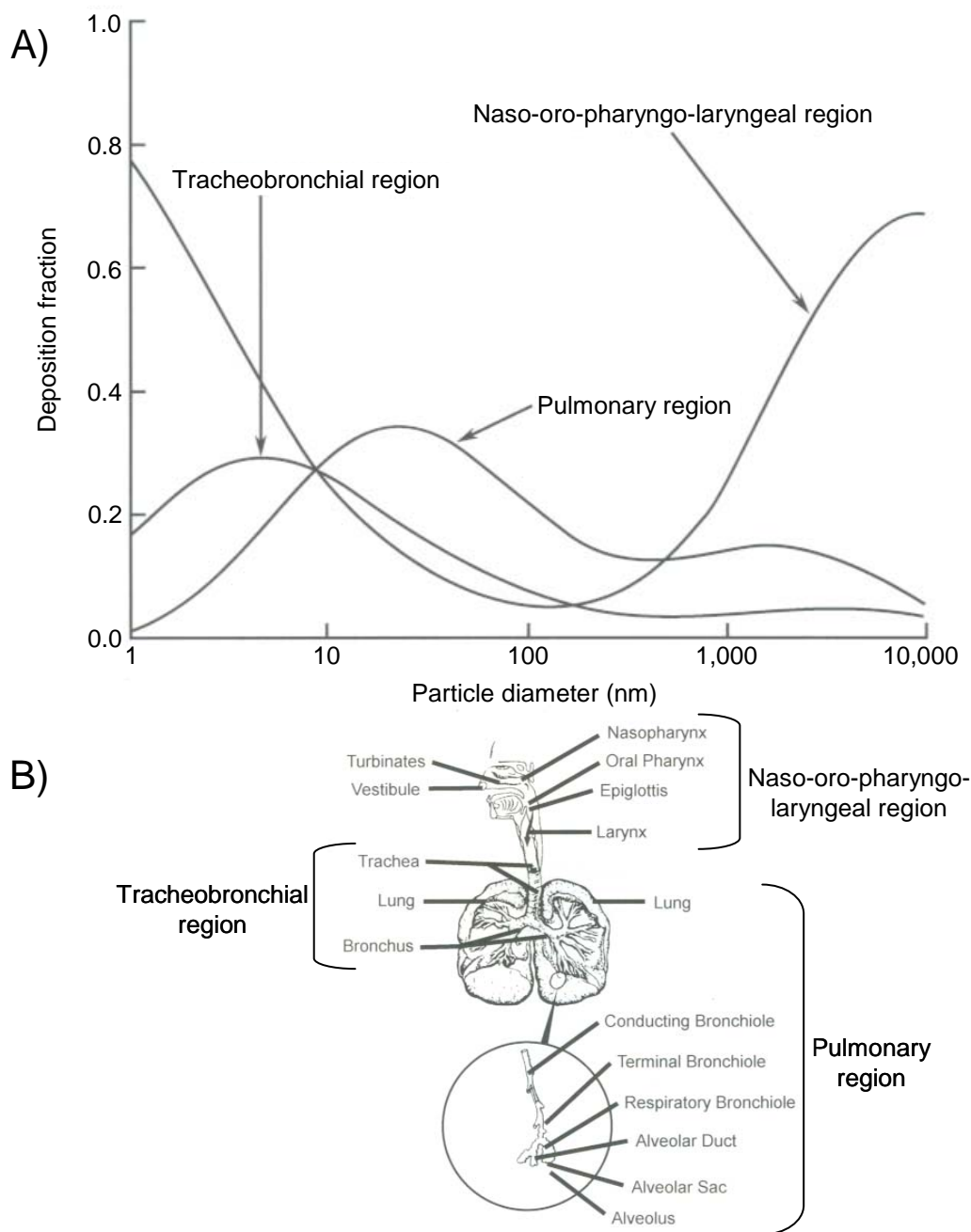


**Figure 1.2** A) Calculated deposition of particles in various regions of the respiratory tract for polydisperse Aerosol. B) Schematic diagram of the human respiratory tract. (Figure 1.2A adapted with permission from Finlayson-Pitts, B.J., and J.N. Pitts, *Chemistry of the Upper and Lower Atmosphere: Theory, Experiments, and Applications*, p. 24., Academic Press, San Diego, CA. Copyright 1999 Academic Press. Figure 1.2B reprinted with permission from Hinds, W.C., *Aerosol Technology: properties, behavior, and measurement of airborne particles*, John Wiley and Sons, Inc., New York. Copyright 1999 John Wiley and Sons, Inc.).

urban areas, as well as in national parks such as Yosemite and the Grand Canyon [Appel *et al.*, 1985; Boylan *et al.*, 2006; Carrico *et al.*, 2005; Day and Malm, 2001; Eatough *et al.*, 2006; Mazurek *et al.*, 1997; Tombach and Brewer, 2005; White and Roberts, 1980]. Aerosols do not only affect the atmosphere aesthetically but can have a major impact on the climate as well. The effect that greenhouse gas species, such as CO<sub>2</sub>, N<sub>2</sub>O, and methane, have on the earth's climate has been studied extensively [Andreae, 2007; Finlayson-Pitts and Pitts, 1999; Hao, 2007; IPCC, 2001; Natr, 2006; Petrova *et al.*, 2006; Seinfeld and Pandis, 1998; Shulk and Editor, 2007]. The amount to which each of these gas phase species warms the atmosphere has been determined with high certainty (Figure 1.3) as reported by the Intergovernmental Panel on Climate Control [IPCC, 2001; IPCC, 2007]. Also shown in Figure 1.3, there is much greater uncertainty as to how aerosols affect the earth's climate. The extent to which aerosols interact with incoming sunlight has to do with their size, shape, and chemical composition [Asano, 1999; Finlayson-Pitts and Pitts, 1999; IPCC, 1994; IPCC, 2001; IPCC, 2007; Seinfeld and Pandis, 1998; Yu *et al.*, 2006]. The chemical composition of a particle will ultimately decide whether the particle absorbs incoming solar radiation or reflects it back to space. The uncertainties in the interaction of solar radiation with the different sizes and compositions of particles generate the large uncertainty bars for aerosols in Figure 1.3.

The influence aerosols have on the climate is not limited to warming and cooling of the atmosphere. Aerosols also act as points of condensation for water, known as cloud condensation nuclei (CCN), which can seed cloud formation. If the atmosphere were completely free of particles, clouds would not be able to form as there would be no suspended surface for water droplets to condense. When the concentration of CCN

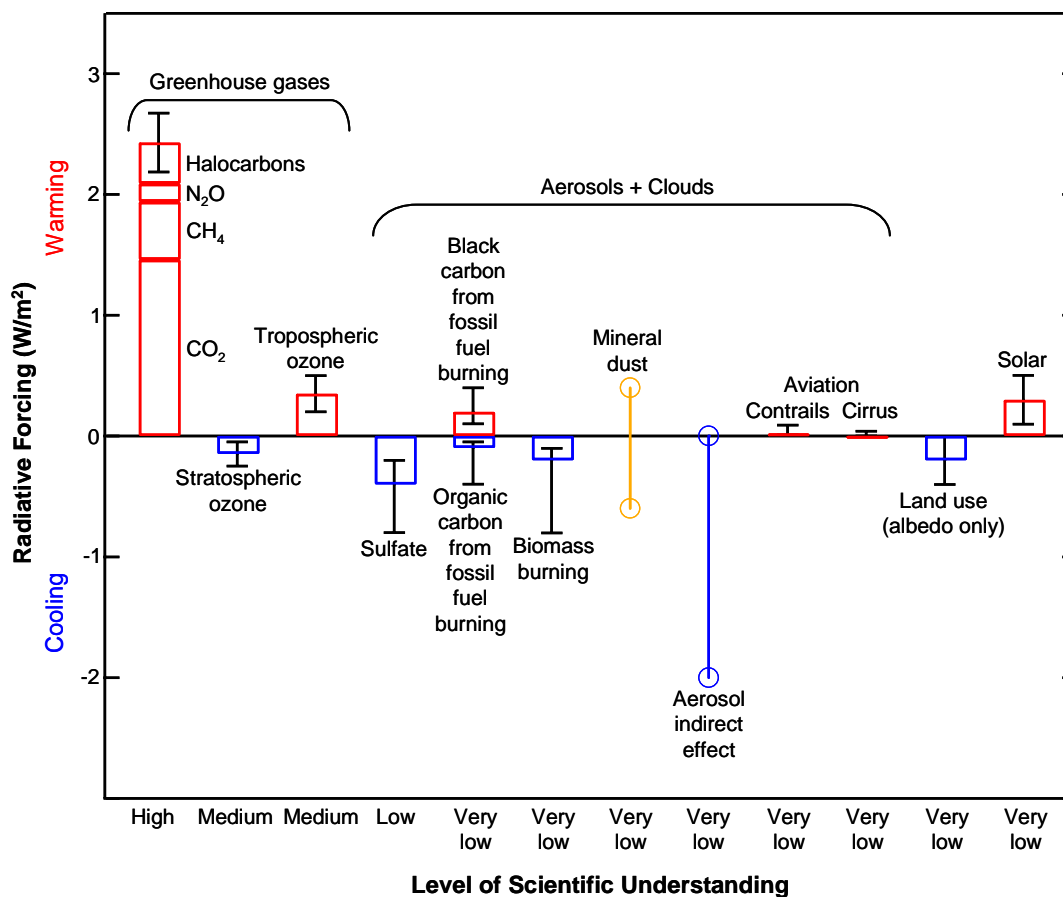


**Figure 1.3** Global annual mean radiative forcing due to various atmospheric agents (adapted with permission from Intergovernmental Panel on Climate Change, *Climate Change 2001: The Scientific Basis*, p. 392. Cambridge University Press, Cambridge, UK. Copyright 2001 Cambridge University Press.).

particles is within an optimal range (which is a function of the water supersaturation), this creates cloud droplets with diameters ideal for precipitation [Curry and Webster, 1999; Kaufman and Tanre, 1994; Petters *et al.*, 2007; Roelofs *et al.*, 2006; Schaefer *et al.*, 1992; Seinfeld and Pandis, 1998; Tomlinson *et al.*, 2007]. However, when the CCN concentration is high, more water droplets are formed but with smaller radii that do not promote precipitation. This condition causes large clouds to form which do not produce any rain [Adhikari *et al.*, 2005; Teller and Levin, 2006].

Aerosols in the atmosphere are generated from a variety of natural and anthropogenic sources. Natural sources include volcanoes, forest and brush fires, wind blown soil and dust, and sea salt from ocean spray. Anthropogenic generated aerosols primarily stem from combustion sources, such as gasoline and diesel vehicles, coal, oil, and biomass fired power plants, industrial operations, and meat cooking, while other non-combustion, anthropogenic sources come from mechanical processes such as mining, landscaping, farming, cement making, and metal working where abrasive materials are used [Finlayson-Pitts and Pitts, 1999; IPCC, 2007; Seinfeld and Pandis, 1998].

The ability to identify the origin (or source) of an aerosol is known as source apportionment. Proper source apportionment of ambient particles is important with regards to understanding their origin, transport, and aging, as well as the role they may play in the environment and possible health effects. The ability to apportion ambient particles quickly and accurately will be very helpful for environmental and health agencies and for monitoring and enforcing emission standards. Proper source apportionment of particles is also useful for global climate and pollution modelers who desire to know the contribution of specific sources in a given region rather than using

estimated numbers based on emission inventories [*Chung et al.*, 2005; *Fraser et al.*, 2000; *Griffin et al.*, 2002; *Ramana and Ramanathan*, 2006; *Ramanathan and Crutzen*, 2003].

## **1.2 Sampling Techniques for Aerosol Source Apportionment**

Several techniques for ambient aerosol source apportionment have been developed over the years. Many of these techniques involve determining organic and inorganic source markers from offline bulk filter analysis using a variety of analytical tools (such as mass spectrometry, chromatography, and microscopy). Other techniques have shown that certain sources can be determined from correlations between particle size data and gas phase measurements as well as with organic gas phase tracer methods. More recent techniques using on-line particle mass spectrometry has proven to be very useful for determining size resolved chemical composition of aerosols and for source apportionment of aerosols. Some of these more widely used techniques are described below.

### **1.2.1 Filter and Impactor Techniques**

Traditional methods of ambient aerosol monitoring involve collecting aerosols on a pre-weighed filter over a specific time and flow rate in order to determine the mass of particles collected. The particles can then be extracted from the filter in bulk, and analyzed with traditional methods such as gas chromatography (GC), high performance liquid chromatography (HPLC), or mass analysis. Because particle composition has been found to change with particle size, this technique evolved into a cascading impactor method where particles of specific size ranges could be collected on impactor substrates



as they traveled through different stages. The apparatus used for this method is called a Micro Orifice Uniform Deposit Impactor (MOUDI) and has become a staple of aerosol monitoring to date [*Kuhlmey et al.*, 1981; *Marple et al.*, 1986; *Marple et al.*, 1991; *McMurry and Marple*, 1986; *Singh et al.*, 2003]. As with the filter techniques, the substrates from MOUDIs are typically extracted and analyzed in bulk with offline techniques.

Filter and impactor sampling methods have proved useful in determining organic chemical markers for various aerosol sources in the atmosphere [*Cass et al.*, 2000; *Kleeman and Cass*, 1998; *Kleeman et al.*, 2000]. However, while the analysis of the particles collected on filters can be useful for determining chemical species and the mass of different species (i.e. EC, OC, metals, ammonium, nitrate, and sulfate), no information is acquired on single particle chemistry or rapid changes in chemical composition. Because the particles are analyzed in bulk, these techniques have to assume uniform composition and density of particles collected on their substrates. There is also the issue of losses of volatile and semi-volatile organics over long sampling times and from storing samples until analysis. Despite the issues with MOUDI sampling, it remains one of the most utilized methods for acquiring quantitative mass information of particulate matter.

### **1.2.2 Particle Sizing Techniques**

On-line particle sizing measurements are being used more and more for source apportionment. One of the key instruments for these measurements is the Scanning Mobility Particle Sizer (SMPS). The SMPS measures particle diameter with a differential mobility analyzer (DMA) which is coupled to a condensation particle counter

(CPC) to measure particle concentration [Chen *et al.*, 1998; Fissan *et al.*, 1983; Flagan, 1998; Knutson and Whitby, 1976; Quant *et al.*, 1995; Wang and Flagan, 1990]. Using an SMPS, particle source contributions are estimated based on the size mode and concentration of ambient aerosols [Lehmann *et al.*, 2003; Reilly *et al.*, 1998; Zhang *et al.*, 2005]. These measurements are typically used for the apportionment of vehicle and other combustion sources by relating the size segregated aerosol concentrations of lab generated samples to those detected in ambient samples. This is also often combined with gas-phase measurements, such as CO, CO<sub>2</sub>, NO<sub>x</sub>, SO<sub>x</sub>, and volatile organic carbon (VOC), and other particle measuring devices, such as an aethalometer for measuring absorbing particles (i.e. elemental carbon), a photoelectric aerosol sensor (PAS) for measuring organic aerosols (specifically PAHs), or a tapered element oscillating microbalance (TEOM) for measuring particle mass concentrations [Bukowiecki *et al.*, 2002; Harrison *et al.*, 1998; Johnson *et al.*, 2005; Shi *et al.*, 1999a; Shi *et al.*, 1999b; Zhang *et al.*, 2005]. The gas phase and additional particle measuring instruments allow for better determination of particle origin from the SMPS measurements by comparing temporal trends of the data between the instruments. However, it is assumed that particles of a certain size will be from a specific source primarily due to its size profile and correlation with gas phase data, regardless of the aerosols chemical composition.

### 1.2.3 Particle Mass Spectrometry Techniques

The drive for obtaining size and chemical composition information on particles in real-time has lead to the development of sophisticated online particle mass spectrometers [Canagaratna *et al.*, 2007; Coe and Allan, 2006; Gard *et al.*, 1997; Hinz and Spengler,

2007; Mallina, 1998; Nash *et al.*, 2006; Prather *et al.*, 1994; Thomson *et al.*, 2000; Wollny, 2003; Zhao *et al.*, 2005]. Online particle mass spectrometry instruments typically include three common elements. The first is that they utilize an aerosol inlet region, such as an aerodynamic lens which focuses incoming particles into a beam, or a converging nozzle followed by skimmer regions to collimate the particle beam and skim away gases. The second commonality between these instruments is that they typically include a particle sizing region. Particle sizing can be done by tracking the particle's time-of-flight between two laser beams or by measuring the time it takes particles to reach a detector after being allowed to enter the instrument via a chopper (or other methods of pulsed introduction). The third element which they share is that they all use some sort of desorption and ionization region, for creating ions of the aerosol, that is followed by a mass spectrometer which allows the determination of the aerosols composition.

Instruments such as the Thermal Desorption Particle Mass Spectrometer (TDPMS) and Aerodyne's Aerosol Mass Spectrometer (AMS) have been used for particle characterization and source apportionment [Canagaratna *et al.*, 2004; Coe and Allan, 2006; Hinz and Spengler, 2007; Nash *et al.*, 2006; Tobias *et al.*, 2001; Tobias *et al.*, 2000]. The TDPBMS and AMS have been shown to be useful in distinguishing organic particle species and even being quantitative for non-refractory aerosol compounds such as organics, ammonium, nitrate and sulfate [Jayne *et al.*, 2000; LaFranchi and Petrucci, 2006; Svane *et al.*, 2004; Tobias *et al.*, 2000]. However, these techniques are unable to detect refractory components (such as dust, sea salt, metals and elemental carbon). The TDPBMS and the commercial version of the AMS do not track

the size of individual particles, but instead control the size range for incoming particles by changing the pressure of the inlet region. Additionally, neither of these instruments acquire the spectrum of single particles; however, a new version of the AMS, which is not yet commercially available, has been recently developed to perform single particle analysis [Cross *et al.*, 2007]. The AMS also has a distinct advantage over the TDPBMS in that the AMS is transportable and can even operate in small aircraft. This mobility allows the AMS to sample a much wider range of ambient aerosol and sources.

Single particle techniques such as aerosol time-of-flight mass spectrometry (ATOFMS) provide an alternative method for aerosol characterization and source apportionment [Bein *et al.*, 2006; Bhawe *et al.*, 2001; Owega *et al.*, 2004; Silva *et al.*, 1999]. The ATOFMS uses a laser to desorb and ionize species from individual particles and thus it can detect all chemical species (refractory and non-refractory) of each particle simultaneously with a dual polarity time-of-flight mass spectrometer [Gard *et al.*, 1997; Su *et al.*, 2004]. The ATOFMS instrument began as an in-lab instrument in the early 1990's and was developed into a transportable instrument within a few years [Gard *et al.*, 1997; Nordmeyer and Prather, 1994]. This transportable version has since been commercialized and marketed by TSI and has become an important tool in aerosol measurements around the world. The pursuit of improving and reducing the size of the instrument has lead to a new version, currently known as aircraft aerosol time-of-flight mass spectrometry (A-ATOFMS), which will become the first version of the ATOFMS instrument to sample in aircrafts [Holecek *et al.*, 2007].

### 1.3 Aerosol Time-of-Flight Mass Spectrometry

The principal technique used in this research is aerosol time-of-flight mass spectrometry (ATOFMS), which is an instrument designed to sample particles over a broad size range and to acquire the size and complete chemical composition of single particles in real-time [Gard *et al.*, 1997; Su *et al.*, 2004]. ATOFMS combines aerodynamic particle sizing along with laser desorption/ionization (LDI) time-of-flight mass spectrometry. Figure 1.4A shows the schematic for the ATOFMS instrument with a standard converging nozzle inlet, while Figure 1.4B shows the ATOFMS instrument with an aerodynamic lens inlet which is used for better transmission of ultrafine particles [Gard *et al.*, 1997; Su *et al.*, 2004]. The version of the instrument in Figure 1.4B is also often referred as ultrafine aerosol time-of-flight mass spectrometry (UF-ATOFMS). Both of these ATOFMS versions can be divided into three distinct regions: 1) the particle inlet region; 2) the light scattering and particle sizing region; and 3) the LDI mass spectrometry region. Each of these regions will be discussed in detail below.

#### 1.3.1 ATOFMS Particle Inlet Region

As was mentioned above, the ATOFMS instrument has two different interfaces designed for the sampling and focusing of particles into the instrument. The first interface developed for the ATOFMS was a converging nozzle inlet. This design consists of a converging nozzle with an orifice opening of 340  $\mu\text{m}$  followed by two conical skimmers. The distance between the nozzle and first skimmer (1.5 mm) is positioned to maximize the amount particle beam focusing into the instrument. The regions between the nozzle and the first skimmer, as well as between the two skimmers, are differentially

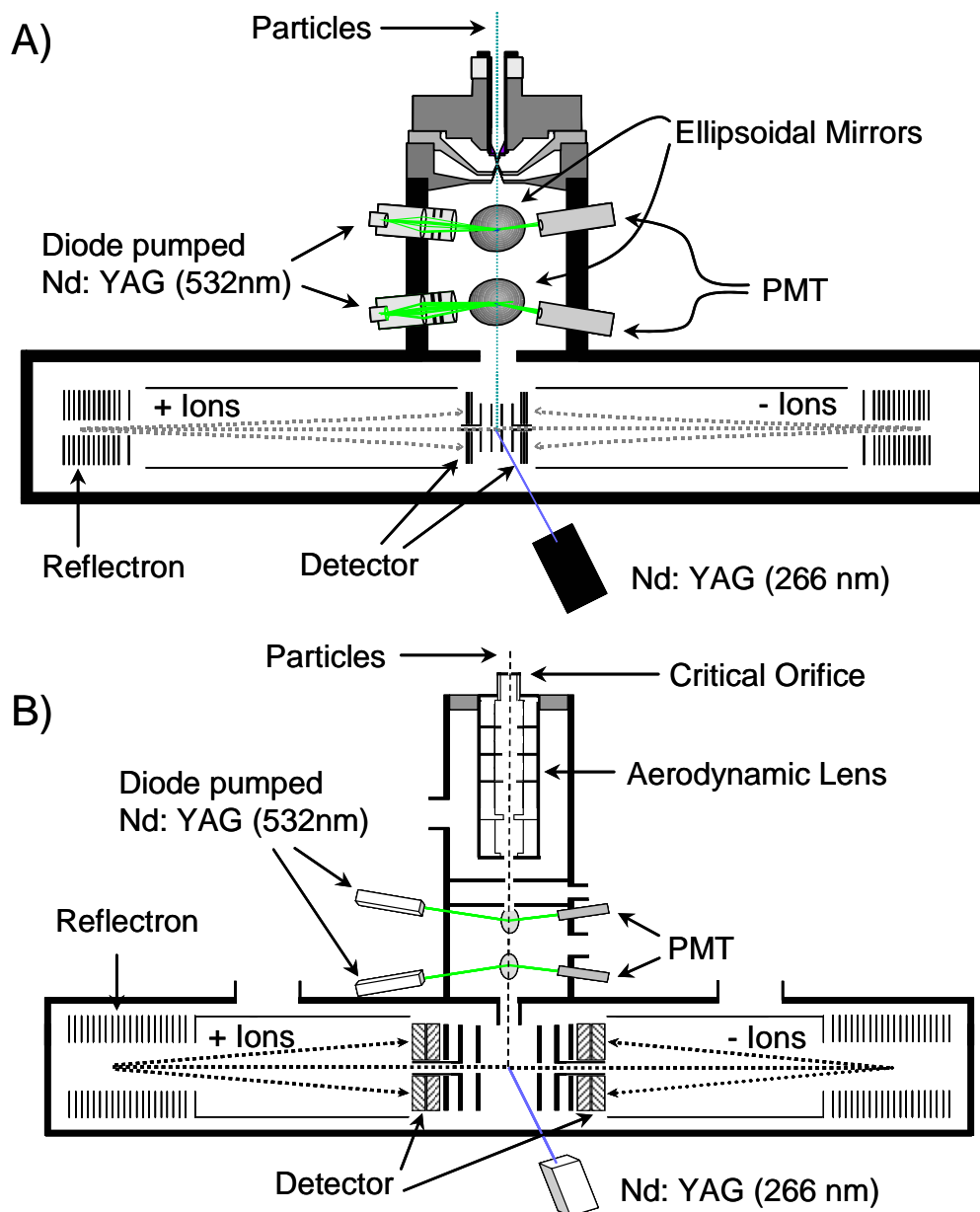


**Figure 1.4** Instrument schematic of the **A)** ATOFMS and **B)** UF-ATOFMS. (Figure 1.2A Reprinted with permission from Gard, E., J.E. Mayer, B.D. Morrical, T. Dienes, D.P. Fergenson, and K.A. Prather, Real-time analysis of individual atmospheric aerosol particles: Design and performance of a portable ATOFMS, *Analytical Chemistry*, 69 (20), 4083-4091, Copyright 1997 American Chemical Society. Figure 1.2B Reprinted with permission from Su, Y.X., M.F. Sipin, H. Furutani, and K.A. Prather, Development and characterization of an aerosol time-of-flight mass spectrometer with increased detection efficiency, *Analytical Chemistry*, 76 (3), 712-719. Copyright 2004 American Chemical Society.).

pumped. In operation, the nozzle region will be about 2.0 Torr, followed by  $2.0 \times 10^{-1}$  Torr after the first skimmer. As particles enter the instrument through the nozzle, they are accelerated to their aerodynamic size-dependent terminal velocity. This is accomplished due to the gas stream carrying the particles undergoing a supersonic expansion as the gas molecules pass through the nozzle and enter the vacuum environment. The two following differentially pumped skimmers help collimate the particle beam and pump the gas away. From there, the particle beam then enters the light scattering and particle sizing region of the instrument. With the standard converging nozzle inlet, the ATOFMS can reliably transmit particles from 200 to 3000 nm. Manipulation in the tuning of the instrument to the extremes can be made to select particles lower than 200 nm or above 3000 nm, but with very poor transmission of such sizes and with severe losses of transmission across the nominal 200 – 3000 nm size range.

The aerodynamic lens inlet was adapted to the ATOFMS instrument in 2001 with the goal of increasing the transmission of particles below 200 nm, and even sub 100 nm [Liu *et al.*, 1995a; Liu *et al.*, 1995b; Su *et al.*, 2004]. Aerosols enter the aerodynamic lens through a critical orifice of about 100  $\mu\text{m}$ , and are drawn in by vacuum which is at 2.1 Torr just after the orifice. The lens is designed with a series of five orifices with successively decreasing diameters (5.0, 4.8, 4.5, 4.3, and 4.0 mm) with relaxation regions between them, followed by a 5.1 mm inner diameter nozzle with a 3.0 mm diameter orifice. As the gas and particles travel through the lens system, they contract and focus at the orifices and are allowed to expand in the relaxation regions. The gas stream that carries the particles plays an important role as the compression of the gas through the

orifices in the lens helps drive the collimation of the particles. Since the particles have greater mass and inertia than the gas molecules, the particle beam does not expand as much as the gas in the relaxation regions, thus allowing the particles to become more tightly focused as they travel through the lens system. The particle beam and gas exit the aerodynamic lens and into a skimmer region which is at  $2.4 \times 10^{-3}$  Torr. Like with the converging nozzle inlet, as the gas stream enters this vacuum, it undergoes a supersonic expansion which accelerates the entrained particles to their aerodynamic size-dependent terminal velocities. Excess gas is pumped away in a differentially pumped skimmer region after the aerodynamic lens. After particles exit the skimmer, they pass into the light scattering and particle sizing region of the instrument.

### **1.3.2 ATOFMS Particle Sizing Region**

Upon exiting the inlet region, particles enter into a sizing region where their aerodynamic diameter is determined based on their time-of-flight. To accomplish this sizing, particles pass through two continuous wave (CW) diode pumped Nd:YAG lasers which are frequency doubled to a wavelength of 532 nm. These two lasers are separated by a known distance (6 cm) and are orthogonal to each other. As particles travel through the lasers, they scatter light which is focused to photomultiplier tubes (PMT) via ellipsoidal mirrors. When a particle passes through the first laser, the scattered light detected by the first PMT sends a signal to a timing circuit which starts a timer. The timer is stopped when the second PMT is triggered by the particle, allowing for the determination of the speed of the particle because the time is measured over a known distance. This method of tracking the particles allows for a calibration curve to be



generated by measuring polystyrene latex sphere (PSL) particles of known size. A third-order polynomial curve of speed versus aerodynamic diameter for the PSL's is generated to create a calibration curve that is used to determine the aerodynamic diameter ( $D_a$ ) of ambient or lab aerosol samples.

For the UF-ATOFMS, the light scattering region has modifications to allow more efficient detection of ultrafine particles. Light scattering for particles entering the instrument above 100 nm is governed by Mie scattering [Hinds, 1998]. The scattering of light by particles at and below 100 nm is very difficult; for this reason, the CW lasers enter the instrument through an optical lens which focuses the laser beam just before the particle stream. This enhancement allows for a greater intensity of laser light to interact with the sub 100 nm particles which improves their detection via light scattering. Additionally, for the work conducted in this thesis, the signal from the PMT's to the timing circuit was amplified more for the UF-ATOFMS than with the standard ATOFMS instrument since the smaller particles scatter less light. The standard inlet ATOFMS instruments have recently been equipped with the same PMT amplifiers.

### **1.3.3 ATOFMS Laser Desorption/Ionization Mass Spectrometry Region**

When a particle has been successfully detected by both lasers in the sizing region, a second timer begins on the timing circuit to allow a third (LDI) laser to fire a single pulse to intercept the particle. For both the ATOFMS and UF-ATOFMS instruments, this third laser is a Q-switched frequency quadrupled Nd:YAG laser at 266 nm generally operating around 1.5 mJ/pulse. This pulse is focused to the center of the source region of the mass spectrometer in alignment with the particle stream. At the focal point, the spot

size of the laser is about 0.5 mm, and the power density is about  $10^8$  W/cm<sup>2</sup>, which is sufficient to vaporize (desorb) the particle and create ions. The instrument utilizes a dual polarity reflectron time-of-flight mass spectrometer to detect both positive and negative ions simultaneously, which are produced in the LDI process. Numerous books and articles have been published on the technique of time-of-flight mass spectrometry (TOFMS) since its conception in 1946 [Cotter, 1997; Cotter, 1999; Grotemeyer, 2001; Stephens, 1946; Uphoff and Grotemeyer, 2003; Weickhardt *et al.*, 1997], so a detailed description of the TOF mass analyzer is not given here.

#### 1.4 ATOFMS Data Analysis

Due to the incorporation of new computer and data acquisition hardware, the rate of particle data acquisition with the ATOFMS has been ever increasing and is currently capable of obtaining single particle spectra up to 10 – 15 Hz. This rate of data acquisition can mean up to tens of millions of particle spectra for just one field measurement study. The generation of such large datasets has spurred the motivation to find better and faster ways to analyze ATOFMS data. The methods for ATOFMS single particle data analysis and classification have been developing and progressing over the years. Some methods have included: sorting through individual spectra by hand, which can be extremely time consuming for large datasets; simple  $m/z$  peak searching using basic table database structures; and databases where mathematical algorithms can be used to cluster the data based on user defined parameters. The major progress has come from incorporating data clustering methods with mathematical algorithms such as Adaptive Resonance Theory-2a (ART-2a), K-means, and Hierarchical Clustering [Lance and Williams, 1967; Murphy *et*

*al.*, 2003; *Phares et al.*, 2001; *Rebotier and Prather*, 2007; *Ward*, 1963; *Wienke et al.*, 1994]. The ART-2a clustering method was chosen by our research group and has been shown to be comparably accurate to other methods [*Rebotier and Prather*, 2007; *Song et al.*, 1999; *Xie et al.*, 1994]. An adaptation of the ART-2a clustering algorithm using predefined particle signatures, or a mass spectral source library, for matching ambient particle spectra is the primary focus of this thesis and is described in detail below.

#### **1.4.1 Particle Clustering using Adaptive Resonance Theory-2a (ART-2a)**

ART-2a converts each mass spectrum into an n-dimensional vector based on the peak area of each  $m/z$ . The dot product of each particle vector is then taken across all the other particle vectors in the dataset in random order and vectors with a dot product above a certain threshold, or vigilance factor (VF), are grouped together in a cluster. If a particle matches to two or more different vectors above the VF, then it will be assigned to the one that provided the highest dot product. The dot product values range from 0 to 1 with a value of 1 indicating the particle spectra are identical. Once a cluster has been generated, the vectors between the particles within the cluster are averaged into a weighted vector which will be used for comparing dot products as each consecutive vector dot product is taken. This process continues on randomly through the entire dataset of particles, creating new clusters whenever a particle vector does not match to an already defined cluster above the VF. After all the particles have been compared and assigned to a specific cluster, a set of clusters is generated. ART-2a then compares all the particle vectors against the defined clusters to ensure each particle is in the correct cluster, and this process recommences for a defined number of iterations.

Since the standard ART-2a clustering method does not converge, meaning that clusters are not combined as their weight vectors become similar (above the VF) and particles do not always go to their previously assigned cluster with each iteration, many clusters can be generated from this analysis. The amount of clusters produced can range from hundreds to thousands depending on how many particles and particle types are in the dataset. In response to the large amount of ART-2a clusters produced, an additional ART-2a regrouping script was created. The ART-2a regrouping script works in the same method as ART-2a on the single particle vectors, except now the vectors that it compares are just those of the clusters generated from the initial ART-2a analysis. Clusters are combined when their dot product comparison results above a predefined VF. This additional regrouping of the ART-2a clusters can reduce the amount of clusters to fewer than 100, which makes the task of classification much easier.

After the particles have been clustered with ART-2a and then regrouped, the spectral ion patterns are visually inspected for the purpose of classification. Based on this visual classification, particle clusters may be even further grouped together by the user to create more general particle types. Similar clusters that appear to belong within the same “class” as each other based on the presence or absence of key species (i.e. elemental carbon (EC), organic carbon (OC), specific metals, sulfate, nitrate) are regrouped by hand. Such classes have minor differences in the relative ion peak patterns among their collective clusters; however, the overall chemical species making up each major type of cluster are the same. One of the key issues with this method of classification and apportionment of particles is that it is dependent upon user interpretation.

### 1.4.2 Classification & Apportionment Using Match-ART-2a with Predefined Clusters

As mentioned above, techniques such as ART-2a have been shown to accurately cluster particle spectra within given similarity thresholds [*Bhave et al.*, 2001; *Murphy et al.*, 2003; *Rebotier and Prather*, 2007; *Song et al.*, 2001; *Tan et al.*, 2002; *Wenzel and Prather*, 2004]. These methods fail to label the particle types they have been used to cluster. The labeling process is still controlled by the user which can result in biases or overly generalized classification. With this in mind, an autonomous approach was developed for clustering and identifying particles. This approach involves creating a mass spectral library of carefully identified and predefined clusters of particle types. To ensure proper classification of sources with this technique, the sources themselves have to be properly sampled individually with an ATOFMS instrument and analyzed with ART-2a. Upon sampling and clustering a collection of sources, the predefined clusters can be combined into a library of clusters (or signatures). These source signatures are used as a “seed” database, where the mass spectra of particles from other studies can be compared to the seeds using a matching version of the ART-2a algorithm [*Allen*, 2006; *Song et al.*, 1999] (YAADA v1.20 – <http://www.yaada.org>).

The match-ART-2a function uses existing ART-2a clusters as source seeds for the purpose of determining whether other particles match those seeds. In this case, ART-2a runs normal with prescribed particle clusters unable to be changed by the addition of new particles to each cluster. Since the clusters do not change as particles are matched to them, this function allows the clusters to stay “true” to the original source signature.

Particles being considered in the matching are either matched exclusively to a particular cluster (above the VF) or not at all. If the particle matches to a particular source seed above the designated dot product VF threshold, then the particle is assigned to that type. If the particle matches to two or more different source seeds above the VF, then it will be assigned to the one that provided the highest dot product. As before, the dot product values range from 0 to 1 with a value of 1 indicating the particle types are identical.

## **1.5 Research Objectives and Synopsis**

The ability to apportion and track particles emitted from specific sources is vital towards advancing our understanding of particle lifetimes, transport, chemical transformation, and overall contribution to regional aerosol. In order to properly apportion atmospheric aerosols, the unique chemical signatures (or fingerprints) from individual sources must first be determined. Since particles in the atmosphere can chemically evolve (or age) over time, the chemical signatures of particles emitted from specific primary sources may change or become masked. Therefore determining the chemical signatures of the freshly emitted source particles is necessary in order to understand the root chemical makeup of particles prior to undergoing atmospheric transformations and to make attempts at source apportionment more feasible. The process of determining specific source signatures, creating a library of source signatures, and adapting it to an autonomous classification method for aerosol source apportionment is goal of the research presented in this thesis.

This method begins in Chapter 2 where particle source signatures for solid fueled rocket motors (SRM) used to launch payloads into outer space were determined by

sampling and characterizing the exhaust wake of a statically fired SRM using UF-ATOFMS and standard ATOFMS. The goal of this study was not only to obtain mass spectral signatures for SRMs, but to test the ability of the ART-2a algorithm to distinguish between particle types with similar mass spectral signatures. This Chapter represents the first attempt at apportioning chemically similar particle types from two distinct sources with ATOFMS. Determining SRM signatures is important because SRMs have been shown to release several tons of alumina and reactive chlorine species into the stratosphere [*Brady et al.*, 1994; *Cofer et al.*, 1989]. While such particles have a very short lifetime in the troposphere, the lifetime, transport, and extent of reaction with the ozone layer in the stratosphere are yet to be fully determined.

In Chapter 3, the chemical signatures of heavy duty diesel vehicle (HDDV) particle exhaust emissions with aerodynamic diameters (Da) 50 to 300 nm are determined. This work was done in part of a series of dynamometer studies for gasoline powered light duty vehicles (LDV) and HDDV aerosol emissions for the expressed purpose of determining unique chemical signatures and distinguishing between the two vehicle types [*Shields et al.*, 2007; *Sodeman et al.*, 2005; *Toner et al.*, 2006].

Chapter 4 investigates whether the ambient exhaust emissions from HDDVs and LDVs can be distinguished from one another. To do this, a library of mass spectral fingerprints was created for both vehicle types and was used to apportion fresh vehicle exhaust particles (50 – 300 nm) detected alongside a major freeway with the UF-ATOFMS using the match-ART-2a method described above. Logistically, a freeway-side location was chosen in a coastal “clean” environment so there would be little influence from sources other than vehicles.

The apportionment process used in Chapter 4 was taken a step further in Chapter 5, where the source signature library was expanded to include the signatures over a much broader size range and for several more specific (HDDV, LDV, dust, sea salt, biomass, and meat cooking) and non-specific sources (aged organic carbon, aged elemental carbon, amine containing particles, PAH's, ammonium rich particles, vanadium particles, and elemental carbon particles). In Chapter 5, the data from two freeway side ATOFMS instruments (50 – 3000 nm) are apportioned using the library matching technique as well as the data from an upwind aerosol background monitoring site.

Finally, Chapter 6 investigates the feasibility of using the ATOFMS mass spectral source library matching method on a global scale and in more polluted environments. This assessment was done by using the matching technique on ATOFMS data collected at two major global cities (Athens, Greece and Mexico City). In addition to testing this apportionment technique for apportionment of ATOFMS data collected around the world, it also tested if the library matching technique could work for data collected with ATOFMS instruments from different research groups.



## 1.6 References

- Adhikari, M., Y. Ishizaka, H. Minda, R. Kazaoka, J.B. Jensen, J.L. Gras, and T. Nakajima, Vertical distribution of cloud condensation nuclei concentrations and their effect on microphysical properties of clouds over the sea near the southwest islands of Japan, *Journal of Geophysical Research, [Atmospheres]*, 110 (D10), D10203/1-D10203/15, 2005.
- Allen, J.O., Software toolkit to analyze single-particle mass spectral data - <http://www.yaada.org>, 2006.
- Andreae, M.O., Atmospheric aerosols versus greenhouse gases in the twenty-first century, *Philosophical Transactions of the Royal Society, A: Mathematical, Physical & Engineering Sciences*, 365 (1856), 1915-1923, 2007.
- Appel, B.R., Y. Tokiwa, J. Hsu, E.L. Kothny, and E. Hahn, Visibility as related to atmospheric aerosol constituents, *Atmospheric Environment (1967-1989)*, 19 (9), 1525-34, 1985.
- Asano, S., Radiative forcing of tropospheric aerosols on climate, *Eerozoru Kenkyu*, 14 (3), 214-220, 1999.
- Bao, L., S. Chen, L. Wu, T.K. Hei, Y. Wu, Z. Yu, and A. Xu, Mutagenicity of diesel exhaust particles mediated by cell-particle interaction in mammalian cells, *Toxicology*, 229 (1-2), 91-100, 2007.
- Barbier, O., G. Jacquillet, M. Tauc, M. Cougnon, and P. Poujeol, Effect of heavy metals on, and handling by, the kidney, *Nephron Physiology*, 99 (4), 105-110, 2005.
- Bein, K.J., Y. Zhao, N.J. Pekney, C.I. Davidson, M.V. Johnston, and A.S. Wexler, Identification of sources of atmospheric PM at the Pittsburgh Supersite-Part II: Quantitative comparisons of single particle, particle number, and particle mass measurements, *Atmospheric Environment*, 40 (Suppl. 2), S424-S444, 2006.
- Benke, G., M. Abramson, and M. Sim, Exposures in the alumina and primary aluminum industry: as historical review, *Annals of Occupational Hygiene*, 42 (3), 173-189, 1998.
- Bhave, P.V., D.P. Fergenson, K.A. Prather, and G.R. Cass, Source apportionment of fine particulate matter by clustering single-particle data: tests of receptor model accuracy, *Environmental Science and Technology*, 35 (10), 2060-2072, 2001.
- Boylan, J.W., M.T. Odman, J.G. Wilkinson, and A.G. Russell, Integrated assessment modeling of atmospheric pollutants in the southern Appalachian Mountains: Part

- II. Fine particulate matter and visibility, *Journal of the Air & Waste Management Association*, 56 (1), 12-22, 2006.
- Brady, B.B., E.W. Fournier, L.R. Martin, and R.B. Cohen, Stratospheric ozone reactive chemicals generated by space launches worldwide, pp. 34 pp., Technology Operations, Aerospace Corp., El Segundo, CA. USA., 1994.
- Bukowiecki, N., D.B. Kittelson, W.F. Watts, H. Burtscher, E. Weingartner, and U. Baltensperger, Real-time characterization of ultrafine and accumulation mode particles in ambient combustion aerosols, *Journal of Aerosol Science*, 33 (8), 1139-1154, 2002.
- Canagaratna, M.R., J.T. Jayne, D.A. Ghertner, S. Herndon, Q. Shi, J.L. Jimenez, P.J. Silva, P. Williams, T. Lanni, F. Drewnick, K.L. Demerjian, C.E. Kolb, and D.R. Worsnop, Chase studies of particulate emissions from in-use New York City vehicles, *Aerosol Science & Technology*, 38 (6), 555-573, 2004.
- Canagaratna, M.R., J.T. Jayne, J.L. Jimenez, J.D. Allan, M.R. Alfarra, Q. Zhang, T.B. Onasch, F. Drewnick, H. Coe, A. Middlebrook, A. Delia, L.R. Williams, A.M. Trimborn, M.J. Northway, P.F. DeCarlo, C.E. Kolb, P. Davidovits, and D.R. Worsnop, Chemical and microphysical characterization of ambient aerosols with the aerodyne aerosol mass spectrometer, *Mass Spectrometry Reviews*, 26 (2), 185-222, 2007.
- Carrico, C.M., S.M. Kreidenweis, W.C. Malm, D.E. Day, T. Lee, J. Carrillo, G.R. McMeeking, and J.L. Collett, Hygroscopic growth behavior of a carbon-dominated aerosol in Yosemite National Park, *Atmospheric Environment*, 39 (8), 1393-1404, 2005.
- Cass, G.R., L.A. Hughes, P. Bhave, M.J. Kleeman, J.O. Allen, and L.G. Salmon, The chemical composition of atmospheric ultrafine particles, *Philosophical Transactions of the Royal Society of London, Series A: Mathematical, Physical and Engineering Sciences*, 358 (1775), 2581-2592, 2000.
- Chen, D.R., D.Y.H. Pui, D. Hummes, H. Fissan, F.R. Quant, and G.J. Sem, Design and evaluation of a nanometer aerosol differential mobility analyzer (Nano-DMA), *Journal of Aerosol Science*, 29 (5/6), 497-509, 1998.
- Chiang, K.-C., and C.-M. Liao, Heavy incense burning in temples promotes exposure risk from airborne PMs and carcinogenic PAHs, *Science of the Total Environment*, 372 (1), 64-75, 2006.
- Chung, C.E., V. Ramanathan, D. Kim, and I.A. Podgorny, Global anthropogenic aerosol direct forcing derived from satellite and ground-based observations, *Journal of Geophysical Research-Atmospheres*, 110 (D24), 2005.

- Coe, H., and J.D. Allan, Mass spectrometric methods for aerosol composition measurements, *Analytical Techniques for Atmospheric Measurement*, 265-310, 2006.
- Cofer, W.R., III, E.L. Winstead, and L.E. Key, Surface composition of solid-rocket exhausted aluminum oxide particles, *Journal of Propulsion and Power*, 5 (6), 674-7, 1989.
- Cooney, D., M. Kazantseva, and A.J. Hickey, Development of a size-dependent aerosol deposition model utilising human airway epithelial cells for evaluating aerosol drug delivery, *ATLA, Alternatives to Laboratory Animals*, 32 (6), 581-590, 2004.
- Cotter, R.J., *Time-of-Flight Mass Spectrometry: Instrumentation and Applications in Biological Research*, 326 pp. pp., 1997.
- Cotter, R.J., The new time-of-flight mass spectrometry, *Analytical Chemistry*, 71 (13), 445A-451A, 1999.
- Cross, E.S., J.G. Slowik, P. Davidovits, J.D. Allan, D.R. Worsnop, J.T. Jayne, D.K. Lewis, M. Canagaratna, and T.B. Onasch, Laboratory and ambient particle density determinations using light scattering in conjunction with aerosol mass spectrometry, *Aerosol Science and Technology*, 41 (4), 343-359, 2007.
- Curry, J.A., and P.J. Webster, *Thermodynamics of Atmospheres and Oceans*, 471 pp., Academic Press, 1999.
- Davies, N.A., M.G. Taylor, and K. Simkiss, The influence of particle surface characteristics on pollutant metal uptake by cells, *Environmental Pollution*, 96 (2), 179-184, 1997.
- Day, D.E., and W.C. Malm, Aerosol light scattering measurements as a function of relative humidity: a comparison between measurements made at three different sites, *Atmospheric Environment*, 35 (30), 5169-5176, 2001.
- de la Fuente, J.M., C.C. Berry, M.O. Riehle, and A.S.G. Curtis, Nanoparticle Targeting at Cells, *Langmuir*, 22 (7), 3286-3293, 2006.
- Dinman, B.D., Alumina-related pulmonary disease, *JOM, J. Occup. Med.*, 30 (4), 328-, 1988.
- Dockery, D.W., C.A. Pope, X.P. Xu, J.D. Spengler, J.H. Ware, M.E. Fay, B.G. Ferris, and F.E. Speizer, An Association between Air-Pollution and Mortality in 6 United-States Cities, *New England Journal of Medicine*, 329 (24), 1753-1759, 1993.

- Eatough, D.J., W. Cui, J. Hull, and R.J. Farber, Fine particulate chemical composition and light extinction at Meadview, AZ, *Journal of the Air & Waste Management Association*, 56 (12), 1694-1706, 2006.
- Elder, A., R. Gelein, J. Finkelstein, R. Phipps, M. Frampton, M. Utell, D.B. Kittelson, W.F. Watts, P. Hopke, C.-H. Jeong, E. Kim, W. Liu, W. Zhao, L. Zhuo, R. Vincent, P. Kumarathasan, and G. Oberdoerster, On-Road Exposure to Highway Aerosols. 2. Exposures of Aged, Compromised Rats, *Inhalation Toxicology*, 16 (Suppl. 1), 41-53, 2004.
- Finlayson-Pitts, B.J., and J.N. Pitts, *Chemistry of the Upper and Lower Atmosphere: Theory, Experiments, and Applications*, 1040 pp., Academic Press, 1999.
- Fissan, H.J., C. Helsper, and H.J. Thielen, Determination of particle size distributions by means of an electrostatic classifier, *Journal of Aerosol Science*, 14 (3), 354-7, 1983.
- Flagan, R.C., History of electrical aerosol measurements, *Aerosol Science and Technology*, 28 (4), 301-380, 1998.
- Fraser, M.P., M.J. Kleeman, J.J. Schauer, and G.R. Cass, Modeling the atmospheric concentrations of individual gas-phase and particle-phase organic compounds, *Environmental Science and Technology*, 34 (7), 1302-1312, 2000.
- Fritschi, L., N. De Klerk, M. Sim, G. Benke, and A.W. Musk, Respiratory morbidity and exposure to bauxite, alumina and caustic mist in alumina refineries, *Journal of Occupational Health*, 43 (5), 231-237, 2001.
- Gard, E., J.E. Mayer, B.D. Morrical, T. Dienes, D.P. Fergenson, and K.A. Prather, Real-time analysis of individual atmospheric aerosol particles: Design and performance of a portable ATOFMS, *Analytical Chemistry*, 69 (20), 4083-4091, 1997.
- Griffin, R.J., D. Dabdub, M.J. Kleeman, M.P. Fraser, G.R. Cass, and J.H. Seinfeld, Secondary organic aerosol 3. Urban/regional scale model of size- and composition-resolved aerosols, *Journal of Geophysical Research, [Atmospheres]*, 107 (D17), AAC5/1-AAC5/14, 2002.
- Grotemeyer, J., *Special Issue: Time-of-Flight Mass Spectrometry. [In: Int. J. Mass Spectrom., 2001; 206(3)]*, 113 pp., 2001.
- Hao, X., Nitrate accumulation and greenhouse gas emissions during compost storage, *Nutrient Cycling in Agroecosystems*, 78 (2), 189-195, 2007.

- Harrison, R.M., M. Jones, and G. Collins, Measurements of the physical properties of particles in the urban atmosphere, *Atmospheric Environment*, 33 (2), 309-321, 1998.
- Hinds, W.C., *Aerosol Technology: Properties, Behavior, and Measurements of Airborne Particles, 2nd Edition*, 464 pp. pp., 1998.
- Hinz, K.-P., and B. Spengler, Instrumentation, data evaluation and quantification in on-line aerosol mass spectrometry, *Journal of Mass Spectrometry*, 42 (7), 843-860, 2007.
- Hirata, M., T. Gotou, and M. Ohba, Thin-film particles of graphite oxide. 2: Preliminary studies for internal micro fabrication of single particle and carbonaceous electronic circuits, *Carbon*, 43 (3), 503-510, 2005.
- Holecck, J.C., K.A. Denkenberger, J.E. Mayer, R.C. Moffet, G. Poon, R.O. Sanchez, T.P. Rebotier, H. Furutani, Y.X. Su, S.A. Guazzotti, and K.A. Prather, Aircraft-ATOFMS Instrument Development., *In Preparation*, 2007.
- IPCC, *Intergovernmental Panel on Climate Change, Climate Change 1994: Radiative Forcing of Climate Change and an Evaluation of the IPCC IS92 Emission Scenarios*, Cambridge University Press, Cambridge, UK, 1994.
- IPCC, *Intergovernmental Panel on Climate Change, Climate Change 2001: The Scientific Basis*, Cambridge University Press, Cambridge, UK, 2001.
- IPCC, *Intergovernmental Panel on Climate Change, Climate Change 2007: The Physical Science Basis AR4*, Cambridge University Press, New York, 2007.
- Jayne, J.T., D.C. Leard, X.F. Zhang, P. Davidovits, K.A. Smith, C.E. Kolb, and D.R. Worsnop, Development of an aerosol mass spectrometer for size and composition analysis of submicron particles, *Aerosol Science & Technology*, 33 (1-2), 49-70, 2000.
- Johnson, J.P., D.B. Kittelson, and W.F. Watts, Source apportionment of diesel and spark ignition exhaust aerosol using on-road data from the Minneapolis metropolitan area, *Atmospheric Environment*, 39 (11), 2111-2121, 2005.
- Kameda, Y., J. Shirai, T. Komai, J. Nakanishi, and S. Masunaga, Atmospheric polycyclic aromatic hydrocarbons: size distribution, estimation of their risk and their depositions in human respiratory tract, *Science of the Total Environment*, 340 (1-3), 71-80, 2005.

- Kaufman, Y.J., and D. Tanre, Effect of variations in supersaturation on the formation of cloud condensation nuclei, *Nature (London, United Kingdom)*, 369 (6475), 45-8, 1994.
- Kleeman, M.J., and G.R. Cass, Source contributions to the size and composition distribution of urban particulate air pollution, *Atmospheric Environment*, 32 (16), 2803-2816, 1998.
- Kleeman, M.J., J.J. Schauer, and G.R. Cass, Size and composition distribution of fine particulate matter emitted from motor vehicles, *Environmental Science and Technology*, 34 (7), 1132-1142, 2000.
- Kleinman, M.T., C. Sioutas, M.C. Chang, A.J.F. Boere, and F.R. Cassee, Ambient fine and coarse particle suppression of alveolar macrophage functions, *Toxicology Letters*, 137 (3), 151-158, 2003.
- Knutson, E.O., and K.T. Whitby, Aerosol classification by electric mobility: apparatus, theory, and applications, *Journal of Aerosol Science*, 6 (6), 443-51, 1976.
- Kreyling, W.G., M. Semmler, and W. Moeller, Ultrafine aerosols and nanoparticles, *Atemwegs- und Lungenkrankheiten*, 31 (8), 411-419, 2005.
- Kuhlmei, G.A., B.Y.H. Liu, and V.A. Marple, A microorifice impactor for submicron aerosol size classification, *American Industrial Hygiene Association Journal (1958-1999)*, 42 (11), 790-5, 1981.
- LaFranchi, B.W., and G.A. Petrucci, A comprehensive characterization of photoelectron resonance capture ionization aerosol mass spectrometry for the quantitative and qualitative analysis of organic particulate matter, *International Journal of Mass Spectrometry*, 258 (1-3), 120-133, 2006.
- Lance, G.N., and W.T. Williams, A General Theory of Classificatory Sorting Strategies .1. Hierarchical Systems, *Computer Journal*, 9 (4), 373, 1967.
- Lehmann, U., M. Mohr, T. Schweizer, and J. Rutter, Number size distribution of particulate emissions of heavy-duty engines in real world test cycles, *Atmospheric Environment*, 37 (37), 5247-5259, 2003.
- Lewtas, J., Complex mixtures of air pollutants: characterizing the cancer risk of polycyclic organic matter, *Environmental Health Perspectives*, 100, 211-18, 1993.
- Lieutier-Colas, F., Deposition of particles in the respiratory tract, *Allergie et immunologie*, 33 (2), 59-63, 2001.

- Liu, D.S., M.K. Shih, and W.H. Huang, Measurement and analysis of contact resistance in wafer probe testing, *Microelectronics Reliability*, 47 (7), 1086-1094, 2007.
- Liu, P., P.J. Ziemann, D.B. Kittelson, and P.H. McMurry, Generating particle beams of controlled dimensions and divergence 1: Theory of particle motion in aerodynamic lenses and nozzle expansions, *Aerosol Science & Technology*, 22 (3), 293-313, 1995a.
- Liu, P., P.J. Ziemann, D.B. Kittelson, and P.H. McMurry, Generating particle beams of controlled dimensions and divergence 2: Experimental evaluation of particle motion in aerodynamic lenses and nozzle expansions, *Aerosol Science & Technology*, 22 (3), 314-324, 1995b.
- Mallina, R.V., Rapid single-particle mass spectrometry (RSMS): inlet design and analysis, 1998.
- Marple, V., K. Rubow, G. Ananth, and H.J. Fissan, Micro-orifice uniform deposit impactor, *Journal of Aerosol Science*, 17 (3), 489-94, 1986.
- Marple, V.A., K.L. Rubow, and S.M. Behm, A microorifice uniform deposit impactor (MOUDI): description, calibration, and use, *Aerosol Science and Technology*, 14 (4), 434-46, 1991.
- Mazurek, M., M.C. Masonjones, H.D. Masonjones, L.G. Salmon, G.R. Cass, K.A. Hallock, and M. Leach, Visibility-reducing organic aerosols in the vicinity of Grand Canyon National Park: properties observed by high resolution gas chromatography, *Journal of Geophysical Research, [Atmospheres]*, 102 (D3), 3779-3793, 1997.
- McMurry, P.H., and V.A. Marple, Measurement of sub 3.0- $\mu$ m size-resolved aerosol chemical composition with microorifice uniform deposit impactors (MOUDI), *Proceedings - APCA Annual Meeting, 79th* (Vol. 3), 86/40.4, 15 pp., 1986.
- Morawska, L., W. Hofmann, J. Hitchins-Loveday, C. Swanson, and K. Mengersen, Experimental study of the deposition of combustion aerosols in the human respiratory tract, *Journal of Aerosol Science*, 36 (8), 939-957, 2005.
- Murphy, D.M., A.M. Middlebrook, and M. Warshawsky, Cluster analysis of data from the particle analysis by laser mass spectrometry (PALMS) instrument, *Aerosol Science and Technology*, 37 (4), 382-391, 2003.
- Mushtakova, V.M., V.A. Fomina, and V.V. Rogovin, Toxic Effect of Heavy Metals on Human Blood Neutrophils, *Biology Bulletin (New York, NY, United States)*, 32 (3), 276-278, 2005.

- Nash, D.G., T. Baer, and M.V. Johnston, Aerosol mass spectrometry: An introductory review, *International Journal of Mass Spectrometry*, 258 (1-3), 2-12, 2006.
- Natr, L., Effect of atmospheric CO<sub>2</sub> concentration on the global climate, *Kvasny Prumysl*, 52 (6), 190-191, 2006.
- Nordmeyer, T., and K.A. Prather, Real-Time Measurement Capabilities Using Aerosol Time-of-Flight Mass Spectrometry, *Analytical Chemistry*, 66 (20), 3540-2, 1994.
- Norramit, P., V. Cheevaporn, N. Itoh, and K. Tanaka, Characterization and carcinogenic risk assessment of polycyclic aromatic hydrocarbons in the respirable fraction of airborne particles in the Bangkok metropolitan area, *Journal of Health Science*, 51 (4), 437-446, 2005.
- Oberdorster, G., E. Oberdorster, and J. Oberdorster, Nanotoxicology: an emerging discipline evolving from studies of ultrafine particles, *Environmental Health Perspectives*, 113 (7), 823-839, 2005.
- Oberdorster, G., Z. Sharp, V. Atudorei, A. Elder, R. Gelein, W. Kreyling, and C. Cox, Translocation of inhaled ultrafine particles to the brain, *Inhalation toxicology*, 16 (6-7), 437-45, 2004.
- Owega, S., G.J. Evans, R.E. Jervis, M. Fila, R. D'Souza, and B.-U.-Z. Khan, Long-range sources of Toronto particulate matter (PM<sub>2.5</sub>) identified by Aerosol Laser Ablation Mass Spectrometry (LAMS), *Atmospheric Environment*, 38 (33), 5545-5553, 2004.
- Penttinen, P., K.L. Timonen, P. Tittanen, A. Mirme, J. Ruuskanen, and J. Pekkanen, Ultrafine particles in urban air and respiratory health among adult asthmatics, *European Respiratory Journal*, 17 (3), 428-435, 2001.
- Petrova, D., P. Kostadinova, E. Sokolovski, and I. Dombalov, Greenhouse gases and environment, *Journal of Environmental Protection and Ecology*, 7 (3), 679-684, 2006.
- Petters, M.D., A.J. Prenni, S.M. Kreidenweis, and P.J. DeMott, On Measuring the Critical Diameter of Cloud Condensation Nuclei Using Mobility Selected Aerosol, *Aerosol Science and Technology*, 41 (10), 907-913, 2007.
- Phares, D.J., K.P. Rhoads, A.S. Wexler, D.B. Kane, and M.V. Johnston, Application of the ART-2a algorithm to laser ablation aerosol mass spectrometry of particle standards, *Analytical Chemistry*, 73 (10), 2338-2344, 2001.
- Pope, C.A., Review: Epidemiological basis for particulate air pollution health standards, *Aerosol Science & Technology*, 32 (1), 4-14, 2000.



- Pope, C.A., R.T. Burnett, M.J. Thun, E.E. Calle, D. Krewski, K. Ito, and G.D. Thurston, Lung cancer, cardiopulmonary mortality, and long-term exposure to fine particulate air pollution, *JAMA, the Journal of the American Medical Association*, 287 (9), 1132-1141, 2002.
- Prather, K.A., T. Nordmeyer, and K. Salt, Real-time characterization of individual aerosol particles using time-of-flight mass spectrometry, *Analytical Chemistry*, 66 (9), 1403-7, 1994.
- Pritchard, R.J., A.J. Ghio, J.R. Lehmann, D.W. Winsett, J.S. Tepper, P. Park, M.I. Gilmour, K.L. Dreher, and D.L. Costa, Oxidant generation and lung injury after particulate air pollutant exposure increase with the concentrations of associated metals, *Inhalation Toxicology*, 8 (5), 457-477, 1996.
- Quant, F.R., R.C. Flagan, and K.D. Horton, Implementation of a scanning mobility particle sizer (SMPS), *Journal of Aerosol Science*, 24 (S1), S83-S84, 1995.
- Ramana, M.V., and V. Ramanathan, Abrupt transition from natural to anthropogenic aerosol radiative forcing: Observations at the ABC-Maldives Climate Observatory, *Journal of Geophysical Research-Atmospheres*, 111 (D20), 2006.
- Ramanathan, V., and P.J. Crutzen, New directions: Atmospheric brown "Clouds", *Atmospheric Environment*, 37 (28), 4033-4035, 2003.
- Ramanathan, V., P.J. Crutzen, J.T. Kiehl, and D. Rosenfeld, Atmosphere - Aerosols, climate, and the hydrological cycle, *Science*, 294 (5549), 2119-2124, 2001.
- Rebotier, T.P., and K.A. Prather, Aerosol time-of-flight mass spectrometry data analysis: A benchmark of clustering algorithms, *Analytica Chimica Acta*, 585 (1), 38-54, 2007.
- Reilly, P.T.A., R.A. Gieray, W.B. Whitten, and J.M. Ramsey, Real-time characterization of the organic composition and size of individual diesel engine smoke particles, *Environmental Science and Technology*, 32 (18), 2672-2679, 1998.
- Roelofs, G.J., P. Stier, J. Feichter, E. Vignati, and J. Wilson, Aerosol activation and cloud processing in the global aerosol-climate model ECHAM5-HAM, *Atmospheric Chemistry and Physics*, 6 (9), 2389-2399, 2006.
- Rosenfeld, D., Aerosols, Clouds, and Climate, *Science (Washington, DC, United States)*, 312 (5778), 1323-1324, 2006.
- Schaefer, B., H.W. Georgii, and R. Staubes, Formation and distribution of cloud condensation nuclei in the marine environment, *Journal of Aerosol Science*, 23 (Suppl. 1), S865-S868, 1992.

- Schlesinger, R.B., and F. Cassee, Atmospheric Secondary Inorganic Particulate Matter: The Toxicological Perspective as a Basis for Health Effects Risk Assessment, *Inhalation Toxicology*, 15 (3), 197-235, 2003.
- Seinfeld, J.H., and S.N. Pandis, *Atmospheric Chemistry and Physics: From Air Pollution to Climate Change*, 1326 pp., John Wiley & Sons, 1998.
- Shi, J.P., R.M. Harrison, and F. Brear, Particle size distribution from a modern heavy duty diesel engine, *Science of the Total Environment*, 235 (1-3), 305-317, 1999a.
- Shi, J.P., A.A. Khan, and R.M. Harrison, Measurements of ultrafine particle concentration and size distribution in the urban atmosphere, *Science of the Total Environment*, 235 (1-3), 51-64, 1999b.
- Shields, L.G., D.T. Suess, and K.A. Prather, Determination of single particle mass spectral signatures from heavy duty diesel vehicle emissions for PM<sub>2.5</sub> source apportionment, *Atmospheric Environment*, 41 (18), 3841-3852, 2007.
- Shulk, B.F., and Editor, *Greenhouse Gases and Their Impact*, 182 pp. pp., 2007.
- Silva, P.J., D.Y. Liu, C.A. Noble, and K.A. Prather, Size and chemical characterization of individual particles resulting from biomass burning of local Southern California species, *Environmental Science & Technology*, 33 (18), 3068-3076, 1999.
- Singh, M., C. Misra, and C. Sioutas, Field evaluation of a personal cascade impactor sampler (PCIS), *Atmospheric Environment*, 37 (34), 4781-4793, 2003.
- Sodeman, D.A., S.M. Toner, and K.A. Prather, Determination of single particle mass spectral signatures from light duty vehicle emissions, *Environmental Science & Technology*, 39 (12), 4569-4580, 2005.
- Song, X.H., N.M. Faber, P.K. Hopke, D.T. Suess, K.A. Prather, J.J. Schauer, and G.R. Cass, Source apportionment of gasoline and diesel by multivariate calibration based on single particle mass spectral data, *Analytica Chimica Acta*, 446 (1-2), 329-343, 2001.
- Song, X.H., P.K. Hopke, D.P. Fergenson, and K.A. Prather, Classification of single particles analyzed by ATOFMS using an artificial neural network, ART-2A, *Analytical Chemistry*, 71(4), 860-865, 1999.
- Stephens, W.E., A pulsed mass spectrometer with time dispersion, *Physical Review*, 69, 691, 1946.

- Su, Y., M.F. Sipin, H. Furutani, and K.A. Prather, Development and characterization of an aerosol time-of-flight mass spectrometer with increased detection efficiency, *Analytical Chemistry*, 76 (3), 712-719, 2004.
- Svane, M., M. Hagstroem, and J. Pettersson, Chemical Analysis of Individual Alkali-Containing Aerosol Particles: Design and Performance of a Surface Ionization Particle Beam Mass Spectrometer, *Aerosol Science and Technology*, 38 (7), 655-663, 2004.
- Tager, I.B., Health effects of aerosols: mechanisms and epidemiology, *Aerosols Handbook*, 619-695, 2005.
- Tan, P.V., O. Malpica, G.J. Evans, S. Owega, and M.S. Fila, Chemically-assigned classification of aerosol mass spectra, *Journal of the American Society for Mass Spectrometry*, 13 (7), 826-38, 2002.
- Teller, A., and Z. Levin, The effects of aerosols on precipitation and dimensions of subtropical clouds: a sensitivity study using a numerical cloud model, *Atmospheric Chemistry and Physics*, 6 (1), 67-80, 2006.
- Thomson, D.S., M.E. Schein, and D.M. Murphy, Particle analysis by laser mass spectrometry WB-57F instrument overview, *Aerosol Science and Technology*, 33 (1-2), 153-169, 2000.
- Tobias, H.J., D.E. Beving, P.J. Ziemann, H. Sakurai, M. Zuk, P.H. McMurry, D. Zarling, R. Waytulonis, and D.B. Kittelson, Chemical analysis of diesel engine nanoparticles using a nano-DMA/thermal desorption particle beam mass spectrometer, *Environmental Science and Technology*, 35 (11), 2233-2243, 2001.
- Tobias, H.J., P.M. Kooiman, K.S. Docherty, and P.J. Ziemann, Real-time chemical analysis of organic aerosols using a thermal desorption particle beam mass spectrometer, *Aerosol Science and Technology*, 33 (1-2), 170-190, 2000.
- Tombach, I., and P. Brewer, Natural background visibility and regional haze goals in the southeastern United States, *Journal of the Air & Waste Management Association*, 55 (11), 1600-1620, 2005.
- Tomlinson, J.M., R. Li, and D.R. Collins, Physical and chemical properties of the aerosol within the southeastern Pacific marine boundary layer, *Journal of Geophysical Research, [Atmospheres]*, 112 (D12), D12211/1-D12211/13, 2007.
- Toner, S.M., D.A. Sodeman, and K.A. Prather, Single particle characterization of ultrafine and accumulation mode particles from heavy duty diesel vehicles using aerosol time-of-flight mass spectrometry, *Environmental Science & Technology*, 40 (12), 3912-3921, 2006.

- Toscano, C.D., and T.R. Guilarte, Lead neurotoxicity: From exposure to molecular effects, *Brain Research Reviews*, 49 (3), 529-554, 2005.
- Uphoff, A., and J. Grotemeyer, The secrets of time-of-flight mass spectrometry revealed, *European Journal of Mass Spectrometry*, 9 (3), 151-164, 2003.
- Wang, S.C., and R.C. Flagan, Scanning electrical mobility spectrometer, *Aerosol Science and Technology*, 13 (2), 230-40, 1990.
- Ward, J.H., Hierarchical grouping to optimize an objective function, *Journal of the American Statistical Association*, 58 (301), 236, 1963.
- Weickhardt, C., F. Moritz, and J. Grotemeyer, Time-of-flight mass spectrometry: state-of-the-art in chemical analysis and molecular science, *Mass Spectrometry Reviews*, 15 (3), 139-162, 1997.
- Wenzel, R.J., and K.A. Prather, Improvements in ion signal reproducibility obtained using a homogeneous laser beam for on-line laser desorption/ionization of single particles, *Rapid Communications in Mass Spectrometry*, 18 (13), 1525-1533, 2004.
- White, W.H., and P.T. Roberts, On the nature and origins of visibility-reducing aerosols in the Los Angeles air basin, *Advances in Environmental Science and Technology*, 10 (Character Origins Smog Aerosols), 715-53, 1980.
- Wienke, D., Y. Xie, and P.K. Hopke, An adaptive resonance theory based artificial neural network (ART-2a) for rapid identification of airborne particle shapes from their scanning electron microscopy images, *Chemometrics & Intelligent Laboratory Systems*, 25 (2), 367-387, 1994.
- Wollny, A.G., Development of a bipolar time-of-flight mass spectrometer for the analysis of the chemical composition of single aerosol particles, pp. i-ix, 1-119, Inst. fuer Chem. und Dynamik der Geosphaere Inst. I: Stratosphaere, Bonn Univ., Bonn, Germany, 2003.
- Xie, Y., P.K. Hopke, and D. Wienke, Airborne particle classification with a combination of chemical composition and shape index utilizing an adaptive resonance artificial neural network, *Environmental Science & Technology*, 28 (11), 1921-1928, 1994.
- Yeh, H.-C., R.G. Cuddihy, R.F. Phalen, and I.Y. Chang, Comparisons of calculated respiratory tract deposition of particles based on the proposed NCRP model and the new ICRP66 model, *Aerosol Science and Technology*, 25 (2), 134-140, 1996.
- Yu, H., Y.J. Kaufman, M. Chin, G. Feingold, L.A. Remer, T.L. Anderson, Y. Balkanski, N. Bellouin, O. Boucher, S. Christopher, P. DeCola, R. Kahn, D. Koch, N. Loeb,

- M.S. Reddy, M. Schulz, T. Takemura, and M. Zhou, A review of measurement-based assessments of the aerosol direct radiative effect and forcing, *Atmospheric Chemistry and Physics*, 6 (3), 613-666, 2006.
- Zhang, K.M., A.S. Wexler, D.A. Niemeier, Y.F. Zhu, W.C. Hinds, and C. Sioutas, Evolution of particle number distribution near roadways. Part III: Traffic analysis and on-road size resolved particulate emission factors, *Atmospheric Environment*, 39 (22), 4155-4166, 2005.
- Zhao, Y., K.J. Bein, A.S. Wexler, C. Misra, P.M. Fine, and C. Sioutas, Field evaluation of the versatile aerosol concentration enrichment system (VACES) particle concentrator coupled to the rapid single-particle mass spectrometer (RSMS-3), *Journal of Geophysical Research, [Atmospheres]*, 110 (D7), D07S02/1-D07S02/11, 2005.

# **2 Single particle analysis of a Minuteman SR19 II rocket motor exhaust plume using Aerosol Time-of-Flight Mass Spectrometry**

## **2.1 Synopsis**

Using aerosol time-of-flight mass spectrometry (ATOFMS), single particle analysis of a static fired Minuteman SR19 II rocket motor exhaust plume was performed at Hill Air Force Base in Utah. Three major particle types were measured in the rocket exhaust and account for 63% of the particles sampled. The top class has positive ions due to aluminum from the rocket fuel/combustion catalyst, tungsten from abrasion to the rocket nozzle, as well as signals from other trace metals. The negative ions consisted of chlorine and chlorine-metal clusters from the fuel oxidizer, as well as aluminum oxide, and tungsten oxides. The second and third most abundant particle types exhibited ion peaks due to elemental carbon (EC), organic carbon (OC), and amines and are most likely from the combustion of the Carboxyl Terminated Poly Butadiene (CTPB) polymer component of the fuel. Suspended soil particles were found to account for 25% of the particles sampled. To distinguish which spectra obtained during the static rocket firing were from suspended soil; samples of soil within the rocket exhaust wake zone and outside the zone were analyzed and consisted of particles in the supermicron size range. This experiment was part of ongoing ATOFMS source characterization work with the

goal of obtaining mass spectral signatures for solid rocket motors (SRMs) and to better understand the emissions from defense operations and how they may impact their local environment.

## 2.2 Introduction

Potentially reactive gasses and particles from solid rocket motor (SRM) combustion emissions and their effects on the environment have been studied since the 1970's. The focus of such studies has been on gas-phase hydrogen chloride (HCl) and other chlorine compounds as well as bare alumina ( $\text{Al}_2\text{O}_3$ ) particles that are produced by the rocket combustion and the effects they could have on stratospheric ozone [Cofer *et al.*, 1989]. While the release of such emissions is on the order of several tons per SRM per firing [Brady *et al.*, 1994], they presently are not considered a significant threat to worldwide stratospheric ozone depletion [Hanning-Lee *et al.*, 1996; World Meteorological Organization, 1999]. Lab based studies of the gas-phase chlorine species on alumina particles have shown to increase the production of reactive chlorine ( $\text{Cl}_2$ ) under stratospheric conditions. However, these results were considered to be of minor significance in the local region of reaction and negligible for the entire stratosphere [Bennett *et al.*, 1997; Molina *et al.*, 1997].

The environmental impacts of static fired SRMs have also been studied. With this being the primary method for SRM testing and disposal, there is a sizable amount of chlorine species and alumina particles injected into the troposphere per SRM firing. Local areas of static firings exhibit high gas and particle phase concentrations immediately following a firing, but return to pre-firing levels within a few hours due to

dispersion/diffusion of the gasses and particles as well as settling of larger particles [Bennett *et al.*, 1997]. While it has been reported that the release of HCl from the exhaust wake can result in increased levels of local acid rain [Aguesse, 1997; Anderson and Keller, 1990; Nadler, 1976], the effect that the alumina particles may have on these local environments is still not completely understood. The health effects due to the exposure to airborne alumina has been studied as well [Benke *et al.*, 1998; Clarke, 1956; Dinman, 1988; Fritschi *et al.*, 2001]. This is particularly important for residents near (or downwind) from such testing facilities since they will be exposed to the transported particles. While it has been determined that bare alumina itself poses no significant toxic health implications, they can contribute to rhinitis and pulmonary fibrosis [Benke *et al.*, 1998; Clarke, 1956; Dinman, 1988; Fritschi *et al.*, 2001]. There have also been findings that indicate there is an increased level of morbidity in mice and rats with increased HCl concentrations on respirated alumina particles [Wohlschlager *et al.*, 1975]. Additionally, it is known that particles emitted in the wake of SRMs are primarily in the ultrafine (<100 nm) and submicron (100 – 1000 nm) size modes [Nadler, 1976; Ross *et al.*, 1999; Schmid *et al.*, 2003]. Particles in this size range are respirable and can cause adverse health effects [Brown *et al.*, 2002; Donaldson *et al.*, 2001; Englert, 2004; Lighty *et al.*, 2000]. However, the actual types of particles emitted from SRMs have not been significantly characterized in health studies.

The objective of the measurements performed in this study was to obtain complete size and chemical composition of SRM exhaust wake particles at the single particle level using ATOFMS and to determine whether it was possible to distinguish such emissions from local soils and dust suspended from the blast. Results from single



particle measurements made with another single particle mass spectrometer, Particle Analysis by Laser Mass Spectrometry (PALMS) have been reported for SRM emissions [Cziczo *et al.*, 2002]. However, the design of the PALMS instrument does not provide accurate sizing information of each particle or the complete chemical composition (both positive and negative spectra) of each particle [Thomson *et al.*, 2000]. The PALMS instrument was used to examine Athena II and Space Shuttle SRM wakes in the upper troposphere. The fuel of the Athena II SRM [Andolz *et al.*, 1998] is similar to that used in the Minuteman SR19 II [Callaghan, 2002] to be used as a basis of comparison between the two studies. Using the ATOFMS instrument, the size and complete chemical composition for both positive and negative ions for each particle can be obtained in real time. The results obtained herein will be compared with those obtained with the PALMS system. It is expected that there will be ion and fragmentation differences seen in the mass spectra due to the different rocket types as well as instrumental differences between the ATOFMS and PALMS. The most notable difference is the desorption/ionization laser used in each system. The PALMS system uses a 193 nm excimer laser (operating at 2 mJ/pulse) [Thomson *et al.*, 2000] and the ATOFMS uses a Nd:YAG laser at 266 nm (operating at 1 mJ/pulse).

## 2.3 Experimental

Exhaust emissions from a Minuteman SR19 stage II rocket motor were collected and analyzed on September 24, 2002 at the static rocket testing area at Hill Air Force Base in Utah. The basic propellant ingredients of this particular motor are ammonium perchlorate oxidizer (73%), aluminum powder (15%), and a binder composed of the

CTPB polymer (12%) [Callaghan, 2002]. The SR19 II rocket motor case is made of titanium and is 52 inches in diameter by 122.5 inches in length [Callaghan, 2002].

In order to ensure the safety of the ATOFMS instruments, they were not located at the rocket test pad where emissions could have been sampled ideally in real-time. Instead, a 300-L stainless steel vessel with one-inch diameter stainless steel sampling line was used to collect the sample. From the front of the vessel (facing towards the rocket) came the 1-inch diameter stainless steel sampling line that stretched 40-feet along the ground, and then 18-feet into the air secured to a large metal “A”-frame that was staked to the ground. Connected to the back of the vessel were two rotary vane pumps drawing a combined flow of 295-lpm which were controlled by an on/off “threshold” trigger on a DustTrak (TSI) provided by the University of Utah.

When the rocket started firing, particle concentrations in the air instantly increased above a set threshold level on the DustTrak, which in turn triggered a power switch for the pumps on the collection chamber. The sampling interval on the DustTrak was set to two second intervals so the trigger would react quickly to the change in concentration. Since the background particle concentration level was at  $0.001 \text{ mg/m}^3$  in this location, it was determined that setting the trigger level at  $0.1 \text{ mg/m}^3$  would not falsely trigger the sampling system by anything other than the rocket wake, as there was no wind, and very little vehicle traffic. When the rocket began firing, the particle concentration rose to over  $246 \text{ mg/m}^3$  (well above the  $100 \text{ mg/m}^3$  maximum limit for the DustTrak) within the first couple of seconds. The particle concentration remained above  $100 \text{ mg/m}^3$  for the first 56 seconds of the 60 second long blast. Once the rocket stopped firing, particle concentrations decreased below the threshold level set on the DustTrak,

**Table 2.1** Soil samples collected from Hill Air Force Base, Utah rocket testing area

<b>Soil Sample</b>	<b>Soil Sample Location</b>	<b>Comments</b>
1	15 meters down wake from sampling chamber	Before Firing
2	South of chamber on access road (on fringe of rocket wake zone)	Before Firing
3	91 meters from rocket (by sampling chamber)	Before Firing
4	Just beyond cement rocket blast pad (36.5 meters from rocket)	Before Firing
5	From observation site 0.64 kilometers from rocket	“Clean” sample
6	From entrance road to HAFB (4-5 kilometers away from site)	“Clean” sample
7	Just beyond cement rocket blast pad (36.5 meters from rocket)	After Firing
8	91 meters from rocket (by sampling chamber)	After Firing

which shut off the power to the pumps. The sample then remained static for 25 minutes to allow the military personnel time to perform a safety check, after which the sample chamber was retrieved. A ball valve for each pump port and the sample port on the chamber were closed and the chamber was taken to the ATOFMS instruments for analysis. The total time after sample collection until sampling began off the chamber was about 30 minutes.

For this study, two ATOFMS instruments were used. The first instrument, with the standard nozzle aerosol inlet and interface can reliably size and chemically characterize particles from 200 to 3000 nm as described in the literature [*Gard et al.*, 1997; *Prather et al.*, 1994]. The second instrument was fitted with a recently developed ultrafine (UF) interface (aerodynamic lens) that can aerodynamically size and chemically characterize particles between 50 and 300 nm [*Su et al.*, 2004]. The ATOFMS instruments along with a Scanning Mobility Particle Sizer (SMPS) (TSI Model 3936L10) and an Aerodynamic Particle Sizer (APS) (TSI Model 3321) sampled off the chamber for just over two hours to obtain complete size and composition information from the exhaust plume of the Solid Rocket Motor.

To distinguish between the soil in the area and rocket emissions, a number of soil samples were collected before and after the rocket blast in the area where the rocket plume traveled over and areas far away from the blast site. Table 2.1 describes the soil samples collected. The soil samples were analyzed and the spectra from the rocket emissions were sorted to segregate particles actually from the rocket from the soil particles suspended by the blast. Due to the fact that the sampling line was knocked down during the test, the ATOFMS data also included local soil/dust that entered the

sampling line during the firing event. Therefore, it was important that the soil/dust samples were collected and analyzed for comparison. The data from the rocket firing and the soil samples collected were imported into Matlab (version 6.1.0.450 Release 12.1) using the YAADA-v1.10 aerosol analysis tool package ([www.yaada.org](http://www.yaada.org)) and analyzed using the ART-2a algorithm [Allen, 2006; Song *et al.*, 1999]. The ART-2a parameters used were: vigilance factor = 0.85, learning rate = 0.05, and 20 iterations.

## **2.4 Results and Discussion**

### **2.4.1 Particle size distributions for the SRM wake and soil samples**

Figure 2.1A shows the combined size distribution for the UF-ATOFMS (50 – 300 nm) and ATOFMS (200 – 3000 nm) as well as for the SMPS and APS data. The SMPS mobility diameter was not corrected since the particles were likely spherical from the vaporized water that was in the rocket blast (assuming the particles were hydrophilic). Water is sprayed onto the test area to cool the test pad and rocket mounts and is instantly vaporized within the rocket wake. As seen in Figure 2.1A, the size distribution of the rocket wake sample shows a peak at 200 nm, with the majority of the particles sized between 100 and 400 nm. The particles sized by the ATOFMS correlate well with the sizing data obtained with the SMPS and APS. The SMPS shows a particle size peak ranging from 100 to 400 nm and the APS shows a peak at 1000 nm. This observed size range agrees with previous measurements of solid rocket exhaust by Cofer *et al.*, where they observed a bimodal size range with peaks at <300 nm and 2000 nm using a scanning electron microscope (SEM) of particles collected on a Teflon filter [Cofer *et al.*, 1987]. However, since the particles were allowed to soak in the collection chamber 30 min

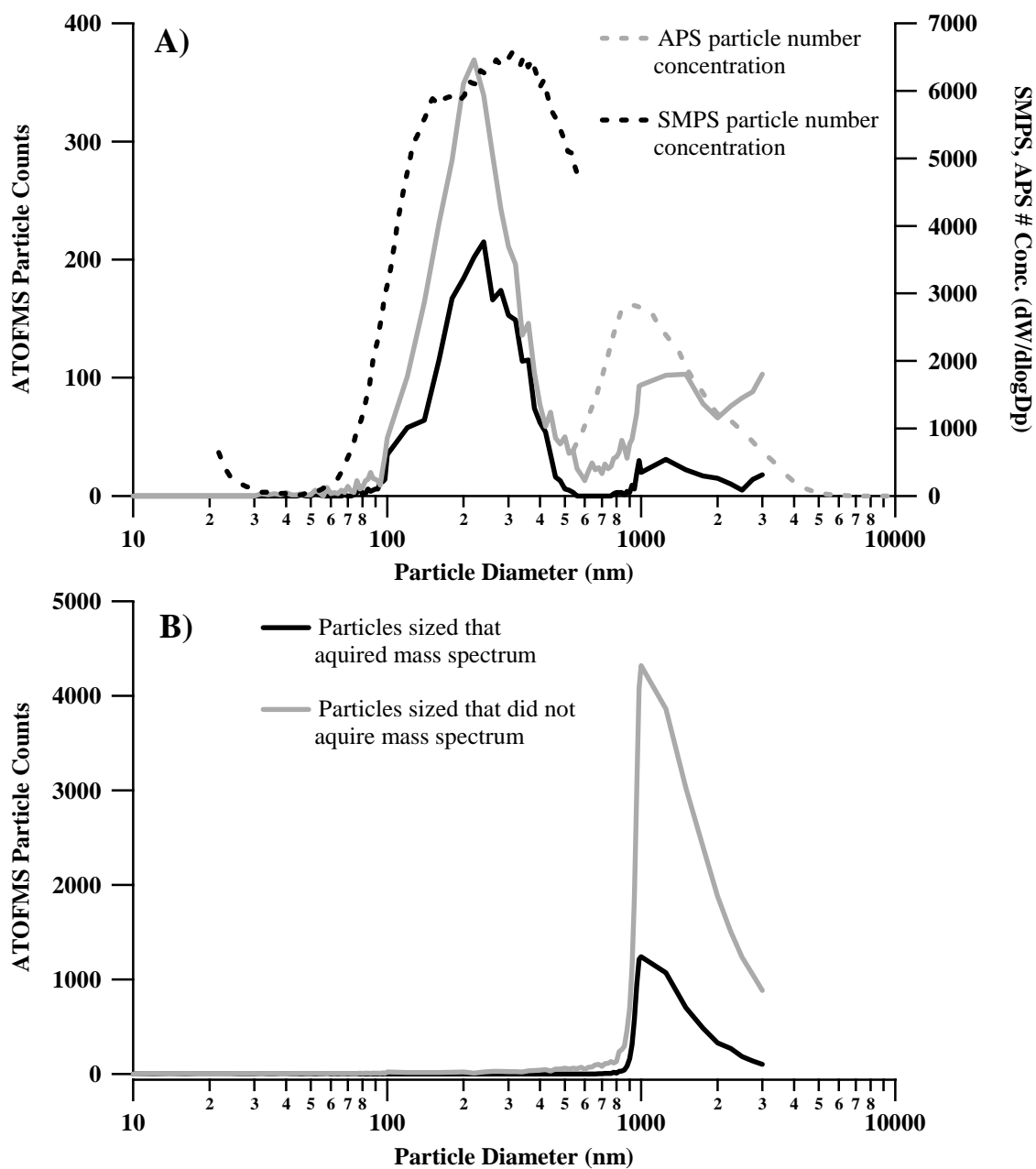














**Figure 2.1** A) Particle size distribution of the Minuteman rocket wake sample. B) Particle size distribution of re-suspended soil samples.

before sampling, it is very likely that these sizes were most likely achieved from smaller sizes that agglomerated and grew over time. The peak observed in the supermicron mode (ranging from 1300 to 2300 nm) can be attributed to suspended soil from the rocket blast and were seen primarily with the standard inlet ATOFMS instrument. Figure 2.1B, shows the size distribution of the resuspended soil samples collected around the testing area. Particles generated from the soil samples were seen most favorably by the standard inlet ATOFMS instrument due to mainly large particles being formed by soil suspension. It is very clear, looking at the particle size range of the resuspended soil samples that the majority of particles seen in the rocket wake sample are from the rocket emissions and not from suspended soil. Additionally, the submicron particles are due to combustion of the SRM fuel while the supermicron particles are mechanically resuspended soil.

#### **2.4.2 SRM exhaust wake particle classes**

Upon analysis of the rocket wake data using the ART2a algorithm, the particle types for the rocket were sorted into 12 classes. Figure 2.2 shows the statistical composition of the rocket wake sample and lists the particle class types in order of abundance. The top three classes make up 63% of the total particles sampled. The fourth and fifth classes seen in the rocket wake match two of the classes from the resuspended soil samples (the top and fourth soil classes), and account for another 21% of particles seen in the rocket wake. The top rocket class (27% of the total) consists of particles with positive ion spectra containing a large peak from  $\text{Al}^+$ , and less intense peaks of  $\text{Na}^+$ ,  $\text{K}^+$ ,  $\text{W}^+$ ,  $\text{Li}^+$ ,  $\text{Fe}^+$ , and  $\text{WO}^+$ . Negative ion spectra from the top rocket class contain a large  $\text{Cl}^-$  peak, as well as peaks for  $\text{AlO}^-$ ,  $\text{Cl}^-$  - metal clusters ( $\text{NaCl}_2^-$ ,  $\text{KCl}_2^-$ ,  $\text{Na}_2\text{Cl}_3^-$ , and  $\text{ZnCl}_3^-$ )

- 1)   $\text{Al}^+$ ,  $\text{Na}^+$ ,  $\text{K}^+$ ,  $\text{W}^+$ ,  $\text{Fe}^+$ ,  $\text{Li}^+$ ,  $\text{WO}^+$ ;  $\text{Cl}^-$ ,  $\text{AlO}^-$ ,  $\text{Cl}^-$ -metal clusters,  $\text{WO}_x^-$  clusters
- 2)   $\text{Al}^+$ , OC, EC, Amines,  $\text{Pb}^+$ ;  $\text{HSO}_4^-$ ,  $\text{AlO}^-$ ,  $\text{PO}_4^-$ ,  $\text{CNO}^-$ ,  $\text{NO}_3^-$ , -187
- 3)  OC, Amines; No negatives
- 4)  **Matches top soil cluster**,  $\text{K}^+$  rich,  $\text{Na}^+$ ,  $\text{Fe}^+$ ,  $\text{Mg}^+$ ,  $\text{Li}^+$ ,  $\text{Al}^+$ , [No (+178,177,175,179)]; Silicates,  $\text{CNO}^-$ ,  $\text{AlO}^-$ ,  $\text{Cl}^-$ ,  $\text{CN}^-$
- 5)  **Matches 4th soil cluster**,  $\text{K}^+$ ,  $\text{Na}^+$ ,  $\text{Li}^+$ ,  $\text{Mg}^+$ ,  $\text{Al}^+$ ;  $\text{Cl}^-$ ,  $\text{OH}^-$ ,  $\text{CN}^-$ ,  $\text{SiO}_3^-$ ,  $\text{HSiO}_3^-$
- 6)  EC, OC/Amines,  $\text{Pb}^+$ ;  $\text{HSO}_4^-$ ,  $\text{NO}_3^-$ ,  $\text{PO}_3^-$ ,  $\text{PO}_4^-$ , -187
- 7)  Soil type with rocket coating
- 8)  EC, OC/Amines;  $\text{PO}_4^-$ ,  $\text{HSO}_4^-$ ,  $\text{NO}_3^-$ ,  $\text{CNO}^-$
- 9)   $\text{Ca}^+$ , OC/EC;  $\text{CNO}^-$ ,  $\text{PO}_3^-$ ,  $\text{PO}_4^-$ ,  $\text{HSO}_4^-$ ,  $\text{SO}_3^-$
- 10)   $\text{Al}^+$ ;  $\text{AlO}^-$ ,  $\text{O}^-$ ,  $\text{OH}^-$  (Supermicron mode only)
- 11)  Soil type with big  $\text{Pb}^+$ ,  $\text{Cu}^+$
- 12)  Unclassified

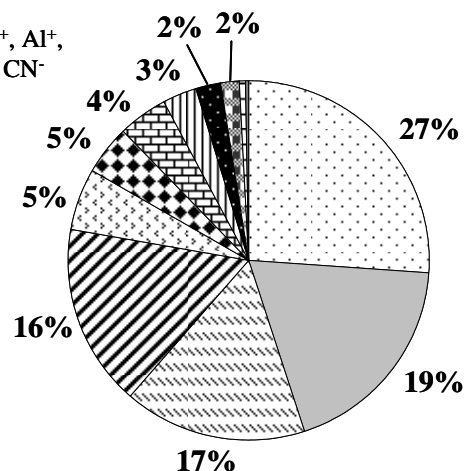


**Figure 2.2** Statistical composition of the Minuteman rocket wake based on ART-2a results of ATOFMS data.



and  $\text{WO}_x^-$  clusters (with  $x = 3, 4$ , and  $5$ ). The tungsten comes from the rocket exhaust nozzle [Gordon and Brown, 1963; Neiman *et al.*, 1961]. During the rocket firing, the alumina particles from the propellant erode the tungsten exhaust nozzle. Figure 2.3A shows a representative spectrum for the top rocket class.

The second rocket particle class makes up about 19% of the total particles sampled. This type has positive ion spectra commonly associated with organic carbon (OC), elemental carbon (EC) ( $m/z$   $^{+12}$ , 24, 36), and amines. The large peak at  $m/z$   $^{+27}$  is most likely from a combination of aluminum and organic carbon. The OC and EC detected on particles is most likely from the combustion of the CTPB polymer component of the fuel. The spectra of this type also show the presence of lead. The negative ion spectra for this class consist of  $\text{AlO}^-$ ,  $\text{HSO}_4^-$ ,  $\text{NO}_3^-$ ,  $\text{PO}_4^-$ ,  $\text{CNO}^-$  and peaks at  $m/z$   $^{-106}$  and  $^{-187}$ . A representative spectrum for the second rocket particle class is shown in Figure 2.3B. The third rocket particle class, making up about 17% of the total, consists of positive spectra attributed to particles containing OC ( $m/z$   $^{+27}$ , 37) and amines ( $m/z$   $^{+58}$ , 86, 118). There were no negative spectra obtained for the particles making up this class.

The fourth, fifth, seventh, and eleventh classes are associated with suspended soil and make up about 25% of the total particles detected. The fourth and fifth classes directly resemble spectra obtained with the soil samples, while the seventh class resembles the same soil samples, but has metal-chloride and tungsten peaks that are likely coatings from the rocket exhaust particles. The sixth class has ion peaks that resemble those in the second class; however, there is no distinct peak due to aluminum, nor a peak for  $\text{CNO}^-$  as detected in the second class. The eighth class is also similar to the second

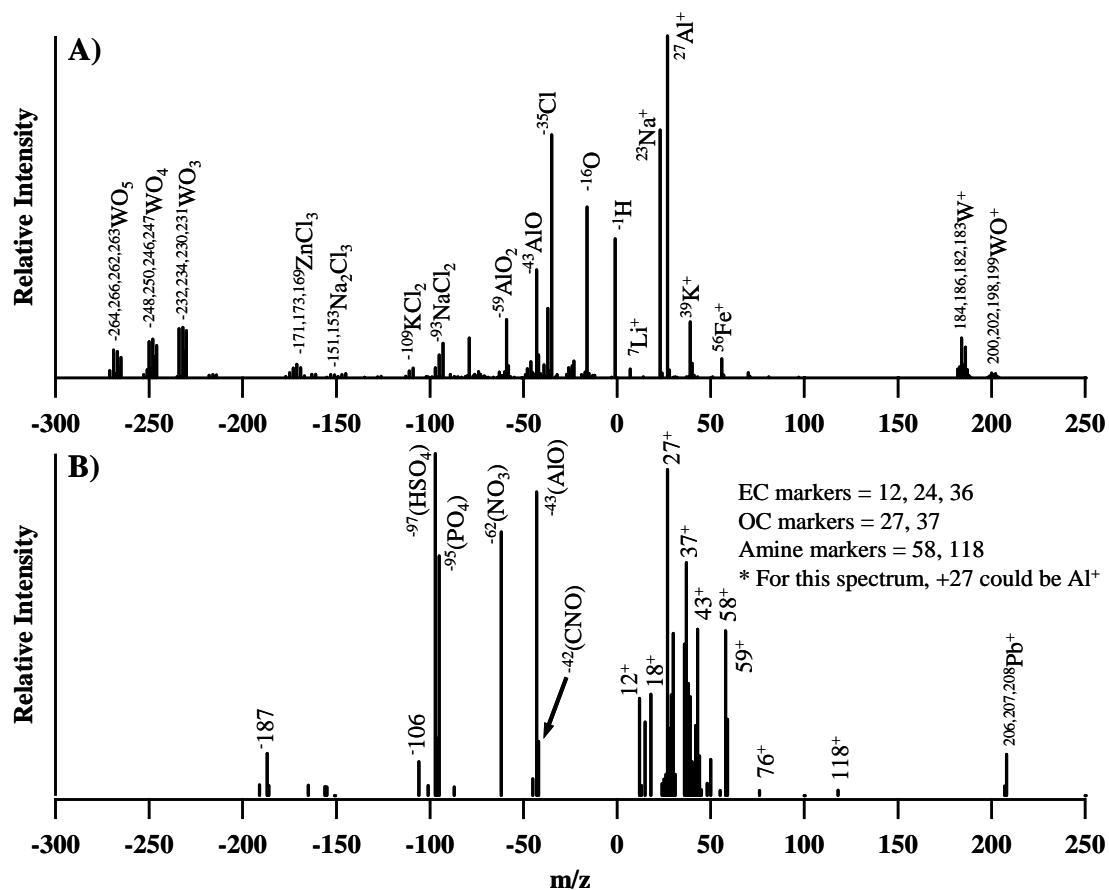


**Figure 2.3** A) Representative spectrum for the top ART-2a class from the Minuteman rocket wake. B) Representative spectrum for EC/OC containing class from the Minuteman rocket wake.

and sixth classes, but does not show the presence of lead. The ninth class is unique to the others in that it shows OC and EC peaks and a large ion peak for calcium in the positive ion mass spectra, as well as phosphate and sulfate ions in the negative ion mass spectra. The mass spectra for the ninth class is typical of vehicle emissions [Shields *et al.*, 2007; Sodeman *et al.*, 2005; Toner *et al.*, 2006] and are probably from the military vehicles that occupied the site just preceding and following the rocket firing. Lastly, the tenth class contains particles that were detected only in the supermicron mode and have peaks attributed to alumina particles.

### 2.4.3 Resuspended soil sample particle classes

Since the static rocket firing suspends a significant amount of soil into the air, soil samples were collected prior to and following the blast. The soil samples (Table 2.1) were resuspended in the lab and the data was analyzed using the same ART-2a parameters as used with the rocket data and resulted in nine different ART-2a classes. Figure 2.4A shows a comparison of the nine ART-2a classes for the eight different soil samples collected. Since the soil samples have similar compositions, their average was taken and compared to the ART-2a classes observed from the rocket wake. Figure 2.4B shows the statistical composition of the average of the soil samples and a brief description of each class (in order of abundance). The top two soil classes alone make up 66% of the total ART-2a soil types and match the soil types seen within the rocket wake.

Figure 2.5A shows a representative spectrum for the top soil particle class which represents 48% of the total soil particles. Positive spectra show a large peak for  $K^+$ , with less intense peaks for  $Na^+$ ,  $Fe^+$ ,  $Ti^+$ ,  $TiO^+$ ,  $Mg^+$ ,  $Al^+$ ,  $Li^+$  and a cluster at  $m/z^+178, 177$ ,

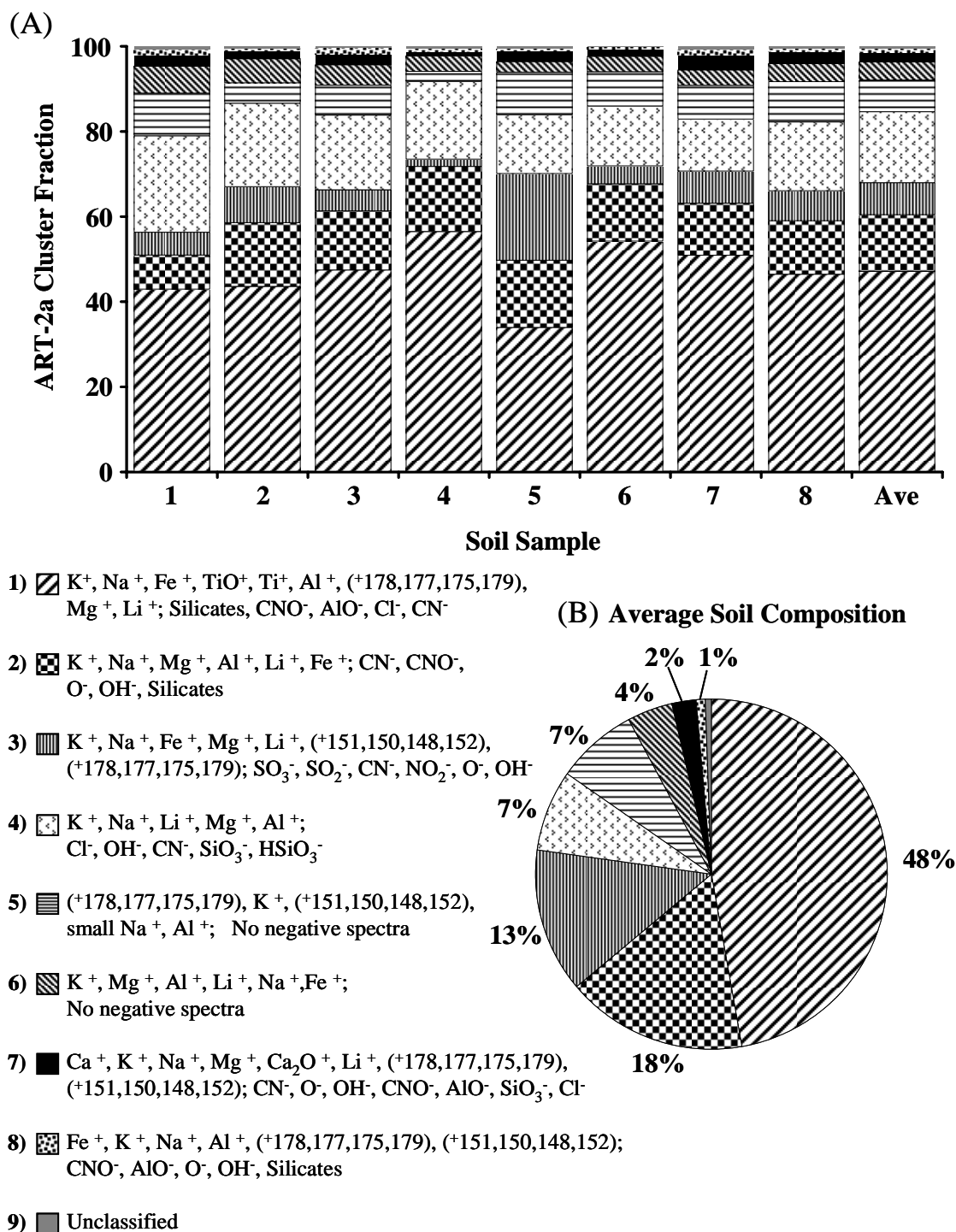


**Figure 2.4** A) Comparison of the re-suspended soil sample statistical compositions based on ART-2a results. B) Average statistical composition of the HAFB re-suspended soil samples.

175, 179 (listed in order of peak intensity). It is difficult to identify the composition of the ions at  $m/z$  <sup>+</sup>178, 177, 175, 179. The third soil class has peaks at  $m/z$  <sup>+</sup>151, 150, 148 and 152 (in order of abundance) which follow the same isotopic patterns and are all  $m/z$  27 less than the respective corresponding peaks at  $m/z$  <sup>+</sup>178, 177, 175, 179). There are many species which could account for the difference in  $m/z$  27 for this kind of particle class, including aluminum or HCN. Negative spectra for the top soil class consist of silicates ( $\text{SiO}_2^-$ ,  $\text{SiO}_3^-$ ,  $\text{HSiO}_3^-$ ,  $\text{HSi}_2\text{O}_5^-$ ),  $\text{OH}^-$ ,  $\text{CN}^-$ ,  $\text{CNO}^-$ ,  $\text{NO}_3^-$ ,  $\text{AlO}^-$  and  $\text{Cl}^-$ .

Figure 2.5B shows the spectrum for the second most abundant soil sample type. The second soil particle class makes up 18% of the soil particles and differs from the first class primarily by not containing the high mass ( $m/z$  <sup>+</sup>178, 177, 175, 179) peaks in the positive ions. The positive ions also have less intense peaks for iron and titanium. In the negative ion spectra, there is no peak for  $\text{HSi}_2\text{O}_5^-$  and the peaks for  $\text{SiO}_2^-$ ,  $\text{SiO}_3^-$ , and  $\text{AlO}^-$  are not as intense as in the top class. The fourth and sixth soil particle classes have similar spectra to the second class and contribute to 7% and 4% of the total soil particles, respectively. The difference for the fourth class is that it does not have any iron or titanium in it, nor does it contain peaks for  $\text{CNO}^-$  or  $\text{AlO}^-$ . Additionally, the fourth class has a very intense peak for  $\text{Cl}^-$  in the negative ions, where  $\text{Cl}^-$  is not present in the second soil class. The difference between the sixth soil particle class and the second is that the sixth class does not yield any negative ion spectra. As with the second class, the peak for  $\text{K}^+$  was the most intense in the positive spectra, but the order of intensities for  $\text{Mg}^+$ ,  $\text{Al}^+$ ,  $\text{Li}^+$ ,  $\text{Na}^+$ , and  $\text{Fe}^+$  are different.

The third most abundant resuspended soil particle type makes up 13% of the total particles detected in the soil samples and has ion peaks for  $\text{K}^+$ ,  $\text{Na}^+$ ,  $\text{Fe}^+$ ,  $\text{Mg}^+$ ,  $\text{Li}^+$ , and

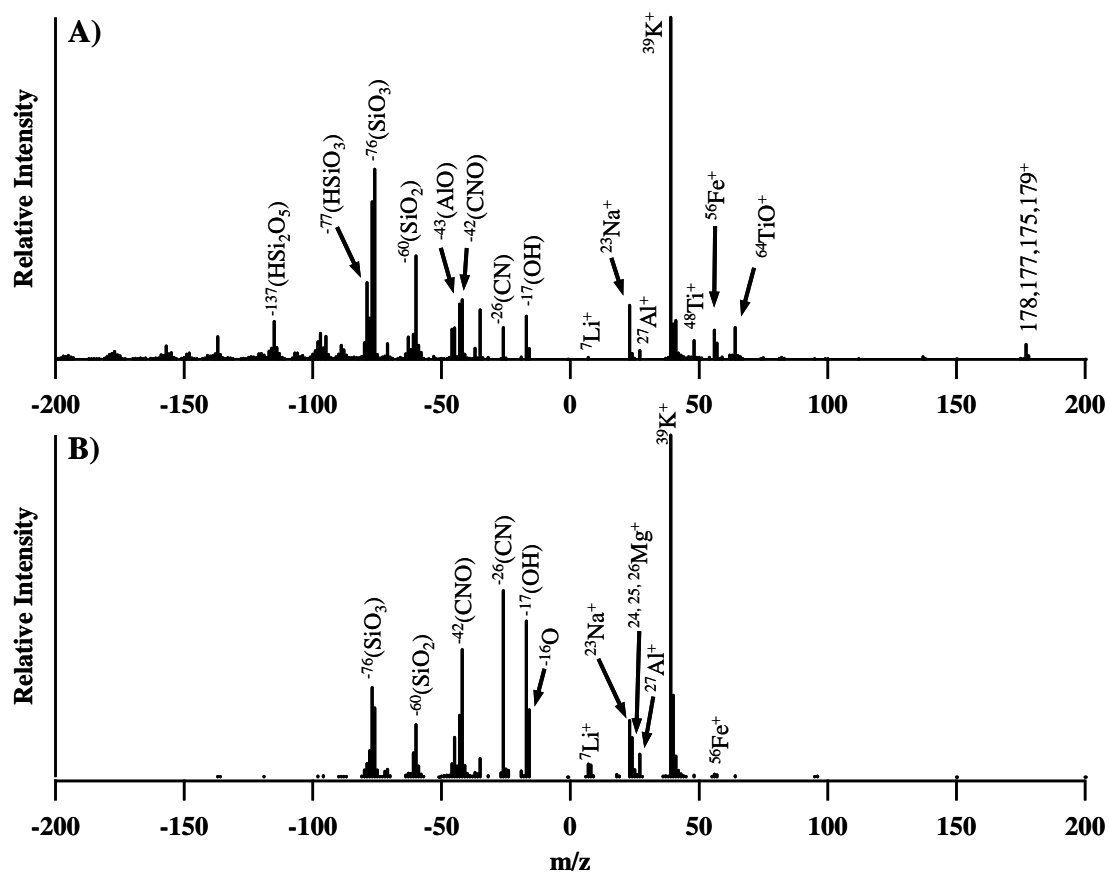


**Figure 2.5** A) Representative spectrum for the top soil particle class based on ART-2a results. B) Representative spectrum of the 2<sup>nd</sup> soil particle class based on ART-2a results.

clusters at  $m/z$  <sup>+</sup>178, 177, 175, 179, and  $m/z$  <sup>+</sup>151, 150, 148, 152 (listed in order of their relative intensities) for the positive spectra. The negative spectra have peaks for  $\text{SO}_3^-$ ,  $\text{SO}_2^-$ ,  $\text{CN}^-$ ,  $\text{NO}_2^-$ ,  $\text{O}^-$ , and  $\text{OH}^-$ , also listed in order of relative intensity. As discussed for the top soil particle type, the high mass peaks likely contain aluminum or HCN since there is an  $m/z$  27 difference between corresponding isotope peaks. The identity of the ions that make these clusters is still under investigation. This soil type is unique for this study in that it contains peaks for  $\text{SO}_3^-$ ,  $\text{SO}_2^-$ , and  $\text{NO}_2^-$ , where none of the other soil classes show the presence of these ions. The fifth particle class contributes to 7% of the soil particles and is similar to the third, but the dominant positive ion peaks are from the  $m/z$  <sup>+</sup>178, 177, 175, 179 cluster, followed by  $\text{K}^+$  and the  $m/z$  <sup>+</sup>151, 150, 148, 152 cluster, and very small peaks due to  $\text{Na}^+$  and  $\text{Al}^+$ . The fifth class did not yield any negative ion spectra.

The seventh and eighth classes also show positive ion peaks for the  $m/z$  <sup>+</sup>178, 177, 175, 179 and  $m/z$  <sup>+</sup>151, 150, 148, 152 clusters. The seventh class, which makes up 2% of the soil particles, is unique to the other soil types in that it shows positive ion peaks for calcium. The most intense peak in the positive ions is  $m/z$  40 ( $\text{Ca}^+$ ), followed by  $\text{K}^+$ ,  $\text{Na}^+$ ,  $\text{Mg}^+$ ,  $\text{Ca}_2\text{O}^+$ ,  $\text{Li}^+$ , and the clusters at  $m/z$  <sup>+</sup>178, 177, 175, 179 and  $m/z$  <sup>+</sup>151, 150, 148, 152. The negative ions have a dominant peak for  $\text{CN}^-$ , followed by  $\text{O}^-$ ,  $\text{OH}^-$ ,  $\text{CNO}^-$ ,  $\text{AlO}^-$ ,  $\text{SiO}_3^-$ , and  $\text{Cl}^-$ . The eighth class, making up 1% of the soil particles, has a dominant peak for iron in the positives, followed by  $\text{K}^+$ ,  $\text{Na}^+$ ,  $\text{Al}^+$ , and the clusters at  $m/z$  <sup>+</sup>178, 177, 175, 179 and  $m/z$  <sup>+</sup>151, 150, 148, 152. The negative spectra have ions for  $\text{CNO}^-$ ,  $\text{AlO}^-$ ,  $\text{O}^-$ ,  $\text{OH}^-$ , and silicates (listed in order of their relative abundance).

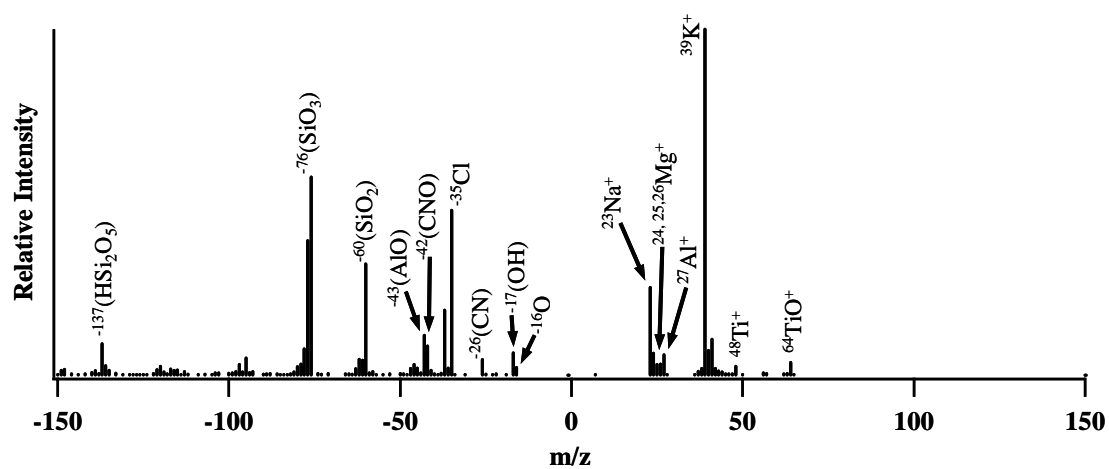


**Figure 2.6** Representative spectrum of the soil particle class detected within the Minuteman rocket wake sample.



Figure 2.6 shows a representative spectrum of a soil particle that was detected within the rocket wake sample. The positive ions have a dominant peak for  $K^+$ , followed by peaks for  $Na^+$ ,  $Al^+$ ,  $Mg^+$ ,  $TiO^+$ ,  $Ti^+$ , and  $Fe^+$ , while the negative ions have peaks for  $Cl^-$ , silicates,  $AlO^-$ ,  $CNO^-$ ,  $OH^-$ ,  $CN^-$  and  $O^-$  (listed in order of relative intensities). The major differences between soil particles within the rocket wake and the resuspended soil particles are that the soil particles within the rocket wake do not have the high mass clusters in the positive spectra, the particles have taken up chlorine which is abundant within the rocket exhaust, and there is no lithium detected on these particles. This rocket wake soil class is very similar to the second particle class from the resuspended soil (which is also similar to the top resuspended soil type minus the peaks at  $m/z^+ 178, 177, 175, 179$ ). This could indicate that the compounds that lead to these high mass peaks are volatile within the rocket wake, which would explain their absence in the soil types seen in the rocket wake particles. Lithium was also not detected in the rocket wake soil particles, most likely due to its higher volatility as compared to the other metals present within the soil particle type. Comparing the acquired spectra and the ART-2a data analysis results between the rocket wake and the soil samples, it is evident that ATOFMS can be used to distinguish between solid rocket motor emissions and suspended soil.

#### **2.4.4 Comparison to the results found with PALMS on the Athena II SRM**

This study demonstrates that particles in the exhaust emissions of static fired SRMs consist mainly of submicron (combustion) particles which are readily distinguishable from local dust or soil sources (that are mechanically resuspended and occur in the supermicron mode). Positive spectra attributed to the rocket wake consist

primarily of aluminum from the rocket fuel/combustion catalyst, and traces of other metals (especially tungsten). Negative spectra consisted of chlorine and chlorine-metal cluster ions from the fuel oxidizer, as well as aluminum oxides, and sulfates. Elemental carbon and organic carbon were seen in many mass spectra as well and are most likely from the combustion of the Carboxyl Terminated Poly Butadiene polymer component of the fuel.

The particle types detected with the ATOFMS instruments for the Minuteman SR19 II SRM agree with those obtained for the Athena II SRM with the PALMS instrument published by Cziczo et al. [Cziczo *et al.*, 2002]. The Athena II wake particles contain Al, Fe, Na, and K in the positive ion spectra and O, OH, Cl, AlO, and AlO<sub>2</sub> in the negative ions and these compounds were also detected in this study. It is also reported by Cziczo et al. that the Athena II wake contained C, Ca, V, Sn, and Pb in the positive ion mass spectra. Carbon was detected in this study in the form of EC and OC along with Pb, but there was no evidence of Sn or V. The PALMS study did not detect the presence of tungsten which reflect the composition of the SRM exhaust nozzles. It was detected in the top particle type for this study. It is also reported for the PALMS study that Ti, I, Ba, Zn, and sulfuric acid fragments were seen in a lesser percentage of the particles. While Ti, I, and Ba were not detected for the SRM wake particles in this study, Zn (in the form of ZnCl<sub>3</sub><sup>-</sup>) was detected in the top class and sulfuric acid (HSO<sub>4</sub><sup>-</sup>) was seen in the second, sixth, eighth, and ninth rocket wake classes. Other ions reported by Cziczo et al. include peaks at  $m/z$  <sup>+</sup>63, 65, 81, and 83 in the positive spectra and  $m/z$  <sup>-</sup>133, 135, and 137 in the negative spectra. These are reported by Cziczo et al. to be possible cluster ions with Cl<sup>-</sup>; however  $m/z$  <sup>+</sup>63 and <sup>+</sup>65 are the isotope peaks for copper. The reason these ions may not

have been detected in the Minuteman SR19 II wake could be due to differences in the LDI lasers used between PALMS and ATOFMS. It could also be due to differences in the composition of the SRM fuel between the two rockets, or even losses from the collection vessel used for this study. Since the PALMS instrument sampled the SRM plume at different intervals from 4 to 36 minutes after launch, it is unfortunate that there was no sizing data obtained in the study by Cziczo et al., which would have allowed for a comparison with the sizing results obtained in this study.

## **2.5 Acknowledgements**

The authors thank Kerry Kelly, and Dave Wagner for their help with collecting the DustTrak data and for helping with the sampling setup. Additionally, we thank Adel Sarofim, JoAnn Lighty from the University of Utah and James (Tom) Callaghan from Hill Air Force Base for their help with coordinating this study. This work was supported by the Strategic Environmental Research and Development Program (SERDP) and the Department of Defense (DOD).

Chapter 2 is in preparation for submission to Atmospheric Science and Technology in 2007. Toner, S.M., D.A. Sodeman, and K.A. Prather, Single particle analysis of a Minuteman SR19 II rocket motor exhaust plume using aerosol time-of-flight mass spectrometry. Copyright 2007, Taylor and Francis, Inc.

## 2.6 References

- Aguesse, T., Environmental impact assessment of solid rocket motors ground tests, *Challenges in Propellants and Combustion: 100 Years after Nobel, [International Symposium on Special Topics in Chemical Propulsion], 4th, Stockholm, May 27-31, 1996*, 106-117, 1997.
- Allen, J.O., Software toolkit to analyze single-particle mass spectral data - <http://www.yaada.org>, 2006.
- Anderson, B.J., and V.W. Keller, A field study of solid rocket exhaust impacts on the near-field environment, pp. 87 pp., Marshall Space Flight Cent., Natl. Aeronaut. Space Adm., Huntsville, AL. USA., 1990.
- Andolz, F.J., T.A. Dougherty, and A.B. Binder, Lunar Prospector Mission Handbook, pp. 63pp, Lockheed Martin Missiles & Space Co., 1998.
- Benke, G., M. Abramson, and M. Sim, Exposures in the alumina and primary aluminum industry: as historical review, *Annals of Occupational Hygiene*, 42 (3), 173-189, 1998.
- Bennett, R.R., J.R. Whimpey, R. Smith-Kent, and A.J. McDonald, Effects of rocket exhaust on the launch site environment and stratospheric ozone, *Challenges in Propellants and Combustion: 100 Years after Nobel, [International Symposium on Special Topics in Chemical Propulsion], 4th, Stockholm, May 27-31, 1996*, 92-105, 1997.
- Brady, B.B., E.W. Fournier, L.R. Martin, and R.B. Cohen, Stratospheric ozone reactive chemicals generated by space launches worldwide, pp. 34 pp., Technology Operations, Aerospace Corp., El Segundo, CA. USA., 1994.
- Brown, J.S., K.L. Zeman, and W.D. Bennett, Ultrafine particle deposition and clearance in the healthy and obstructed lung, *American Journal of Respiratory and Critical Care Medicine*, 166 (9), 1240-7., 2002.
- Callaghan, J., Static Test SR19 Minuteman II Stage 2 Rocket Motor, Test Directive number: TD LM-02-SR19-AA22069, in *Department of The Air Force Test Directive number: TD LM-02-SR19-AA22069*, pp. 14, Department of the Air Force: Air Force Material Command Ogden Air Logistics Center, Hill Air Force Base, Utah, HILL AIR FORCE BASE, UTAH 84056, 2002.
- Clarke, C.A., Effects of aluminium oxide on the lungs of mice, *J. Dental Research*, 35, 693-5, 1956.

- Cofer, W.R., III, G.G. Lala, and J.P. Wightman, Analysis of mid-tropospheric space shuttle exhausted aluminum oxide particles, *Atmospheric Environment (1967-1989)*, 21 (5), 1187-96, 1987.
- Cofer, W.R., III, E.L. Winstead, and L.E. Key, Surface composition of solid-rocket exhausted aluminum oxide particles, *Journal of Propulsion and Power*, 5 (6), 674-7, 1989.
- Cziczo, D.J., D.M. Murphy, D.S. Thomson, and M.N. Ross, Composition of individual particles in the wakes of an Athena II rocket and the space shuttle, *Geophysical Research Letters*, 29 (21), 33/1-33/4, 2002.
- Dinman, B.D., Alumina-related pulmonary disease, *JOM, J. Occup. Med.*, 30 (4), 328-, 1988.
- Donaldson, K., V. Stone, A. Clouter, L. Renwick, and W. MacNee, Ultrafine particles, *Occupational and Environmental Medicine*, 58 (3), 211-216, 2001.
- Englert, N., Fine particles and human health--a review of epidemiological studies, *Toxicology Letters*, 149 (1-3), 235-242, 2004.
- Fritschi, L., N. De Klerk, M. Sim, G. Benke, and A.W. Musk, Respiratory morbidity and exposure to bauxite, alumina and caustic mist in alumina refineries, *Journal of Occupational Health*, 43 (5), 231-237, 2001.
- Gard, E., J.E. Mayer, B.D. Morrical, T. Dienes, D.P. Fergenson, and K.A. Prather, Real-time analysis of individual atmospheric aerosol particles: Design and performance of a portable ATOFMS, *Analytical Chemistry*, 69 (20), 4083-4091, 1997.
- Gordon, G.M., and D.A. Brown, Tungsten and rocket motors, pp. 72 pp., NASA (Natl. Aeron. Space Admin.), 1963.
- Hanning-Lee, M.A., B.B. Brady, L.R. Martin, and J.A. Syage, Ozone decomposition on alumina: implications for solid rocket motor exhaust, *Geophysical Research Letters*, 23 (15), 1961-1964, 1996.
- Lighty, J.S., J.M. Veranth, and A.F. Sarofim, Combustion aerosols: Factors governing their size and composition and implications to human health, *Journal of the Air & Waste Management Association*, 50 (9), 1565-1622, 2000.
- Molina, M.J., L.T. Molina, R. Zhang, R.F. Meads, and D.D. Spencer, The reaction of  $\text{ClONO}_2$  with HCl on aluminum oxide, *Geophysical Research Letters*, 24 (13), 1619-1622, 1997.

- Nadler, M.P., Environmental study of toxic exhausts, pp. 104 pp., Naval Weapons Center, China Lake, CA. USA., 1976.
- Neiman, A.S., O. Preston, and D.A. Brown, Tungsten and rocket motors, *United States Department of Commerce, Office of Technical Services, AD [ASTIA Document], 255,252*, 44 pp., 1961.
- Prather, K.A., T. Nordmeyer, and K. Salt, Real-time characterization of individual aerosol particles using time-of-flight mass spectrometry, *Analytical Chemistry*, *66* (9), 1403-7, 1994.
- Ross, M.N., P.D. Whitefield, D.E. Hagen, and A.R. Hopkins, In situ measurement of the aerosol size distribution in stratospheric solid rocket motor exhaust plumes, *Geophysical Research Letters*, *26* (7), 819-822, 1999.
- Schmid, O., J.M. Reeves, J.C. Wilson, C. Wiedinmyer, C.A. Brock, D.W. Toohey, L.M. Avallone, A.M. Gates, and M.N. Ross, Size-resolved particle emission indices in the stratospheric plume of an Athena II rocket, *Journal of Geophysical Research-Atmospheres*, *108* (D8), 2003.
- Shields, L.G., D.T. Suess, and K.A. Prather, Determination of single particle mass spectral signatures from heavy duty diesel vehicle emissions for PM<sub>2.5</sub> source apportionment, *Atmospheric Environment*, *41* (18), 3841-3852, 2007.
- Sodeman, D.A., S.M. Toner, and K.A. Prather, Determination of single particle mass spectral signatures from light duty vehicle emissions, *Environmental Science & Technology*, *39* (12), 4569-4580, 2005.
- Song, X.H., P.K. Hopke, D.P. Fergenson, and K.A. Prather, Classification of single particles analyzed by ATOFMS using an artificial neural network, ART-2A, *Analytical Chemistry*, *71*(4), 860-865, 1999.
- Su, Y.X., M.F. Sipin, H. Furutani, and K.A. Prather, Development and characterization of an aerosol time-of-flight mass spectrometer with increased detection efficiency, *Analytical Chemistry*, *76* (3), 712-719, 2004.
- Thomson, D.S., M.E. Schein, and D.M. Murphy, Particle analysis by laser mass spectrometry WB-57F instrument overview, *Aerosol Science and Technology*, *33* (1-2), 153-169, 2000.
- Toner, S.M., D.A. Sodeman, and K.A. Prather, Single particle characterization of ultrafine and accumulation mode particles from heavy duty diesel vehicles using aerosol time-of-flight mass spectrometry, *Environmental Science & Technology*, *40* (12), 3912-3921, 2006.

Wohlschlager, J., L.C. DiPasquale, and E.H. Vernot, Toxicity of solid rocket motor exhaust - effects of hydrogen chloride, hydrogen fluoride and alumina on rodents, pp. 275-85, Univ. California, Irvine, CA.; Toxic Hazards Research Unit, Dayton, OH. USA., 1975.

World Meteorological Organization, Scientific Assessment of Ozone Depletion, in *Scientific Assessment of Ozone Depletion: 1998*, WMO, 1999.

### **3 Single particle characterization of ultrafine and accumulation mode particles from heavy duty diesel vehicles using aerosol time-of-flight mass spectrometry**

#### **3.1 Synopsis**

The aerodynamic size and chemical composition of individual ultrafine and accumulation mode particle emissions ( $D_a = 50 - 300$  nm) were characterized to determine mass spectral signatures for heavy duty diesel vehicle (HDDV) emissions that can be used for atmospheric source apportionment. As part of this study, six in-use HDDVs were operated on a chassis dynamometer using the heavy heavy-duty diesel truck (HHDDT) five-cycle driving schedule under different simulated weight loads. The exhaust emissions passed through a dilution/residence system to simulate atmospheric dilution conditions, after which an ultrafine aerosol time-of-flight mass spectrometer (UF-ATOFMS) was used to sample and characterize the HDDV exhaust particles in real-time. This represents the first study where refractory species including elemental carbon and metals are characterized directly in HDDV emissions using on-line mass spectrometry. The top three particle classes observed with the UF-ATOFMS comprise 91% of the total particles sampled and show signatures indicative of a combination of elemental carbon (EC) and engine lubricating oil. In addition to the vehicle make/year,



the effects of driving cycle and simulated weight load on exhaust particle size and composition were investigated.

### 3.2 Introduction

Of the various anthropogenic sources of particles, diesel powered vehicles have become an increasing environmental concern. While they tend to have lower fuel consumption and CO<sub>2</sub> emissions, on a per vehicle basis they produce one to two orders of magnitude more particulate matter emissions than do gasoline powered vehicles [Kittelson, 1998]. Many studies have been conducted on the particulate matter released in diesel emissions. These studies have included insight into the possible health effects [Dybdahl *et al.*, 2004; Pourazar *et al.*, 2004; Reed *et al.*, 2004; Zhao *et al.*, 2004], as well as size and number concentrations of particles emitted by diesel vehicles [Khalek *et al.*, 2003; Kwon *et al.*, 2003; Lehmann *et al.*, 2003; Lyyranen *et al.*, 1999a; Moosmuller *et al.*, 2001; Reilly *et al.*, 1998; Sakurai *et al.*, 2003a; Schauer *et al.*, 1999; Shi *et al.*, 2000; Virtanen *et al.*, 2004; Yanowitz *et al.*, 1999]. Many of these studies have shown that the emissions from diesel engines produce high number concentrations of ultrafine particles, especially during idle and low RPM engine operating conditions. Certain studies have probed the composition of diesel particulate matter using filter and/or impactor techniques, such as Micro Orifice Uniform Deposit Impactors (MOUDI), to collect particles in different size ranges. Analysis of the particles collected on filters can be useful for determining organic species and the mass of different species; however no information is acquired on single particle chemistry or rapid changes in chemical composition. Detailed information on the individual particle types emitted by diesel

engines is crucial for understanding their origin as well as the type and level of environmental and health impacts they may have. With such a large fraction of particles emitted from diesel vehicles formed in the accumulation and ultrafine size ranges, it is important to be able to accurately apportion these particles and single particle analysis provides a potentially more direct approach for doing this.

Single particle mass spectrometry techniques, such as aerosol time-of-flight mass spectrometry (ATOFMS), have been used in a number of studies for characterizing particles in the fine (100 – 1000 nm) and coarse (> 1000 nm) size ranges. Recently, the ATOFMS instrument incorporated an aerodynamic lens for improved transmission of smaller accumulation mode and ultrafine particles and is referred to as an ultrafine aerosol time-of-flight mass spectrometer (UF-ATOFMS) [Su *et al.*, 2004]. In this study, the UF-ATOFMS was used to characterize individual ultrafine and accumulation mode diesel exhaust particles. Other particle mass spectrometers, such as the thermal desorption particle beam mass spectrometer (TDPBMS) [Sakurai *et al.*, 2003b; Tobias *et al.*, 2001; Tobias *et al.*, 2000] and the Aerodyne aerosol mass spectrometer (AMS) [Canagaratna *et al.*, 2004; Jayne *et al.*, 2000], have been used to characterize particles emitted from diesel engines. The TDPBMS and AMS have been shown to be useful in distinguishing organic carbon particles; however, these techniques cannot measure refractory components in particles, such as elemental carbon which can represent a significant fraction of diesel emissions particularly in the 50-100 nm size range [Shi *et al.*, 2000; Watson *et al.*, 1994].

The goal of this study is to chemically characterize ultrafine and accumulation mode (50 – 300nm, D<sub>a</sub>) diesel exhaust particles to determine single particle mass spectral

signatures that are unique to heavy duty diesel vehicles (HDDVs). These signatures will be grouped with those obtained from previous ATOFMS studies for HDDV exhaust (100 – 3000nm,  $D_a$ ) and gasoline vehicle (LDV) exhaust (50 – 3000nm,  $D_a$ ) to perform ambient source apportionment of HDDV and LDV exhaust particles. Finally, in order to examine whether the acquired dynamometer signatures are representative of particles sampled in ambient air, an initial comparison is presented of the acquired HDDV signatures with those obtained during a recent freeway-side ATOFMS study.

### 3.3 Experimental

Six HDDVs were analyzed in July and August, 2001 at the Ralph's Distribution center in Riverside, CA. A description of each truck is provided in Table 3.1, including the vehicle/engine year, manufacturer, engine power, miles driven, and driving cycles performed. The HDDVs were tested under the same sampling conditions, including the driving schedule and dilution conditions, so the major aerosol chemical disparities observed between trucks can be attributed to the differences between trucks and not sampling and/or instrumental variability [Suess and Prather, 2002].

The sampling conditions consisted of driving each truck on a heavy duty dynamometer operated by West Virginia University personnel. The transportable heavy duty vehicle emissions testing laboratory (THDVETL) was used to obtain reproducible aerosol emissions from HDDV and is described elsewhere [Bata *et al.*, 1991; Clark *et al.*, 1995]. For this study, the heavy heavy-duty diesel truck (HHDDT) five-cycle driving schedule under different simulated weight loads was used to determine the effect of driving conditions on the exhaust particle's chemical composition. The HHDDT five-

**Table 3.1** Heavy Duty Diesel Vehicles (HDDVs) tested and driving cycles performed.

E55CRC (truck)	Vehicle Model Year	Vehicle Manufacturer	Engine Model Year	Engine Manufacturer	Engine Model	Engine Power (hp)	Mileage	Tests Performed
E55CRC-27	2000	Freightliner	1999	Detroit	Diesel Series 60	500	420,927	C*
E55CRC-28	1999	Freightliner	1998	Detroit	Diesel Series 60	500	539,835	IC, A*
E55CRC-30	1999	Freightliner	1998	Detroit	Diesel Series 60	500	138,553	IC, A
E55CRC-31	1998	Kenworth	1997	Cummins	N14-460E+	460	587,265	A, B
E55CRC-32	1992	Volvo	1991	Caterpillar	3406B	280	595,258	A
E55CRC-33	1985	Freightliner	1984	Caterpillar	3,406	310	988,823	A

**Five cycle test at A) 56,000 lbs / B) 66,000 lbs / C) 75,000 lbs**

**30 min idle**

10 min soak

**17 min creep**

10 min soak

**11 min transit**

10 min soak

**34 min cruise with speeds at 55 mph**

10 min soak

**13 min "high speed" HDDT\_S cycle at 65 mph** \*(31 min "high speed" HHDDT65 at 65 mph)

stop cycle

**56,000 lbs idle-creep cycle (IC)**

Idle truck for 30 min

run at "creep" speeds for 17 min

10 min soak with engine off

repeat 5x

cycle schedule was developed by the California Air Resources Board (CARB) and consists of an idle, creep, transient, cruise, and high-speed cycle. The idle stage consists of the truck idling for 30 minutes with no acceleration periods. The creep stage consists of small accelerations and decelerations, maintaining speeds less than 10 mph, which simulates heavy traffic conditions. The transient stage consists of fast and short periods of accelerations and decelerations with speeds up to 50 mph and is a simulation of city-street and some highway driving conditions. The cruise cycle mimics driving conditions encountered on highways and maintains speeds between 50 - 60 mph for the majority of the cycle. The final cycle of the 5-cycle test, named HDDT\_S / HHDDT65, is a simulation of higher speed driving and acceleration, with speeds up to 65 mph. The high-speed cycle was altered during the study from a 31 minute test (HHDDT65) to a 13 minute test (HDDT\_S) in an effort to provide stress relief to the dynamometer system.

Three different (on axle) simulated weight loads were used to determine the effect of engine load on exhaust emissions. These loads were 56,000 lbs, 66,000 lbs, and 75,000 lbs, representing increasingly laden driving conditions. The different loads were not tested on all HDDVs; however, all vehicles except one were tested at the 56,000 lbs load. Only one truck was able to be tested at 75,000 lbs and one other at 66,000 lbs due to stress issues on the dynamometer. The truck tested at 66,000 lbs was also tested at 56,000 lbs, and the differences in loads, as it pertains to particle composition, are discussed.

Upon exiting the exhaust pipe of the HDDV, the diesel exhaust is passed through a constant volume sampling system, which is part of the THDVETL [Bata *et al.*, 1991; Clark *et al.*, 1995], and is used for primary dilution. Secondary dilution was achieved by

**Table 3.2** Dilution ratios (DR) for each HDDV and cycle

HDDV	Cycle	Cycle time (sec)	Dilution Ratio Information		Cycle DR
			WVU Primary Dilution	UCD Secondary Dilution	
E55CRC-27 5-cycle 75,000lbs	Idle	1800	130.0	10.0	1300.0
	Creep	1032	77.0	10.0	770.0
	Trans	688	17.0	10.0	170.0
	Cruise	2083	12.0	9.7	116.4
	HHDDT65	739	7.0	9.0	63.0
E55CRC-28 Idle/Creep	Idle/Creep	2831	117.9	5.2	618.2
	Idle/Creep	2831	117.4	5.2	615.5
	Idle/Creep	2831	119.7	5.2	627.4
	Idle/Creep	2831	117.1	5.2	614.1
	Idle/Creep	2831	121.4	5.2	636.6
E55CRC-28 5-cycle 56,000lbs	Idle	1799	139.9	30.1	4211.0
	Creep	1031	101.0	35.2	3555.2
	Trans	687	24.4	26.6	649.0
	Cruise	2082	13.0	26.6	345.8
	HHDDT65	1899	12.0	27.8	333.6
E55CRC-30 Idle/Creep	Idle/Creep	2831	110.2	5.2	573.0
	Idle/Creep	2831	110.5	5.2	573.3
	Idle/Creep	2831	111.2	5.2	577.0
	Idle/Creep	2831	113.4	5.2	588.4
	Idle/Creep	2831	115.1	5.2	597.0
E55CRC-30 5-cycle 56,000lbs	Idle/Creep	2831	113.9	5.2	590.7
	Idle	1799	121.9	10.0	1221.1
	Creep	1031	73.3	10.0	734.1
	Trans	687	19.7	9.7	189.8
	Cruise	2082	13.4	9.3	125.2
E55CRC-31 5-cycle 56,000lbs	HDDT_S	759	9.1	9.0	82.6
	Idle	1799	133.3	10.0	1334.9
	Creep	1031	78.7	10.0	788.0
	Trans	687	20.7	10.0	207.7
	Cruise	2082	13.4	9.7	129.2
E55CRC-31 5-cycle 66,000lbs	HDDT_S	759	9.8	9.3	91.4
	Idle	1799	129.4	10.0	1296.0
	Creep	1031	80.2	10.0	803.6
	Trans	687	20.5	10.0	205.7
	Cruise	2082	15.0	9.7	144.6
E55CRC-32 5-cycle 56,000lbs	HDDT_S	759	10.1	9.3	93.8
	Idle	1799	120.2	9.7	1160.6
	Creep	1031	84.4	10.0	845.8
	Trans	687	26.0	9.7	251.1
	Cruise	2082	14.8	9.0	133.6
E55CRC-33 5-cycle 56,000lbs	HDDT_S	759	12.2	8.8	106.8
	Idle	1799	122.7	10.0	1229.3
	Creep	1031	84.2	10.0	843.2
	Trans	687	24.7	9.5	234.1
	Cruise	2082	15.1	8.8	132.6
	HDDT_S	759	10.1	8.5	85.8

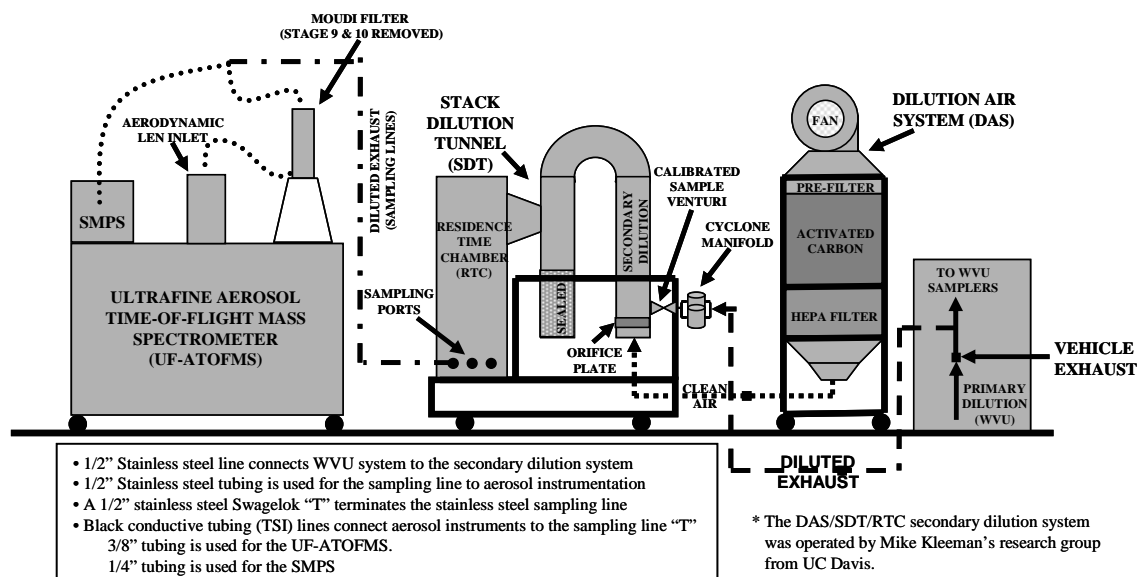


**Figure 3.1** Sampling set-up used for HDDV dynamometer experiment. (Figure derived from *Robert et al.* 2007)

sampling off of the primary dilution tunnel with a Stack Dilution Tunnel (SDT) at a constant flow [McDonald *et al.*, 2000]. The secondary dilution with the SDT was used to simulate realistic atmospheric dilution conditions, allowing for equilibrium to be established for semivolatile organic carbon species between the gas and particle phase [Hildemann *et al.*, 1989]. Dilution ratios for each HDDV and cycle performed are summarized in Table 3.2.

For this study, an ultrafine aerosol time-of-flight mass spectrometer (UF-ATOFMS) was used to size and chemically characterize HDDV exhaust particles between 50 and 300 nm. The UF-ATOFMS instrument along with a scanning mobility particle sizer (SMPS) (TSI Model 3936L10 – Minnesota) sampled off of a SDT residence chamber continuously for each truck testing period. Stainless steel sampling lines were used to sample from the residence chamber to the instrumentation and were coupled to the instruments with black conductive tubing (TSI). A more detailed description of the driving cycles and the sampling conditions is provided in the supporting information. A diagram of the sampling system is provided in Figure 3.1 [Robert *et al.*, 2007].

Data obtained from this study were imported into Matlab 6.1.0.450 (Release 12.1) and analyzed with the ART-2a neural network data analysis algorithm [Hopke and Song, 1997; Song *et al.*, 1999; Xie *et al.*, 1994] using a vigilance factor of 0.85, learning rate of 0.05 and 20 iterations. This method of analysis has been shown to be reliable for ATOFMS data and is used for this study to allow comparisons to be made to previous and future studies using the same technique. Single particle HDDV emissions (100 – 3000nm) have been sampled and reported with a standard-inlet ATOFMS instrument previously [Shields *et al.*, 2007] and will be used as a basis of comparison in this chapter.



### 3.4 Results and Discussion

#### 3.4.1 Description of Particle Types Observed with UF-ATOFMS

Formation studies of diesel exhaust particles in the accumulation and ultrafine size mode have been studied and described elsewhere [Burtscher *et al.*, 1998; Kittelson, 1998; Tobias *et al.*, 2001]. These previous accounts of HDDV exhaust have mainly focused on size profiles of the exhaust particles, or chemical composition obtained using bulk analysis methods. In addition, studies using thermal desorption mass spectrometry for on-line chemical composition analysis have focused on the non-refractory materials and thus the associations between elemental carbon and other species such as metals have not been probed (18, 20, 22). This study is unique in reporting the results from *single particle* analysis of the full range of chemical species in ultrafine and accumulation mode particles sampled directly from HDDV.

As previously stated, the data were imported into Matlab and analyzed with the ART-2a neural network data analysis technique, where particles were grouped into clusters (classes) based on their similarity of mass spectra. ART-2a does not converge and thus creates multiple chemically similar clusters while making the initial particle clusters. Thus, a secondary cluster regrouping function was run on the particle clusters to group clusters together within the original vigilance factor. Resulting clusters were then sorted and grouped by hand into classes of the same type. About 10% of the particles were unclassified after these steps because each of these particles resulted in its own ART-2a cluster due to miscalibrated ion peaks in the spectra. These unclassified particles were reanalyzed with ART-2a at a lower vigilance factor ( $VF = 0.4$ ) which allowed them to be grouped into a smaller number of clusters. Those clusters were found to match the

original ART-2a clusters and were combined with those classes. Using this data analysis technique, seven main particle classes resulted for this HDDV data set with 100% of the sampled particles being classified. Representative spectra / weight-matrices for the seven classes are shown in Figure 3.2 (A-G), and Figure 3.3 shows the statistical breakdown of these classes by percentage. It is important to note that these seven classes serve as simplified representations of the particle types to illustrate the major signatures observed and their relative abundances. The representative spectra in Figure 3.2 are shown in order of particle class abundance.

The top particle class (Figure 3.2A and labeled as *EC*, *Ca*, *OC*, *Phosphate* in Figure 3.3) made up 78% of the particles sampled by UF-ATOFMS in the ultrafine and accumulation particle modes. The positive ion mass spectra for this class consist of elemental carbon (EC) ( $^{12}\text{C}_1^+$ ,  $^{24}\text{C}_2^+$ ,  $^{36}\text{C}_3^+$ ,  $^{48}\text{C}_4^+$ ,  $^{60}\text{C}_5^+$ ), calcium ( $^{40}\text{Ca}^+$ ,  $^{56}\text{CaO}^+$ ), and organic carbon (OC) with peaks at  $m/z$  27<sup>+</sup>, 29<sup>+</sup>, and 37<sup>+</sup>. The negative ion spectra contain peaks due to phosphate ( $^{-97}\text{H}_2\text{OPO}_3$ ,  $^{-79}\text{PO}_3$ ,  $^{-63}\text{PO}_2$ ) and some EC ( $^{-24}\text{C}_2$ ,  $^{-36}\text{C}_3$ ). The peak at  $m/z$  -97 can also be attributed to  $^{-97}\text{HSO}_4$ . Based on the spectrum, the EC particles in this class show primarily short chain carbon envelopes ( $\text{C}_n^+$  where  $n < 6$ ). Another note regarding the EC peaks in this class is that the peak for  $^{36}\text{C}_3^+$  is larger than that for  $^{12}\text{C}_1^+$ . This finding is reproducible for ultrafine HDDV particles and will be addressed later in the discussion of the prospects for ambient apportionment. It has been shown that as particle size decreases (especially in the ultrafine and low accumulation size range), the extent of fragmentation through laser desorption/ionization (LDI) techniques increases [Schoolcraft *et al.*, 2001; Schoolcraft *et al.*, 2000] which results in smaller carbon ion clusters as the particles become smaller. The calcium and phosphate

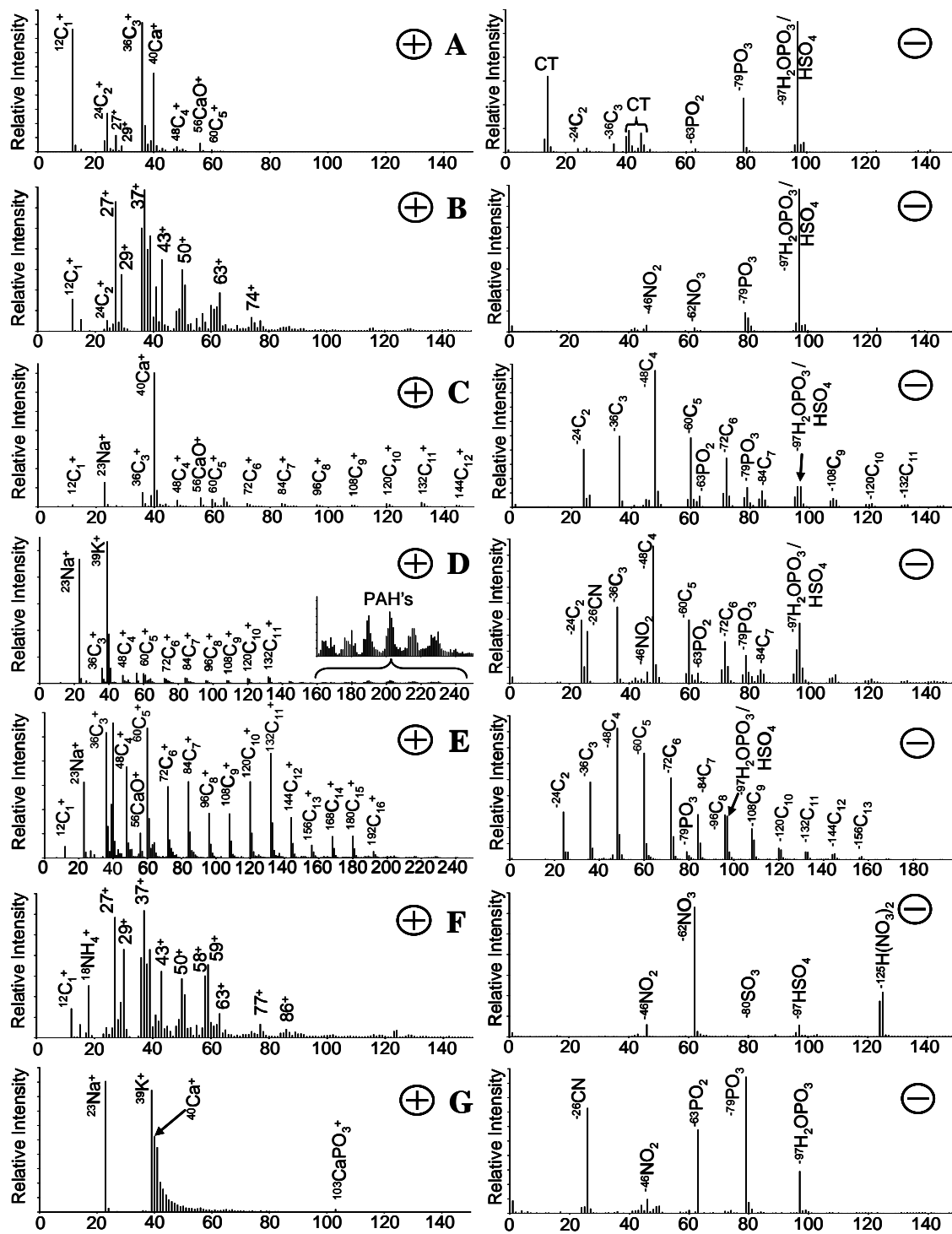


**Figure 3.2 (A – G),** Positive and negative ion representative mass spectra / weight matrices for the particle classes sampled in HDDV exhaust. Peaks labeled “CT” in negative ion spectra indicate signal “cross-talk”, or noise, from the positive ion detector.

in this class most likely come from additives typically used in diesel engine lubrication oil [Gautam *et al.*, 1999; Harrison *et al.*, 2003; Rudnick, 2003]. Calcium is added to vehicle lubricants commonly in the form of calcium carbonate and calcium sulfonate to act as a detergent to neutralize acidic combustion byproducts and to prevent accumulation of deposits in the engine [Rudnick, 2003]. Phosphate is typically added to engine lubricants in the form of zinc dialkyldithiophosphate (ZDDP) and functions as an anti-wear agent [Gautam *et al.*, 1999]. An in-lab analysis with an ATOFMS of the oil and fuel samples sampled from each truck during the HDDV study shows the presence of these additives in similar amounts to those detected in the HDDV exhaust spectra [Spencer *et al.*, 2006]. The lack of zinc detected in this particle type as well as others is likely due to the low sensitivity of ATOFMS to this metal. For other particle types, the  $m/z$  peaks of Zn ( $m/z$  64, 66, 68) can be masked by peaks from organic carbon. These findings suggest that this main class of particles seen in HDDV exhaust can be attributed to engine lubricating oil and/or coagulation of lubricating oil and EC particles from incomplete combustion. These results agree with the findings by other researchers that lubricating oil is detected in the majority of diesel exhaust particles [Canagaratna *et al.*, 2004; Jung *et al.*, 2003; Lyyranen *et al.*, 1999b; Okada *et al.*, 2003; Sakurai *et al.*, 2003b; Tobias *et al.*, 2001; Vilhunen *et al.*, 1999].

The second most abundant particle type is shown in Figure 3.2B (labeled as *OC*, *EC*, *Phosphate*, *Sulfate* in Figure 3.3) and makes up 8% of the particles characterized with the UF-ATOFMS. The positive ion mass spectra of this class are dominated by organic carbon ion fragments, which are labeled by mass-to-charge (as there are many possibilities to their organic compositions), and to a lesser extent, the presence of EC ion

peaks. Even though LDI can cause extensive fragmentation of organic species present on particles which makes it difficult to identify the parent species, it is possible to identify certain organic classes of molecules. In the case of this positive ion spectrum, the presence of  $m/z$  51<sup>+</sup>, 63<sup>+</sup>, and 74<sup>+</sup> can be attributed to aromatic species as shown previously with an ATOFMS [Silva and Prather, 2000]. The presence of low mass organic fragments  $m/z$  27<sup>+</sup>, 29<sup>+</sup>, 37<sup>+</sup>, 43<sup>+</sup> and 50<sup>+</sup> are typically associated with long-chain aliphatic organics, but can also result from the fragmentation of many other types of organic species. The negative ion mass spectrum shows peaks indicative of sulfate, phosphate, and small amounts of nitrate (<sup>-46</sup>NO<sub>2</sub>, <sup>-62</sup>NO<sub>3</sub>). The presence of NO<sub>x</sub> species in the particles can indicate incomplete combustion of air in the engine or possible high exhaust temperatures. They could also derive from oxidation of the nitrogen-containing organics from the diesel fuel [Arens *et al.*, 2001; Hughey *et al.*, 2001]. Given that HDDVs produce a higher fraction of EC compared to OC [Kleeman *et al.*, 2000; Lowenthal *et al.*, 1994], it is somewhat surprising there is an OC particle type that does not contain an EC core. However, it should be noted that while all HDDVs produced this particle type, most of the particles in this OC class came from one HDDV (E55CRC-30). Given the large surface area of EC particles produced in diesel emissions, it is likely this particle type was produced by large amounts of OC species condensing on EC particle cores.

The third most abundant particle type observed makes up 7% of the HDDV exhaust particles classified with the UF-ATOFMS and is represented in Figure 3.2C (labeled as *Ca*, *Na*, *EC*, *Phosphate*, *Sulfate* in Figure 3.3). This particular class contains a strong ion signal due to calcium (<sup>40</sup>Ca<sup>+</sup>) in the positive ion mass spectra, as well as less

intense peaks due to sodium ( $^{23}\text{Na}^+$ ), long-chained EC ( $\text{C}_n^+$  where  $n \geq 6$ ), and potassium ( $^{39}\text{K}^+$ ). The negative ion mass spectra are also dominated by long-chained EC and contain peaks due to  $^{-97}\text{H}_2\text{OPO}_3$ / $^{-97}\text{HSO}_4$ ,  $^{-79}\text{PO}_3$ , and  $^{-63}\text{PO}_2$ . The spectra suggest the particles contained lubricating oil as they are very similar to the top class, except for the spectra in this class contain sodium and higher  $m/z$  EC fragments. Sodium can come from a variety of sources, including impurities in the lubricating oil and/or from the diesel fuel. Diesel fuel samples analyzed in lab with an ATOFMS show the presence of sodium more frequently than in the oil samples [Spencer *et al.*, 2006]. The most reasonable explanations for the higher  $m/z$  carbon ion fragments are that the EC peaks in this particle type are produced by larger soot agglomerates, or differences in the laser desorption/ionization (LDI) process. It is known that soot can form long-chain EC/soot agglomerates, which grow to their largest sizes in the accumulation mode [Arens *et al.*, 2001; Kittelson, 1998; Shi *et al.*, 2000; Van Gulijk *et al.*, 2004; Walker, 2004]. One cannot exclude the possibility that these particles experienced different powers during the LDI process. It has been shown that there are differences with ATOFMS spectra for the same particle type based solely on the LDI laser [Wenzel and Prather, 2004]. As shown in Wenzel *et al.*, these effects result from ionizing the particle in cold or hot spots of an inhomogeneous laser beam where the power density is different enough to cause softer or harder ionization, respectively. The techniques used by Wenzel *et al.* for LDI beam homogenization were not used for this study.

The fourth most abundant classified particle type makes up 3% of the total particles and is represented in Figure 3.2D (labeled as *Na, K, Ca, EC, PAH, Phosphate, Nitrate, Sulfate* in Figure 3.3). This class consists of positive ion mass spectra with

strong potassium ( $^{39}\text{K}^+$ ) and sodium ( $^{23}\text{Na}^+$ ) signals, as well as smaller peaks attributed to EC ( $\text{C}_{1-11}^+$ ) and polycyclic aromatic hydrocarbons (PAH's) in the higher mass range ( $m/z$  163, 168, 176, 180, 190, 202, 216, 226 and 230). ATOFMS is very sensitive to alkali metals, and thus the large peak intensities of both potassium and sodium make it difficult to see EC and PAH's in the representative weight matrix areas. The negative ion mass spectra for this class consist of EC, phosphates, sulfate,  $^{-46}\text{NO}_2$  and  $^{-26}\text{CN}$ . Particles in this class appear to contain a mixture of diesel oil and fuel combustion by-products. The presence of sodium and potassium with such a strong intensity resembles the spectra seen in the lab-analyzed diesel fuel samples [Spencer *et al.*, 2006]. The presence of PAH's has been seen in both fuel and oil samples and could be from either source, or could have formed during combustion and condensed onto the particles. The ATOFMS lab-analyzed fuel samples from Spencer *et al.* 2006 showed much more PAH content in diesel fuel than in gasoline fuel which is consistent with previous literature findings [Rhead and Hardy, 2003; Zielinska *et al.*, 2004].

The fifth most abundant class, making up 2% of the total HDDV exhaust particles, is represented in Figure 3.2E (labeled EC, Ca, Na, OC, Phosphate, Sulfate in Figure 3.3). This class has positive ion mass spectra containing calcium, long-chained EC ( $\text{C}_{1-16}^+$ ), sodium, and some minor peaks attributed to OC. The negative ion mass spectra are composed of long-chained EC ( $\text{C}_{1-13}^-$ ),  $^{-97}\text{H}_2\text{OPO}_3$ / $^{-97}\text{HSO}_4$ , and  $^{-79}\text{PO}_3$ . While this class has a very similar composition to that of the third class, it differs by having much more intense EC ion intensities, as well as the presence of some OC. Despite these differences, this class does appear to be derived from the same process as the third class and it may have just experienced slightly higher laser powers.

The sixth class, represented in Figure 3.2F (labeled *OC, Amines, Nitrates, Sulfates* in Figure 3.3), makes up 1% and appears to be from incomplete combustion of the diesel fuel. The positive ions for this class are composed primarily of peaks due to OC, as well as peaks due to amines (or possibly nitrogen containing organics) at  $m/z$  58<sup>+</sup>, 59<sup>+</sup>, and 86<sup>+</sup> [Angelino *et al.*, 2001], and peaks due to aromatic organics ( $m/z$  63<sup>+</sup> and 77<sup>+</sup>). While the negative ion spectra contain peaks for  $^{-46}\text{NO}_2$ ,  $^{-62}\text{NO}_3$ ,  $^{-125}\text{H}(\text{NO}_3)_2$ ,  $^{-80}\text{SO}_3$ , and  $^{-97}\text{HSO}_4$  (generally labeled as nitrates and sulfates, respectively). The negative ion peaks due to nitrate are an indication of incomplete combustion, and the presence of the sulfate species (with no presence of phosphate species) indicates that this is more likely from the combustion of fuel than from the lubricating oil. This source assignment is corroborated by the laboratory ATOFMS analysis of diesel fuel [Spencer *et al.*, 2006].

The final class, making up the remaining 1% of the total particles, is represented in Figure 3.2G (labeled *Na, K rich w/Ca, Phosphates, Nitrates* in Figure 3.3). This class is very unique, compared to the other classes, in that it is only composed of inorganic species. The positive ion mass spectra contain sodium, potassium, calcium and calcium phosphate ( $^{103}\text{CaPO}_3^+$ ), while the negative ion mass spectra contain phosphates ( $^{-97}\text{H}_2\text{OPO}_3$ ,  $^{-79}\text{PO}_3$ ,  $^{-63}\text{PO}_2$ ),  $^{-26}\text{CN}$ , and  $^{-46}\text{NO}_2$ . The species present in this class would indicate that the particles contained salts from the additives in the lubricating oil and fuel.



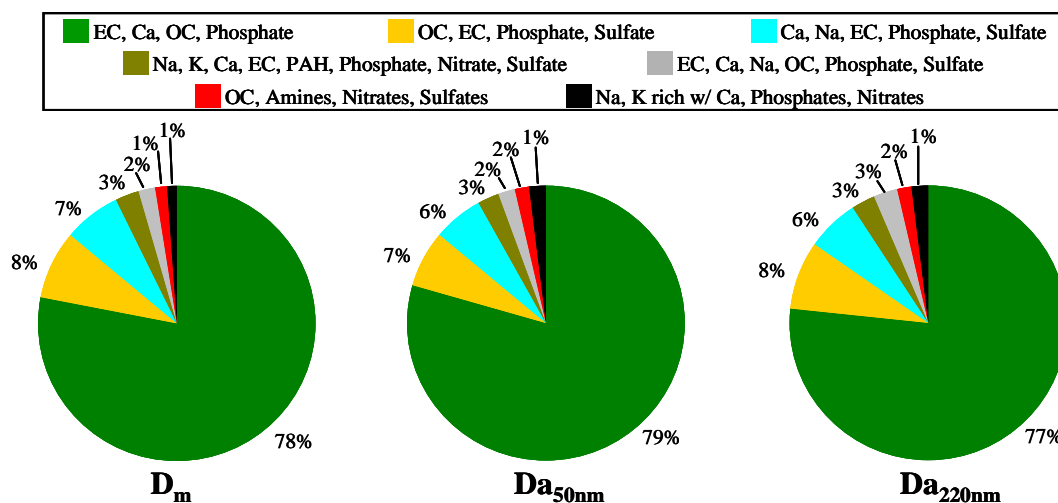


**Figure 3.3** Statistical breakdown of the scaled particle classes observed from the HDDV exhaust. Particle statistics are shown for data scaled directly to SMPS data ( $D_m$ ) and for SMPS data that was converted to  $D_a$  using shape factors and densities for diesel particles, as described in Park *et al.*, with mobility diameters of 50 nm ( $Da_{50nm}$  and  $Da_{220nm}$ ).

### 3.4.2 Analysis of Size Segregated Chemical Composition for each HDDV

To establish proper statistical representation of the particle classes, the UF-ATOFMS particle counts were scaled to particle counts detected with an SMPS. The same methods for scaling particle number concentration as described in Sodeman *et al.* and Robert *et al.* were used on the data in this study [Robert *et al.*, 2007; Sodeman *et al.*, 2005]. The SMPS size bins were combined to ensure that there were enough UF-ATOFMS particle counts in each bin to provide reliable particle statistics. The rule set for scaling required each size bin to contain at least ten particles detected by the UF-ATOFMS. Since UF-ATOFMS measures the particles aerodynamic diameter ( $D_a$ ) and it is being scaled to an instrument (SMPS) that measures the particle mobility diameter ( $D_m$ ), it was necessary to examine that scaling to  $D_m$  without converting  $D_m$  to  $D_a$  was acceptable. This verification was done by using the equation for converting  $D_a$  to  $D_m$  as described in Van Gulijk *et al.* using the dynamic shape factors and particle densities as described in Park *et al.* [Park *et al.*, 2004a; Van Gulijk *et al.*, 2004]. The shape factors reported in Park *et al.* are 1.11 and 2.21, and the particles densities are 1.27 and 1.78 g/cm<sup>3</sup> for particles with mobility diameters of 50 and 200 nm, respectively. Figure 3.3 displays the results of this conversion for the percentages of the scaled classes. These results show that there is never more than a 1% deviation in a particle class contribution whether scaling to  $D_m$  or converting  $D_m$  to  $D_a$  with the shape factor and density of particles at 50 nm ( $Da_{50nm}$ ) or of particles at 220 nm ( $Da_{220nm}$ ). While  $D_m$  and  $D_a$  for diesel exhaust particles are not identical, it can be seen that there is a very minor difference in the particle class statistics when scaling using the two different types of particle diameters. Thus, no modifications were made to the data to adjust for different

chemical types for scaling since it was determined to be negligible for this study over this size range with the UF-ATOFMS.

Studies by Tobias *et al.* and Sakurai *et al.* investigated the chemical composition of particles as a function of size in HDDV engine emissions, but not at the single particle level, or using instruments with the ability to detect inorganic or refractory species (i.e. EC) [Sakurai *et al.*, 2003b; Tobias *et al.*, 2001]. One of the unique measurement capabilities of ATOFMS or any single particle mass spectrometer that uses a laser for the desorption/ionization step is that OC, EC, and inorganic species can all be detected and their associations within single particles can be measured in real time. This allows one to obtain size-resolved chemical composition information about the particle classes observed for each HDDV as shown in Figure 3.4. The UF-ATOFMS particle classes shown in Figure 3.4 are scaled to the SMPS number concentrations for combined size bins per gram of CO<sub>2</sub> for each HDDV on each test. The data in each plot have been multiplied by a factor (as indicated on each plot) to keep them all on the same scale. Data missing from a certain size bin indicates that there were not enough UF-ATOFMS particle counts for that particular bin to make scaling of that size bin statistically reliable.

As Figure 3.4 shows, the main particle type for generally all size bins and for each HDDV is the first particle class (*EC, Ca, OC, Phosphate*). This is particularly true for the smaller size bins, but as particle size increases, the composition changes for some HDDVs. E55CRC-30 (Figure 3.4D,E) is an anomaly to this scenario, where the idle/creep cycle (3.4D) is dominated by the second particle class (*OC, EC, Phosphate, Sulfate*) for all size bins and still contains a significant amount of particles in this class

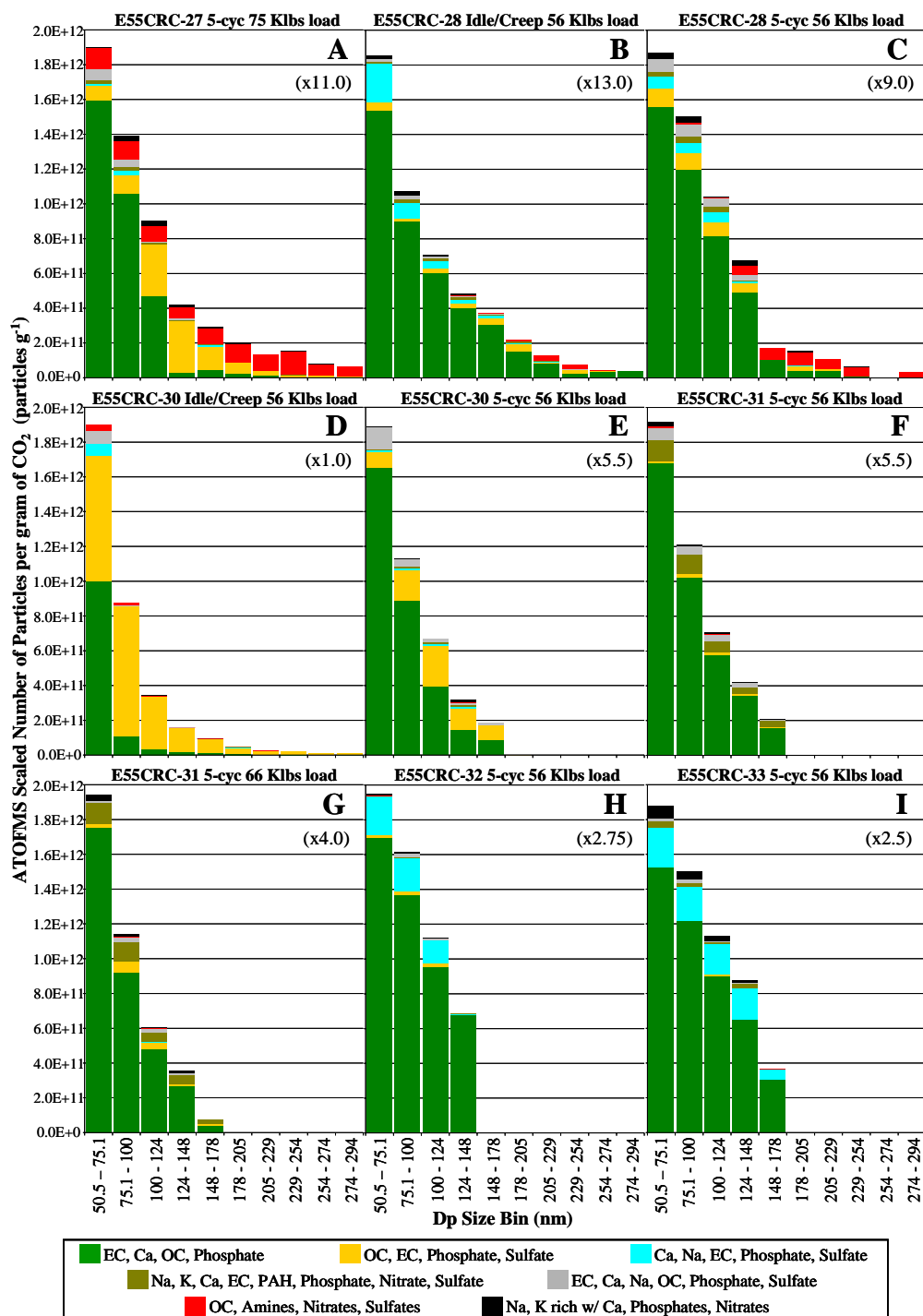


**Figure 3.4 (A - I), UF-ATOFMS size segregated chemical composition of particles observed for each HDDV for each driving test scaled number to SMPS per gram of CO<sub>2</sub>.** Size bins are created from SMPS data, where bins were combined to provide 20-25nm size bins. The simulated on-axis weight load is provided for each HDDV.

even for the 5-cycle test (3.4E). Since the HDDVs E55CRC-27, 28, and 30 (Figure 3.4A-D) have enough counts to show scaled data out to 294 nm, trends in particle composition can be examined as size increases. The larger size bins show that some of the more minor classes (especially the OC-containing classes) start to become more prevalent as particle size increases. This is an indication of semivolatile organic vapors condensing onto HDDV exhaust particle EC cores to create larger particles with contributions from organic carbon species [Spencer and Prather, 2006]. For each HDDV, from 50-178 nm, the overall particle class breakdown per size bin seems to be relatively constant (excluding E55CRC-27 and 30). In addition, each of the HDDVs tested were found to emit the same particle types. The difference between the HDDVs is the proportions of each particle type emitted.

Another feature to note about Figure 3.4 concerns the number concentration as a function of size for each HDDV. The scale is set by E55CRC-30 (Figure 3.4D) during the idle/creep cycle, where particle concentrations peaked in the 50-75 nm size bin. The number concentrations fall quite dramatically with this particular HDDV as particle size increases, as expected for an idle/creep cycle. The size distribution of the idle/creep cycle for E55CRC-28 (Figure 3.4B) does not show this type of trend though, which is particularly interesting since they are of the same make/model and year (and E55CRC-28 has higher engine mileage). Another interesting note is in regards to E55CRC-31 which ran the 5-cycle test at simulated on-axle weight loads of 56,000 lbs and 66,000 lbs (Figures 3.4F, 3.4G). The particulate emissions for the 66,000 lbs test were a little over 1.5 times more per size bin than for the 56,000 lbs test. However, it is noticeable that for each size bin, the relative particle composition remains fairly constant between the two

loads. Another trend that can be noted from all the HDDVs (excluding E55CRC-30) is that particle number concentrations over all size bins (50-294 nm) tend to increase with older HDDV models.

### 3.4.3 Particle Composition as a Function of Driving Cycle & HDDV

Prior HDDV exhaust studies have included in-depth analysis of particle size distributions based on engine load and speed [*Khalek et al.*, 2003; *Kwon et al.*, 2003; *Lehmann et al.*, 2003; *Lyyranen et al.*, 1999a; *Moosmuller et al.*, 2001; *Reilly et al.*, 1998; *Sakurai et al.*, 2003a; *Schauer et al.*, 1999; *Shi et al.*, 2000; *Virtanen et al.*, 2004]. For this study, size information was obtained with the UF-ATOFMS instrument as well as with a scanning mobility particle sizer (SMPS). The SMPS provides an accurate representation of the particle number concentrations and was used in this study to scale the UF-ATOFMS data. The average size distributions (from SMPS) for all HDDVs during each of the five-cycle tests are shown in Figure 3.5. While each of these represents an average for all HDDVs tested on each cycle, the general size profile for each stage of the 5-cycle test is relatively consistent for each HDDV. Figure 3.5 shows that particle number concentrations peak in the ultrafine size mode under lower engine loads during the idle and creep cycles (lower rpm), which is consistent with the aforementioned studies. Also, as engine loads increase (increasing rpm), the particle number concentrations go down in the ultrafine mode and shift more to the accumulation mode range (transient, cruise, HHDDT). The vertical dashed lines on the plot indicate the particle sizing range of the UF-ATOFMS. Since the lower particle size limit of the

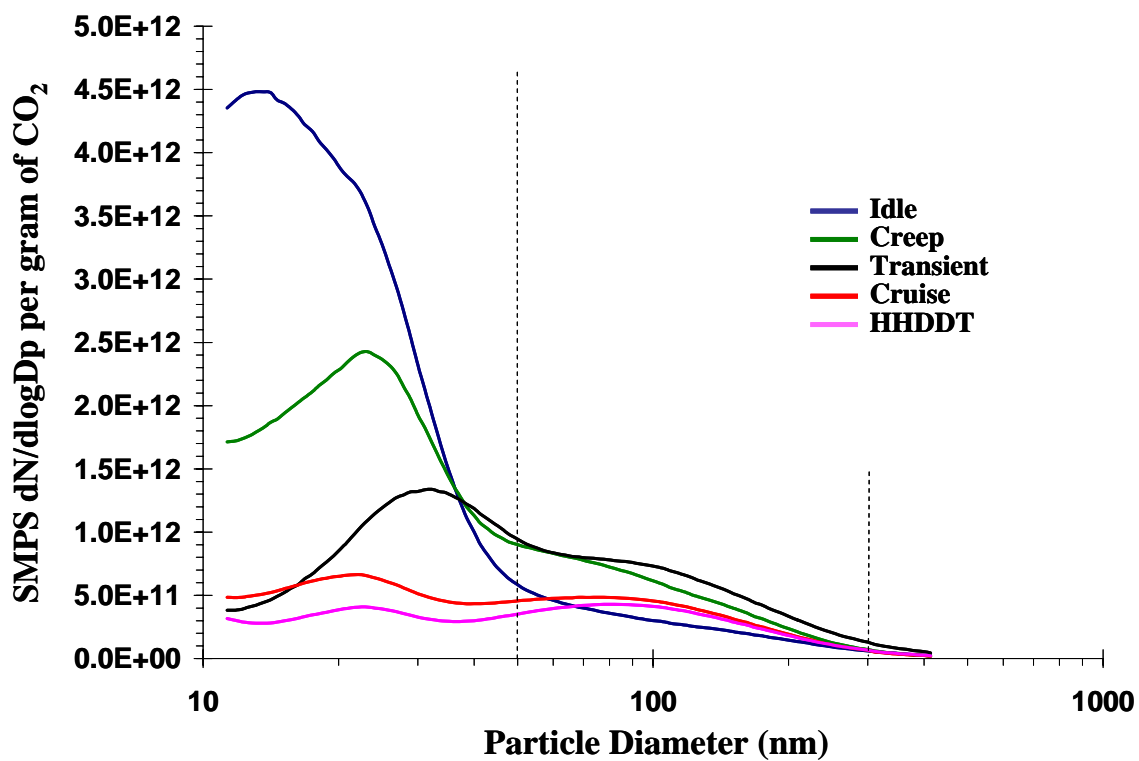


**Figure 3.5** Average SMPS size distributions for all HDDVs during the 5-cycle tests. The vertical dashed lines represent the sizing range of the UF-ATOFMS.

UF-ATOFMS is 50 nm, the relative ordering of particle number concentrations produced during each cycle will be different for the UF-ATOFMS.

It is expected that different HDDVs will have somewhat different particle compositions in their exhaust. Differences in fuel, oil, engine technology and engine wear play a role in these particle composition variations. Figure 3.6(A-I) shows the UF-ATOFMS particle classes scaled to the SMPS number concentrations per gram of CO<sub>2</sub> for each HDDV on each test cycle. The measured CO<sub>2</sub> concentrations for each cycle are also included in this plot to show the trend of CO<sub>2</sub> emission. Since the UF-ATOFMS is unable to detect particles below 50 nm, the number concentration trends per cycle for these plots in Figure 3.6 will follow the trend for each cycle within the dashed lines shown in Figure 3.5. Also, the data from each plot in Figure 3.6 have been multiplied by a factor (indicated on each plot) to keep them all on the same scale.

As shown, the specific driving conditions can produce different types of particles. This is more clearly shown for the minor classes, as they can occur in relatively high abundance for just one cycle for a particular HDDV. E55CRC-27 and 30 show the most variation due to a major contribution from OC particles. These plots (as well as those in Figure 3.4) show that not all HDDVs produce the same abundance of particle types. This is even true for E55CRC-28 and -30 (Figure 3.6B-E), which are the same make/model and year, but emit different amounts of the same particle types on the same driving cycles.

Since there were only six HDDVs tested in this study, it is difficult to make generalizations for all HDDVs and driving cycles based on these results. One trend that remains consistent is the presence of the top particle class (*EC, Ca, OC, Phosphate*) for



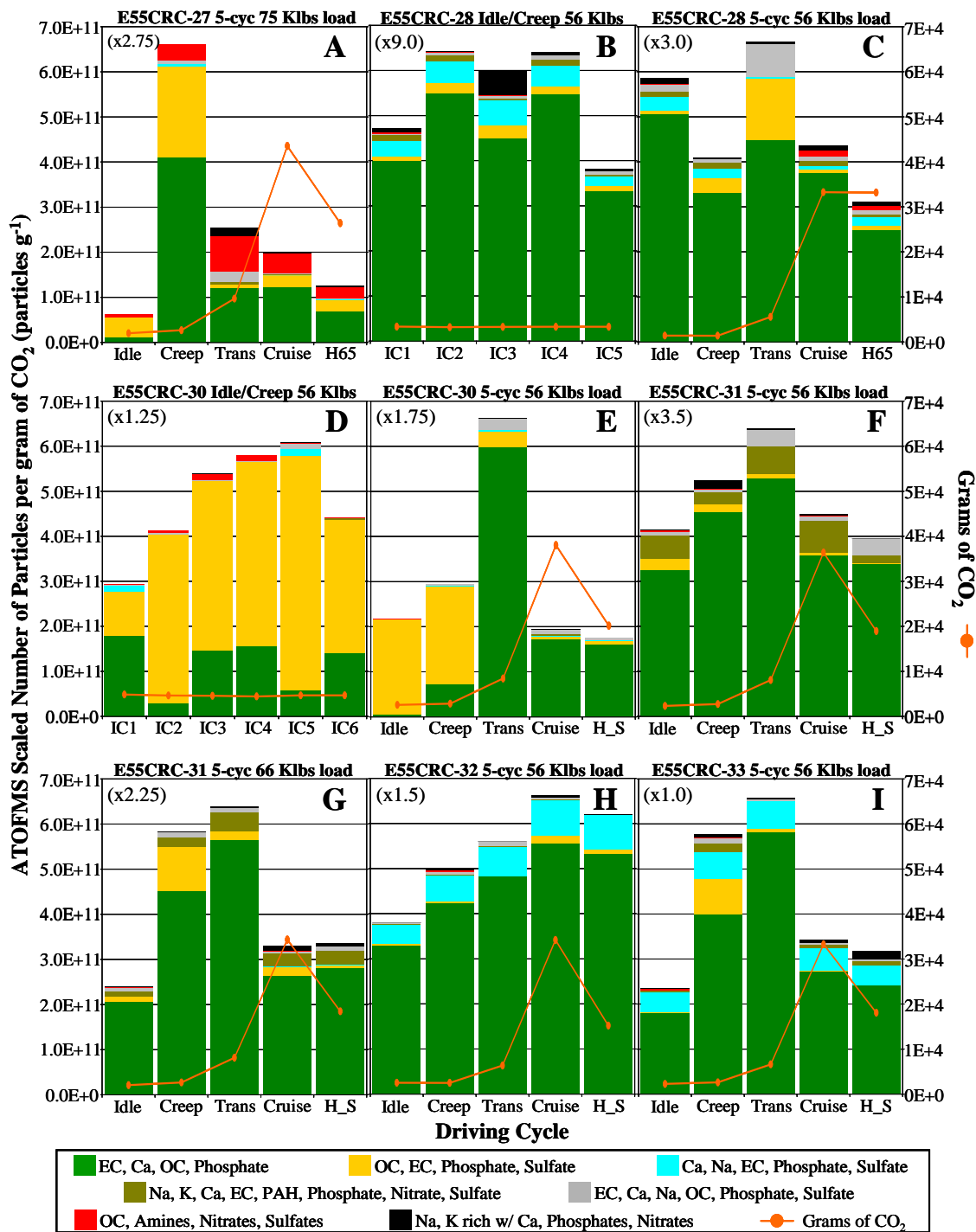


**Figure 3.6 (A – I),** UF-ATOFMS particle classes scaled number to SMPS per gram of CO<sub>2</sub> for each HDDV on each test cycle. Measured CO<sub>2</sub> concentrations for each cycle are included for each HDDV. The simulated on-axis weight load is provided for each HDDV. *Note: The high-speed HHDDT65 cycle is denoted as H65, and the modified high-speed HDDT\_S cycle is denoted as H\_S.*

all HDDVs tested. While this may not have always been the dominant class for every cycle and size bin, it was consistently emitted from each HDDV tested and may therefore be useful for ambient apportionment purposes as discussed later. In general, only one HDDV (E55CRC-30) emitted high amounts of OC particles both in number concentration measured with the UF-ATOFMS and mass concentration measured on filters by the Kleeman group [Robert *et al.*, 2007].

### 3.4.4 Composition and Reproducibility Over a Larger Size Range

A previous study on HDDV particle emissions was conducted with a standard inlet ATOFMS on the same dynamometer system in Riverside, CA in 2001 [Shields *et al.*, 2007]. While the ATOFMS instrument used for the HDDV earlier study was tuned to characterize particles down to 100 nm, it had a much lower transmission efficiency for smaller particles than the UF-ATOFMS [Su *et al.*, 2004]. The size overlap allows for comparison of particle types detected by two different ATOFMS instruments; however, it is important to note that the UF-ATOFMS will have better compositional statistics at smaller sizes based on its higher transmission efficiency.

As with the particle classes observed in this study, the top particle classes from the 2001 study were dominated by particles attributed to EC and diesel lubricating oil. With the standard inlet ATOFMS, as particle size becomes smaller, the classes match well with those obtained with UF-ATOFMS. The top particle class seen with both instruments in the 100 to 300nm size range is the *EC, Ca, OC, Phosphate* type. When the ion intensities between the two weight matrices are plotted against each other, an  $R^2$  value of 0.95 is obtained for the top ART-2a cluster of this class between the two studies.

The other main class seen with the standard inlet ATOFMS matches the third most abundant class (*Ca*, *Na*, *EC*, *Phosphate*, *Sulfate*) seen with the UF-ATOFMS and also shows a strong correlation ( $R^2 = 0.95$ ). The sixth and seventh classes are also seen in this overlapping size range between the two studies with  $R^2$  correlations of 0.88 and 0.87. The other particle types detected with the UF-ATOFMS (the 2<sup>nd</sup>, 4<sup>th</sup>, and 5<sup>th</sup> classes listed in this paper) were also observed in the previous study with the standard inlet instrument; however, the particle counts for these types were not sufficient to be included as their own classes and were grouped into a “minor classes” category. Because of the overall higher transmission of particles in this size range in the UF-ATOFMS, there is a better statistical representation of the classes containing fewer particles that allows them to be classified into their own distinct chemical category with the UF-ATOFMS.

The above evaluation focuses on the comparison of particle signatures only for particles of the same size. When comparing the composition of all particle sizes, both instruments detected similar OC and EC particle types; however, the ordering of abundance changes. Such classes include the top class, the third class, the sixth class and the seventh class with  $R^2$  correlations of 0.89, 0.81, 0.78 and 0.76 respectively. These correlations were higher than expected given that the two instruments detect the majority of their particles in different size ranges. In general, for particles classified as the same type in the two studies, the larger particles detected with the standard inlet ATOFMS show more aged/complex spectra than those detected with the UF-ATOFMS for the same classified particle type in the smaller sizes. Specifically, higher mass EC ion peaks and more negative ion peaks were detected from particles with the standard inlet ATOFMS than with the UF-ATOFMS, which is reflected in the lower  $R^2$  correlations for the EC

types. This could be reflective of larger soot agglomerates at larger sizes leading to more extensive EC carbon cluster ion patterns [Park *et al.*, 2004b; Van Gulijk *et al.*, 2004]. The fact that the chemistry and particle types do not change significantly as particle size increases, only the intensities increase, suggests that particle growth via agglomeration is the main growth mechanism for these particles types. In the atmosphere, since particle composition can be affected by gases and particles from different sources with different compositions, one might expect larger ambient particles to have distinctly different compositions than smaller particles [Jacobson and Seinfeld, 2004]. In fact, this is indeed what is observed in ambient ATOFMS studies. For a further description of the unique larger particles detected with the standard inlet instrument, see Shields *et al.*, 2007.

### **3.4.5 Prospects for Apportionment**

One of the key goals of this study involved obtaining source signatures for HDDVs that can be used for source apportionment of ambient particles. A question exists as to whether mass spectral signatures from different sources obtained from laboratory and dynamometer experiments can be detected during ambient studies and used for source apportionment. Part of this comes from concern that the particle sizes and compositions sampled from the tailpipe of HDDVs (through the dilution and residence systems) do not properly mimic the dilution and aging that occurs on these particles in real on-road driving [Graskow *et al.*, 2000; Kawai *et al.*, 2004]. Certain sources, such as sea salt, dust, light duty gasoline powered vehicles, biomass burning, coal combustion, meat cooking, and fireworks have proven to be readily distinguishable in ATOFMS ambient measurements by using source signatures to apportion them [Gard

*et al.*, 1998; Guazzotti *et al.*, 2003; Liu *et al.*, 1997; Liu *et al.*, 2003; Silva *et al.*, 2000; Silva *et al.*, 1999; Sodeman *et al.*, 2005; Suess, 2002]. A far bigger challenge involves distinguishing exhaust particles from gasoline and diesel powered vehicles in an ambient environment. Comparing the source signatures for gasoline powered light duty vehicles (LDV) obtained in Sodeman *et al.* [Sodeman *et al.*, 2005] versus those obtained for HDDV with UF-ATOFMS has shown that the particles from these sources are distinguishable from one another and will be described in further detail in the following chapters [Toner *et al.*, 2007]. In short, some features that can be used to distinguish HDDV from LDV are more intense peaks for calcium and phosphate, and the intensity of the peak at  $^{36}\text{C}_3^+$  is greater than that of  $^{12}\text{C}_1^+$  in EC particles emitted from HDDV particles. While there is some similarity between LDV and HDDV exhaust particle types, they are mathematically discernible with ART-2a.

Figure 3.7 displays the top three ART-2a clusters/classes from this HDDV characterization study compared to the 1<sup>st</sup>, 9<sup>th</sup>, and 5<sup>th</sup> most abundant classes observed with the UF-ATOFMS sampling alongside a freeway (in the 50 – 300 nm size range). When ion peak intensities for each  $m/z$  of the weight matrices (representative spectra) in the classes being compared are plotted against one another, very close correlations exist with  $R^2$  values of 0.89, 0.95, and 0.97 for HDV1-FWY1, HDV2-FWY9, and HDV3-FWY5 respectively. As shown here, the dynamometer classes are detected in ambient air with almost identical signatures at the single particle level, thus showing promise that dynamometer signatures can be used for future ambient source apportionment. A more detailed analysis of the ambient freeway study concerning the ability to match fresh

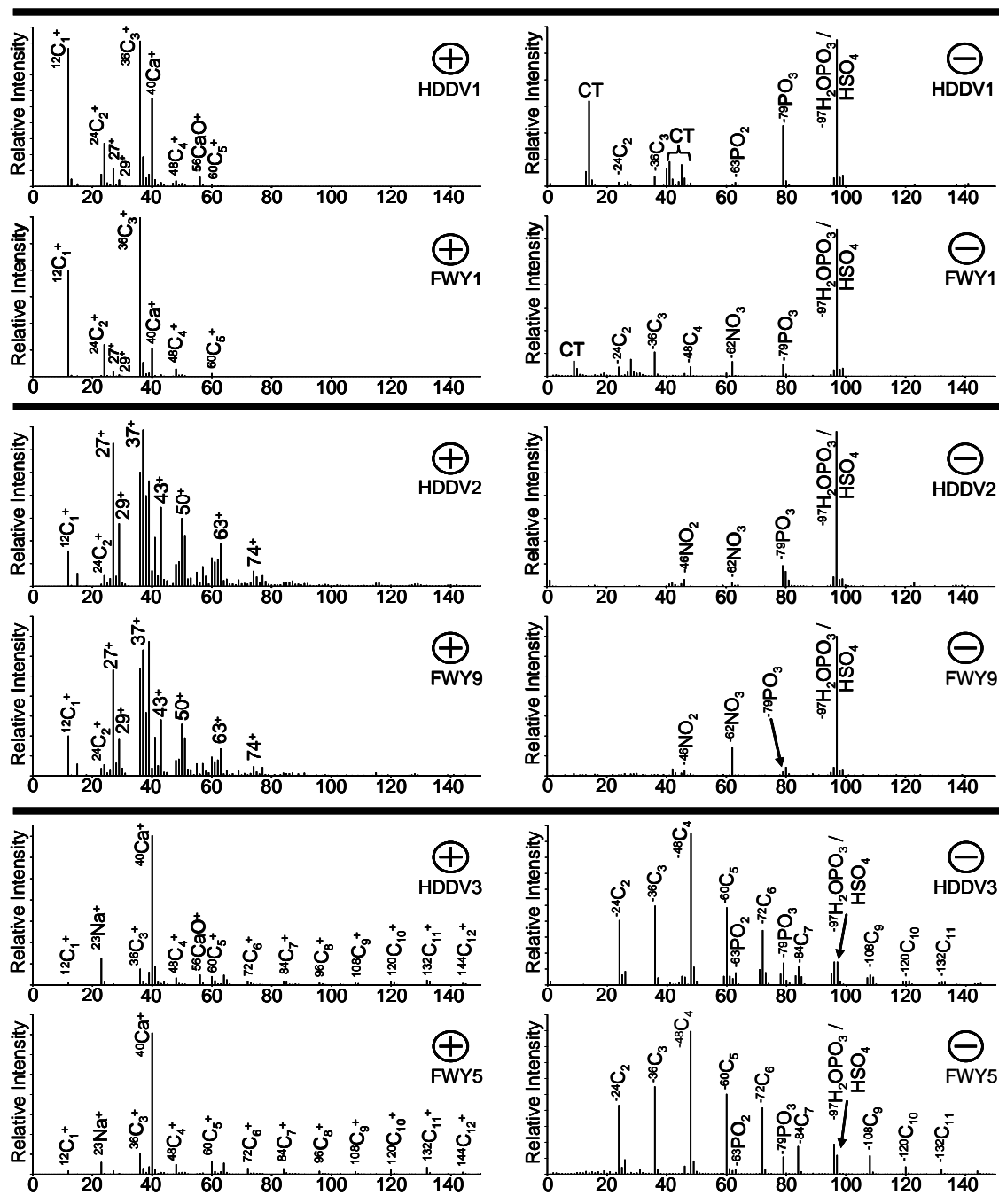


**Figure 3.7** Comparison of the top three HDDV particle classes with those observed of the same type in an ambient freeway study with the UF-ATOFMS. HDDV classes are labeled as HDDV# (+/-) and the classes from the freeway study are labeled as Fwy# (+/-). The “#” for HDDV and Fwy refers to the cluster result as classified with ART-2a. The freeway study was classified using the same ART-2a parameters as the HDDV study. Similar classes are placed side-by-side.

dynamometer emissions with fresh ambient roadside emissions will be discussed in the following chapters. The issue of ambient aging and how this affects apportionment will also be addressed.

### **3.5 Acknowledgements**

The authors thank Nigel Clark and the personnel at the WVU portable HDDV dynamometer facility in Riverside, CA (including Tom Long, Curt Leasor, Chris Rowe and Adam Leach) for their assistance in vehicle testing providing gas phase data. We also sincerely thank Michael Kleeman, Michael Robert, and Chris Jakober for operating the secondary dilution and residence chamber. Lastly, we thank William Vance from the California Air Resources Board (CARB) for all the help he provided with the WVU data. Funding for this project was supplied by CARB – Contract 00-331.

Chapter 2 is reproduced with permission from Toner S.M., D.A. Sodeman, and K.A. Prather, Single particle characterization of ultrafine and accumulation mode particles from heavy duty diesel vehicles using aerosol time-of-flight mass spectrometry, *Environmental Science & Technology*, 40 (12), 3912-3921, 2006. Copyright 2006, American Chemical Society.

### 3.6 References

- Angelino, S., D.T. Suess, and K.A. Prather, Formation of Aerosol Particles from Reactions of Secondary and Tertiary Alkylamines: Characterization by Aerosol Time-of-Flight Mass Spectrometry, *Environmental Science and Technology*, 35 (15), 3130-3138, 2001.
- Arens, F., L. Gutzwiller, U. Baltensperger, H.W. Gaeggeler, and M. Ammann, Heterogeneous Reaction of NO<sub>2</sub> on Diesel Soot Particles, *Environmental Science and Technology*, 35 (11), 2191-2199, 2001.
- Bata, R., N. Clark, M. Gautam, A. Howell, T. Long, J. Loth, D. Lyons, G. Palmer, J. Smith, and W. Wang, A Transportable Heavy Duty Engine Testing Laboratory, *SAE Trans.*, 100, 433-440, 1991.
- Burtscher, H., S. Kunzel, and C. Huglin, Characterization of Particles in Combustion Engine Exhaust, *Journal of Aerosol Science*, 29 (4), 389-396, 1998.
- Canagaratna, M.R., J.T. Jayne, D.A. Ghertner, S. Herndon, Q. Shi, J.L. Jimenez, P.J. Silva, P. Williams, T. Lanni, F. Drewnick, K.L. Demerjian, C.E. Kolb, and D.R. Worsnop, Chase studies of particulate emissions from in-use New York City vehicles, *Aerosol Science & Technology*, 38 (6), 555-573, 2004.
- Clark, N.N., M. Gautam, R.M. Bata, W.-G. Wang, J.L. Loth, G.M. Palmer, and D.W. Lyons, Technical Report: Design and operation of a new transportable laboratory for emissions testing of heavy duty trucks and buses, *Int. J. of Vehicle Design*, 2 (3/4), 308-322, 1995.
- Dybdahl, M., L. Risom, J. Bornholdt, H. Autrup, S. Loft, and H. Wallin, Inflammatory and genotoxic effects of diesel particles in vitro and in vivo, *Mutation Research*, 562 (1-2), 119-131, 2004.
- Gard, E.E., M.J. Kleeman, D.S. Gross, L.S. Hughes, J.O. Allen, B.D. Morrical, D.P. Fergenson, T. Dienes, M.E. Galli, R.J. Johnson, G.R. Cass, and K.A. Prather, Direct observation of heterogeneous chemistry in the atmosphere, *Science (Washington, D. C.)*, 279 (5354), 1184-1187, 1998.
- Gautam, M., K. Chitoor, M. Durbha, and J.C. Summers, Effect of diesel soot contaminated oil on engine wear - investigation of novel oil formulations, *Tribology International*, 32 (12), 687-699, 1999.
- Graskow, B.R., M.R. Ahmadi, J.E. Morris, and D.B. Kittelson, Influence of fuel additives and dilution conditions on the formation and emission of exhaust particulate matter from a direct injection spark ignition engine, *Society of Automotive*



- Engineers, [Special Publication] SP, SP-1551 (Diesel and Gasoline Performance and Additives)*, 261-271, 2000.
- Guazzotti, S.A., D.T. Suess, K.R. Coffee, P.K. Quinn, T.S. Bates, A. Wisthaler, A. Hansel, W.P. Ball, R.R. Dickerson, C. Neususs, P.J. Crutzen, and K.A. Prather, Characterization of carbonaceous aerosols outflow from India and Arabia: biomass/biofuel burning and fossil fuel combustion, *Journal of Geophysical Research, [Atmospheres]*, 108 (D15), ACL13/1-ACL13/14, 2003.
- Harrison, R.M., R. Tilling, M.S.C. Romero, S. Harrad, and K. Jarvis, A study of trace metals and polycyclic aromatic hydrocarbons in the roadside environment, *Atmospheric Environment*, 37 (17), 2391-2402, 2003.
- Hildemann, L.M., G.R. Cass, and G.R. Markowski, A dilution stack sampler for collection of organic aerosol emissions: design, characterization and field tests, *Aerosol Science and Technology*, 10 (1), 193-204, 1989.
- Hopke, P.K., and X.H. Song, Classification of Single Particles by Neural Networks Based on the Computer-Controlled Scanning Electron Microscopy Data, *Analytica Chimica Acta*, 348 (1-3), 375-388, 1997.
- Hughey, C.A., C.L. Hendrickson, R.P. Rodgers, and A.G. Marshall, Elemental composition analysis of processed and unprocessed diesel fuel by electrospray ionization Fourier transform ion cyclotron resonance mass spectrometry, *Energy & Fuels*, 15 (5), 1186-1193, 2001.
- Jacobson, M.Z., and J.H. Seinfeld, Evolution of nanoparticle size and mixing state near the point of emission, *Atmospheric Environment*, 38 (13), 1839-1850, 2004.
- Jayne, J.T., D.C. Leard, X. Zhang, P. Davidovits, K.A. Smith, C.E. Kolb, and D.R. Worsnop, Development of an aerosol mass spectrometer for size and composition analysis of submicron particles, *Aerosol Science and Technology*, 33 (1-2), 49-70, 2000.
- Jung, H., D.B. Kittelson, and M.R. Zachariah, The influence of engine lubricating oil on diesel nanoparticle emissions and kinetics of oxidation, *Society of Automotive Engineers, [Special Publication] SP, SP-1802 (Diesel Particulate Systems, Engines and Components, and Engine Performance Additives)*, 217-226, 2003.
- Kawai, T., Y. Goto, and M. Odaka, Influence of dilution process on engine exhaust nanoparticles, *Society of Automotive Engineers, [Special Publication] SP, SP-1862 (Emissions Measurement & Testing)*, 113-119, 2004.
- Khalek, I.A., M. Spears, and W. Charmley, Particle size distribution from a heavy-duty diesel engine: Steady-state and transient emission measurement using two dilution

- systems and two fuels, *Society of Automotive Engineers, [Special Publication] SP, SP-1755* (Diesel Emission Measurement and Modeling), 1-11, 2003.
- Kittelson, D.B., Engines and Nanoparticles - a Review, *Journal of Aerosol Science*, 29 (5-6), 575-588, 1998.
- Kleeman, M.J., J.J. Schauer, and G.R. Cass, Size and composition distribution of fine particulate matter emitted from motor vehicles, *Environmental Science and Technology*, 34 (7), 1132-1142, 2000.
- Kwon, S.-B., K.W. Lee, K. Saito, O. Shinozaki, and T. Seto, Size-Dependent Volatility of Diesel Nanoparticles: Chassis Dynamometer Experiments, *Environmental Science and Technology*, 37 (9), 1794-1802, 2003.
- Lehmann, U., M. Mohr, T. Schweizer, and J. Rutter, Number size distribution of particulate emissions of heavy-duty engines in real world test cycles, *Atmospheric Environment*, 37 (37), 5247-5259, 2003.
- Liu, D.-Y., D. Rutherford, M. Kinsey, and K.A. Prather, Real-Time Monitoring of Pyrotechnically Derived Aerosol Particles in the Troposphere, *Analytical Chemistry*, 69 (10), 1808-1814, 1997.
- Liu, D.-Y., R.J. Wenzel, and K.A. Prather, Aerosol time-of-flight mass spectrometry during the Atlanta Supersite Experiment: 1. Measurements, *Journal of Geophysical Research, [Atmospheres]*, 108 (D7), SOS 14/1-SOS 14/16, 2003.
- Lowenthal, D.H., B. Zielinska, J.C. Chow, J.G. Watson, M. Gautam, D.H. Ferguson, G.R. Neuroth, and K.D. Stevens, Characterization of heavy-duty diesel vehicle emissions, *Atmospheric Environment*, 28 (4), 731-43, 1994.
- Lyyranen, J., J. Jokiniemi, E.I. Kauppinen, and J. Joutsensaari, Aerosol characterisation in medium-speed diesel engines operating with heavy fuel oils, *Journal of Aerosol Science*, 30 (6), 771-784, 1999a.
- Lyyranen, J., J. Jokiniemi, E.I. Kauppinen, and J. Joutsensaari, Aerosol characterization in medium-speed diesel engines operating with heavy fuel oils, *Journal of Aerosol Science*, 30 (6), 771-784, 1999b.
- McDonald, J.D., B. Zielinska, E.M. Fujita, J.C. Sagebiel, J.C. Chow, and J.G. Watson, Fine particle and gaseous emission rates from residential wood combustion, *Environmental Science & Technology*, 34 (11), 2080-2091, 2000.
- Moosmuller, H., W.P. Arnott, C.F. Rogers, J.L. Bowen, J.A. Gillies, W.R. Pierson, J.F. Collins, T.D. Durbin, and J.M. Norbeck, Time resolved characterization of diesel

- particulate emissions. 1. Instruments for particle mass measurements, *Environmental Science & Technology*, 35 (4), 781-787, 2001.
- Okada, S., C.-B. Kweon, J.C. Stetter, D.E. Foster, M.M. Shafer, C.G. Christensen, J.J. Schauer, A.M. Schmidt, A.M. Silverberg, and D.S. Gross, Measurement of trace metal composition in diesel engine particulate and its potential for determining oil consumption: ICPMS (inductively coupled plasma mass spectrometer) and ATOFMS (Aerosol time of Flight mass spectrometer) measurements, *Society of Automotive Engineers, [Special Publication] SP, SP-1737* (CI Engine Combustion Processes & Performance with Alternative Fuels), 59-72, 2003.
- Park, K., D.B. Kittelson, and P.H. McMurry, Structural properties of diesel exhaust particles measured by transmission electron microscopy (TEM): Relationships to particle mass and mobility, *Aerosol Science & Technology*, 38 (9), 881-889, 2004a.
- Park, K., D.B. Kittelson, M.R. Zachariah, and P.H. McMurry, Measurement of Inherent Material Density of Nanoparticle Agglomerates, *Journal of Nanoparticle Research*, 6 (2-3), 267-272, 2004b.
- Pourazar, J., A.J. Frew, A. Blomberg, R. Helleday, F.J. Kelly, S. Wilson, and T. Sandstrom, Diesel exhaust exposure enhances the expression of IL-13 in the bronchial epithelium of healthy subjects, *Respiratory Medicine*, 98 (9), 821-5., 2004.
- Reed, M.D., A.P. Gigliotti, J.D. McDonald, J.C. Seagrave, S.K. Seilkop, and J.L. Mauderly, Health Effects of Subchronic Exposure to Environmental Levels of Diesel Exhaust, *Inhalation Toxicology*, 16 (4), 177-193, 2004.
- Reilly, P.T.A., R.A. Gieray, W.B. Whitten, and J.M. Ramsey, Real-Time Characterization of the Organic Composition and Size of Individual Diesel Engine Smoke Particles, *Environmental Science and Technology*, 32 (18), 2672-2679, 1998.
- Rhead, M.M., and S.A. Hardy, The sources of polycyclic aromatic compounds in diesel engine emissions, *Fuel*, 82 (4), 385-393, 2003.
- Robert, M.A., C.A. Jakober, and M.J. Kleeman, Size and composition distributions of particulate matter emissions 2. Heavy duty diesel vehicles, *submitted for publication*, 2007.
- Rudnick, L.R., *Lubricant additives : chemistry and applications*, xiii, 735 pp., Marcel Dekker, New York, 2003.

- Sakurai, H., K. Park, P.H. McMurry, D.D. Zarling, D.B. Kittelson, and P.J. Ziemann, Size-Dependent Mixing Characteristics of Volatile and Nonvolatile Components in Diesel Exhaust Aerosols, *Environmental Science and Technology*, 37 (24), 5487-5495, 2003a.
- Sakurai, H., H.J. Tobias, K. Park, D. Zarling, K.S. Docherty, D.B. Kittelson, P.H. McMurry, and P.J. Ziemann, On-line measurements of diesel nanoparticle composition and volatility, *Atmospheric Environment*, 37 (9-10), 1199-1210, 2003b.
- Schauer, J.J., M.J. Kleeman, G.R. Cass, and B.R.T. Simoneit, Measurement of emissions from air pollution sources. 2. C-1 through C-30 organic compounds from medium duty diesel trucks, *Environmental Science & Technology*, 33 (10), 1578-1587, 1999.
- Schoolcraft, T.A., G.S. Constable, B. Jackson, L.V. Zhigilei, and B.J. Garrison, Molecular dynamics simulations of laser disintegration of amorphous aerosol particles with spatially nonuniform absorption, *Nuclear Instruments & Methods in Physics Research, Section B: Beam Interactions with Materials and Atoms*, 180, 245-250, 2001.
- Schoolcraft, T.A., G.S. Constable, L.V. Zhigilei, and B.J. Garrison, Molecular dynamics simulation of the laser disintegration of aerosol particles, *Analytical chemistry*, 72 (21), 5143-50., 2000.
- Shi, J.P., D. Mark, and R.M. Harrison, Characterization of particles from a current technology heavy-duty diesel engine, *Environmental Science & Technology*, 34 (5), 748-755, 2000.
- Shields, L.G., D.T. Suess, and K.A. Prather, Determination of single particle mass spectral signatures from heavy duty diesel vehicle emissions for PM<sub>2.5</sub> source apportionment, *Atmospheric Environment*, 41 (18), 3841-3852, 2007.
- Silva, P.J., R.A. Carlin, and K.A. Prather, Single particle analysis of suspended soil dust from Southern California, *Atmospheric Environment*, 34 (11), 1811-1820, 2000.
- Silva, P.J., D.-Y. Liu, C.A. Noble, and K.A. Prather, Size and Chemical Characterization of Individual Particles Resulting from Biomass Burning of Local Southern California Species, *Environmental Science and Technology*, 33 (18), 3068-3076, 1999.
- Silva, P.J., and K.A. Prather, Interpretation of mass spectra from organic compounds in aerosol time-of-flight mass spectrometry, *Analytical Chemistry*, 72 (15), 3553-3562, 2000.

- Sodeman, D.A., S.M. Toner, and K.A. Prather, Determination of single particle mass spectral signatures from light duty vehicle emissions, *Environmental Science & Technology*, 39 (12), 4569-4580, 2005.
- Song, X.H., P.K. Hopke, D.P. Fergenson, and K.A. Prather, Classification of single particles analyzed by ATOFMS using an artificial neural network, ART-2A, *Analytical Chemistry*, 71(4), 860-865, 1999.
- Spencer, M.T., and K.A. Prather, Using ATOFMS to determine OC/EC mass fractions in particles, *Aerosol Science and Technology*, 40 (8), 585-594, 2006.
- Spencer, M.T., L.G. Shields, S.M. Toner, D.A. Sodeman, and K.A. Prather, Comparison of oil and fuel particle chemical signatures with particle emissions from heavy and light duty vehicles, *Atmospheric Environment*, 40 (27), 5224-5235, 2006.
- Su, Y., M.F. Sipin, H. Furutani, and K.A. Prather, Development and characterization of an aerosol time-of-flight mass spectrometer with increased detection efficiency, *Analytical Chemistry*, 76 (3), 712-719, 2004.
- Suess, D.T., Single particle mass spectrometry combustion source characterization and atmospheric apportionment of vehicular, coal, and biofuel exhaust emission, Ph.D. thesis, University of California, Riverside, Riverside, 2002.
- Suess, D.T., and K.A. Prather, Reproducibility of single particle chemical composition during a heavy duty diesel truck dynamometer study, *Aerosol Science and Technology*, 36 (12), 1139-1141, 2002.
- Tobias, H.J., D.E. Beving, P.J. Ziemann, H. Sakurai, M. Zuk, P.H. McMurry, D. Zarling, R. Waytulonis, and D.B. Kittelson, Chemical Analysis of Diesel Engine Nanoparticles Using a Nano-DMA/Thermal Desorption Particle Beam Mass Spectrometer, *Environmental Science and Technology*, 35 (11), 2233-2243, 2001.
- Tobias, H.J., P.M. Kooiman, K.S. Docherty, and P.J. Ziemann, Real-time chemical analysis of organic aerosols using a thermal desorption particle beam mass spectrometer, *Aerosol Science and Technology*, 33 (1-2), 170-190, 2000.
- Toner, S.M., L.G. Shields, D.A. Sodeman, and K.A. Prather, Using mass spectral source signatures to apportion exhaust particles from gasoline and diesel powered vehicles in a freeway study using UF-ATOFMS., *Atmospheric Environment*, doi:10.1016/j.atmosenv.2007.08.005, 2007.
- Van Gulijk, C., J.C.M. Marijnissen, M. Makkee, J.A. Moulijn, and A. Schmidt-Ott, Measuring diesel soot with a scanning mobility particle sizer and an electrical low-pressure impactor: performance assessment with a model for fractal-like agglomerates, *Journal of Aerosol Science*, 35 (5), 633-655, 2004.

- Vilhunen, J.K., A. Von Bohlen, M. Schmeling, L. Rantanen, S. Mikkonen, R. Klockenkamper, and D. Klockow, Trace element determination in diesel particulates by total-reflection x-ray fluorescence analysis, *Mikrochimica Acta*, 131 (3-4), 219-223, 1999.
- Virtanen, A.K.K., J.M. Ristimaeki, K.M. Vaaraslahti, and J. Keskinen, Effect of Engine Load on Diesel Soot Particles, *Environmental Science and Technology*, 38 (9), 2551-2556, 2004.
- Walker, A.P., Controlling particulate emissions from diesel vehicles, *Topics in Catalysis*, 28 (1-4), 165-170, 2004.
- Watson, J.G., J.C. Chow, D.H. Lowenthal, L.C. Pritchett, and C.A. Frazier, Differences in the carbon composition of source profiles for diesel- and gasoline-powdered vehicles, *Atmospheric Environment*, 28 (15), 2493-505, 1994.
- Wenzel, R.J., and K.A. Prather, Improvements in ion signal reproducibility obtained using a homogeneous laser beam for on-line laser desorption/ionization of single particles, *Rapid Communications in Mass Spectrometry*, 18 (13), 1525-1533, 2004.
- Xie, Y., P.K. Hopke, and D. Wienke, Airborne Particle Classification with a Combination of Chemical Composition and Shape Index Utilizing an Adaptive Resonance Artificial Neural Network, *Environmental Science & Technology*, 28 (11), 1921-1928, 1994.
- Yanowitz, J., M.S. Graboski, L.B.A. Ryan, T.L. Alleman, and R.L. McCormick, Chassis dynamometer study of emissions from 21 in-use heavy duty diesel vehicles, *Environmental Science & Technology*, 33 (2), 209-216, 1999.
- Zhao, H.W., M.W. Barger, J.K.H. Ma, V. Castranova, and J.Y.C. Ma, Effects of exposure to diesel exhaust particles (DEP) on pulmonary metabolic activation of mutagenic agents, *Mutation Research*, 564 (2), 103-113, 2004.
- Zielinska, B., J. Sagebiel, W.P. Arnott, C.F. Rogers, K.E. Kelly, D.A. Wagner, J.S. Lighty, A.F. Sarofim, and G. Palmer, Phase and Size Distribution of Polycyclic Aromatic Hydrocarbons in Diesel and Gasoline Vehicle Emissions, *Environmental Science and Technology*, 38 (9), 2557-2567, 2004.

# **4 Using mass spectral source signatures to apportion exhaust particles from gasoline and diesel powered vehicles in a freeway study using UF-ATOFMS**

## **4.1 Synopsis**

Single particle mass spectrometry techniques such as aerosol time-of-flight mass spectrometry (ATOFMS) offer a unique approach for on-line source apportionment of ambient aerosols. Source signatures, or mass spectral "fingerprints", have been obtained using ATOFMS from a variety of sources with an emphasis placed on distinguishing between emissions from different types of vehicles. In this study, the signatures from previous source tests of diesel powered heavy duty vehicles (HDDV) and gasoline powered light duty vehicles (LDV) are matched to particle spectra acquired during a freeway-side study performed over a month in southern California to source apportion the particles. Using a relatively high matching (vigilance) factor of 0.85, particle mass spectral signatures from the vehicle source studies matched 83% of the freshly emitted particles detected alongside the freeway. The particle contributions alongside the freeway in the ultrafine and accumulation size range (aerodynamic diameter = 50–300nm) were apportioned to 32% LDV, 51% HDDV, and 17% from other sources. This paper discusses the apportionment process used and the methods used for validation with peripheral instrumentation.

## 4.2 Introduction

Many studies have shown that vehicle emissions represent a major source of pollution in urban areas [*Fruin et al.*, 2001; *Marshall et al.*, 2003; *Mysliwiec and Kleeman*, 2002; *Rogge et al.*, 1993; *Vanvorst and George*, 1997]. With growing concern over the health effects pertaining to pollution from vehicles [*Pope*, 2000; *Riediker et al.*, 2004; *Seagrave et al.*, 2002], a goal of major federal and state agencies is to set regulations which will lead to a reduction of pollutants from these sources. The first step in this process involves distinguishing between the emissions from gasoline powered light duty vehicle (LDV), heavy duty diesel vehicle (HDDV), and other combustion sources in ambient aerosols which will allow state and federal air control agencies to quantify the relative contributions from the major pollution sources and develop effective control strategies.

Several methods have been used for aerosol source apportionment using a variety of techniques. Filter and impactor sampling methods, such as Micro Orifice Uniform Deposit Impactors (MOUDI), are useful in collecting particles that can be chemically analyzed using a variety of off-line techniques. These techniques have proved useful in determining organic markers for various aerosol sources in the atmosphere [*Cass et al.*, 2000; *Kleeman and Cass*, 1998; *Kleeman et al.*, 2000]. On-line measurements are being used more and more for source apportionment. Some of these instruments include Scanning Mobility Particle Sizers (SMPS), where particle source contributions are estimated based on the measured size modes of the particles [*Lehmann et al.*, 2003; *Reilly et al.*, 1998; *Zhang et al.*, 2005]. Other on-line instruments, such as Thermal Desorption Particle Mass Spectrometers (TDPMS) and Aerosol Mass Spectrometers (AMS) have



been used for particle source apportionment as well [*Canagaratna et al.*, 2004; *Tobias et al.*, 2001; *Tobias et al.*, 2000]. However, these thermal desorption techniques are unable to detect refractory components (such as inorganic compounds and elemental carbon), and they do not sample single particles. Single particle techniques such as aerosol time-of-flight mass spectrometry (ATOFMS) provide an alternative method for source apportionment [*Bein et al.*, 2006; *Bhave et al.*, 2001; *Owega et al.*, 2004; *Silva et al.*, 1999]. The ATOFMS uses a laser to desorb and ionize species from individual particles and thus can detect all chemical species (refractory and non-refractory) of each particle simultaneously with a dual polarity time-of-flight mass spectrometer [*Gard et al.*, 1997; *Su et al.*, 2004]. An ultrafine aerosol time-of-flight mass spectrometer (UF-ATOFMS) was used in this study, because the majority of particles emitted in both LDV and HDDV exhaust are in the ultrafine size range (aerodynamic diameter ( $D_a$ ) < 100nm).

The purpose of this study involves determining whether mass spectral signatures obtained from previous vehicle dynamometer characterization studies are representative of those detected in an area with fresh roadside emissions [*Shields et al.*, 2007; *Sodeman et al.*, 2005; *Toner et al.*, 2006]. Logistically, a freeway-side location was chosen in a coastal “clean” environment so there would be little influence from sources other than vehicles. Also, in such a location, the particles would be less aged which would “skew” the mass spectral signatures. A major objective of this study is to test whether the ART-2a neural network clustering algorithm matching method can be used to distinguish mass spectral signatures from very similar vehicle sources. Finally, upon method validation, the goal is to apportion aerosols near the roadway and determine their overall contribution to the total ambient aerosol at the freeway location.

### 4.3 Experimental

This study was conducted in San Diego, California from Jul. 21-Aug. 25, 2004. The sampling site was stationed in a low-use parking lot during the summer on the UCSD campus directly adjacent to the I-5 freeway (GPS position 32°52'49.74"N 117°13'40.95"W) with the sampling line within 10 meters of the freeway. The site housed a suite of instruments including an UF-ATOFMS. This same UF-ATOFMS instrument was used in two previous studies for the characterization of aerosols from LDVs and HDDVs [Sodeman *et al.*, 2005; Toner *et al.*, 2006]. A summary of the instrumentation operated at the site (that will be discussed in this paper) is provided in Table 4.1. Meteorological stations were operated on each side of the freeway for complete wind trajectory information. A digital Webcam was used for freeway traffic monitoring and recorded digital video continuously throughout the study.

Traffic counts were determined by counting individual LDVs and HDDVs on both sides of the freeway for the first five minutes of each hour. The number of vehicles counted in the first five minutes was multiplied by twelve in order to approximate the total LDV and HDDV counts for the entire hour. The LDV fleet consisted primarily of newer vehicles (model year 2000 or newer), which was determined by routine traffic observations and from the video. The HDDV fleet along this portion of the freeway was predominantly tractor trailers, with a much smaller contribution from buses and medium sized diesel delivery trucks.

**Table 4.1** List of instrumentation.

Instrument	Make & Model	Measurement	Units	Sample Resolution	Sampling Period
Ultrafine Aerosol Time-of-Flight Mass Spectrometer (UF-ATOFMS)		size range: 50-300nm		real-time	Jul 21 to Aug 25, 2004
Scanning Mobility Particle Sizer (SMPS)	TSI Model 3936L10	particle number conc. (10-500nm)	#/cm <sup>3</sup>	5 min	Jul 21 to Aug 25, 2004
Aethalometer	Magee Scientific 'Spectrum' AE-3 Series	optical absorption cross-section per unit mass	µg/m <sup>3</sup>	5 min	Jul 21 to Aug 25, 2004
Chemiluminescence NO-NO <sub>2</sub> -NO <sub>x</sub> Analyzer	Thermo Environmental Instruments (TEI) Model 42C	NO & NO <sub>x</sub> concentration levels	ppb	1 min	Aug 5 to Aug 25, 2004
CO Analyzer	Advanced Pollution Instrumentation (API) Model M300	CO concentration levels	ppm	5 min	Jul 30 to Aug 10 & Aug 13 to Aug 25, 2004
Webcam	Creative Model PD1001	traffic video surveillance		1 sec	Jul 21 to Aug 25, 2004

The particle mass spectra from the vehicles studies were previously analyzed and clustered with the ART-2a clustering algorithm as described in Sodeman *et al* and Toner *et al* [Sodeman *et al.*, 2005; Toner *et al.*, 2006]. The ART-2a algorithm and its use for single particle characterization are described in detail elsewhere [Song *et al.*, 1999; Xie *et al.*, 1994]. ART-2a has been compared to other approaches [Rebotier and Prather, 2007] where it is shown that ART-2a yielded very comparable results to other clustering techniques including several variants of hierarchical clustering as well as K-means clustering. For the PM emissions in vehicle studies, the ART-2a parameters used were a vigilance factor (VF) of 0.85, learning rate of 0.05, and 20 iterations. The resulting mass spectral signatures (clusters) were used to apportion particles detected near the freeway using the same ART-2a algorithm, but using a matching approach. The match-ART-2a function (YAADA v1.20 – <http://www.yaada.org>) uses existing ART-2a clusters as source “seeds” for the purpose of determining whether other particles match those seeds. In this case, ART-2a runs normal with prescribed particle clusters unable to be changed by the addition of new particles to each cluster. Since the clusters do not change as particles are matched to them, this function allows the clusters to stay “true” to the original source signature. Particles being considered in the matching are either matched exclusively to a particular cluster (above the VF) or not at all. If a particle matches above the threshold for two or more clusters, it will be added to the one with which yields the highest dot product. The VF used for match-ART-2a for this study is 0.85 which represents a very high VF. If the dynamometer signatures are truly representative of the signatures from vehicles, this VF should be effective because the vehicle emissions are expected to be fresh near the freeway. In a more aged environment, it is likely a lower

VF will be necessary to match a reasonable number of particles. The effect of varying VF for source matching is discussed in Appendix 2.

The results obtained from match-ART-2a were compared to various peripheral data, to validate the results of the matching technique. Such peripheral instruments are described in Table 4.1. The outcome of these comparisons will be discussed below.

## **4.4 Results and discussion**

### **4.4.1 Creation and Comparison of Particle Seeds From Source Studies**

As described in the Experimental section, the particles detected with the UF-ATOFMS during the freeway-side study were analyzed via a matching version of the ART-2a algorithm. The particle clusters used for matching (as the reference library) were obtained in previous LDV and HDDV dynamometer studies [*Shields et al.*, 2007; *Sodeman et al.*, 2005; *Toner et al.*, 2006]. While the papers written on these studies refer to distinct particle classes, these classes are descriptive of the many (~100) ART-2a clusters resulting from the studies. Since ART-2a does not converge, these classes were grouped by running ART-2a and then regrouped using a function that combines resulting ART-2a clusters that match above a set vigilance factor (regrouped VF = 0.90). These regrouped clusters can then be even further grouped based on visual inspection of the ion patterns. Similar clusters that appear to belong within the same “class” as each other based on the presence or absence of key species (i.e. elemental carbon (EC), organic carbon (OC), sulfate, nitrate) are regrouped by hand. Such classes have minor differences in the relative ion peak patterns among their collective clusters, however; the overall chemical species making up each major type of cluster are the same.

For matching purposes, instead of using the combined weight matrices from the regrouped representative particle classes, the top ART-2a clusters that account for ~90% of the particles from each vehicle study were used. Additionally, it was hypothesized that the top particle types detected in the vehicle studies should also be the top types detected in the fresh emissions near the highway. In order to create source seeds more representative of the freeway environment, only particles generated during warm/hot engine conditions for both HDDV and LDV studies were used to make the source seed clusters. These clusters still correspond to their representative classes described in previous papers (as stated earlier), however, there are minor differences in some clusters that make it more advantageous to use the separate ART-2a clusters for matching purposes. In addition, clusters generated by running ART-2a on the UF-ATOFMS freeway detected particles were also incorporated into the source seed library. The majority of these clusters were attributed to HDDVs, as their weight matrices correlated much better to the HDDV library source seeds than to the LDV seeds. The seeds are also separated by size, where ultrafine (50–100nm) and accumulation mode (100–140nm & 140-1000nm) mass spectral libraries have been created for each source. This is done because there are distinct chemical differences for each source based on size, and these size ranges show the largest chemical distinctions. For example, as found in the dynamometer studies using UF-ATOFMS, LDVs produce more organic carbon than elemental carbon particles for sizes above 100 nm. Two separate libraries were made for the accumulation mode to compensate for a regional background elemental carbon particle type that was detected above 140nm during the freeway study. This particle type will be discussed in a future publication [Toner *et al.*, 2007]. For this manuscript, the

matching results obtained from both accumulation mode libraries are combined to represent the UF-ATOFMS accumulation mode results (100-300nm). This was done because the trends in HDDV/LDV apportionment were found to be very similar between the two accumulation mode libraries once the regional background EC particles above 140 nm were identified as non-freeway particles. Further details on the number of seeds in the vehicle source library and the frequency at which they match particles for this study are provided in Appendix 1.

Since HDDVs and LDVs combust chemically similar fuels, it is important to first investigate the similarity between the HDDV and LDV exhaust particle types from the dynamometer source studies. The first method used to compare these particle types involved taking the representative area matrix for each class described for each study and calculating the dot product between them. The area matrices used to represent the particle classes are similar to the weight matrices that ART-2a yields except that the area matrices are not weighted. The area matrices represent an average of all particles within a particular class. Since ART-2a distinguishes particle types bases on their dot products, this type of comparison between the two studies allows one to determine if the area matrices of the general particle types would be distinguishable using ART-2a. Figure 4.1 displays a color mapped table of this comparison, with cooler colors (i.e. blue) indicating less similarity (lower dot product) and warmer colors (i.e. red) indicating more similarity (higher dot product). The labels for the classes are based on the most abundant ion peaks in the mass spectra and are described in detail in previous source characterization manuscripts by Sodeman et al. and Toner et al. [Sodeman *et al.*, 2005; Toner *et al.*, 2006]. Figure 4.1 shows that some of the dot product comparisons between the two

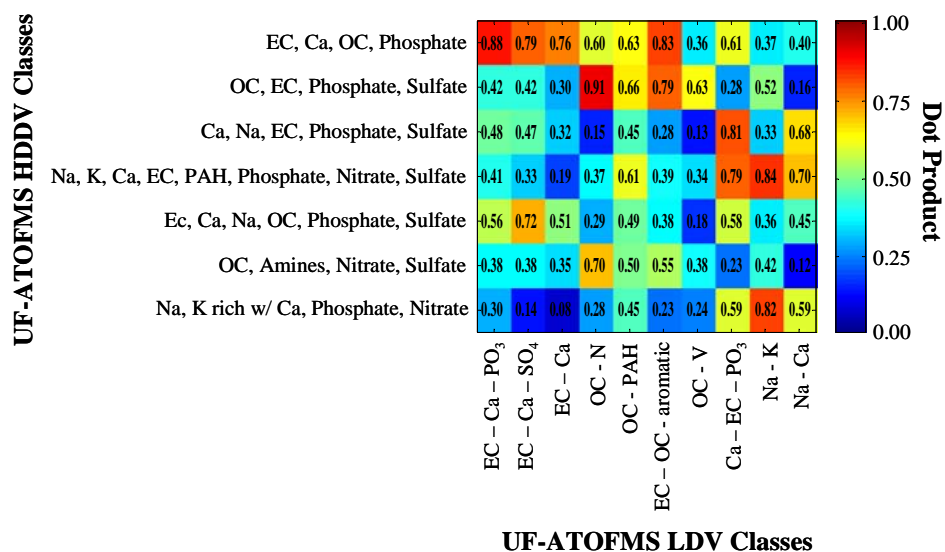


**Figure 4.1** Dot product comparisons of the representative area matrices between the general classes from the HDDV and LDV dynamometer experiments using UF-ATOFMS. Classes are labeled in the same manner as in the manuscripts from Sodeman *et al.* 2005 and Toner *et al.* 2006.



source studies result in strong matches (i.e. orange and red colors). As expected, those classes that match the best are chemically similar types; i.e. the EC, Ca, OC, Phosphate classes from HDDV matching to the EC-Ca-PO<sub>3</sub> class from LDV (note this was produced by a smoking LDV). Also, the OC, EC, Phosphate, and Sulfate classes from HDDV match to the OC-N class from LDV. While these classes have dot products above the vigilance factor used for ART-2a analysis ( $VF = 0.85$ ), they are visually distinct (as described in the two manuscripts) and still readily distinguishable using the matching procedure. One of the major problems with this comparison is the fact that the area matrices represent an average of the particles within the class and are not weighted to the majority. As stated previously though, the representative spectra of the general classes are not used for apportionment matching purposes. Instead, the size segregated mass spectral libraries for HDDV and LDV particles, as described above, are used. Using size information in the apportionment turns out to be quite important because those particles that are chemically similar between sources fall into quite different size ranges.

Another method for comparing the two studies involves taking the particles from the dynamometer studies detected with the UF-ATOFMS and matching them to the HDDV/LDV reference library clusters using a non-exclusive matching process with ART-2a. This process adds a matched particle to HDDV, LDV, or combination of both cluster types if the particle matches above a vigilance factor of 0.85. This method of matching allows for determining the amount of similarity of the particle types between the two studies. Between 19 – 33% of the HDDV dynamometer particles and 30 – 49% of the LDV dynamometer particles matched both the HDDV and LDV reference clusters. These results are shown in Figure 4.2. With such a large degree of overlap between the

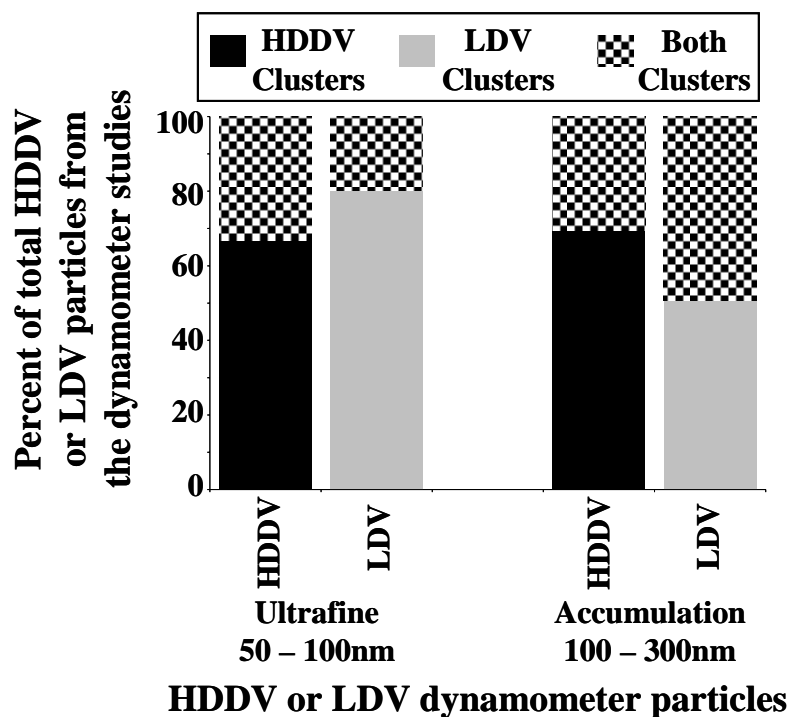


**Figure 4.2** ART-2a matching error analysis using non-exclusive matching of HDDV and LDV dynamometer particles. For each, the fraction of HDDV and LDV particles that matched to the HDDV, LDV, or both HDDV and LDV clusters from the HDDV/LDV reference library are shown for ultrafine (50–100nm) and accumulation (100–300nm) mode particles.

particle types from both clusters, it would appear to be a challenging task to distinguish between HDDV and LDV particles using the ART-2a matching method. This is not the case though as particles within the overlapping region turn out to be quite distinguishable for reasons described below.

The main goal of this paper involves using ART-2a to distinguish between HDDV and LDV particles in an environment dominated by relatively fresh vehicle emissions. To accomplish this, an exclusive matching procedure was used where particles were matched to the HDDV/LDV reference clusters and they either matched exclusively or not at all. If a particle matched to more than one cluster above the vigilance factor, it was placed in the cluster to which it matched the most closely (i.e. the highest dot-product value). If a particle did not match to either HDDV or LDV, it was placed into the “other” category. Particles falling into the “other” category included sea salt, dust, biomass burning, and other sources not related to LDV or HDDV exhaust emissions. Quality assurance of this matching technique was carried out by using the same HDDV/LDV cluster library to match to particles from the previous source studies. The amount of error in matching was calculated based on the number of particles from the known source that matched to the incorrect source. Figure 4.3 shows the matching fraction of particles from each study to the same HDDV/LDV reference library. The most error (mismatching) is about 4%, which occurs for the larger accumulation mode particles from the LDV source particles matching to HDDV clusters within the reference library. Given this low error, this provides confidence in the ART-2a apportionment approach used in this study. The errors associated with matching to the source seeds at varying

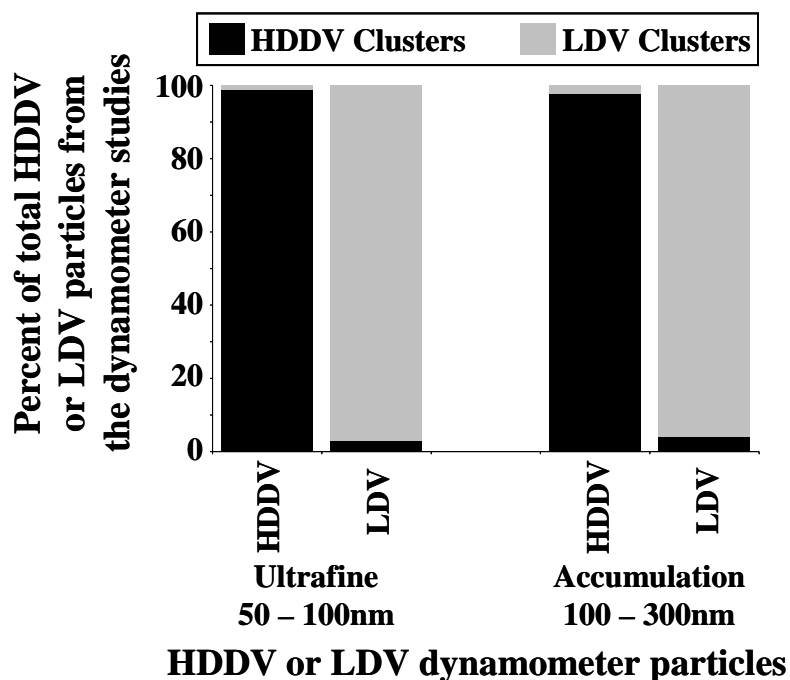


**Figure 4.3** ART-2a matching error analysis using exclusive matching of HDDV and LDV dynamometer particles. For each, the fraction of HDDV and LDV particles that matched to the HDDV or LDV clusters from the HDDV/LDV reference library are shown for ultrafine (50–100nm) and accumulation (100–300nm) mode particles.

VF's, as well as results from using source seeds created at a lower VF, are discussed in Appendix 2.

#### **4.4.2 Particles Detected that Match to HDDV/LDV Source Seeds**

The ART-2a algorithm was used to cluster the particles detected with the UF-ATOFMS during the freeway-side study using a VF of 0.85. This approach creates the top particle types separately from the match-ART-2a technique to determine how closely the resulting clusters compare with those from the vehicle studies. Figure 4.4 (A-D) shows the representative ART-2a weight matrices (WM) /spectra from this analysis that match to the top particle types from the dynamometer studies. The top particle classes from the HDDV and LDV vehicle source characterization studies were used for this comparison because they should theoretically be the top particle types seen in a vehicle dominated environment. Indeed, this is the case, where the majority of the top ten freeway ART-2a results match to the top HDDV dynamometer classes. The top HDDV particle type detected from the dynamometer studies is the top type detected during this freeway-side study (as shown in Figure 4.4A) and matches with an  $R^2$  of 0.97 when the  $m/z$  peak pattern and intensities are plotted against each other. Figure 4.4B shows the second most abundant type from the HDDV dynamometer studies compared to the second most abundant type detected during the freeway study which matches with an  $R^2$  of 0.98. This particle class is also the most abundant type detected in 100 – 400 nm particles detected with a standard inlet ATOFMS [Shields *et al.*, 2007]. The spectra shown in Figure 4.4C represent the third cluster from the freeway ART-2a results which match the top LDV type from the dynamometer study with an  $R^2$  of 0.99. The last

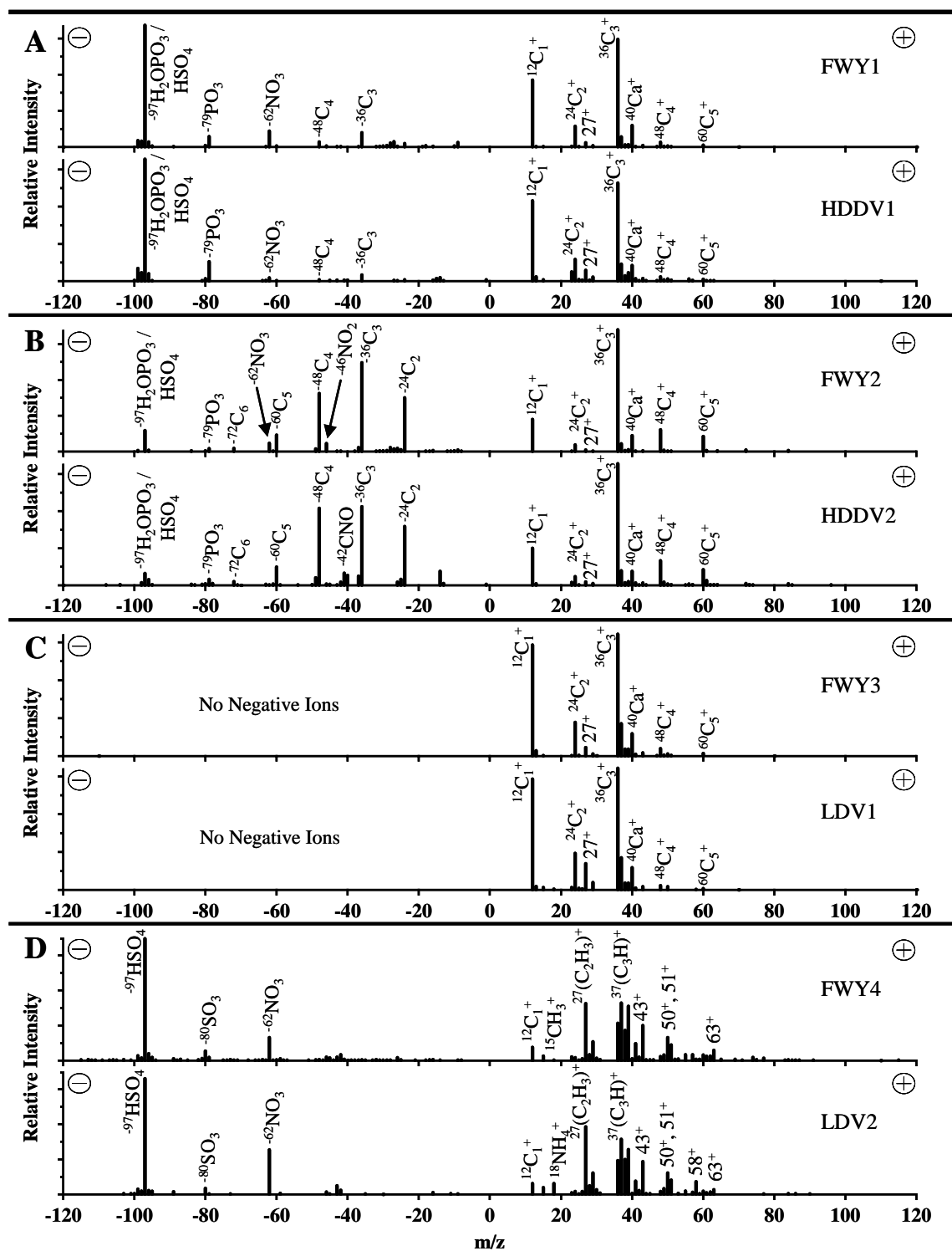


**Figure 4.4** Weight matrices of the top particle types detected during freeway study that match to vehicle study signatures.

spectra (Figure 4.4D) show the sixth freeway particle cluster that matches the third most abundant type from the LDV dynamometer study ( $R^2 = 0.98$ ).

There has been speculation as to whether mass spectral signatures from different sources obtained from laboratory and dynamometer experiments can be detected during ambient studies and used for source apportionment purposes. Such questions result from the concern that the dilution and residence systems used during source characterization studies do not properly mimic real-world dilution and aging conditions that occur in on-road driving exhaust [Graskow *et al.*, 2000; Kawai *et al.*, 2004]. The freeway-side study was chosen to lessen the effects of aging on the particle signatures. It was expected that the “fresh” emissions would be more comparable to the particle signatures obtained from the dynamometer experiments. The high  $R^2$  values for the comparison of particle classes confirms the chemistry of the particle types detected in dynamometer studies are consistent with those produced in ambient environments.

The high  $R^2$  values serves as further validation that the ART-2a clustering technique is a reliable method for ATOFMS particle mass spectral clustering. A discussion of whether mathematical clustering algorithms can properly separate and cluster similar particle types has been addressed in the literature [Bhave *et al.*, 2001; Phares *et al.*, 2001; Song *et al.*, 2001]. Some concerns about ART-2a have included that too low of a vigilance factor will yield a manageable number of end clusters, but will not distinguish between different types of particles. Also, too high of a vigilance factor will yield too many clusters to properly classify all particles. Through laboratory work conducted with ATOFMS data of known particle types, the proper vigilance factor for source apportionment using ART-2a has been found to be 0.85 [Wenzel and Prather,

2004]. While this tends to create many clusters for ambient data sets, the number is quite manageable because similar clusters can still be mathematically regrouped (which greatly reduces the number of clusters). For example, in this freeway study 2,763 clusters were generated after running ART-2a ( $VF = 0.85$ ) on fine mode particles, but mathematically regrouping these clusters using a  $VF$  of 0.90 reduces the number to 370 clusters (of which, the top 72 represent 90% of the total freeway-side particles detected with the UF-ATOFMS). The  $R^2$  values obtained for these comparisons show that these techniques work very well and should lessen concerns about their legitimacy.

#### 4.4.3 Temporal Trends and Correlations with UF-ATOFMS Data

A number of peripheral instruments accompanied the UF-ATOFMS instrument for this study to test the apportionment process being used. Previous vehicle apportionment studies show that  $NO_x$  emissions can be used as a tracer gas for HDDV emissions [Funasaka *et al.*, 1998; Gorse, 1984; Johnson, 2004]. Also, an aethalometer measures absorptivity by particles and can be used as an indicator of elemental carbon (or soot) containing particles (particularly at  $\lambda = 880\text{nm}$ ). Indeed, previous HDDV and LDV source studies show more EC associated with HDDVs [Shields *et al.*, 2007; Sodeman *et al.*, 2005; Toner *et al.*, 2006]. CO gas emissions have been shown to act as a tracer for LDV emissions [Gorse, 1984]; however, the CO monitor used in this study was not running during all the time periods. Figure 4.5 (A,B) shows a plot of  $NO_x$  vs. aethalometer data as well as HDDV counts (from video footage) vs. aethalometer. The time periods for the two plots are different as the  $NO_x$  monitor began later in the study. However, the plot between the  $NO_x$  and aethalometer (Figure 4.5A) show a good



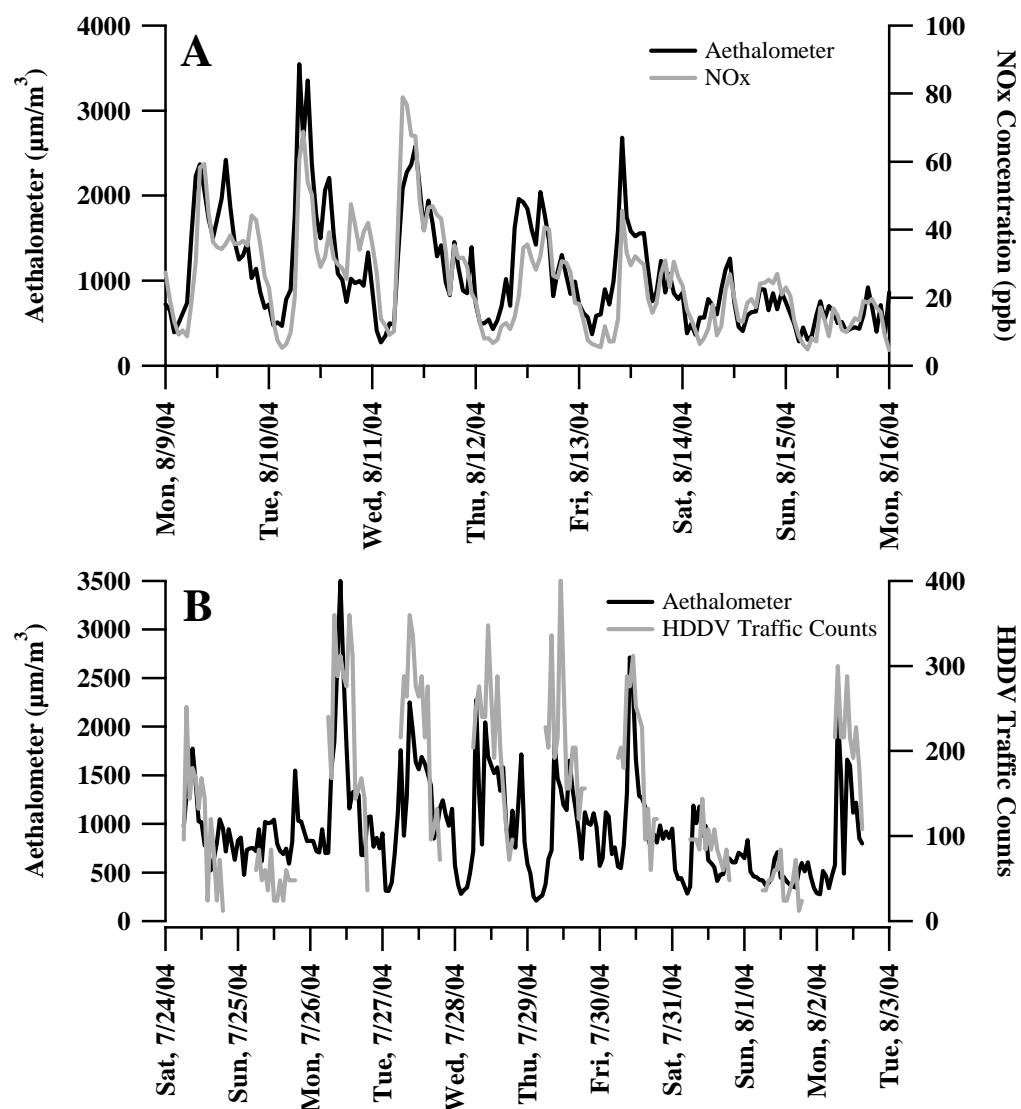


**Figure 4.5** Temporal plots of A) NOx gas data vs. aethalometer data; and B) HDDV video counts vs. aethalometer data. Both NOx and aethalometer data show a good correlation with each other ( $R^2 = 0.7$ ). The HDDV video counts also track the aethalometer data.

correlation ( $R^2 = 0.7$ ), tracking for the remainder of the study, which suggests it is safe to assume that they most likely tracked during the time period before the  $\text{NO}_x$  instruments arrival. This correlation can allow the use of the aethalometer data trends as a surrogate for the  $\text{NO}_x$  concentrations during periods when the  $\text{NO}_x$  data were not available. Figure 4.5B shows the comparison of HDDV video counts versus the aethalometer trends. The breaks in the counts come at night when there is insufficient light to properly distinguish between vehicles. The trends in HDDV counts versus aethalometer data also show a very strong correlation. Since HDDV's are shown to emit a larger mass of black carbon compared to LDV's [Robert *et al.*, 2007a; Robert *et al.*, 2007b], it is expected that the HDDV counts should be closely correlated with the aethalometer data. HDDVs make up about 2% of the fleet for this particular region of the freeway, and when HDDV traffic counts peak, there is generally a very large amount of LDV traffic as well. Even though HDDVs make such a low contribution to the traffic on this stretch of freeway, their particle emissions are quite prevalent and readily discernable.

Figures 4.6 and 4.7 shows the time series of the ART-2a matching results for the fine and ultrafine mode particles, respectively. Using the fractions from both the ultrafine and fine mode temporal plots, on average 83% of the aerosols detected near this roadside with the UF-ATOFMS are attributed to vehicle exhaust emissions, with 32% apportioned to LDV and 51% to HDDV emissions. For the fine mode particles ( $D_a = 100\text{--}300\text{nm}$ ), 66% of the aerosols are attributed to vehicle exhaust emissions, with 25% from LDV and 41% from HDDV. And, for ultrafine particles ( $D_a = 50\text{--}100\text{nm}$ ), 95% of the aerosols are apportioned to vehicles, with 37% from LDV and 58% from HDDV. The fact that such a large number of particles in the roadside environment matched to the

vehicle seeds using a relatively high vigilance factor (0.85) produces confidence that the seeds used in the source library are representative of a broad range of vehicles. If a particular particle type had been missed in the seeds, it would be apparent in a large number of "other" particles.

Figure 4.6 shows the ART-2a matching results for fine mode particles ( $D_a = 100\text{--}300\text{nm}$ ) along with wind data and video traffic counts for July 24 to Aug 03, 2004. This time period is of particular interest because MOUDI samplers ran at the same time and the source apportionment results from both approaches will be compared in a future study. The plot of the unscaled matching counts shows that both wind and traffic counts play a major role in the particle concentrations for this site. The matching counts peak around 9:00 each morning, which is when HDDV traffic counts peak. This also occurs just prior to, and during the beginning of daily peak wind speeds. The sampling site was located on the east side of the freeway because the prevailing daily wind blows from the west ( $270^\circ$ ). This allowed for the ideal positioning to detect freeway traffic exhaust particles. The matched fraction and unscaled count plots show that there is a larger number of diesel particles detected (relative to LDV matched particles), which follow the trend in diesel traffic observed from the video footage. It is interesting to note that the detection of LDV particles is always lower than that of HDDV particles for the fine particle mode. This was expected, as roadside and ambient studies have shown that HDDV's contribute a much higher concentration of particles even in LDV dominated areas [Imhof *et al.*, 2005; Kittelson *et al.*, 2006; Zhang *et al.*, 2005; Zhao and Hopke, 2004]. Vehicle studies have also shown that HDDV's emit a significantly higher fraction

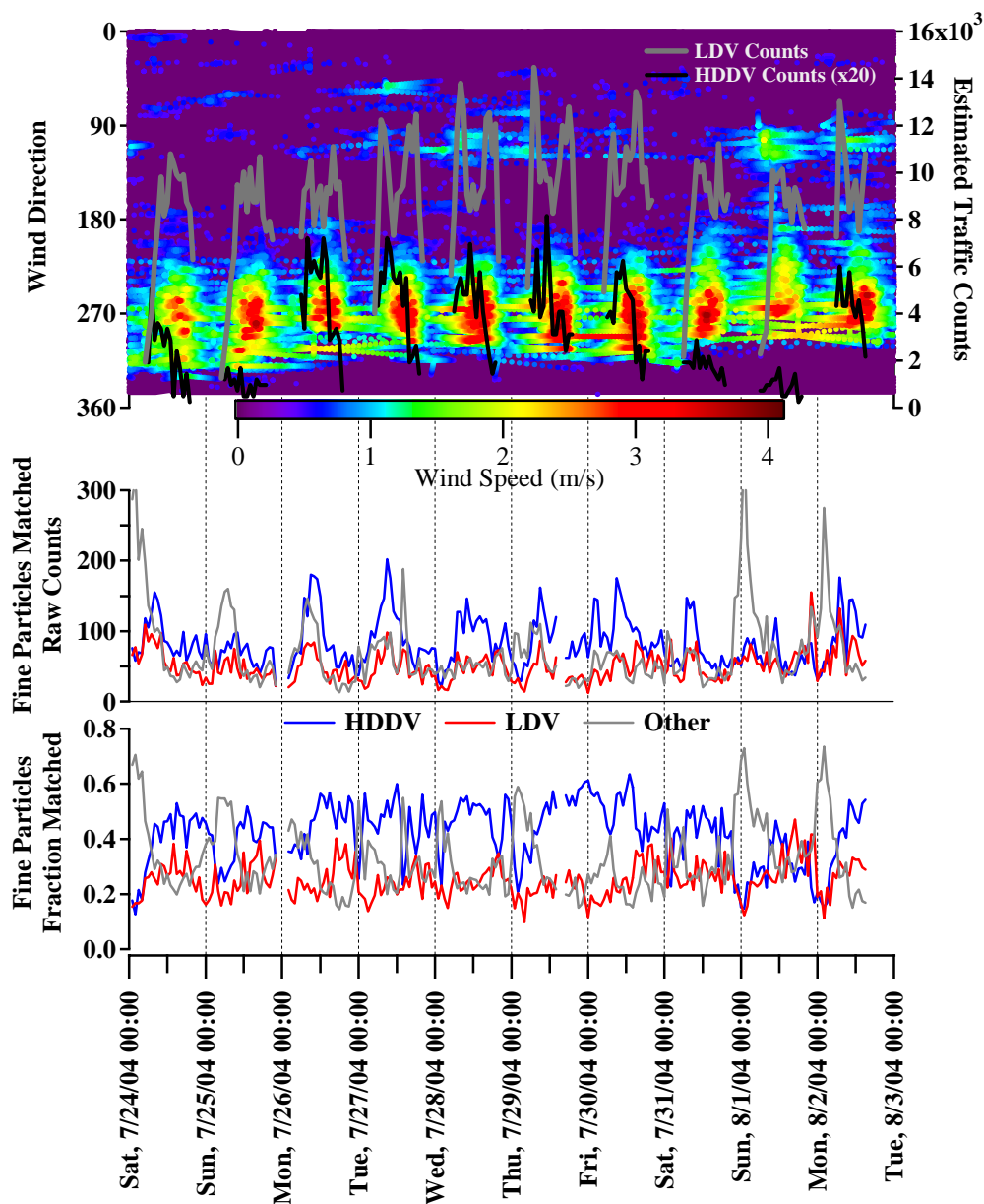


**Figure 4.6** Top: Wind data (blowing from: N = 0°/360°, E = 90°, S = 180°, W = 270°) along with LDV & HDDV traffic counts (from video). HDDV counts are multiplied by 20 to keep them on the same scale as LDV traffic counts. Middle: HDDV/LDV/Other ART-2a matching result unscaled counts from UF-ATOFMS data. Bottom: HDDV/LDV/Other ART-2a matching fraction results from UF-ATOFMS data. Data shown are accumulation mode particles ( $D_a = 100\text{--}300\text{nm}$ ) for July 24 to Aug 03, 2004.

of fine particles compared to LDV's [Shields *et al.*, 2007; Sodeman *et al.*, 2005; Toner *et al.*, 2006]. Another note to make about Figure 4.6 is that the temporal trend for the fraction of particles attributed to other sources has no correlation with the fractions matched to HDDV or LDV. This randomness of the accumulation mode "Other" type indicates that the particles within this class are not associated with either fresh HDDV or LDV emissions.

Figure 4.7 shows the times series of the ART-2a matching results for ultrafine particles ( $D_a = 50\text{--}100\text{nm}$ ) along with SMPS data and video traffic counts for July 24 to Aug 03, 2004. Traffic counts are shown on both Figure 4.6 and 4.7 to allow for comparison. This figure depicts how strong of a role the traffic counts play on the particle concentrations detected at this site. Comparing the ultrafine unscaled matched counts to the SMPS data illustrates how well the UF-ATOFMS particle detection tracks the changes in particle concentrations at this site. Since ultrafine particles provide an indication of freshly emitted particles, it was expected that the UF-ATOFMS ultrafine counts would track the SMPS data and the vehicle counts. This figure also shows how strong an influence the LDV emissions, though still less than HDDV emissions, have on the ultrafine particle concentrations in this area versus the fine mode particles. The fraction plot shows that there is a fairly consistent trend between the LDV and HDDV contribution to the ultrafine mode. As was discussed for Figure 4.6 in reference to the fine particles, HDDV's are known to emit a greater number of ultrafine particles in comparison to LDV's [Shields *et al.*, 2007; Sodeman *et al.*, 2005; Toner *et al.*, 2006]. Once again, this can account for the larger number of HDDV particles detected by the UF-ATOFMS than for LDV's, despite the dominating LDV traffic counts. Another note

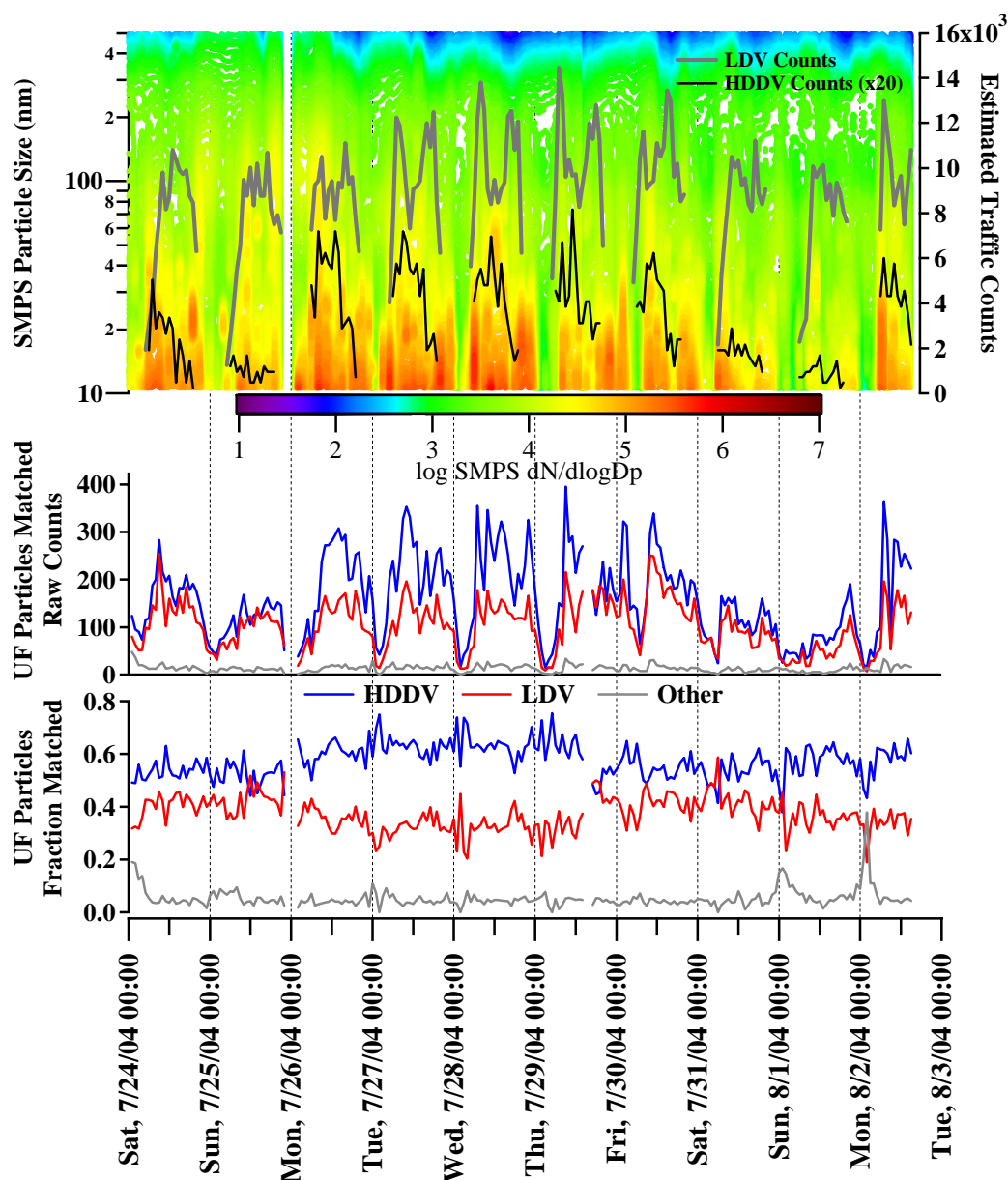


**Figure 4.7** Top: SMPS data along with LDV & HDDV traffic counts (from video). HDDV counts are multiplied by 20 to keep them on the same scale as LDV traffic counts. Middle: HDDV/LDV/Other ART-2a matching result unscaled counts from UF-ATOFMS data. Bottom: HDDV/LDV/Other ART-2a matching fraction results from UF-ATOFMS data. Data shown are ultrafine mode particles ( $D_a = 50\text{--}100\text{nm}$ ) for July 24 to Aug 03, 2004.

to make about Figure 4.7 is that it clearly shows a difference in weekday versus weekend traffic and particle detection. The first Saturday (7/24/04) had a high amount of traffic, including HDDV traffic, and shows almost the same amount of matching contributions as the weekdays. The first Sunday (7/25/04), as well as the following weekend show a reduced amount of HDDV traffic and, hence, a lower number of particles matching to HDDVs. When HDDV traffic increased on the weekdays, the number of HDDV apportioned particles were much greater than those apportioned to LDV's. It wasn't until Friday (7/30/04) that the LDV detected UF particle counts began to resemble those for HDDV's, and they remained about even through the weekend. Then, on Monday (8/02/04), the HDDV emissions began to dominate again. Also, an interesting feature to note about Figures 4.6 & 4.7 is that while the weekend LDV video counts remained relatively high (especially compared to the HDDV counts), the fraction of LDV and HDDV particles did not seem to change by the same magnitude. The weekend HDDV fraction goes down by about 10% for the UF particles and 9% for the accumulation mode particles, while the LDV fraction goes up by 7% for the UF particles and 2% for the accumulation mode. Also, the LDV apportioned counts go down despite the video traffic counts staying relatively high due to the fact that the winds were not as strong towards the site on the weekend (i.e. see 7/31 and 8/1 in Figure 3.6) as they were throughout the week. On 8/1, in addition to the winds not being as strong, they had more of an influence from the southwest and the east.

Figure 4.8 shows correlation plots along with a temporal plot of particles matched to HDDV and LDV along with aethalometer data ( $\lambda = 880\text{nm}$ ). There is a stronger correlation between the aethalometer and the HDDV matched particles ( $R^2 = 0.77$ ) than

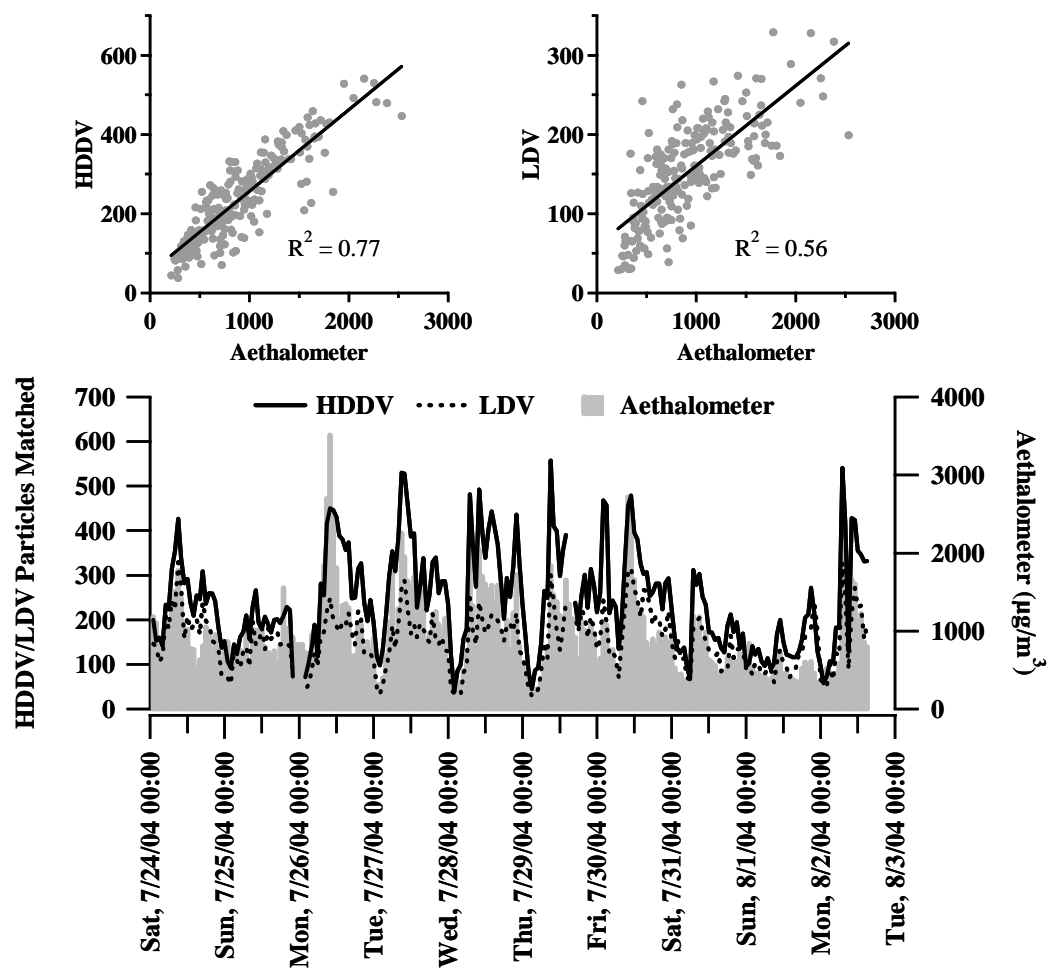


**Figure 4.8** Time series of aethalometer data with HDDV/LDV apportioned particles. The  $R^2$  values for aethalometer to HDDV is 0.77, and 0.56 for the aethalometer to LDV.



with the LDV matched particles ( $R^2 = 0.56$ ). Aethalometers measure the absorptivity of particles in the UV to IR regions, and since HDDVs emit a larger number of elemental carbon than do LDVs, the trends of aethalometer data should reflect trends in HDDV exhaust particles. Based on the trends of the  $\text{NO}_x$  and aethalometer data with the ATOFMS data, the observed correlations provide support to the ART-2a apportionment approach used in this study. The results presented in this paper represent the first step in using mass spectral source signatures acquired in LDV and HDDV dynamometer source characterization studies for ambient source apportionment. As expected, a high percentage (83%) of the ultrafine and accumulation mode aerosols sampled near the freeway are attributed to vehicle exhaust emissions, with 32% and 51% being attributed to LDV and HDDV, respectively. Future studies using different algorithms, including Hierarchical clustering and Positive Matrix Factorization, will be performed and the results will be compared to those obtained in this study. Also, comparisons will be made between single particle source apportionment results and standard organic tracer methods [Schauer *et al.*, 1996]. Such comparisons will be necessary for determining the most appropriate method for performing source apportionment using single particle mass spectral data.

#### **4.5 Acknowledgements**

The authors thank Dan Cayan and Alex Revchuk of the Scripps Institution of Oceanography (SIO) at UCSD for setting up the micro-meteorological stations and providing data for this study. We also thank UCSD and their facilities management for all their cooperation and help with setting up power to the sampling site, as well as the

members from the Prather group who helped in transporting equipment to the site. This work was supported by the California Air Resources Board (CARB) (Contract 00-331) as well as the EPA Science to Achieve Results Program through a subcontract from the University of Rochester PM and Health Center Grant R827453.

Chapter 4 is reproduced with permission from Toner, S.M., L.G. Shields, D.A. Sodeman, and K.A. Prather, Using mass spectral source signatures to apportion exhaust particles from gasoline and diesel powered vehicles in a freeway study using UF-ATOFMS, *Atmospheric Environment*, doi:10.1016/j.atmosenv.2007.08.005, 2007. Copyright 2007, Elsevier.

## 4.6 References

- Bein, K.J., Y. Zhao, N.J. Pekney, C.I. Davidson, M.V. Johnston, and A.S. Wexler, Identification of sources of atmospheric PM at the Pittsburgh Supersite-Part II: Quantitative comparisons of single particle, particle number, and particle mass measurements, *Atmospheric Environment*, 40 (Suppl. 2), S424-S444, 2006.
- Bhave, P.V., D.P. Fergenson, K.A. Prather, and G.R. Cass, Source apportionment of fine particulate matter by clustering single-particle data: tests of receptor model accuracy, *Environmental Science and Technology*, 35 (10), 2060-2072, 2001.
- Canagaratna, M.R., J.T. Jayne, D.A. Ghertner, S. Herndon, Q. Shi, J.L. Jimenez, P.J. Silva, P. Williams, T. Lanni, F. Drewnick, K.L. Demerjian, C.E. Kolb, and D.R. Worsnop, Chase studies of particulate emissions from in-use New York City vehicles, *Aerosol Science & Technology*, 38 (6), 555-573, 2004.
- Cass, G.R., L.A. Hughes, P. Bhave, M.J. Kleeman, J.O. Allen, and L.G. Salmon, The chemical composition of atmospheric ultrafine particles, *Philosophical Transactions of the Royal Society of London, Series A: Mathematical, Physical and Engineering Sciences*, 358 (1775), 2581-2592, 2000.
- Fruin, S.A., M.J. St Denis, A.M. Winer, S.D. Colome, and F.W. Lurmann, Reductions in human benzene exposure in the California South Coast Air Basin, *Atmospheric Environment*, 35 (6), 1069-1077, 2001.
- Funasaka, K., T. Miyazaki, T. Kawaraya, K. Tsuruho, and T. Mizuno, Characteristics of particulates and gaseous pollutants in a highway tunnel, *Environmental Pollution*, 102 (2-3), 171-176, 1998.
- Gard, E., J.E. Mayer, B.D. Morrical, T. Dienes, D.P. Fergenson, and K.A. Prather, Real-time analysis of individual atmospheric aerosol particles: Design and performance of a portable ATOFMS, *Analytical Chemistry*, 69 (20), 4083-4091, 1997.
- Gorse, R.A., Jr., On-road emission rates of carbon monoxide, nitrogen oxides, and gaseous hydrocarbon, *Environmental Science and Technology*, 18 (7), 500-7, 1984.
- Graskow, B.R., M.R. Ahmadi, J.E. Morris, and D.B. Kittelson, Influence of fuel additives and dilution conditions on the formation and emission of exhaust particulate matter from a direct injection spark ignition engine, *Society of Automotive Engineers, [Special Publication] SP, SP-1551* (Diesel and Gasoline Performance and Additives), 261-271, 2000.
- Imhof, D., E. Weingartner, C. Ordonez, R. Gehrig, M. Hill, B. Buchmann, and U. Baltensperger, Real-world emission factors of fine and ultrafine aerosol particles

- for different traffic situations in Switzerland, *Environmental Science and Technology*, 39 (21), 8341-8350, 2005.
- Johnson, T.V., Diesel emission control technology - 2003 in review, *Society of Automotive Engineers, [Special Publication] SP, SP-1835* (Diesel Emissions), 1-14, 2004.
- Kawai, T., Y. Goto, and M. Odaka, Influence of dilution process on engine exhaust nanoparticles, *Society of Automotive Engineers, [Special Publication] SP, SP-1862* (Emissions Measurement & Testing), 113-119, 2004.
- Kittelson, D.B., W.F. Watts, J.P. Johnson, J.J. Schauer, and D.R. Lawson, On-road and laboratory evaluation of combustion aerosols-Part 2: Summary of spark ignition engine results, *Journal of Aerosol Science*, 37 (8), 931-949, 2006.
- Kleeman, M.J., and G.R. Cass, Source contributions to the size and composition distribution of urban particulate air pollution, *Atmospheric Environment*, 32 (16), 2803-2816, 1998.
- Kleeman, M.J., J.J. Schauer, and G.R. Cass, Size and composition distribution of fine particulate matter emitted from motor vehicles, *Environmental Science and Technology*, 34 (7), 1132-1142, 2000.
- Lehmann, U., M. Mohr, T. Schweizer, and J. Rutter, Number size distribution of particulate emissions of heavy-duty engines in real world test cycles, *Atmospheric Environment*, 37 (37), 5247-5259, 2003.
- Marshall, J.D., W.J. Riley, T.E. McKone, and W.W. Nazaroff, Intake fraction of primary pollutants: motor vehicle emissions in the South Coast Air Basin, *Atmospheric Environment*, 37 (24), 3455-3468, 2003.
- Mysliwiec, M.J., and M.J. Kleeman, Source apportionment of secondary airborne particulate matter in a polluted atmosphere, *Environmental Science & Technology*, 36 (24), 5376-5384, 2002.
- Owega, S., G.J. Evans, R.E. Jervis, M. Fila, R. D'Souza, and B.-U.-Z. Khan, Long-range sources of Toronto particulate matter (PM<sub>2.5</sub>) identified by Aerosol Laser Ablation Mass Spectrometry (LAMS), *Atmospheric Environment*, 38 (33), 5545-5553, 2004.
- Phares, D.J., K.P. Rhoads, A.S. Wexler, D.B. Kane, and M.V. Johnston, Application of the ART-2a algorithm to laser ablation aerosol mass spectrometry of particle standards, *Analytical Chemistry*, 73 (10), 2338-2344, 2001.

- Pope, C.A., Review: Epidemiological basis for particulate air pollution health standards, *Aerosol Science & Technology*, 32 (1), 4-14, 2000.
- Rebotier, T.P., and K.A. Prather, Aerosol time-of-flight mass spectrometry data analysis: A benchmark of clustering algorithms, *Analytica Chimica Acta*, 585 (1), 38-54, 2007.
- Reilly, P.T.A., R.A. Gieray, W.B. Whitten, and J.M. Ramsey, Real-time characterization of the organic composition and size of individual diesel engine smoke particles, *Environmental Science and Technology*, 32 (18), 2672-2679, 1998.
- Riediker, M., W.E. Cascio, T.R. Griggs, M.C. Herbst, P.A. Bromberg, L. Neas, R.W. Williams, and R.B. Devlin, Particulate matter exposure in cars is associated with cardiovascular effects in healthy young men, *American Journal of Respiratory & Critical Care Medicine*, 169 (8), 934-940, 2004.
- Robert, M.A., C.A. Jakober, and M.J. Kleeman, Size and composition distributions of particulate matter emissions 2. Heavy duty diesel vehicles, *submitted for publication*, 2007a.
- Robert, M.A., C.A. Jakober, S. VanBergen, and M.J. Kleeman, Size and composition distributions of particulate matter emissions 1. Light duty gasoline vehicles, *submitted for publication*, 2007b.
- Rogge, W.F., L.M. Hildemann, M.A. Mazurek, G.R. Cass, and B.R.T. Simoneit, Sources of fine organic aerosol 2: Noncatalyst and catalyst-equipped automobiles and heavy-duty diesel trucks, *Environmental Science & Technology*, 27 (4), 636-651, 1993.
- Schauer, J.J., W.F. Rogge, L.M. Hildemann, M.A. Mazurek, G.R. Cass, and B.R.T. Simoneit, Source apportionment of airborne particulate matter using organic compounds as tracers, *Atmospheric Environment*, 30 (22), 3837-3855, 1996.
- Seagrave, J., J.D. McDonald, A.P. Gigliotti, K.J. Nikula, S.K. Seilkop, M. Gurevich, and J.L. Mauderly, Mutagenicity and in vivo toxicity of combined particulate and semivolatile organic fractions of gasoline and diesel engine emissions, *Toxicological Sciences*, 70 (2), 212-226, 2002.
- Shields, L.G., D.T. Suess, and K.A. Prather, Determination of single particle mass spectral signatures from heavy duty diesel vehicle emissions for PM<sub>2.5</sub> source apportionment, *Atmospheric Environment*, 41 (18), 3841-3852, 2007.
- Silva, P.J., D.Y. Liu, C.A. Noble, and K.A. Prather, Size and chemical characterization of individual particles resulting from biomass burning of local Southern California species, *Environmental Science & Technology*, 33 (18), 3068-3076, 1999.

- Sodeman, D.A., S.M. Toner, and K.A. Prather, Determination of single particle mass spectral signatures from light duty vehicle emissions, *Environmental Science & Technology*, 39 (12), 4569-4580, 2005.
- Song, X.H., N.M. Faber, P.K. Hopke, D.T. Suess, K.A. Prather, J.J. Schauer, and G.R. Cass, Source apportionment of gasoline and diesel by multivariate calibration based on single particle mass spectral data, *Analytica Chimica Acta*, 446 (1-2), 329-343, 2001.
- Song, X.-H., P.K. Hopke, D.P. Fergenson, and K.A. Prather, Classification of single particles analyzed by ATOFMS using an artificial neural network, ART-2A, *Analytical Chemistry*, 71 (4), 860-865, 1999.
- Su, Y., M.F. Sipin, H. Furutani, and K.A. Prather, Development and characterization of an aerosol time-of-flight mass spectrometer with increased detection efficiency, *Analytical Chemistry*, 76 (3), 712-719, 2004.
- Tobias, H.J., D.E. Beving, P.J. Ziemann, H. Sakurai, M. Zuk, P.H. McMurry, D. Zarling, R. Waytulonis, and D.B. Kittelson, Chemical analysis of diesel engine nanoparticles using a nano-DMA/thermal desorption particle beam mass spectrometer, *Environmental Science and Technology*, 35 (11), 2233-2243, 2001.
- Tobias, H.J., P.M. Kooiman, K.S. Docherty, and P.J. Ziemann, Real-time chemical analysis of organic aerosols using a thermal desorption particle beam mass spectrometer, *Aerosol Science and Technology*, 33 (1-2), 170-190, 2000.
- Toner, S.M., L.G. Shields, and K.A. Prather, Source apportionment of freeway-side PM<sub>2.5</sub> using ATOFMS, *manuscript in preparation*, 2007.
- Toner, S.M., D.A. Sodeman, and K.A. Prather, Single particle characterization of ultrafine and accumulation mode particles from heavy duty diesel vehicles using aerosol time-of-flight mass spectrometry, *Environmental Science & Technology*, 40 (12), 3912-3921, 2006.
- Vanvorst, W.D., and S. George, Impact of the California Clean Air Act, *International Journal of Hydrogen Energy*, 22 (1), 31-38, 1997.
- Wenzel, R.J., and K.A. Prather, Improvements in ion signal reproducibility obtained using a homogeneous laser beam for on-line laser desorption/ionization of single particles, *Rapid Communications in Mass Spectrometry*, 18 (13), 1525-1533, 2004.
- Xie, Y., P.K. Hopke, and D. Wienke, Airborne particle classification with a combination of chemical composition and shape index utilizing an adaptive resonance artificial neural network, *Environmental Science & Technology*, 28 (11), 1921-1928, 1994.

- Zhang, K.M., A.S. Wexler, D.A. Niemeier, Y.F. Zhu, W.C. Hinds, and C. Sioutas, Evolution of particle number distribution near roadways. Part III: Traffic analysis and on-road size resolved particulate emission factors, *39* (22), 4155-4166, 2005.
- Zhao, W., and P.K. Hopke, Source apportionment for ambient particles in the San Geronio wilderness, *Atmospheric Environment*, *38* (35), 5901-5910, 2004.

# 5 Source apportionment of freeway-side PM<sub>2.5</sub> using ATOFMS

## 5.1 Synopsis

Several approaches for ambient aerosol source apportionment have been developed over the years. A number of these techniques involve determining organic and inorganic source markers from offline bulk filter analysis using a variety of analytical tools (such as mass spectrometry, chromatography, and microscopy). Some other methods have inferred that certain sources can be determined from correlations between particle size data and gas phase measurements. The technique presented here involves using a mass spectral source signature library to apportion single particles detected with an aerosol time-of-flight mass spectrometer (ATOFMS). The source signature library has been developed through a series of source and ambient characterization studies and currently contains signatures for heavy duty diesel vehicles (HDDV), light duty gasoline vehicles (LDV), dust, sea salt, biomass, and meat cooking. There are also additional non-source specific signatures, determined from the data acquired for several ambient ATOFMS studies, for aged organic carbon, aged elemental carbon, amine containing particles, PAH's, ammonia rich particles, vanadium particles, and elemental carbon particles. Using the ART-2a algorithm to match individual ambient particle mass spectra to the source signature library, it was found that 97% of ambient particles (50 – 3000 nm)



detected with two ATOFMS instruments near a freeway matched the library signatures. The use of the ART-2a source signature matching method shows that particles from gasoline powered vehicles can be readily distinguished from heavy duty diesel powered vehicles in roadside ambient measurements. Additionally, it was discovered that regional background particles matching with specific elemental carbon and vanadium signatures from ship emissions dominate and overwhelm the local emissions; however, the library matching method is able to identify their presence and distinguish them from local emissions.

## 5.2 Introduction

Recent studies have shown that vehicle emissions are a major source of pollution in urban areas [*Buzcu-Guven et al.*, 2007; *Fruin et al.*, 2001; *Kleeman et al.*, 2007; *Marshall et al.*, 2003; *Mysliwiec and Kleeman*, 2002; *Rogge et al.*, 1993; *Vanvorst and George*, 1997]. With an ever growing concern over the health effects associated with vehicle emissions, a goal of major federal and state agencies is to set regulations which lead to a reduction in these pollutants [*Pope*, 2000; *Riediker et al.*, 2004; *Seagrave et al.*, 2002]. The ability to apportion gasoline powered light duty vehicles (LDV), heavy duty diesel vehicles (HDDV), and other combustion emissions in ambient aerosols will allow city and state agencies to channel their efforts and resources into targeting the major polluters (LDV, HDDV, and other combustion sources) in their area. Distinguishing between LDV and HDDV exhaust aerosols may represent the greatest challenge (compared to other combustion sources) due to the similar chemical characteristics of the PM in their emissions, which result from their similar fuel and oil composition [*Allen et*

*al.*, 2001; *Fraser et al.*, 2003; *Kleeman et al.*, 2000; *Miguel et al.*, 1998; *Rogge et al.*, 1993; *Watson et al.*, 1994].

The purpose of this work is to test whether aerosol mass spectral source signatures acquired from ATOFMS source characterization studies, including vehicle dynamometer studies, can be used to apportion ambient aerosols in a freeway-side study. A freeway-side location was chosen in a coastal area because this location should be dominated by particles from fresh vehicle exhaust emissions and should display a relatively low concentration of aged or transformed particles. The background particles are expected to be mostly sea salt since this is a coastal region. The steps involved in data quality assurance will be discussed as well as how particle size measurements and gas phase instrumentation can be incorporated for aerosol source apportionment.

### 5.3 Experimental

The experimental setup used for this study has been described in Chapter 4 [*Toner et al.*, 2007]. The study was conducted from July 21 to August 25, 2004 at two sites. First, a “clean” upwind site was stationed at the Prather Laboratory in Urey Hall at the University of California, San Diego (UCSD) with the goal of determining the signatures of background ambient aerosols (GPS position 32°52’31.66’’N 117°14’28.64’’W). This site is relatively close to the ocean (within 950 meters) so the prevailing winds (from the west) should introduce little-to-no fresh source emissions. This site housed a standard inlet ATOFMS instrument [*Gard et al.*, 1997] along with an aerodynamic particle sizer (APS) (TSI Model 3321 – Minnesota) and a scanning mobility particle sizer (SMPS) (TSI Model 3936L10 – Minnesota). The second site was located at a trailer stationed in a

**Table 5.1** List of instrumentation used at the freeway and upwind sampling sites

Instrument	Make & Model	Measurement	Units	Sample Resolution	Site	Sampling Period
Ultrafine Aerosol Time-of-Flight Mass Spectrometer (UF-ATOFMS)		size range: 50–300 nm		real-time	Freeway	Jul 21 to Aug 25, 2004
Standard Aerosol Time-of-Flight Mass Spectrometer (ATOFMS) 1		size range: 200–3000 nm		real-time	Freeway	Jul 21 to Aug 25, 2004
Standard Aerosol Time-of-Flight Mass Spectrometer (ATOFMS) 2		size range: 200–3000nm		real-time	Upwind	Jul 21 to Aug 2, 2004
					Freeway	Aug 10 to Aug 25, 2004
Aerodynamic Particle Sizer (APS) 1	TSI Model 3321	particle number conc. (0.5–20 $\mu$ m)	#/cm <sup>3</sup>	5 min	Freeway	Jul 21 to Aug 25, 2004
Aerodynamic Particle Sizer (APS) 2	TSI Model 3321	particle number conc. (0.5–20 $\mu$ m)	#/cm <sup>3</sup>	5 min	Upwind	Jul 21 to Aug 2, 2004
Scanning Mobility Particle Sizer (SMPS) 1	TSI Model 3936L10	particle number conc. (10–500nm)	#/cm <sup>3</sup>	5 min	Freeway	Jul 21 to Aug 25, 2004
Scanning Mobility Particle Sizer (SMPS) 2	TSI Model 3936L10	particle number conc. (10–500nm)	#/cm <sup>3</sup>	5 min	Upwind	Jul 21 to Aug 2, 2004
Aethalometer	Magee Scientific 'Spectrum' AE-3 Series	optical absorption cross-section per unit mass	$\mu$ m/m <sup>3</sup>	5 min	Freeway	Jul 21 to Aug 25, 2004
Nephelometer	Radiance Model M903	light scattering coefficient (bscat)	km <sup>-1</sup>	5 min	Freeway	Jul 21 to Jul 22 & Jul 25 to Aug 25, 2004
Photoelectric Aerosol Sensor (PAS)	EcoChem Model 2000	concentration of total particle-bound PAH	ng/m <sup>3</sup>	5 min	Freeway	Jul 30 to Aug 25, 2004
Tapered Element Oscillating Microbalance (TEOM)	Rupprecht & Patashnick (R & P) Series 1400a	mass concentration (PM <sub>2.5</sub> )	$\mu$ g/m <sup>3</sup>	30 min	Freeway	Jul 21 to Aug 25, 2004
Chemiluminescence NO-NO <sub>2</sub> -NO <sub>x</sub> Analyzer	Thermo Environmental Instruments (TEI) Model 42C	NO & NO <sub>x</sub> concentration levels	ppb	1 min	Freeway	Aug 5 to Aug 25, 2004
CO Analyzer	Advanced Pollution Instrumentation (API) Model M300	CO concentration levels	ppm	5 min	Freeway	Jul 30 to Aug 10 & Aug 13 to Aug 25, 2004
Webcam	Creative Model PD1001	traffic video surveillance		1 sec	Freeway	Jul 21 to Aug 25, 2004

low-use parking lot (particularly during the summer) on the UCSD campus directly adjacent to the I-5 freeway (GPS position 32°52'49.74"N 117°13'40.95"W) with the sampling line within 10 meters of the freeway. The trailer housed a suite of instruments including an ATOFMS and UF-ATOFMS [Su *et al.*, 2004]. A detailed summary of the instrumentation operated at both sites is provided in Table 5.1. Dr. Michael Kleeman's research group (UC Davis) also sampled PM at both sites with micro orifice uniform deposit impactors (MOUDI's), Anderson Impactors, an APS, and an SMPS. The Kleeman group sampled from July 21 - August 1. Their measurements focused on obtaining size-resolved concentrations of organic and metal tracers to be used for conventional source apportionment. Ultimately, when their results become available, a comparison will be made between the ATOFMS apportionment results and the impactor-based predictions. Meteorological stations were operated on each side of the freeway for complete wind trajectory information.

## **5.4 Results and Discussion**

### **5.4.1 Quality Assurance of ATOFMS Data**

Data from the three ATOFMS instruments as well as all peripheral instruments were loaded into a database that allows for direct comparison of the temporal trends of gas phase, particle phase, and meteorological data. Before beginning data analysis of the ATOFMS particle types, quality assurance (QA) graphs were prepared for all three instruments over the relevant size ranges of the study. The purpose of these graphs is to examine whether any anomalies occurred during sampling that would result in improper interpretation of the acquired data.

A question that often arises with ATOFMS data concerns whether any chemical biases are leading to particles being “missed” in the LDI analysis step. In order to check for the presence of chemical biases, temporal plots are compared of the number of particles which scatter light to the number of particles which scatter light and produce a mass spectrum. If there is a chemical bias, where a particular type is being “missed”, it will show up as lots of “scatters” with very few “scatters + mass spectra” [Wenzel *et al.*, 2003]. These plots were made for all three ATOFMS instruments over multiple size ranges for the full duration of the study. An example of this type of plot is shown in Figure 5.1A for the UF-ATOFMS. As can be seen, there are no major deviations between the scatters and scatters + mass spectra over the time of the study, indicating that there are major period with missed particle types. It is important to note that the smallest sized particles have the highest probability of showing a chemical bias since smaller particles are more “pure” (i.e. less chemically complex). In the freeway study, there was no major evidence of any particle types being missed by the ATOFMS in any of the size ranges examined (50 – 3000 nm). This is not surprising since the particle emissions from vehicles strongly absorb the ultraviolet light at 266 nm used for the laser desorption/ionization process with the ATOFMS. It should also be noted that all temporal plots for ATOFMS data shown in this manuscript show unscaled ATOFMS number concentrations. As will be shown, the unscaled temporal trends of the ATOFMS track the peripheral instruments without scaling; the main reason for scaling is to obtain atmospherically representative concentrations that can be directly compared to results from other studies.

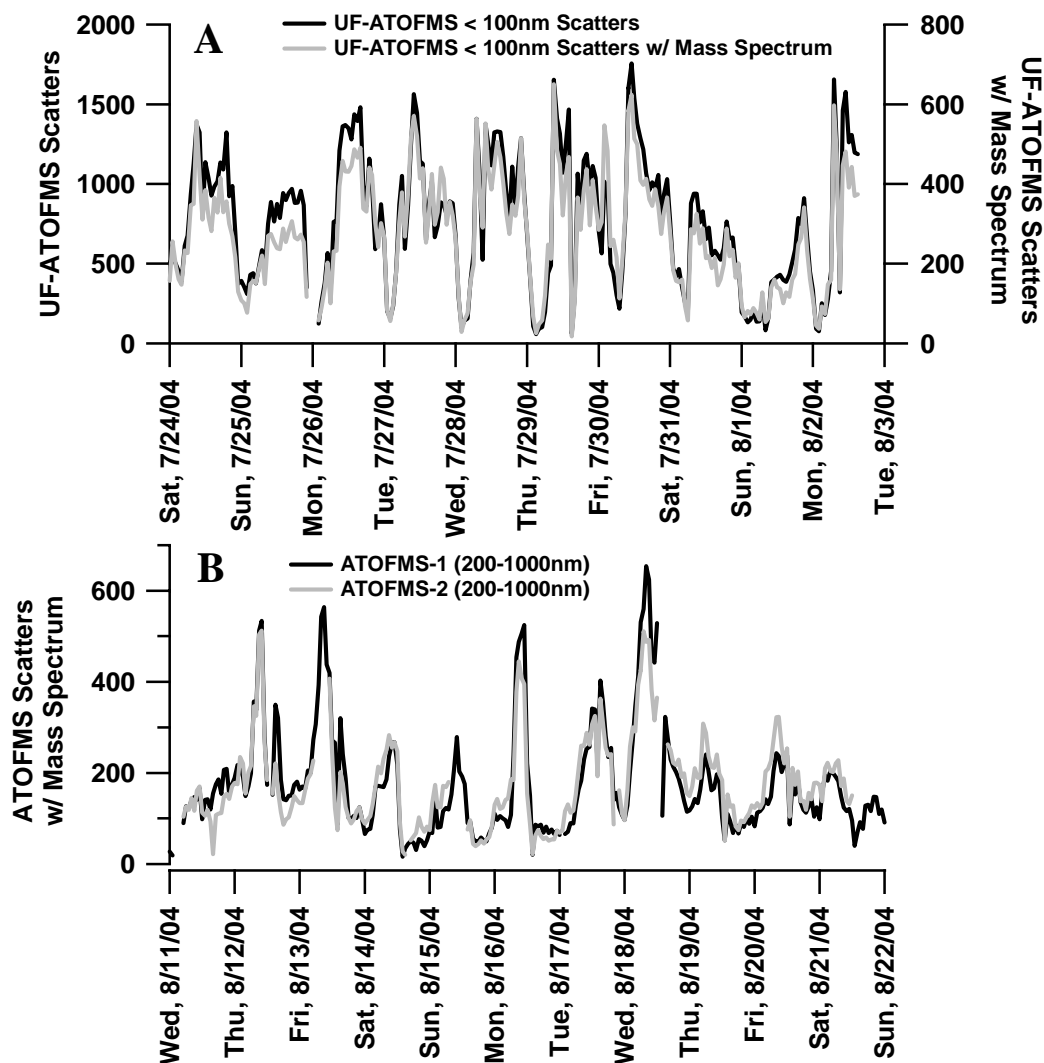


**Figure 5.1** A) QA plot of UF-ATOFMS particle scatters vs. particles scattered that produced a mass spectrum to determine if there are any chemical biases or particle types being missed. B) Comparison of the two standard inlet ATOFMS instruments particle detections when running side-by-side at the freeway site. Plots are in one hour resolution.

As part of the QA process, it is also important to compare the temporal trends for the two standard inlet ATOFMS instruments when they were sampling side-by-side for the last part of the study near the freeway. Figure 5.1B shows this comparison, demonstrating how when the instruments were located at the same site almost identical trends in particle counts are obtained, demonstrating the reproducibility of the ATOFMS systems.

#### **5.4.2 Comparison with standard particle counts**

Comparing the ATOFMS size distribution measurements with those from other particle size measuring instruments is an additional method for determining whether the trends observed with the ATOFMS reflect ambient particle concentrations. Figure 5.2A shows a comparison of the SMPS against the UF-ATOFMS for sub-100 nm particle counts. Despite being on different absolute scales, it is evident that the basic temporal trends measured by these two instruments track one another quite well ( $R^2 = 0.60$ ), providing additional validation of the ATOFMS temporal trends. In general, the ultrafine counts increased during periods when the winds were blowing from the west directly from the freeway to the sampling site. At night, the wind speeds typically became quite low ( $< 1.0$  m/s), the traffic was reduced, and the ultrafine particle counts were at their lowest. This pattern was repeated each day over the entire study.

The two standard inlet ATOFMS systems measured particles in the larger size modes (200 – 3000 nm). Figure 5.2B shows a comparison of the ATOFMS by the freeway with the APS for submicron counts. The APS only samples particles down to 500 nm so a slightly different size range is covered. The standard ATOFMS detected

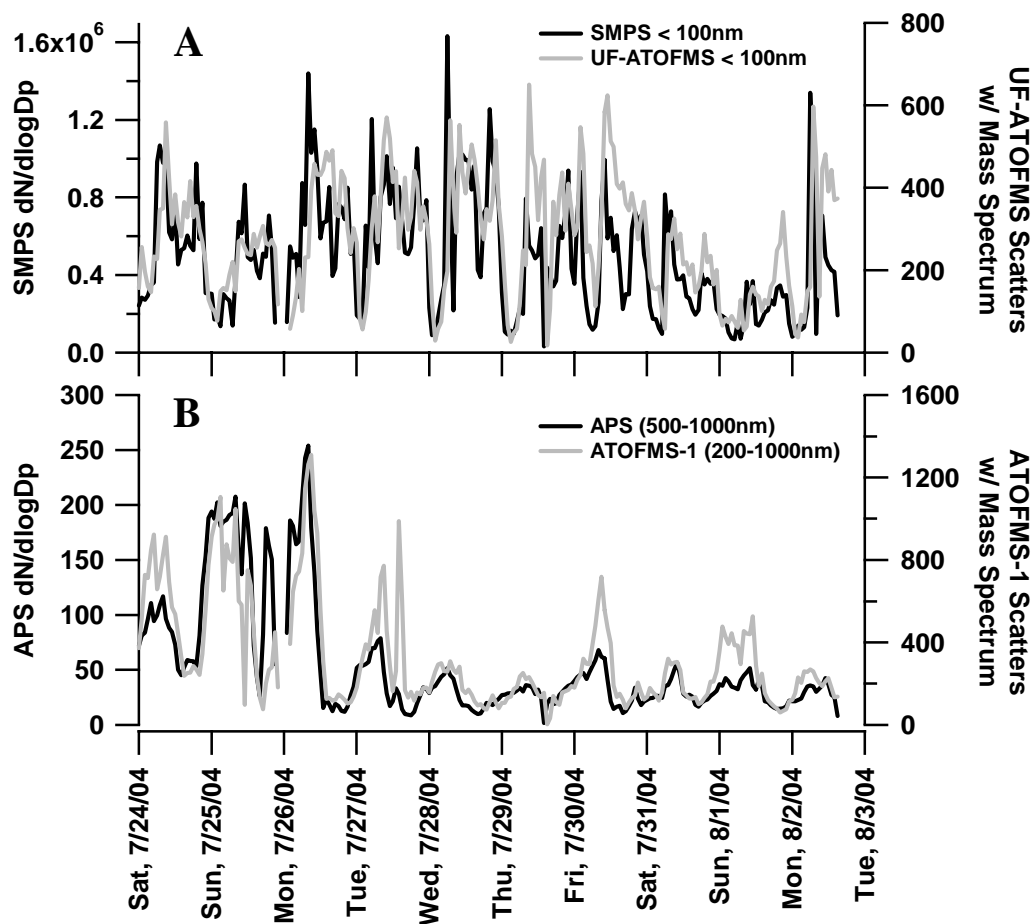


**Figure 5.2** A) Comparison of sub-100 nm particle counts with the SMPS to sub-100 nm particles detected (that produced mass spectra) with the UF-ATOFMS at the freeway site. B) Comparison of fine mode particles (500 – 1000 nm) with the APS to fine mode particles (200 – 1000 nm) detected (that produced mass spectra) with the standard inlet ATOFMS at the freeway site. Plots are in one hour resolution.



very few particles below 300 nm due to limitations in the transmission efficiency of the inlet. The important thing to note about this comparison is how strongly correlated the trends are ( $R^2 = 0.70$ ), offering further credence to the temporal variations measured with the ATOFMS. Figure 5.2A-B shows the ATOFMS instruments tracking particle number concentrations measured using traditional particle sizing instruments over a broad range of sizes. This validation step is extremely important to future studies probing the temporal variability of different source contributions to the various ambient particles sampled by ATOFMS.

### 5.4.3 Comparison of particle phase and gas phase data

It is interesting to compare the UF-ATOFMS measurements with gas phase measurements. Figure 5.3A and 5.3B show a comparison of gas phase CO and NO<sub>x</sub> concentration measurements versus UF-ATOFMS counts, indicating time periods when fresh emissions were impacting the sampling site. Figure 5.3C shows an expanded view of each gas phase species plotted over a larger time span. Typically it is expected that time periods where UF particles and CO peak may be related to LDV exhaust periods [Gorse, 1984], whereas increases in NO<sub>x</sub> concentrations could be more indicative of HDDV emissions [Funasaka *et al.*, 1998; Gorse, 1984; Johnson, 2004]. When comparing the trends between CO and NO<sub>x</sub> emissions though, their trends tracked each other very closely ( $R^2 = 0.71$ ). Since the trends are so similar, one cannot generalize that the CO is for LDVs and the NO<sub>x</sub> represents HDDVs in this case. More likely, these trends follow so closely because they are tracking both the trends in traffic as well as wind patterns. The CO and NO<sub>x</sub> values presented here (where the CO emissions are

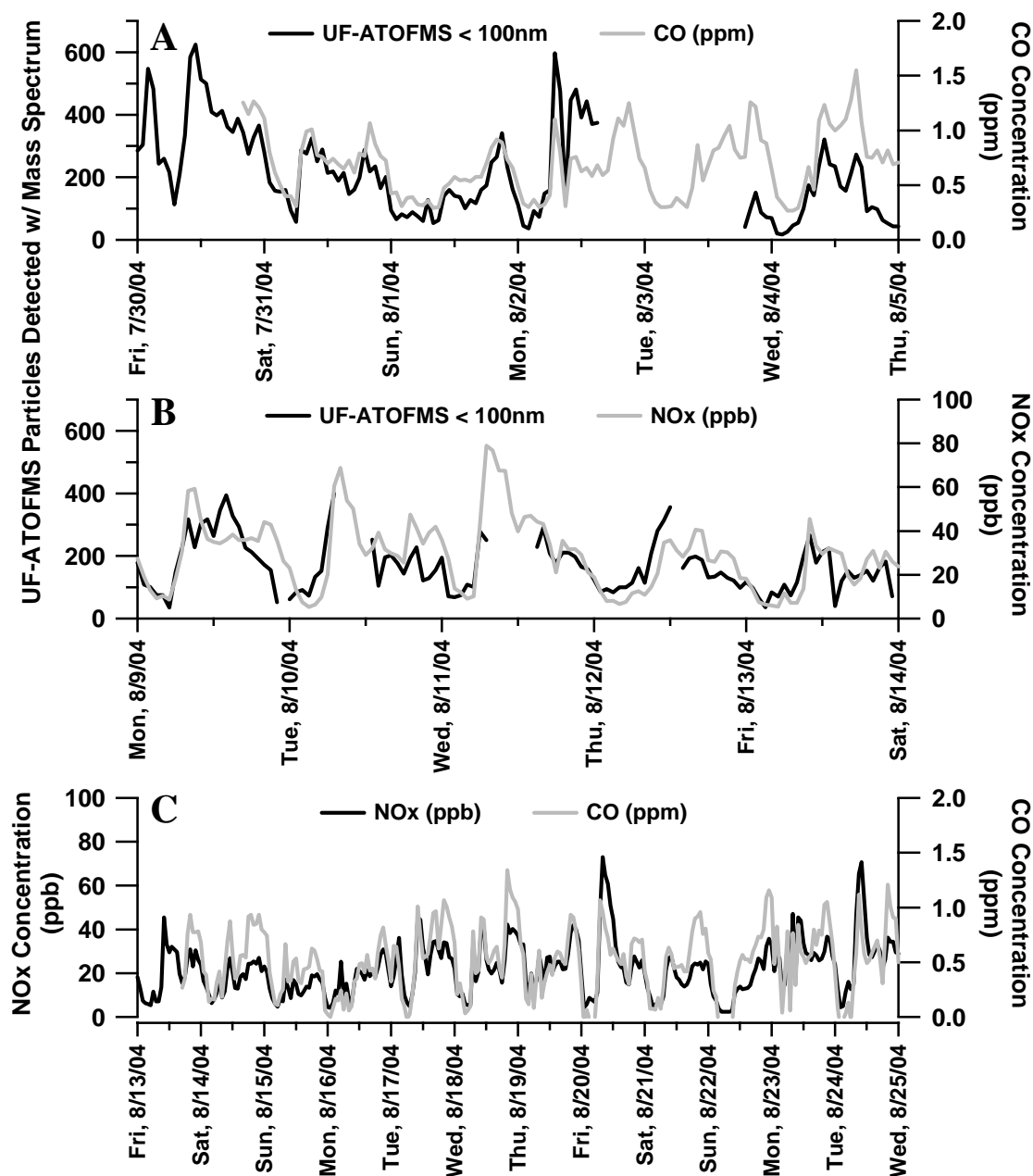


**Figure 5.3** A) Comparison of sub-100 nm UF-ATOFMS particles detected that produced mass spectra with CO measurements. B) Comparison of sub-100 nm UF-ATOFMS particles detected that produced mass spectra with NO<sub>x</sub> measurements. C) Comparison of CO and NO<sub>x</sub> measurements at the freeway site. Plots are in one hour resolution.

continuously higher than the NO<sub>x</sub> emissions) are consistent with previous findings for areas with similar traffic conditions [*Gorse*, 1984; *Pelkmans and Debal*, 2006].

#### 5.4.4 Comparison of temporal trends from peripheral instruments

Analysis of gas phase species such as NO<sub>x</sub> and CO coupled with aethalometer data can provide insight into the time periods when vehicle exhaust plumes were impacting the sampling site. There is some speculation as to whether this combination of instruments coupled with ultrafine size distribution measurements made with an SMPS can be used to identify HDDV impacted events [*Johnson et al.*, 2005; *Lehmann et al.*, 2003; *Reilly et al.*, 1998; *Wahlin et al.*, 2001; *Zhang et al.*, 2005]. Figure 5.4A shows a comparison of the aethalometer and NO<sub>x</sub> measurements made over a time period when all instruments were operational. In general, the trends observed between the ultrafine particle concentrations (<100 nm), CO, aethalometer, and NO<sub>x</sub> measurements tracked each other, following peak wind speeds, which occurred mostly during daytime hours. Likewise, in Figure 5.4B, the data from the nephelometer (which detects light scattering particles) has similar trends as the aethalometer. This correlation is a strong indication that the local winds control when the particles reach the sampling site.

By comparing the aethalometer and NO<sub>x</sub> concentrations, one can see the trends track extremely well. In addition, one can see increases during weekdays versus weekends as has been reported in previous studies [*Charron and Harrison*, 2005; *Johnson et al.*, 2005; *Wahlin et al.*, 2001]. This has been attributed to a relative increase in HDDV traffic during the week in Chapter 4. However, based on traffic count data, in addition to fewer HDDVs being on the road on weekends, there are also fewer LDVs

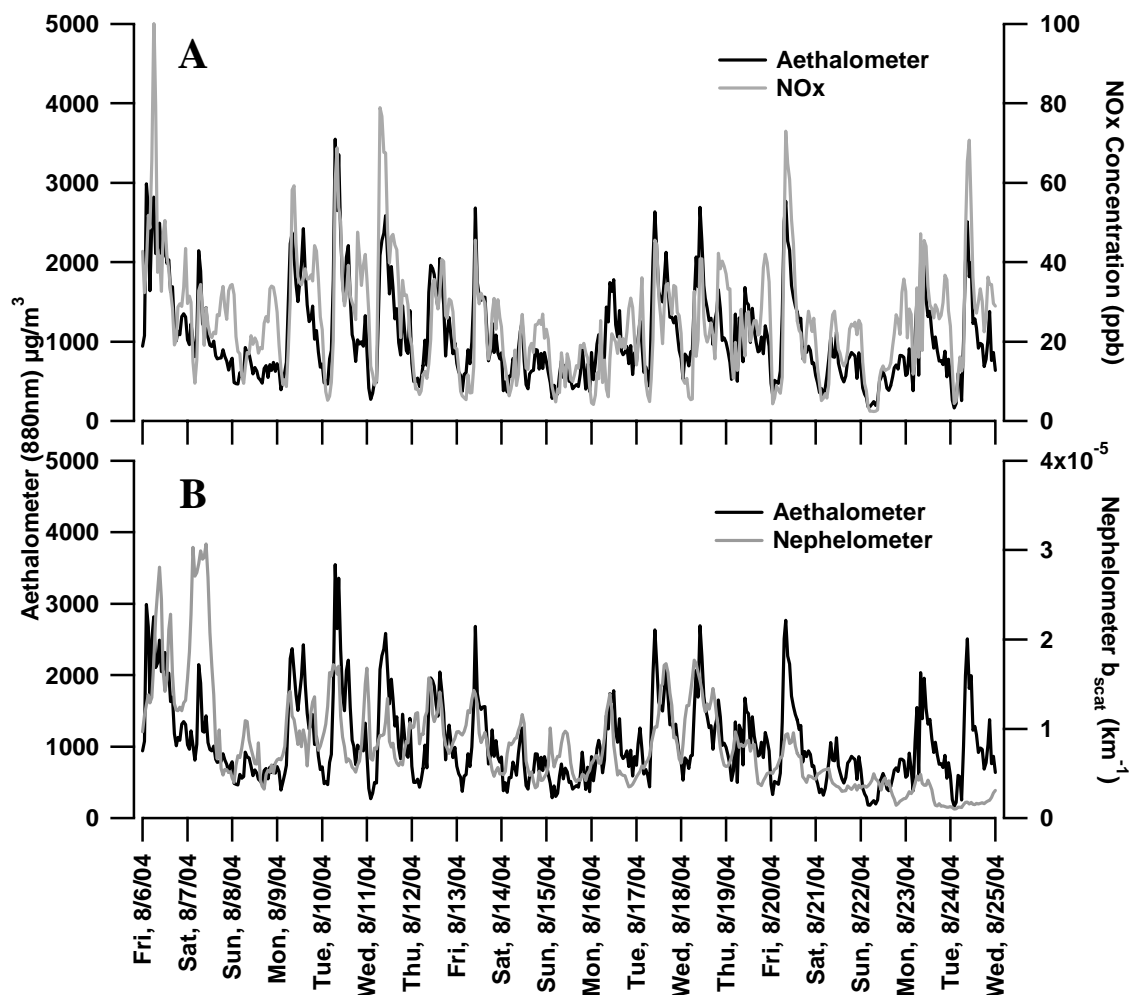


**Figure 5.4** A) Comparison of aethalometer and NO<sub>x</sub> measurements at the freeway site. B) Comparison of aethalometer and nephelometer measurements at the freeway site. Plots are in one hour resolution.

overall [Toner *et al.*, 2007]. Therefore, the traffic flow is lower on this stretch of freeway during the weekends compared to the weekdays.

#### 5.4.5 Upwind/Downwind Sampling

A major goal of the freeway study involved determining the contributions of vehicle emissions to ambient air near a major freeway. As previously described, an upwind sampling site was established so a comparison could be made between source contributions at a freeway-impacted site and a background (upwind) site. In addition to composition measurements being made with the ATOFMS and filters (Kleeman, UC-Davis), size distribution measurements were made using an APS and SMPS at both locations.

Figure 5.5A shows the APS and SMPS concentrations for the period between Jul. 24 and Aug. 3, 2004 at the freeway sampling site. Figure 5.5B shows the same data for the upwind sampling site. As can be seen, there is a constant band of particles with sizes from 250 – 800 nm at the two locations, suggesting a strong regional contribution to the ambient PM levels at both sites. It is important to note that the wind was blowing from the upwind site (onshore) towards the freeway site during daytime hours when the concentrations show maxima at both locations. This figure shows that the concentrations of accumulation mode particles above 200 nm at the upwind/background site were not always lower than those at the freeway site as one would expect if the freeway was the major source of PM in this area.

The ultrafine mode and low size end of the accumulation mode (50 – 300 nm) show higher concentrations at the freeway location (Figure 5.5A), suggesting fresh

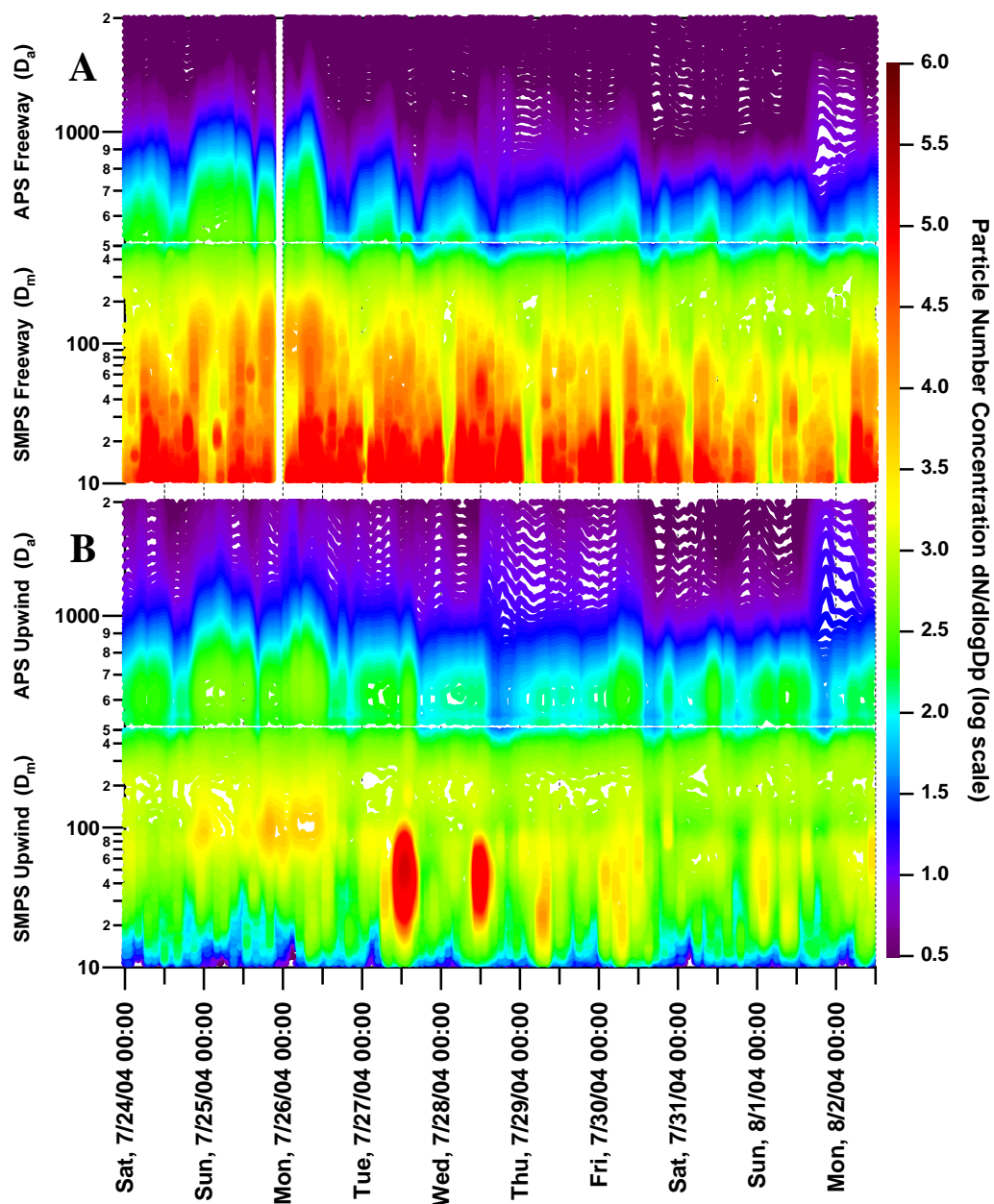


**Figure 5.5** A) SMPS and APS particle number concentrations at the freeway site from. B) SMPS and APS particle number concentrations at the upwind sampling site. Both plots are shown from Jul. 24 to Aug. 3, 2004 in order to directly compare the two sites. The data is shown in log scale.

vehicle emissions from the freeway are contributing to particles in the 50 – 300 nm size range. However, it is interesting to note that on July 27 and 28, at around noon, significantly higher ultrafine and accumulation mode concentrations are observed at the upwind lab site indicating contributions from a local source. The standard instrument (ATOFMS-2) was sampling at the upwind location during this period. An examination of the single particle composition revealed a unique single particle signature that has been detected as a major particle type in meat cooking emissions in previous meat cooking studies conducted in our laboratory [Silva, 2000]. A large potential source of PM on the UCSD campus near the sampling site is a cafeteria where food is grilled. The peak in emissions corresponds to the period of the day when the most people eat at this establishment. Notably, a meat cooking aroma is often detected at the upwind site.

On July 29 and 30, ultrafine concentrations at the upwind site peaked at approximately 6:00 am (Figure 5.5B) and most likely came from traffic on a local road that borders the UCSD campus located close to the upwind site (about 300 m away) which is highly traveled at this hour of the day. In general, ultrafine particle concentrations show the highest spatial variability and represent ideal markers for local source inputs, as they spike only near the emission source. The ultrafine particles are also the most straightforward to identify and apportion since they have undergone very little aging and thus their signatures closely resemble the source (in this case dynamometer testing) signatures.

As shown in Figure 5.5, regional background PM concentrations made significant contributions to the accumulation mode. Figure 5.6 compares the size distributions of the ATOFMS instruments [upwind (5.6A) and freeway (5.6B,C)] for the same time period as

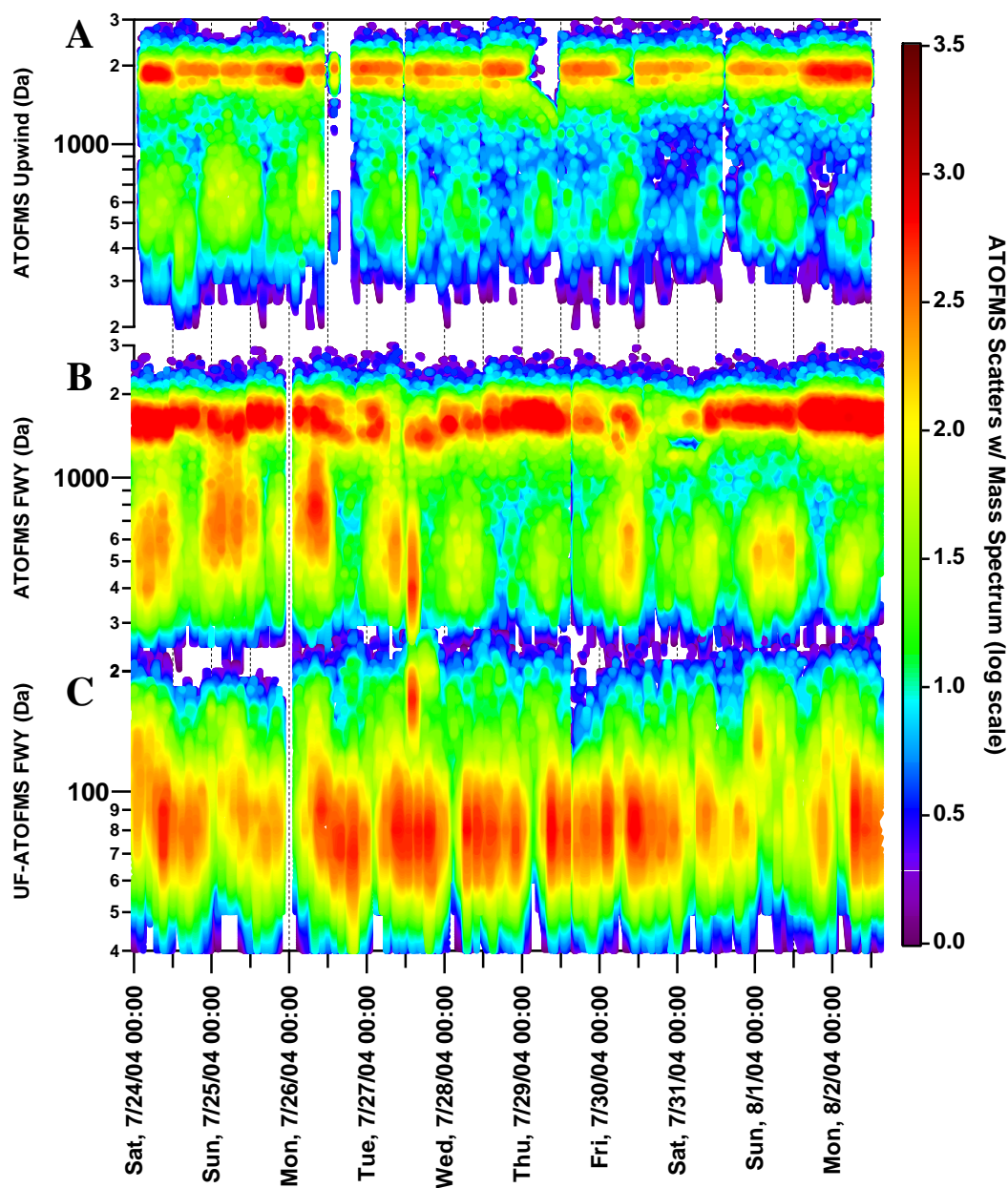


**Figure 5.6** Particle size distribution data of: A) Standard inlet ATOFMS at the upwind sampling site. B) Standard inlet ATOFMS at the freeway sampling site. C) UF-ATOFMS at the freeway site. The particle size data shown is only for particles that were detected that produced a mass spectrum with the particular ATOFMS instrument. The data shown is from Jul. 24 to Aug. 3, 2004 in order to compare the two sites and to the APS and SMPS data shown in Figure 5.5.



the comparison of APS and SMPS data compared in Figure 5.5. One can see that the accumulation mode size distributions show very similar trends between the upwind and freeway sites. While the freeway site shows higher concentrations in the accumulation mode, the upwind site shows peaks at the same times. The difference in concentrations may be due to the topography of the area. Since the freeway site is located in a lower, valley-like area, the background aerosols may be more prevalent at this site than at the upwind site which is closer to the coast and at a higher elevation. Evident in this figure is a relatively high PM concentration in the accumulation mode from July 24-27. It can also be seen that the accumulation mode peaks at nighttime and early morning hours, which corresponds to when the local wind speeds are at their lowest levels. This suggests that the accumulation mode particles are either due to smaller particles growing via condensation and/or agglomeration or from background particles at higher altitude settling to ground level. The latter of these scenarios is the most likely because of specific particle types detected that are unique to these time periods.

Due to these accumulation mode background contributions, other particle types were detected during this study that did not match to the vehicle dynamometer signatures. Figure 5.7 (A,B) shows the mass spectra for two such particle types: vanadium and elemental carbon (EC). These particle types peaked during the first few days of the study (July 24-27) in the accumulation mode at both sites usually when the local winds were low, likely indicating a regional contribution. The temporal trends for the vanadium and EC particle types are shown in Figure 5.7 (C,D). HYSPLIT model [Draxler and Rolph, 2003] 24-hour back trajectories during these peak times show the winds at 500 m coming (southward) down along the California coastline, passing directly over the major shipping

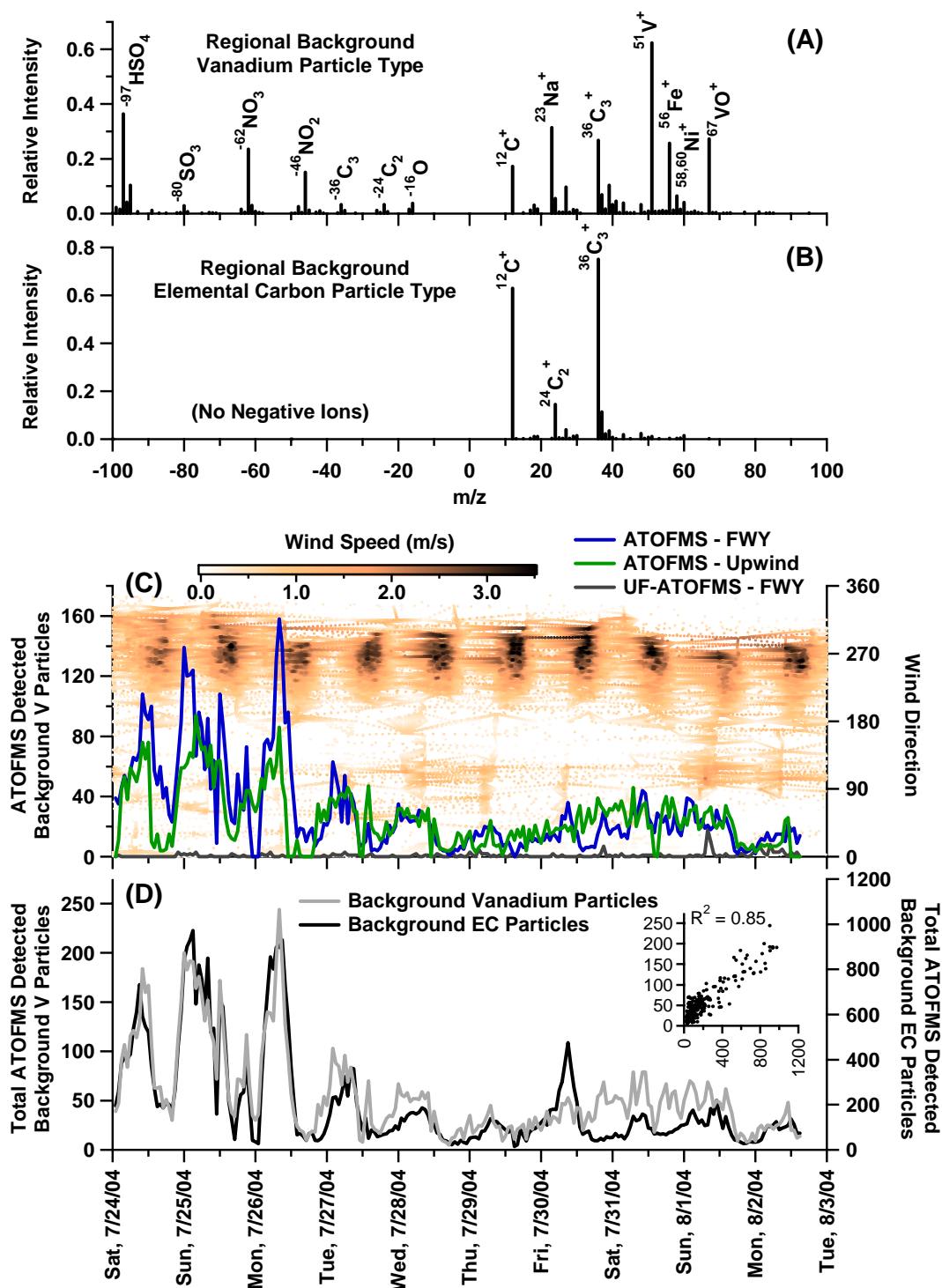


**Figure 5.7** Positive and negative ion mass spectra for the regional background (A) vanadium and (B) EC particle types. (C) The temporal trends of the vanadium particle type detected with all three ATOFMS instruments compared to wind data. (D) Temporal trends (and correlation) of total background vanadium particles versus the total background EC particles for the three ATOFMS instruments.

ports in Long Beach and San Pedro. The HYSPLIT model back-trajectories are shown in Figure 5.8. When comparing the temporal trends of the vanadium & EC particles to the HYSPLIT back trajectories, it can be seen that largest peaks (7/24-7/26) occur when the nighttime wind trajectories are strong and coming straight down the southern California coast from the Los Angeles area. The days with smaller peaks occur when the nighttime trajectories are either not as strong, or are coming into the sampling site from out over the ocean.

Oil combustion has been shown to be the primary source for atmospheric vanadium aerosols [Divita *et al.*, 1996; Phares *et al.*, 2003; Tolocka *et al.*, 2004; Xie *et al.*, 2006]. Vanadium particles have also been shown to come from vehicles, dust, and industrial sources [Ondov *et al.*, 1989; Rossini Oliva and Fernandez Espinosa, 2007; Sodeman *et al.*, 2005]. The correlation between V, Fe, and Ni associated with this type (as shown in Figure 5.7A) agree with findings by Xie *et al.* 2006 for ship oil combustion emissions [Xie *et al.*, 2006]. It is interesting to compare the temporal trend for these V-particles in the accumulation mode versus the ultrafine mode. On August 1, the number concentration of these particles shows a spike with the UF-ATOFMS that is not apparent in the accumulation mode, mostly likely indicating a local source. The temporal trends for the background vanadium and EC type, as well as the correlation between EC and V particle types, are shown in Figure 5.7D. As can be seen, the EC and vanadium trends track each other very strongly ( $R^2 = 0.85$ ), especially from 7/24 to 7/30, with only minor variations occurring between 7/30 and 8/1. This correlation is an indication that the EC and V particle types are transported together and are likely from the same source. The relationship between these types of vanadium and elemental carbon particles and the use

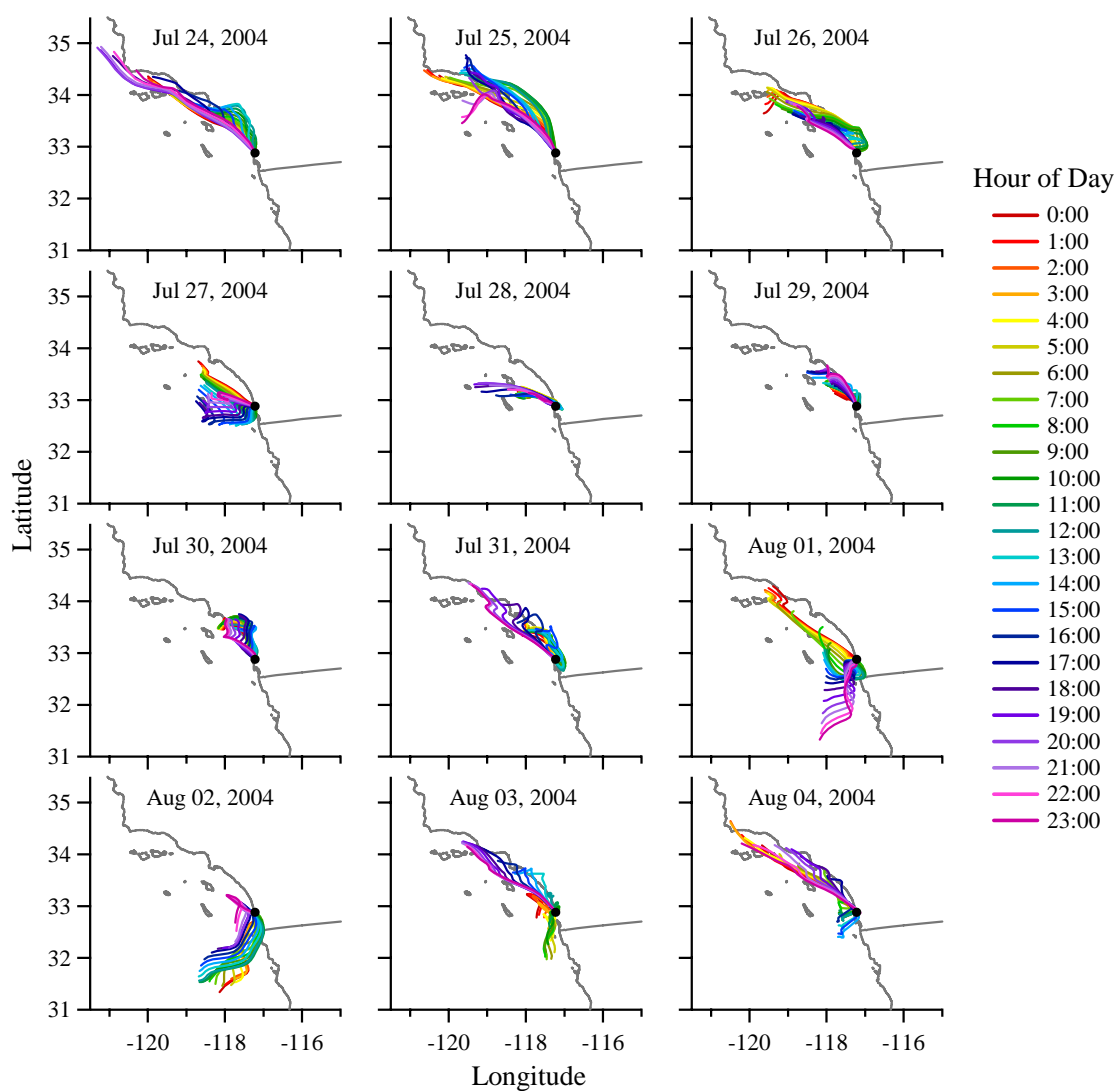


**Figure 5.8** Hourly HYSPLIT model 24-hour back trajectories at 500 m for each day at the freeway study site.

of these signatures for apportioning ship emissions will be discussed in a future publication [Ault *et al.*, 2007].

In general, all of the major particle types observed at the freeway site were also detected at the laboratory site. The similarities between the major particle types sampled by the standard ATOFMS instrument that was initially located at the upwind site (ATOFMS-2) and then moved to the freeway site were compared by taking the dot product of the top clusters detected at each site. All of the particle types detected at both sites had matching clusters with vigilance (similarity) factors of 0.85 and greater, meaning their mass spectral signatures were very similar to one another (a dot product of 1 indicates they are identical to one another). It is important to keep in mind that slight modifications due to uptake of organic carbon, ammonium, nitrate, and other secondary species will not have much of an effect on the comparison as the ART-2a weight vectors are sensitive to the most intense peaks in the spectra. The particle types deemed as “unique” at both sites were mainly sea salt particles. This is because they had undergone less processing in general at the upwind site since it is closer to the ocean. The spectral modifications due to heterogeneous processing involve the loss of one peak from a relatively complex particle spectrum and the addition of another. For example, the uptake of  $\text{NO}_x$  or  $\text{SO}_x$  species on a sea salt particle will displace the chlorine on the particle which will result in the ATOFMS spectrum of the “aged” particle having different negative ion peaks than a fresh sea salt spectrum [Gard *et al.*, 1998]. Reducing the vigilance factor to 0.7 instead of 0.85 resulted in all particle types at the freeway site, including sea salt, matching the clusters at the upwind site. As would be expected, the rank order (based on the number of particles in each cluster) of the various types and their

relative contributions to ambient PM was different at the two sites (i.e. there was more sea salt detected at the upwind site than at the freeway site, and more vehicle emissions detected at the freeway site than at the upwind site).

#### **5.4.6 Data Analysis Used for Apportionment**

The same method described in Chapter 4 for source apportionment using mass spectral source signatures was also used here [Toner *et al.*, 2007]. In short, several ATOFMS source characterization studies have been conducted for the purpose of obtaining unique mass spectral signatures for each source. The particle source library includes signatures for HDDV and LDV exhaust emissions, coal burning, biomass burning, meat cooking, sea salt, dust, and industrial emissions; as well as non-source specific signatures for aged elemental carbon (aged EC), aged organic carbon (aged OC), amines, NH<sub>4</sub>-containing, vanadium-containing, EC particles, and PAH-containing particles. These source signatures are used as a “seed” database, where the mass spectra of particles from other studies can be compared to the seeds using a matching version of the ART-2a algorithm [Allen, 2006; Song *et al.*, 1999] (YAADA v1.20 – <http://www.yaada.org>). Each particle mass spectrum is compared to all the mass spectra (ART-2a weight matrices) in the source database one at a time taking the dot product between each. If the particle matches to a particular source seed above a designated dot product vigilance factor (VF) threshold, then the particle is assigned to that type. If the particle matches to two or more different source seeds above the VF, then it will be assigned to the one that provided the highest dot product. The dot product values range

from 0 to 1 with a value of 1 indicating the particle types are identical. For this analysis, a relatively high VF of 0.85 was used.

The ART-2a matching method has shown that a significant fraction of the HDDV and LDV particle types acquired during dynamometer sampling are indeed representative of those produced near a roadway [Toner *et al.*, 2007; Toner *et al.*, 2006]. The results in Chapter 4 also show that the particles detected near the freeway are readily matched to particles from the vehicle dynamometer studies [Toner *et al.*, 2007]. These previous results focused on particles sampled with the UF-ATOFMS sampling near the freeway in the 50 – 300 nm size range, because particles in this size regime denote freshly emitted particles that would have a greater probability of originating from vehicular traffic on the freeway. The previous results also focused mainly on matching LDV and HDDV particles, since those would be the most similar types and thus, the potentially hardest to distinguish from one another. For this paper, the particles from the UF-ATOFMS and the two standard ATOFMS instruments were subjected to the same mass spectral matching procedures. However, since there is such a large size range sampled by these instruments, particles are only matched to source library particles of the same size range. Therefore, ultrafine particles (50 – 100 nm) are only matched to source particles in the same size range, and likewise for small accumulation mode particles (SAM) (100 – 140 nm), larger accumulation mode particles (LAM) (140 – 1000 nm), and supermicron particles (1000 – 3000 nm). Size segregated matching ensures that particle types from one source that may be similar to those of another source, but having very different particle size ranges, don't conflict with each other. The reason the accumulation mode was split into two libraries (for this study) was because of the regional background EC

and vanadium types discussed earlier which were found to influence the apportionment of the accumulation mode particles with sizes above 140 nm [Toner *et al.*, 2007]. As previously mentioned, the source library currently contains signatures for HDDVs, LDVs, dust, sea salt, biomass, and meat cooking, along with non-source specific signatures for aged organic carbon, aged elemental carbon, amine containing particles, PAH's, ammonia rich particles, vanadium particles, and elemental carbon particles. The signatures for HDDVs and LDVs were primarily obtained from dynamometer studies. Additionally, some of the HDDV and LDV signatures were obtained directly from ambient sampling after such particles were found to match with the dynamometer seeds. Other sources, such as biomass, dust, sea salt, and meat cooking were obtained from both lab studies and previous ambient measurements. The seeds for aged organic carbon, aged elemental carbon, amine containing particles, PAH's, ammonia rich particles, vanadium particles, and elemental carbon particles were obtained directly from classified ambient data from several different studies. As mentioned earlier though, the vanadium and elemental carbon seeds (many of which were derived from this study) may actually be signatures for ship emissions [Ault *et al.*, 2007].

#### **5.4.7 Source Apportionment Using ART-2a**

As described, ART-2a analysis was used to “match” ambient data to source seeds for the duration of the study. Figure 5.9 shows the size resolved apportionment for the first part of the study (Jul. 24 to Aug. 3, 2004) and averaged over those days. In Chapter 4, the one hour temporal apportionment of LDV and HDDV particles is shown for this same time period [Toner *et al.*, 2007]. From those results, it was shown that for ultrafine



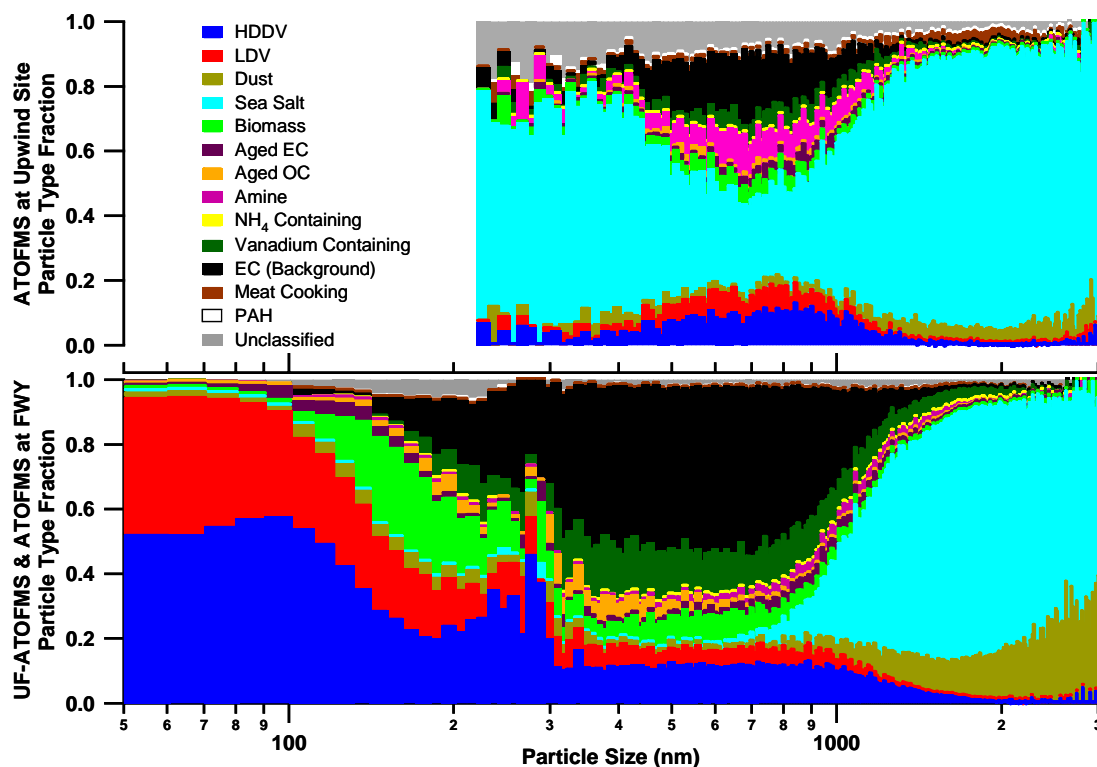


**Figure 5.9** Size resolved source apportionment of the particles detected at the upwind (top) and freeway (bottom) sampling sites. Both plots are averages for ATOFMS data acquired from July 24 to Aug 3, 2004. In the bottom plot for the freeway site, the sizing region of overlap between the UF-ATOFMS and standard inlet ATOFMS is 200 – 300 nm.

particles, 37% of the particles were apportioned to LDVs and 58% to HDDVs. For accumulation mode particles ( $Da = 100 - 300$  nm), 25% were LDV and 41% were HDDV. It was also shown that the trends of the apportioned particles tracked very well with LDV and HDDV vehicle counts. It is important to note that those results were only for particles detected with the UF-ATOFMS. Thus, when examining Figure 5.9, the ultrafine apportionment at the freeway site shows the same apportionment percentages as in Chapter 4. With the data from the standard ATOFMS being incorporated into the apportionment, size fraction trends through the region between 200 – 300 nm (where the two instruments overlap in particle size detection) for the HDDV apportionment is not as smooth due to the low number counts between 200 – 300 nm for both ATOFMS instruments. The trends of the other particle types in the 200 – 300 nm region are also not as smooth for the same reason as for the HDDV and LDV trends. The UF-ATOFMS was tuned to transmit ultrafine particles most effectively for this study by sampling ambient air drawn through a MOUDI with a 50% size cut at 100 nm to remove most of the particles larger than 200 nm, and thus making the transmission of particles above 200 nm relatively low [Su *et al.*, 2004]. Likewise, the detection of particles below 300 nm by the standard inlet ATOFMS was low for this study. These size detection barriers for each instrument can be seen quite clearly in Figure 5.6 (B,C). The relatively low detection efficiency of particles for each instrument between 200 and 300 nm during this study accounts for the lack of a smooth transition for the particle types in the 200 – 300 nm size range.

As shown in Figure 5.9, ATOFMS allows for the determination of aerosol apportionment with very fine (10 nm) size resolution. This is important, because it can

be seen that the fraction of particle types changes with size, especially above 100 nm. Above 100 nm, particles associated with biomass burning start to contribute to the ambient particles at the site, as well as particles apportioned to aged EC and aged OC. Most noticeable is the contribution from the EC (background) and vanadium-containing particle types starting around 140 nm (particularly for the EC background period). As discussed earlier, the regional background types were detected primarily at night, when local wind speeds were very low and when HYSPLIT back trajectories (Figure 5.8) come down the California coastline over Long Beach. These regional background types make up a major fraction of the particles from 200 – 1000 nm. The overall apportionment fractions stay relatively constant between 300 – 800 nm. Above 800 nm, sea salt particles start to contribute and become the dominant type above 1000 nm.

While seeds for non-aged and aged sources are included in the source signature library for non-vehicle sources, it should be noted that the sources are not currently being distinguished between aged and non-aged species to keep the apportionment simple. However, the majority of the particles from non-vehicle sources above 100 nm are coated with sulfate, nitrate, ammonium, as well as secondary organic aerosols (SOA) and that the amount of sec species increases with size based on ion intensities as one would expect.

When comparing the upwind site to the freeway site in Figure 5.9, one can see that sea salt particles dominated the detected particles at the upwind site. Interestingly, the particles apportioned to LDVs and HDDVs at the upwind site were primarily detected from 300 – 1000 nm. This observation could be an indication of growth of the vehicle particles as they were transported from the nearby roadway that is 200 meters upwind

from this site. Unfortunately, there was not another UF-ATOFMS at the upwind site to see if there was an influence of vehicle emission on the UF mode. As shown in Figure 5.5B, there was very little contribution to the UF mode at the upwind site except when cooking emissions from a nearby cafeteria impacted the site. Over the 400 – 1000 nm size range, there is a greater fraction of amine-containing particles that do not match to any source library particles, a possible indication of aging occurring on the vehicle particles as they were transported to this site. A commonality between the freeway site and the upwind site is the detection of the regional background vanadium and EC particles over the same size range. As explained earlier, while the freeway site shows a higher contribution than the upwind site (40% of the total particles at the freeway versus 10% at the upwind site over the 140 – 1000 nm size range), the difference may be due to the topography of the area. The fact that the EC and vanadium particles are detected over the same size range is further evidence that these particles are part of a regional background as shown in Figure 5.7.

#### **5.4.8 Size Resolved Source Apportionment Temporal Series**

As previously mentioned, the initial time series of the ATOFMS source apportioned freeway particles using the mass spectral source library was presented in Chapter 4. In that chapter, the focus was on the apportionment of HDDV and LDV emissions in the ultrafine size range. The particles that were not apportioned to HDDV and LDV were designated as “other” particles [Toner *et al.*, 2007]. For this current study, a mass spectral source signature library with additional clusters besides HDDV and LDV signatures was used. Therefore, many of the particles originally designated as

“other” are now apportioned, as can be seen in size resolved apportionment results presented in Figure 5.9. Figure 5.10 (A-D) shows the time series of the ultrafine and accumulation mode apportionment results at the freeway site, similar to those shown in Chapter 4, but with less particles in the “other” category. Figure 5.10 is ordered from the smallest size range at the top down to the largest size range at the bottom. Evident in this figure is the influence of non-vehicle particle types with the increase in particle size, just as Figure 5.9 shows. Also, the time series shows that certain particle types, such as biomass, are more prevalent on the weekends than the weekdays. Another interesting feature is the Aged OC class spikes on July 27, 2004 in the UF-ATOFMS 140 – 300 nm size range and the ATOFMS 200 – 1000 nm size range. This spike can also be seen in the ATOFMS number concentration plot in Figure 5.6, occurring at the same time across the same size ranges. The particles that matched to the Aged OC signatures during this time are fairly unique, as they only spiked with the two instruments on this one day during the study. One of the main points of Figure 5.10 is to show that even near a freeway, one is not just being exposed to freeway aerosols. During times with a high regional background influence, the freeway related PM above 100 nm represented a relatively small fraction of the overall concentrations.

The time series of the ATOFMS (300 – 1000 nm) particle fractions in Figure 5.10 compliment Figures 5.7 & 5.9. As shown in Figure 5.10, the EC background type dominates the particles between 300 and 1000 nm, with a strong contribution from the vanadium particles as well. The time series in Figure 5.7 shows that the EC & vanadium made a large contribution to the particle concentrations from 7/24 – 7/27. This is also quite evident in Figure 5.10 for the ATOFMS 300 – 1000 nm time series.

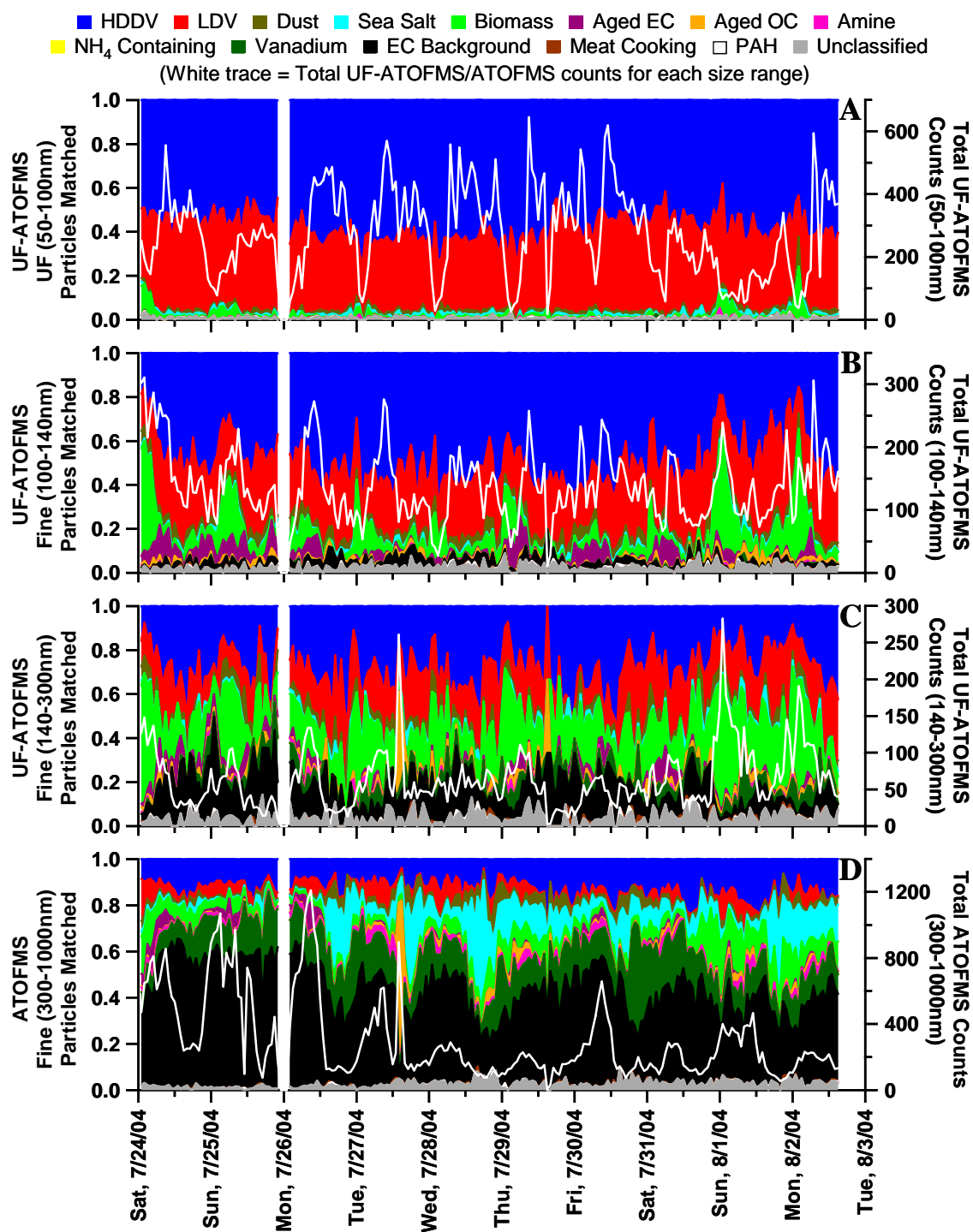


**Figure 5.10** Time series of the size segregated source apportionment fractions for the freeway site ultrafine and accumulation mode particles detected with the UF-ATOFMS and ATOFMS.

One should note that all results presented here are based on a relatively simplistic univariate data analysis approach using ART-2a. However, even with this simplistic approach, the results demonstrate how single particle data can be used to apportion source contributions to ambient data. Particle aging, coating, agglomeration, and water uptake will play important roles in affecting particle source apportionment in other studies using this source library technique. These changes will, undoubtedly, make matching to source signatures more challenging, particularly at locations further from the source. Many of the sources, such as biomass, sea salt, and dust are readily distinguishable whether or not the particles are aged. The biggest challenge with aging will be with differentiating LDV and HDDV exhaust particles from one another. However, there are unique features to the HDDV and LDV sources that should make matching consistent, whether the particles have aged or not. One of the most important factors is that HDDV particles tend to have more calcium and phosphate associated with them in an elemental carbon/calcium type particle (EC-Ca) [Shields *et al.*, 2007; Toner *et al.*, 2006]. LDV particles have much less calcium and/or phosphate associated with them, but do produce elemental carbon particles in the UF size mode [Sodeman *et al.*, 2005]. These kinds of distinctions could be used to identify HDDV and LDV particles in highly aged environments that do not match to the source seeds.

One of the ultimate goals of this study is to eventually compare single particle source apportionment with impactor filter samples acquired during this study. Single particle measurements hopefully can distinguish between unique vehicle source signatures superimposed on a high ambient background concentrations that may not be apparent in MOUDI mass concentrations where only slight changes are due to vehicle

emissions (at least for the accumulation mode). Also, once the data are available, the source percentage predictions made with ART-2a on the ATOFMS data will be compared with organic tracer MOUDI and impactor based method results from this study obtained by the Kleeman research group from UC-Davis. Additionally, future analysis using different clustering algorithms, such as Hierarchical clustering and Positive Matrix Factorization, will be used in comparison to the results found in this chapter and Chapter 4 [Toner *et al.*, 2007].

## 5.5 Acknowledgements

The authors thank Dan Cayan and Alex Revchuk of the Scripps Institution of Oceanography (SIO) at UCSD for setting up the micro-meteorological stations and providing their data for this study. We also thank UCSD and their facilities management for all their cooperation and help with setting up power to the freeway site. Lastly, we thank Michael Kleeman and Michael Robert from UC-Davis for their collaboration with this study. The HYSPLIT transport and dispersion model used in this publication was provided by the NOAA Air Resources Laboratory (ARL). Funding for this study was provided by the California Air Resources Board (CARB) (Contract 00-331).

Chapter 5 is reproduced with permission from Toner, S.M., L.G. Shields, and K.A. Prather, Source apportionment of freeway-side PM<sub>2.5</sub> using ATOFMS, *Atmospheric Environment*, Submitted for publication, 2007. Copyright 2007, Elsevier.



## 5.6 References

- Allen, J.O., Software toolkit to analyze single-particle mass spectral data - <http://www.yaada.org>, 2006.
- Allen, J.O., P.R. Mayo, L.S. Hughes, L.G. Salmon, and G.R. Cass, Emissions of size-segregated aerosols from on-road vehicles in the Caldecott Tunnel, *Environmental Science & Technology*, 35 (21), 4189-4197, 2001.
- Ault, A.P., H. Furutani, G. Dominguez, M.H. Thiemens, and K.A. Prather, A mass spectral fingerprint of ship emission particles by aerosol time-of-flight mass spectrometry and applications for source apportionment, *In Preparation*, 2007.
- Buzcu-Guven, B., G. Brown Steven, A. Frankel, R. Hafner Hilary, and T. Roberts Paul, Analysis and apportionment of organic carbon and fine particulate matter sources at multiple sites in the midwestern United States, *Journal of the Air & Waste Management Association*, 57 (5), 606-619, 2007.
- Charron, A., and R.M. Harrison, Fine (PM<sub>2.5</sub>) and Coarse (PM<sub>2.5-10</sub>) Particulate Matter on A Heavily Trafficked London Highway: Sources and Processes, *Environmental Science and Technology*, 39 (20), 7768-7776, 2005.
- Divita, F., Jr., J.M. Ondov, and A.E. Suarez, Size spectra and atmospheric growth of V-containing aerosol in Washington, DC, *Aerosol Science and Technology*, 25 (3), 256-273, 1996.
- Draxler, R.R., and G.D. Rolph, HYSPLIT (HYbrid Single-Particle Lagrangian Integrated Trajectory) Model access via NOAA ARL READY Website (<http://www.arl.noaa.gov/ready/hysplit4.html>). NOAA Air Resources Laboratory, Silver Spring, MD., 2003.
- Fraser, M.P., B. Buzcu, Z.W. Yue, G.R. McGaughey, N.R. Desai, D.T. Allen, R.L. Seila, W.A. Lonneman, and R.A. Harley, Separation of fine particulate matter emitted from gasoline and diesel vehicles using chemical mass balancing techniques, *Environmental Science & Technology*, 37 (17), 3904-3909, 2003.
- Fruin, S.A., M.J. St Denis, A.M. Winer, S.D. Colome, and F.W. Lurmann, Reductions in human benzene exposure in the California South Coast Air Basin, *Atmospheric Environment*, 35 (6), 1069-1077, 2001.
- Funasaka, K., T. Miyazaki, T. Kawaraya, K. Tsuruho, and T. Mizuno, Characteristics of particulates and gaseous pollutants in a highway tunnel, *Environmental Pollution*, 102 (2-3), 171-176, 1998.

- Gard, E., J.E. Mayer, B.D. Morrical, T. Dienes, D.P. Fergenson, and K.A. Prather, Real-time analysis of individual atmospheric aerosol particles: Design and performance of a portable ATOFMS, *Analytical Chemistry*, 69 (20), 4083-4091, 1997.
- Gard, E.E., M.J. Kleeman, D.S. Gross, L.S. Hughes, J.O. Allen, B.D. Morrical, D.P. Fergenson, T. Dienes, M.E. Galli, R.J. Johnson, G.R. Cass, and K.A. Prather, Direct observation of heterogeneous chemistry in the atmosphere, *Science*, 279 (5354), 1184 -1187, 1998.
- Gorse, R.A., Jr., On-road emission rates of carbon monoxide, nitrogen oxides, and gaseous hydrocarbon, *Environmental Science and Technology*, 18 (7), 500-7, 1984.
- Johnson, J.P., D.B. Kittelson, and W.F. Watts, Source apportionment of diesel and spark ignition exhaust aerosol using on-road data from the Minneapolis metropolitan area, *Atmospheric Environment*, 39 (11), 2111-2121, 2005.
- Johnson, T.V., Diesel emission control technology - 2003 in review, *Society of Automotive Engineers, [Special Publication] SP, SP-1835* (Diesel Emissions), 1-14, 2004.
- Kleeman, M.J., J.J. Schauer, and G.R. Cass, Size and composition distribution of fine particulate matter emitted from motor vehicles, *Environmental Science & Technology*, 34 (7), 1132-1142, 2000.
- Kleeman, M.J., Q. Ying, J. Lu, M.J. Mysliwiec, R.J. Griffin, J. Chen, and S. Clegg, Source apportionment of secondary organic aerosol during a severe photochemical smog episode, *Atmospheric Environment*, 41 (3), 576-591, 2007.
- Lehmann, U., M. Mohr, T. Schweizer, and J. Rutter, Number size distribution of particulate emissions of heavy-duty engines in real world test cycles, *Atmospheric Environment*, 37 (37), 5247-5259, 2003.
- Marshall, J.D., W.J. Riley, T.E. McKone, and W.W. Nazaroff, Intake fraction of primary pollutants: motor vehicle emissions in the South Coast Air Basin, *Atmospheric Environment*, 37 (24), 3455-3468, 2003.
- Miguel, A.H., T.W. Kirchstetter, R.A. Harley, and S.V. Hering, On-road emissions of particulate polycyclic aromatic hydrocarbons and black carbon from gasoline and diesel vehicles, *Environmental Science & Technology*, 32 (4), 450-455, 1998.
- Mysliwiec, M.J., and M.J. Kleeman, Source apportionment of secondary airborne particulate matter in a polluted atmosphere, *Environmental Science & Technology*, 36 (24), 5376-5384, 2002.

- Ondov, J.M., C.E. Choquette, W.H. Zoller, G.E. Gordon, A.H. Biermann, and R.E. Heft, Atmospheric behavior of trace elements on particles emitted from a coal-fired power plant, *Atmospheric Environment (1967-1989)*, 23 (10), 2193-204, 1989.
- Pelkmans, L., and P. Debal, Comparison of on-road emissions with emissions measured on chassis dynamometer test cycles, *Transportation Research Part D-Transport and Environment*, 11 (4), 233-241, 2006.
- Phares, D.J., K.P. Rhoads, M.V. Johnston, and A.S. Wexler, Size-resolved ultrafine particle composition analysis 2. Houston, *Journal of Geophysical Research, [Atmospheres]*, 108 (D7), SOS 8/1-SOS 8/14, 2003.
- Pope, C.A., Review: Epidemiological basis for particulate air pollution health standards, *Aerosol Science & Technology*, 32 (1), 4-14, 2000.
- Reilly, P.T.A., R.A. Gieray, W.B. Whitten, and J.M. Ramsey, Real-time characterization of the organic composition and size of individual diesel engine smoke particles, *Environmental Science and Technology*, 32 (18), 2672-2679, 1998.
- Riediker, M., W.E. Cascio, T.R. Griggs, M.C. Herbst, P.A. Bromberg, L. Neas, R.W. Williams, and R.B. Devlin, Particulate matter exposure in cars is associated with cardiovascular effects in healthy young men, *American Journal of Respiratory & Critical Care Medicine*, 169 (8), 934-940, 2004.
- Rogge, W.F., L.M. Hildemann, M.A. Mazurek, G.R. Cass, and B.R.T. Simoneit, Sources of fine organic aerosol 2: Noncatalyst and catalyst-equipped automobiles and heavy-duty diesel trucks, *Environmental Science & Technology*, 27 (4), 636-651, 1993.
- Rossini Oliva, S., and A.J. Fernandez Espinosa, Monitoring of heavy metals in topsoils, atmospheric particles and plant leaves to identify possible contamination sources, *Microchemical Journal*, 86 (1), 131-139, 2007.
- Seagrave, J., J.D. McDonald, A.P. Gigliotti, K.J. Nikula, S.K. Seilkop, M. Gurevich, and J.L. Mauderly, Mutagenicity and in vivo toxicity of combined particulate and semivolatile organic fractions of gasoline and diesel engine emissions, *Toxicological Sciences*, 70 (2), 212-226, 2002.
- Shields, L.G., D.T. Suess, and K.A. Prather, Determination of single particle mass spectral signatures from heavy duty diesel vehicle emissions for PM<sub>2.5</sub> source apportionment, *Atmospheric Environment*, 41 (18), 3841-3852, 2007.
- Silva, P.J., Source profiling and apportionment of airborne particles: A new approach using aerosol time-of-flight mass spectrometry. Ph.D. Dissertation, University of California, Riverside, p 428, 2000.

- Sodeman, D.A., S.M. Toner, and K.A. Prather, Determination of single particle mass spectral signatures from light duty vehicle emissions, *Environmental Science & Technology*, 39 (12), 4569-4580, 2005.
- Song, X.H., P.K. Hopke, D.P. Fergenson, and K.A. Prather, Classification of single particles analyzed by ATOFMS using an artificial neural network, ART-2A, *Analytical Chemistry*, 71(4), 860-865, 1999.
- Su, Y., M.F. Sipin, H. Furutani, and K.A. Prather, Development and characterization of an aerosol time-of-flight mass spectrometer with increased detection efficiency, *Analytical Chemistry*, 76 (3), 712-719, 2004.
- Tolocka, M.P., D.A. Lake, M.V. Johnston, and A.S. Wexler, Number concentrations of fine and ultrafine particles containing metals, *Atmospheric Environment*, 38 (20), 3263-3273, 2004.
- Toner, S.M., L.G. Shields, D.A. Sodeman, and K.A. Prather, Using mass spectral source signatures to apportion exhaust particles from gasoline and diesel powered vehicles in a freeway study using UF-ATOFMS., *Atmospheric Environment*, doi:10.1016/j.atmosenv.2007.08.005, 2007.
- Toner, S.M., D.A. Sodeman, and K.A. Prather, Single particle characterization of ultrafine and accumulation mode particles from heavy duty diesel vehicles using aerosol time-of-flight mass spectrometry, *Environmental Science & Technology*, 40 (12), 3912-3921, 2006.
- Vanvorst, W.D., and S. George, Impact of the California Clean Air Act, *International Journal of Hydrogen Energy*, 22 (1), 31-38, 1997.
- Wahlin, P., F. Palmgren, and R. Van Dingenen, Experimental studies of ultrafine particles in streets and the relationship to traffic, *Atmospheric Environment*, 35, S63-S69, 2001.
- Watson, J.G., J.C. Chow, D.H. Lowenthal, L.C. Pritchett, C.A. Frazier, G.R. Neuroth, and R. Robbins, Differences in the carbon composition of source profiles for diesel-powered and gasoline-powered vehicles, *Atmospheric Environment*, 28 (15), 2493-2505, 1994.
- Wenzel, R.J., D.Y. Liu, E. Edgerton, and K.A. Prather, Aerosol time-of-flight mass spectrometry during the Atlanta Supersite Experiment: 2. Scaling procedures, *Journal of Geophysical Research-Atmospheres*, 108 (D7), 8427, 2003.
- Xie, Z.Q., L.G. Sun, J.D. Blum, Y.Y. Huang, and W. He, Summertime aerosol chemical components in the marine boundary layer of the Arctic Ocean, *Journal of Geophysical Research-Atmospheres*, 111 (D10), 2006.

Zhang, K.M., A.S. Wexler, D.A. Niemeier, Y.F. Zhu, W.C. Hinds, and C. Sioutas, Evolution of particle number distribution near roadways. Part III: Traffic analysis and on-road size resolved particulate emission factors, *Atmospheric Environment*, 39 (22), 4155-4166, 2005.

# **6 Source apportionment of PM<sub>2.5</sub> in Athens (Greece) and Mexico City using an ATOFMS derived mass spectral source library**

## **6.1 Synopsis**

Using a variation of the ART-2a algorithm along with an aerosol time-of-flight mass spectrometry (ATOFMS) derived mass spectral source library, source apportionment of ambient aerosols for two major global cities (Athens, Greece and Mexico City, Mexico) was carried out. From these results, it was found that the ambient primary aerosols at both locations show a strong influence from biomass burning and dust. The Athens site also shows strong contributions from both diesel and gasoline powered vehicle emissions, sea salt, and a combination of elemental carbon and vanadium particles that could be due to ship emissions. While the aerosols at both sites show signs of aging and associations with secondary organic carbon, nitrate, sulfate, and ammonium, the Mexico City site was found to have more aged aerosols than Athens, and (along with biomass burning and dust) shows contributions from diesel and gasoline vehicle emissions, industrial emissions, meat cooking, and non-source specific amines, PAH's, aged organic and elemental carbon. The results obtained with the source signature matching technique are compared to general particle classification results and

show that the source signature matching technique is applicable to worldwide ambient ATOFMS data.

## 6.2 Introduction

Proper source apportionment of ambient particles is important with regards to understanding their origin, as well as determining the roles they may play in the environment and affecting human health. The ability to apportion ambient particles quickly and accurately will be very helpful for environmental and health agencies and for monitoring and enforcing emission standards. This kind of application is also useful for global climate and pollution modelers who desire to know the contribution of specific sources in a given region rather than using estimated numbers from emission inventories [Chung *et al.*, 2005; Fraser *et al.*, 2000; Griffin *et al.*, 2002; Ramana and Ramanathan, 2006; Ramanathan and Crutzen, 2003]. Traditional methods of ambient aerosol classification and apportionment typically use filter or impactor based applications where aerosols are collected on a substrate and then analyzed with offline techniques [Cass *et al.*, 2000; Kleeman and Cass, 1998; Kleeman *et al.*, 2000]. Other methods have apportioned particles to sources based strictly on the size distribution and concentration of ambient aerosols [Lehmann *et al.*, 2003; Reilly *et al.*, 1998; Zhang *et al.*, 2005a]. More recent techniques using mass spectrometry on single particles, such as aerosol time-of-flight mass spectrometry (ATOFMS) [Gard *et al.*, 1997; Su *et al.*, 2004], have proven very useful for determining the size resolved chemical composition of aerosols [Bein *et al.*, 2006; Bhave *et al.*, 2001; Owega *et al.*, 2004; Silva *et al.*, 1999]. One of the issues with the single particle mass spectrometry techniques is that the classification, labeling,

and apportionment of particles based on their mass spectrum is dependent upon user interpretation. This can result in inconsistencies with labeling of similar classes and apportionment.

The methods for ATOFMS single particle data analysis and classification have been developing and progressing over the years. Some methods have included: sorting through individual spectra by hand, which can be extremely time consuming for large datasets; simple  $m/z$  peak searching using basic table database structures; and databases where mathematical algorithms can be used to cluster the data based on user defined parameters. The major progress has come from incorporating data clustering methods with mathematical algorithms such as ART-2a, K-means, and Hierarchical Clustering [Lance and Williams, 1967; Murphy *et al.*, 2003; Phares *et al.*, 2001; Rebotier and Prather, 2007; Ward, 1963]. These techniques have been shown to accurately cluster particle spectra within given similarity thresholds [Bhave *et al.*, 2001; Murphy *et al.*, 2003; Rebotier and Prather, 2007; Song *et al.*, 2001; Tan *et al.*, 2002; Wenzel and Prather, 2004]. These methods fail to label (or classify) the particle types they have been used to cluster. That process is still determined by the user which can succumb to biases or overly generalized classification. The use of a mass spectral source library for apportioning ATOFMS single particle data has been described and shown to work with minimal error in a fresh emission environment [Toner *et al.*, 2007a; Toner *et al.*, 2007b]. The next progressive step is to use the method on more aged environments and/or other global areas to see if a mass spectral library developed for one location is representative of the same sources around the world. The goal of this study is to test the mass spectral source library matching method on ATOFMS data collected in more polluted



environments (Athens, Greece and Mexico City) to determine if the library signatures are applicable in other locations and with other ATOFMS instruments.

### 6.3 Experimental

The use of a single mass spectral library for source apportionment of ATOFMS data, for any sampling location, is a very desirable commodity. To date, ATOFMS ambient particle mass spectral data are typically clustered using the ART-2a algorithm and then visually characterized [Bhave *et al.*, 2001; Song *et al.*, 1999]. The inherent weakness of such a method is that user bias can sway the classification results, and the homogeneity of an ART-2a cluster can vary depending on the parameters used for clustering. Using a mass spectral library, built from ART-2a generated clusters from various source characterization studies, is a novel approach to eliminating user bias when classifying single particle data. This approach can also help reduce misclassification of particles because the clusters within the source library do not change as particles are added to them during the apportionment step. The library matching method uses a variation of the ART-2a algorithm known as match-ART-2a ([www.yaada.org](http://www.yaada.org)) [Allen, 2006]. This method is different than the standard ART-2a clustering method by having particle clusters (or seeds) already defined. These seeds are the particle source signatures from the source library which are described below. As particle spectra are compared mathematically, taking the dot product, to the seed spectra in the library, they either will match to specific source seeds above a defined vigilance (or similarity) factor (VF), or they may not match to any of the source seeds. If the particle matches to a particular source seed above a designated dot product VF threshold, then the particle is assigned to

that type. If the particle matches to two or more different source seeds above the VF, then it will be assigned to the one that provided the highest dot product. The dot product values range between 0 and 1, where a dot product of 1 means the particle spectra are identical. Particles that do not match to any of the source seeds are grouped in an unclassified category.

The current source library contains seeds for seven specific sources (gasoline powered light duty vehicles (LDV), heavy duty diesel vehicles (HDDV), biomass burning, dust, sea salt, meat cooking, and industrial emissions) and has seeds for seven other general particle types (elemental carbon (EC), aged organic carbon (aged OC), aged elemental carbon (aged EC), amines, PAH's, vanadium-containing, and  $\text{NH}_4$ -containing) for particles that may not match into any of the seven specific sources. The source specific seeds were obtained from both laboratory and ambient field studies conducted with the ATOFMS. For example, the HDDV and LDV clusters were generated from data acquired from dynamometer studies as well as from a freeway-side study. Likewise, the dust source signatures were obtained from lab studies of resuspended dust and soil as well as from dust particle classes detected from various ATOFMS studies around the world. The sea salt, industrial, and non-source specific seeds were generated exclusively from particle classes detected from ATOFMS ambient studies. The non-source specific aged types were created from ATOFMS ambient studies where the particle types exhibit ion peaks attributed to aging (i.e. SOA, nitrate, sulfate, and ammonium) and are too convoluted to assign to a specific source. While there are not a vast amount of specific sources currently in the library, the current types represent major particle types found in urban, marine, and rural areas [Kim *et al.*, 2005; Kleeman and Cass, 1998; Liu *et al.*,

2003; *Park and Kim*, 2005; *Pastor et al.*, 2003; *Querol et al.*, 2001; *Swietlicki et al.*, 1996; *Ward et al.*, 2006; *Ying and Kleeman*, 2006; *Zhao and Hopke*, 2006]. The library is adaptive and can have more source signatures added to it as future source characterization and ambient studies are conducted. Such sources include a variety of industrial emissions, coal combustion, and cigarette smoking, as well as increasing the detail on the vehicle source seeds and with more aged source particle types.

It is very important to test the source library on multiple ATOFMS instruments in order to insure that they can be universal for the ATOFMS community around the world. The library, as it currently stands, is not completely universal just yet. Since the library is open-source, it can always have new source spectra added to it or even have ones removed if they are found to interfere with proper apportionment. The idea is for the library to be openly available to the ATOFMS community and for it to evolve as users modify the library with their own source data.

The source signature library matching technique was previously tested on ATOFMS ambient data obtained in a location dominated by “fresh” emissions near a freeway (Chapters 4 and 5) [*Toner et al.*, 2007a; *Toner et al.*, 2007b]. To test whether particles can be apportioned in different environments, as well as with ATOFMS instruments used by different research groups, data from two different global locations were chosen. The first study is Athens, Greece (37°59'12.24"N 23°43'30.73"E), which was conducted in August of 2003 using a TSI 3800 ATOFMS owned and operated by the Harrison research group out of the University of Birmingham [*Dall'Osto and Harrison*, 2006]. The second study is Mexico City, Mexico (19°29'23.60"N 99°08'55.60"W), which was conducted in March of 2006 with an in-house built ATOFMS instrument that

was also used for some of the original source characterization studies used to build the source library [Moffet *et al.*, 2007]. The experimental methods as well as the general classification of the particles are described for both studies in the literature [Dall'Osto and Harrison, 2006; Moffet *et al.*, 2007]. A map for both locations is included in Appendix 3 (Figure A3.1). The ATOFMS data from both of these studies were analyzed (separately) using the source library with match-ART-2a at a VF of 0.85 which represents a very high VF. This is the same VF used in Chapter 4 which showed a low error of 4% for aerosol apportionment at  $VF = 0.85$  [Toner *et al.*, 2007b]. The same VF is used again for this study to test if such a high VF can be used to apportion particles in more polluted (and aged) regions. The effect of varying the VF are shown and discussed in the Appendix 3. The source apportionment results from the mass spectral library matching method are discussed and compared to the traditional ART-2a classified particles reported in the literature for both studies [Dall'Osto and Harrison, 2006; Moffet *et al.*, 2007].

## **6.4 Results and Discussion**

### **6.4.1 Source apportionment of ambient particles in Athens, Greece**

The ambient particles detected with the ATOFMS used by Dall'Osto *et al.* in Athens, Greece were analyzed using the match-ART-2a technique with the mass spectral source signature library. As was previously mentioned, a VF of 0.85 was used for the library matching process. For this particular analysis, the submicron (200 – 1000 nm) and supermicron (1000 – 3000 nm) particles were analyzed separately in order to illustrate the chemical differences that typically distinguish the two modes. The

submicron mode particles are typically due to combustion sources and/or agglomeration and condensation processes, while the supermicron mode aerosols are typically represented by mechanically driven processes. Figure 6.1 shows the temporal series of the submicron (Figure 6.1A) and supermicron (Figure 6.1B) apportioned particles along with their respective total ATOFMS particle counts (white trace). It is apparent by looking at Figure 6.1 that there is a large number of particles that are not apportioned to any sources (i.e. unclassified) by this matching process at  $VF = 0.85$ . The reason for this is because the data collected for this study has many spectra with low signal to noise and a large fraction (~15% in the submicron and over 35% in the supermicron) of spectra with miscalibrated peaks [Dall'Osto and Harrison, 2006]. These noisy and miscalibrated spectra typically do not match to the source library spectra, especially at a high VF of 0.85, as their ion peaks simply do not match. For this reason, matching was also carried out at a lower VF and with a different technique using only the positive ions for the unclassified particles to see how these parameters affect the matching process. The results from the lower VF matching and positive ion matching are shown in Figures A3.2, A3.3, and A3.4 in Appendix 3. The process of positive ion is also described in Appendix 3.

As shown in Figure 6.1A, biomass burning contributes to the majority (~33%) of ambient submicron particles. This result agrees with findings in Dall'Osto et al., 2006; however, the particles attributed to biomass by library source matching were more generically labeled as secondary carbon by Dall'Osto et al. Despite being labeled as secondary carbon by Dall'Osto et al., inspection of these particles revealed that they contain a large peak due to potassium and exhibit very strong similarities to the biomass

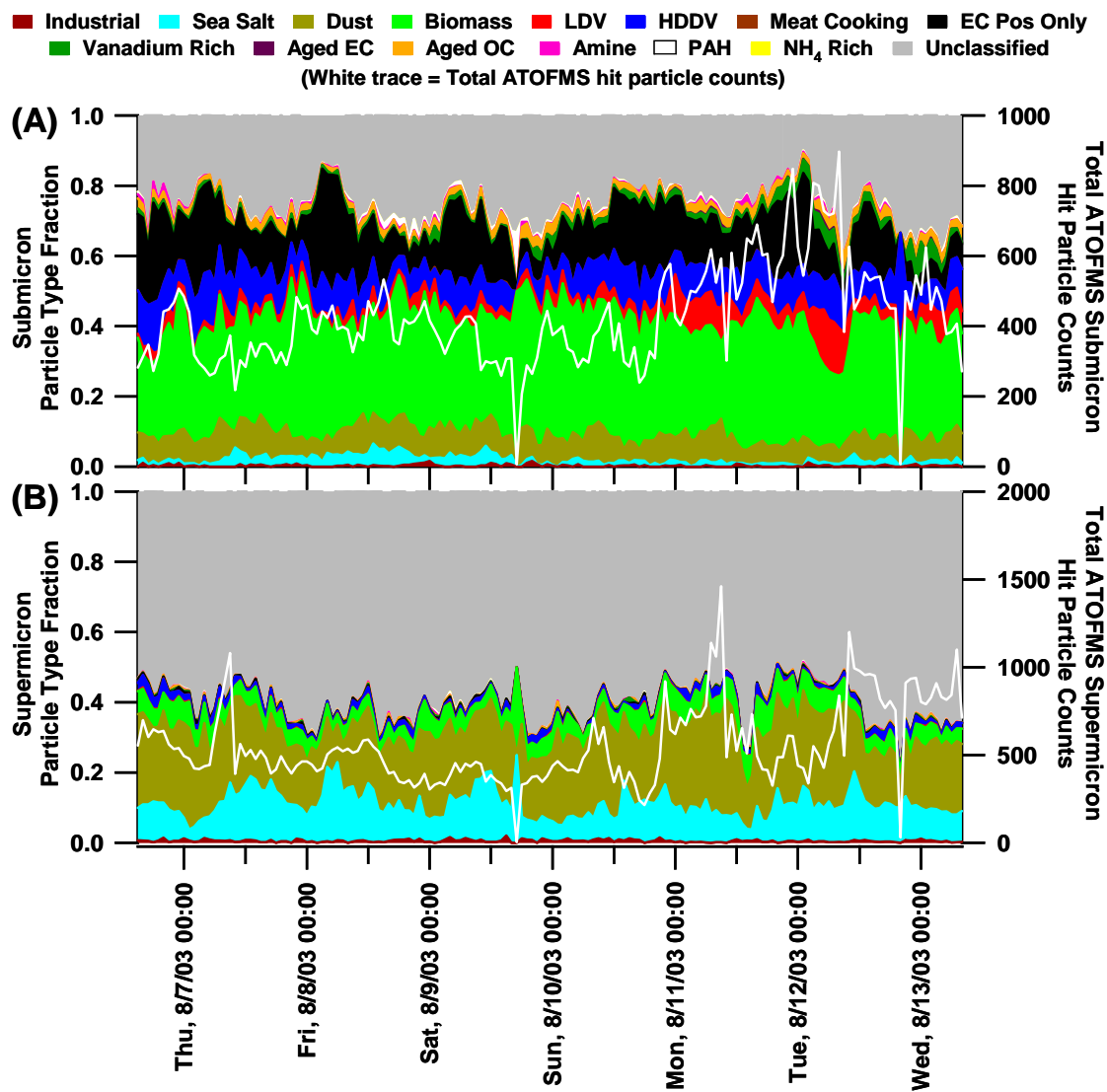


**Figure 6.1** Temporal series of the mass spectral source library matching results for Athens, Greece ambient A) submicron particles; and B) supermicron particles.

signatures (matching with dot products  $> 0.9$ ). The summer of 2003 produced record temperatures and an intense wildfire season throughout Europe. These wildfires have a major impact on the air quality over the Mediterranean area [Hodzic *et al.*, 2007], and explain why biomass aerosols appears as a consistent background during this study. Since these biomass particles have been transported to the Athens site, it is likely that much of the carbon they contain is due to the uptake of secondary organic carbon. Elemental carbon particles (EC Pos Only) make up the next largest fraction (14%) of particles for the submicron mode. This particle type has been shown before to correlate with vanadium particles in a coastal environment, and may be indicative of ship emissions [Ault *et al.*, 2007; Toner *et al.*, 2007a]. The other major contributors to the submicron particles are dust, HDDV, and LDV at 7%, 9%, and 4% respectively. There are also more minor contributions from sea salt, aged OC, vanadium, amines, and industrial emissions. It is interesting to note that there is no strong diurnal variation for any of the source fractions, nor with the total ATOFMS submicron counts. This may be another indication of a fairly constant regional background as described for the biomass particles.

As can be seen in Figure 6.1B for the supermicron mode, the majority of the classified particles are from dust (21%) and sea salt (11%). Both local and transported dust have been shown to be a major fraction to the particulate matter in Athens in prior studies [Eleftheriadis *et al.*, 1998; Metzger *et al.*, 2006; Papayannis *et al.*, 2005], as well as by Dall'Osto *et al.* for this study [Dall'Osto and Harrison, 2006]. This is a good indication that the matching results for the classified particles are accurate. The particles apportioned to sea salt do show some temporal variations, which may a function of local

winds. Since much of Greece is surrounded by the Mediterranean Sea, and the closest coastline to the sampling site is 6.5 km, it seems very reasonable that there be a contribution from sea salt to the supermicron mode. As shown in Figure 6.1B, almost 60% of the supermicron particles were not classified by the library matching technique though. As stated earlier, this is because over 35% of the supermicron spectra have miscalibrated ion peaks for this study. In Appendix 3, Figure A3.3, it is shown that many of these miscalibrated spectra are just for the negative ions (as by the results of a positive ion matching process), and are primarily for dust and sea salt particles, which become 39% and 19% of the particles, respectively, after matching this way. Also contributing to the supermicron mode are particles from biomass burning, industrial emissions, diesel emissions, and some aged OC and amines. The matching percentages for each source are summarized in Table 6.1 (and Table A3.1 in Appendix 3).

Figure 6.2 shows the size resolved source apportionment of the ATOFMS detected ambient particles for Athens, Greece. As can be seen in this figure, biomass particles represent the major fraction of the submicron particles, but only down to 250 nm. To note, the biomass particles are not 100% pure biomass particles since they have transported to the Athens site and contain secondary species (organics, nitrate, and sulfate) on them. The influence from both HDDV and LDV emissions can be seen throughout the full size range of the submicron particles, but below 250 nm the influence from diesel emissions is detected as the major particle type. As described by Dall'Osto et al., the sampling site was located alongside a road with moderate traffic, with more trafficked roads in relatively close proximity to the site. These findings agree with other roadside studies, even with high LDV to HDDV traffic ratios, that the smaller particles



**Table 6.1** Percent of Athens, Greece particles matched to the mass spectral source library at different match-ART-2a Vigilance Factors (VF)

Particle Source	Matching VF = 0.85		Matching VF = 0.85**		Matching VF = 0.75	
	Sub %	Super %	Sub %	Super %	Sub %	Super %
Industrial	0.29	0.54	0.72	1.37	0.48	1.23
Sea Salt	1.78	10.45	2.77	19.30	2.66	19.36
Dust	7.18	21.09	11.95	38.64	11.62	41.81
Biomass	32.56	5.11	34.41	6.30	36.57	7.06
LDV	4.30	0.12	5.02	0.18	8.33	0.28
HDDV	8.90	1.42	8.90	1.42	10.37	4.27
Meat Cooking	0.01	0.00	0.01	0.00	0.01	0.00
EC (Positive only)	14.03	0.35	14.03	0.35	13.44	0.37
Vanadium Rich	1.82	0.15	2.04	0.26	2.60	0.29
Aged EC	0.07	0.00	0.07	0.00	0.09	0.00
Aged OC	2.34	0.36	2.34	0.36	4.73	1.02
Amine Containing	0.39	0.07	0.60	0.14	1.36	0.14
PAH Containing	0.62	0.07	0.62	0.07	0.06	0.04
NH4 Containing	0.00	0.00	0.00	0.00	0.00	0.00
Unclassified	25.72	60.26	16.51	31.60	7.69	24.13

Sub = Submicron particles (200-1000nm)

Super = Supermicron particles (1000-3000nm)

\*\* Matching at VF = 0.85 including rematching unclassified particles using positive ion only matching

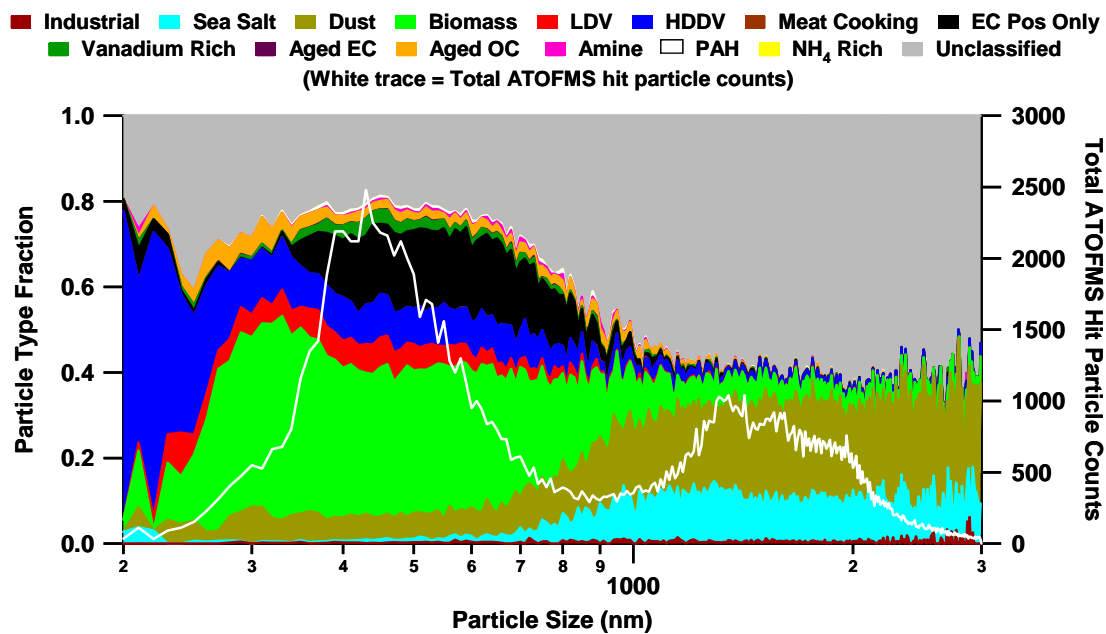


**Figure 6.2** Size resolved source apportionment of the ATOFMS detected ambient particles for Athens, Greece.

will be dominated by vehicle traffic of which diesel emission can be the largest contributor [Imhof *et al.*, 2005; Kittelson *et al.*, 2006; Toner *et al.*, 2007b; Zhang *et al.*, 2005a; Zhao and Hopke, 2004]. The EC positive ion only type as well as vanadium particles are shown to peak between 300 and 1000 nm, just as in a previous coastal ATOFMS study [Toner *et al.*, 2007a]. As was discussed in Chapters 4 and 5, these two classes combined in this size range may be due to ship emissions, however their temporal  $R^2$  correlation for Athens is 0.5, which may indicate separate sources for this site. The analysis of a current ATOFMS study is underway to determine if these signatures are ship emissions [Ault *et al.*, 2007]. As discussed for Figure 6.1B, it can be seen that both dust and sea salt make up the majority of the classified particles in Figure 6.2. In Appendix 3, Figure A3.4, it is shown that the majority of the unclassified supermicron particles in Figure 6.2 are from miscalibrated dust and sea salt.

#### **6.4.2 Source Signature Matching for Athens, Greece**

While the ATOFMS mass spectral library contains many spectra for each source, it is interesting to examine the top spectra to which the particles are matched for each study. Figure 6.3 shows the top library spectra that the ambient Athens particles matched to for each specific source, while Figure 6.4 shows the top non-source specific source spectra that were matched. The particle types are listed in order (as in Figures 6.1 and 6.2) across Figures 6.3 and 6.4.

Despite not being one of the major particle types in the Athens ambient aerosol, it is interesting to note that the particles which match to the industrial spectrum (Figure 6.3) are matching to a library cluster that was produced from the Mexico City dataset. This

industrial particle type is characterized by the large ion signals due to sodium and potassium, as well as the presence of aluminum, iron, zinc, and lead, as described in the literature [Moffet *et al.*, 2007]. Such particles, described by Moffet *et al.*, are consistent with those associated with high temperature combustion sources such as waste incinerators [Hu *et al.*, 2003; Moffet *et al.*, 2007]. Particles containing these metals have also been detected in prior Athens aerosol characterization studies [Kanas *et al.*, 2004; Karageorgos and Rapsomanikis, 2007; Scheff and Valiozis, 1990; Valavanidis *et al.*, 2006; Vassilakos *et al.*, 2007].

The top sea salt, dust, biomass, LDV, and HDDV library clusters that were matched are typical of those seen in other ATOFMS studies [Dall'Osto and Harrison, 2006; Guazzotti *et al.*, 2003; Guazzotti *et al.*, 2001; Qin and Prather, 2006; Silva *et al.*, 2000; Sodeman *et al.*, 2005; Toner *et al.*, 2006]. The majority of the sea salt and biomass particles detected for this Athens study show signs of aging due to the uptake and oxidation of NO<sub>x</sub> species. The biomass particles, as well as the HDDV and LDV particles, also show the presence of HSO<sub>4</sub><sup>-</sup> (*m/z* -97) and SOA (*m/z* +43). The top dust type for Athens is dominated by the presence of calcium which is consistent with the findings by Dall'Osto *et al.*, and others for Athens PM<sub>2.5</sub> [Dall'Osto and Harrison, 2006; Eleftheriadis *et al.*, 1998; Metzger *et al.*, 2006]. This dust type has been shown to be transported from the Saharan desert in previous studies and is commonly detected in the Mediterranean area [Eleftheriadis *et al.*, 1998; Formenti *et al.*, 2003; Ganor, 1991; Papayannis *et al.*, 2005]. The presence of the large nitrate ion peak (*m/z* -62) is also an indication that this dust type has been transported and aged.

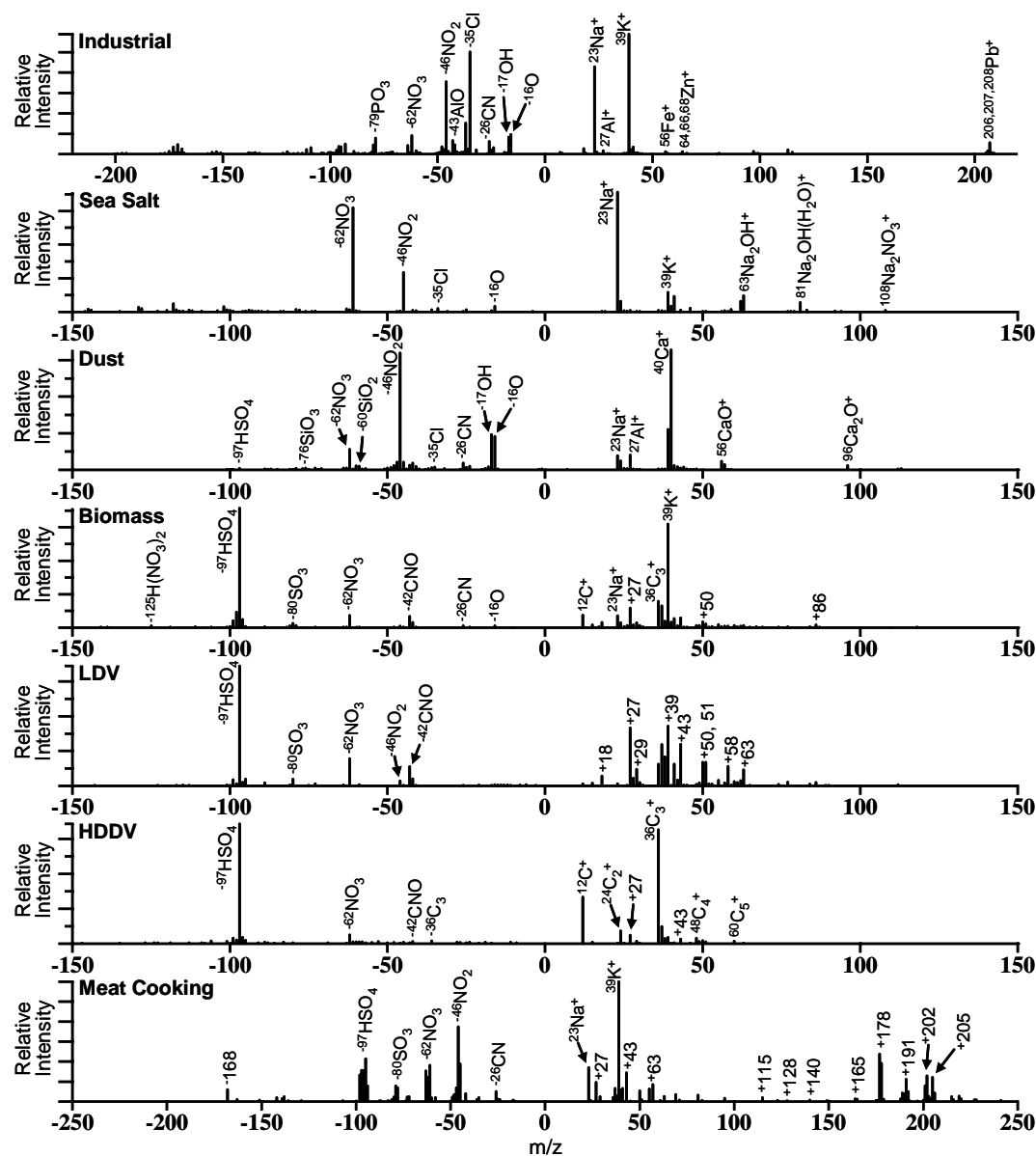


**Figure 6.3** The top matching mass spectral source signatures for each source for Athens, Greece ATOFMS data.

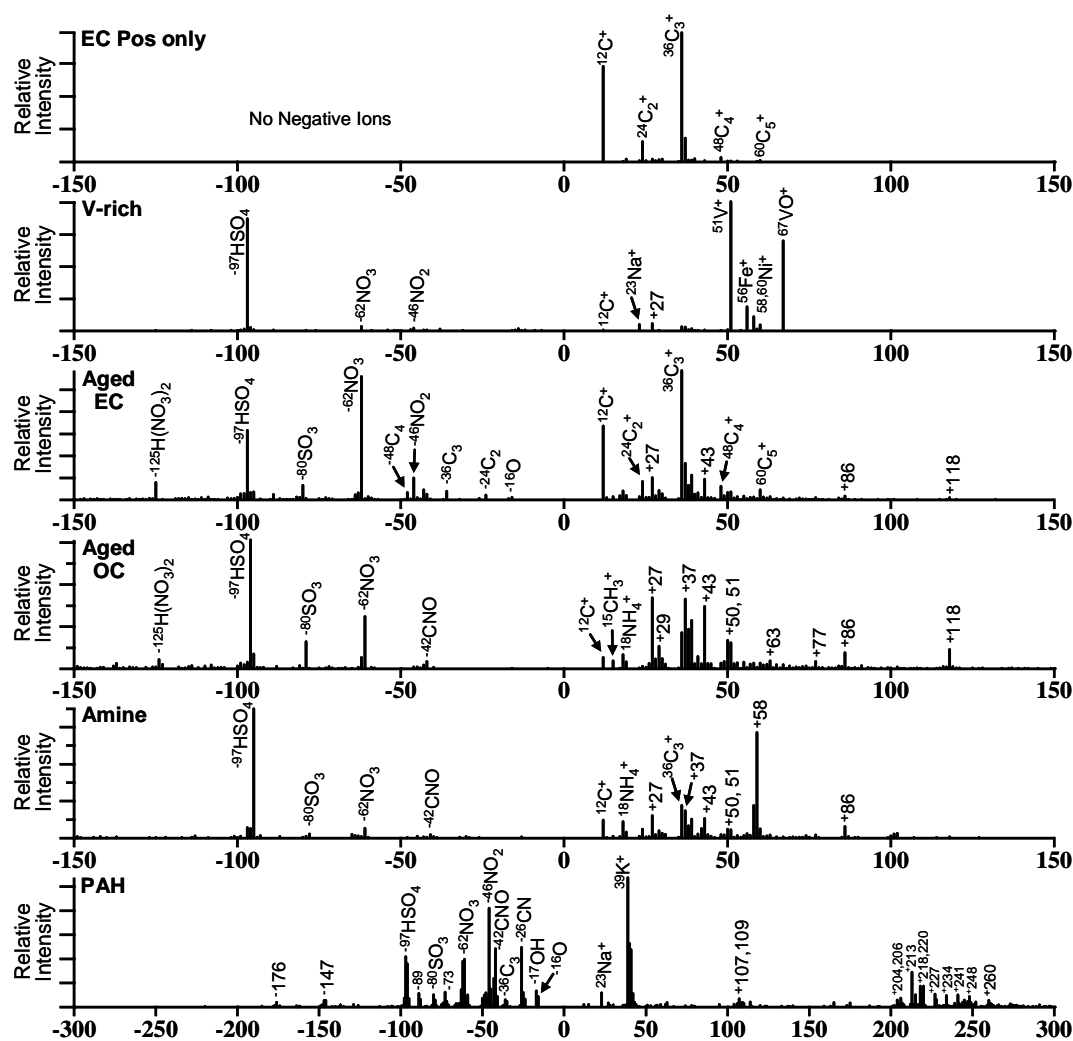


**Figure 6.4** The top matching non-source specific mass spectral signatures for each type for Athens, Greece ATOFMS data.

Figure 6.4 shows the top non-source specific library clusters that were matched to for the Athens dataset. The EC pos only type (characterized by EC peaks at  $m/z$  12, 24, 36, 48, and 60, and the lack of negative ions) and the vanadium (V-rich) particle types are very similar to the ones described in Chapter 5 [Toner *et al.*, 2007a]. As noted earlier, these particles may be due to ship exhaust emissions as indicated in Chapter 5, but their low  $R^2$  correlation for the Athens data may suggest different sources for this site. Further analysis is underway to confirm this, as these are relatively general particle types that could be produced from a number of different sources. The aged EC and aged OC types both show the presence of nitrate, ammonium, SOA ( $m/z$   $^{+}43$ ), and sulfate species, indicating secondary species are prevalent in Athens. The presence of  $m/z$  -125 [ $\text{H}(\text{NO}_3)_2^-$ ], which is also on the biomass particles, is an indication of a large amount of nitrate species on these particles.

### 6.4.3 Source apportionment of ambient particles in Mexico City

As was done for the Athens data, the ambient particles detected with the ATOFMS used by Moffet *et al.* in Mexico City were analyzed using the match-ART-2a technique with the mass spectral source signature library. For this particular analysis, the submicron (180 – 1000 nm) and supermicron (1000 – 3000 nm) particles were analyzed separately, as done by Moffet *et al.* for direct comparison of the results. Figure 6.5A and 6.5B shows the temporal series of the submicron and supermicron apportioned particles in the same manner as in Moffet *et al.* For submicron particles apportioned with the source library matching method in Figure 6.5A, it was found that the majority (34%) of the submicron particles were attributed to biomass burning. It has been noted in the

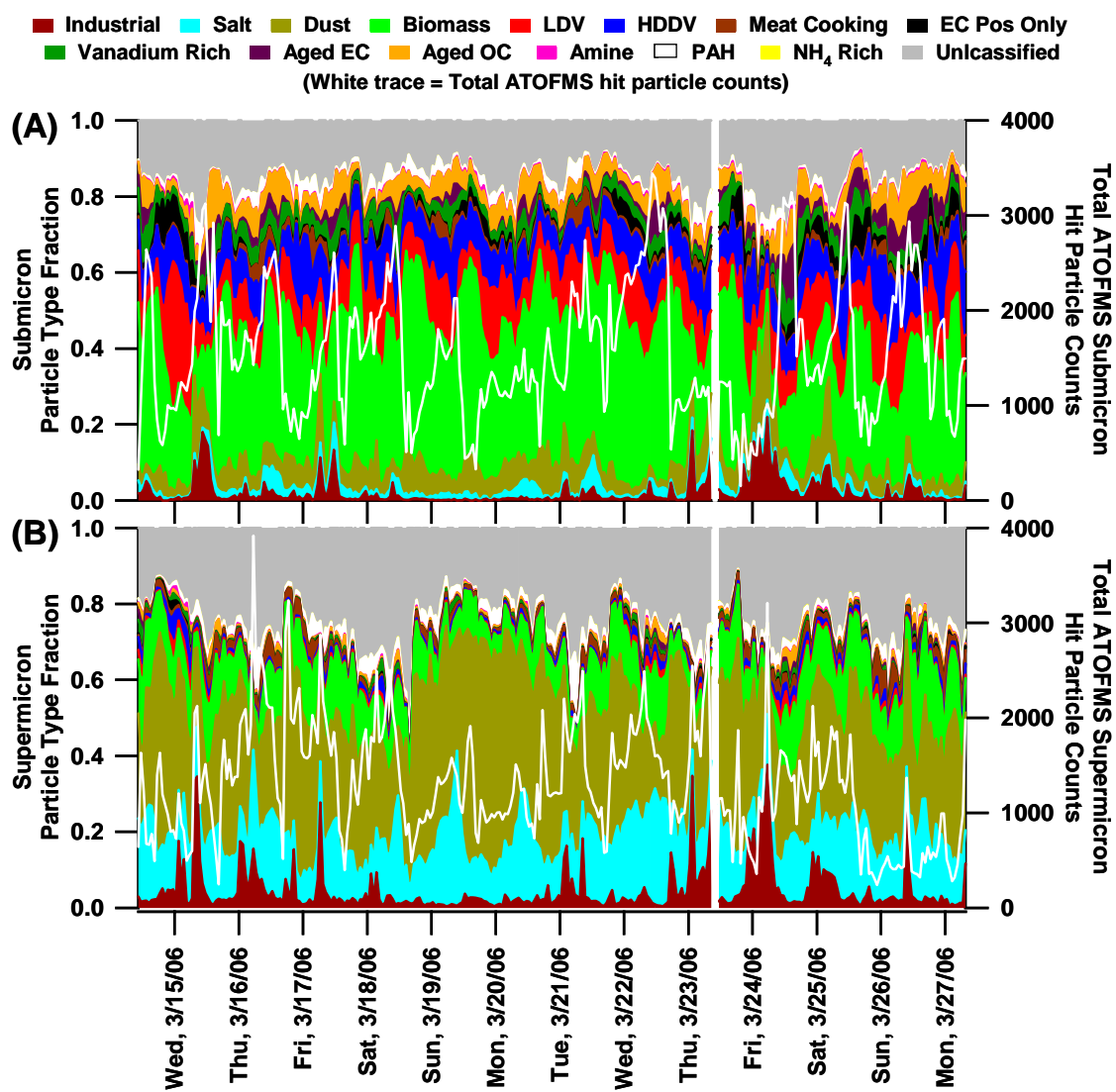


**Figure 6.5** Temporal series of the mass spectral source library matching results for Mexico City ambient A) submicron particles; and B) supermicron particles.



literature that there were many visible brush and agricultural fires around Mexico City during this study [Fast *et al.*, 2007; Moffet *et al.*, 2007]. Vehicle emissions and dust make up the next largest fractions with 11% LDV, 10% HDDV, and 6% dust. Aged OC (5%), aged EC (3%), vanadium particles (4%), meat cooking (2%), and PAH containing particles (2%) also make notable contributions to the submicron matched particles. Upon further evaluation of the apportionment results, it was found that 44% of the particles apportioned to LDV are similar (with dot products above 0.85) to the aged OC seeds as well. As studies on Mexico City particulate matter have indicated that secondary organic species dominate the particle mass [Baumgardner *et al.*, 2000; Chow *et al.*, 2001; Doran *et al.*, 2007; Salcedo *et al.*, 2006; Volkamer *et al.*, 2006; Zavala *et al.*, 2006], this could be an indication that some of the aged OC particles have been incorrectly apportioned as LDV. However, it has been shown that LDVs produce a large number of OC particles above 100 nm [Sodeman *et al.*, 2005]. Therefore, a large amount of these particles can actually be from primary LDV emissions but have undergone aging and have become coated with secondary organic species. The biomass and vehicle particles show diurnal trends which agree with the findings in Moffet *et al.*, 2007. The particles matched to the meat cooking library signatures generally peak during the morning and early afternoon hours, which is when local street vendors were observed to be cooking. Additionally, the particles that matched to the industrial seeds (representing 2% of the submicron matched particles) have episodal occurrences, which also agrees with the findings by Moffet *et al.* [Moffet *et al.*, 2007]. Another 2% of the submicron particles, labeled as “Salt”, were matched to sea salt clusters in the source library. Since Mexico City is a considerable distance (about 250 km) from the ocean, the presence of such particles could be from the

dry lake bed of Lake Texcoco (located ~15 km east) which has regions of salt flats [Chow *et al.*, 2002; Moffet *et al.*, 2007; Moya *et al.*, 2004; San Martini *et al.*, 2007; Vega *et al.*, 2001]. Due to the fact that these particles are in the submicron mode, they could also be from combustion processes originating from industry or from paper refuse incineration. The submicron salt particles closely resemble the supermicron salt particles; however, about 55% of the submicron salt particles show the presence of elemental and organic carbon.

As can be seen in Figure 6.5B for the supermicron mode, the majority of matched particles are from dust (34%), salt (15%), and biomass (11%) particles. The salt particles show a diurnal pattern, and spike during time periods when the winds are coming from the east and north-east [Moffet *et al.*, 2007]. As mentioned for the submicron salt, with the Texcoco dry lake bed being located east/northeast of the sampling site, it makes it the likely candidate for the source of these salt particles. The particles matched to the industrial library seeds occur in early morning episodes, at the same times as in the submicron mode, and make up 5% of the particles in the supermicron mode. The matching percentages for each source are summarized in Table 6.2 (and in Table A3.2 in the Supporting Information).

It is also apparent from Figure 6.5 that the amount of unclassified particles for the Mexico City ATOFMS data (submicron = 16% & supermicron = 25%) is much less than that for the Athens dataset. This is primarily because there are fewer miscalibrated spectra for the Mexico City dataset. As with the Athens dataset though, there is a larger fraction of miscalibrated spectra in for the supermicron particles (~10%) than in the submicron particles (~3%) in the Mexico City dataset. It is hypothesized that the

**Table 6.2** Percent of Mexico City particles matched to the mass spectral source library at different match-ART-2a Vigilance Factors (VF).

Particle Source	Matching VF = 0.85		Matching VF = 0.85**		Matching VF = 0.75	
	Sub %	Super %	Sub %	Super %	Sub %	Super %
Industrial	2.19	4.56	2.42	4.82	3.23	5.53
Salt	1.99	15.19	2.52	18.16	2.38	17.04
Dust	6.26	34.01	7.63	39.32	7.76	40.20
Biomass	34.07	10.99	35.59	12.02	36.48	12.68
LDV	11.19	0.96	11.71	1.03	14.79	1.65
HDDV	9.84	1.43	9.81	1.42	10.55	2.41
Meat Cooking	1.77	2.17	1.77	2.16	1.74	2.15
EC (Positive only)	2.19	0.21	2.19	0.21	2.26	0.22
Vanadium Rich	4.03	0.69	4.40	0.95	5.00	0.95
Aged EC	2.78	0.30	2.77	0.30	2.84	0.35
Aged OC	5.32	1.00	5.32	1.00	6.25	2.29
Amine Containing	0.37	0.17	0.74	0.42	0.85	0.28
PAH Containing	2.17	3.06	1.57	2.73	1.35	2.43
NH4 Containing	0.00	0.03	0.00	0.03	0.00	0.10
Unclassified	15.83	25.23	11.56	15.44	4.51	11.72

Sub = Submicron particles (180-1000nm)

Super = Supermicron particles (1000-3000nm)

\*\* Matching at VF = 0.85 including rematching unclassified particles using positive ion only matching

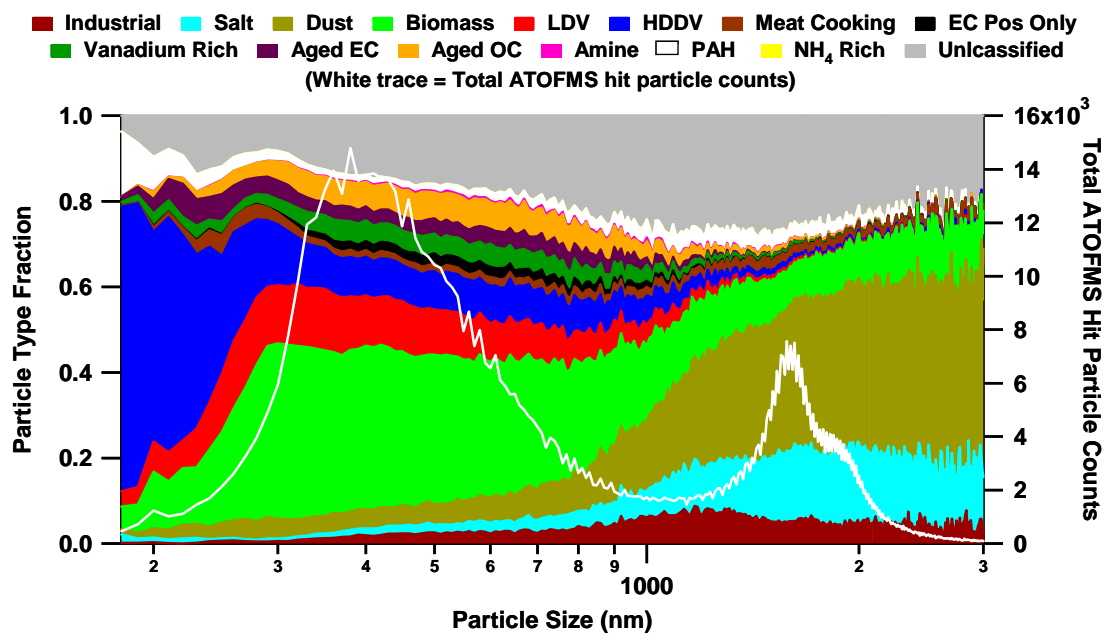


**Figure 6.6** Size resolved source apportionment of the ATOFMS detected ambient particles for Mexico City.

extremely large ion signals (which often exceed acquisition board scale) produced from inorganic particle species, such as dust and salt, detected in the supermicron mode may be the reason for these miscalibrated spectra. Further experiments are needed to confirm this hypothesis though. The unmatched particles that are not miscalibrated are either from sources not in the current mass spectral library, or are particle types that are far more aged than their equivalent types in the library.

Figure 6.6 shows the size resolved source apportionment of the ATOFMS detected ambient particles for Mexico City. Similar to what was seen for Athens, Greece; biomass particles represent the major fraction of the submicron particles down to 250 nm. As with Athens, the influence from both HDDV and LDV emissions can be seen throughout the submicron particles, and below 250 nm the influence from diesel emissions is detected as the major particle type. A major difference between the aerosol for the two locations is the near absence of the EC positive ion only type in Mexico City. There is a small amount detected (about 2%) in Mexico City, but, as will be shown below, the spectra for this type is different from the EC particles detected in Athens. Likewise, the top vanadium type detected in Mexico City is different than the one seen in Athens, and does not resemble the vanadium particles thought to be from ship emissions [Ault *et al.*, 2007; Toner *et al.*, 2007a]. When comparing Figure 6.6 to Figure 6.2, it can be seen that the presence of aged OC, aged EC, meat cooking, and PAH-containing particles are more prevalent at the Mexico City site than at the Athens, Greece site.

#### 6.4.4 Source Signature Matching for Mexico City

The top source library spectra that the ambient Mexico City particles matched to for each specific source are shown in Figure 6.7, while Figure 6.8 shows the top non-source specific source spectra that were matched. Since the source signatures for industrial particles were generated from the Mexico City dataset, it is of no surprise that the top industrial type matched is the same as the top industrial type described by Moffet et al., 2007. As mentioned before, this industrial particle type is characterized by the large ion signals due to sodium and potassium, as well as the presence of aluminum, iron, and lead, and is consistent with particles associated with high temperature combustion sources such as waste incinerators [Hu et al., 2003; Moffet et al., 2007].

The top salt type, which matched to sea salt signatures, is also described by Moffet et al. as a Na-K class. As previously mentioned, these particles likely come from the Texcoco dry lake bed which has salt flat regions. This wind suspended salt (or dust) is very similar to aged sea salt in that it has ion peaks for sodium-water clusters, as well as sodium nitrate and sodium sulfate (as shown in Figure 6.7). The top dust type matched in Mexico City, while containing sodium and potassium, is different from the salt type. The dust contains ion markers for  $\text{Al}^+$ ,  $\text{Li}^+$ , silicates and phosphate, and does not have sodium nitrate or sodium sulfate as in the salt type.

The top biomass type matched in Mexico City is very similar to that matched for the Athens dataset except that the Mexico City biomass type is more aged, as it has larger ion peaks for  $\text{NO}_3^-$  ( $m/z$  -62) and  $\text{H}(\text{NO}_3)_2^-$  ( $m/z$  -125). As described by Moffet et al., the majority of the secondary species found on the particles in Mexico City is from  $\text{NO}_x$ , SOA and ammonium. The LDV top matched type is the same library signature that was

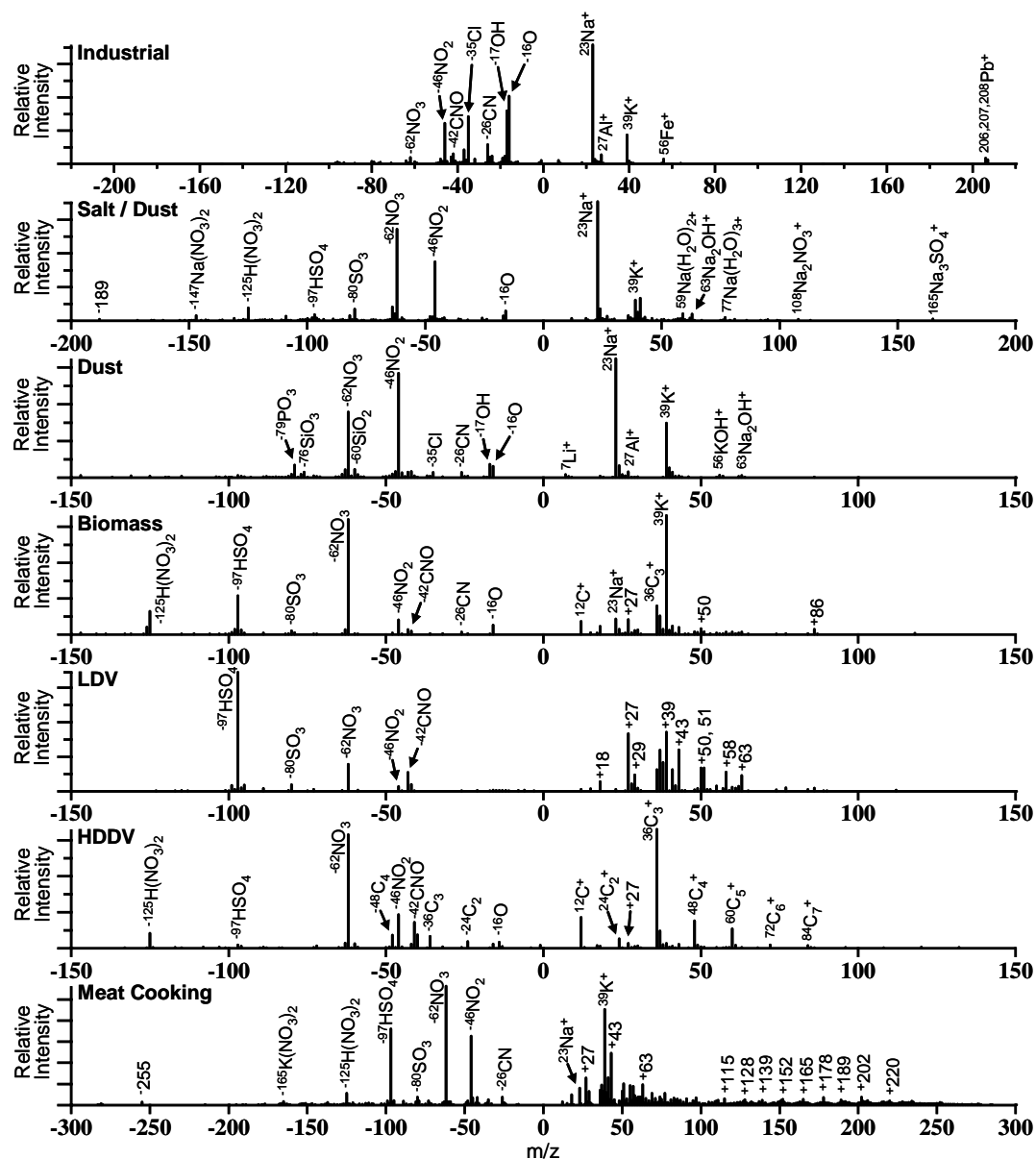


**Figure 6.7** The top matching mass spectral source signatures for each source for Mexico City ATOFMS data.

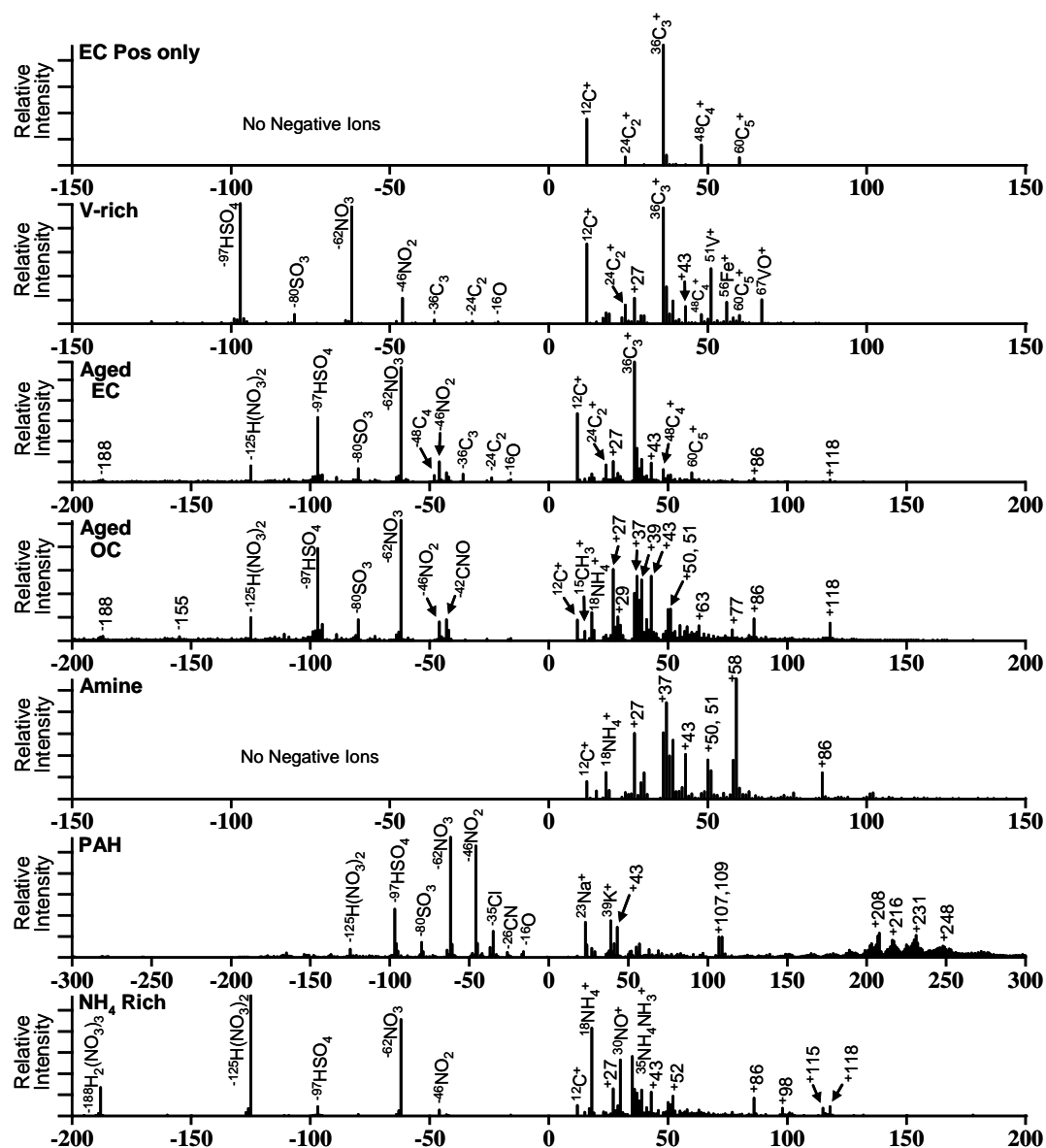


**Figure 6.8** The top matching non-source specific mass spectral signatures for each type for Mexico City ATOFMS data.



the top type for the Athens dataset, however the top HDDV matched type is very different from the Athens type and shows aging ion peaks due to the uptake of  $\text{NO}_x$  species. This is expected as Mexico City is more polluted than Athens, and has more sources (vehicles and industry) that release gas phase  $\text{NO}_x$  (which is the precursor for particle phase nitrate). This HDDV signature is one that was generated from slightly aged particles detected at a freeway-side study [Toner *et al.*, 2007b]. While the Mexico City sampling site was located in an industrial area, it has been reported that there was considerable traffic both from gasoline and diesel vehicles in the area around the sampling site [Moffet *et al.*, 2007]. The top meat cooking matched type detected in Mexico City exhibits the presence of oleic acid ( $m/z$  -255), which is often used as a tracer for meat cooking emissions [Robinson *et al.*, 2006; Rogge *et al.*, 1991]. As mentioned in Moffet *et al.*, 2007, a busy roadway near the sampling site had street vendors who were often cooking meat during the morning through the afternoon.

Figure 6.8 shows the top non-source specific library clusters that were matched to for the Mexico City dataset. As was mentioned in the discussion for the Athens data, the EC pos only and vanadium-containing particles matched in Mexico are different than those matched in Athens. These types are hypothesized to come from ship emissions in Athens, Greece, however, they are more likely from other sources in Mexico City since Mexico City is a considerable distance from the ocean. While EC is commonly emitted from a variety of combustion sources, vanadium is often used as a heavy oil marker which can also come from a variety of sources, including vehicle emissions [Shields *et al.*, 2007; Sodeman *et al.*, 2005], industrial emissions [Noble and Prather, 1996; Tolocka *et al.*, 2004], and from oil fired power plants [Hsieh and Tsai, 2003; Suarez and Ondov,

2002]. The EC positive ion only type is different than the one detected in Athens in that the ion intensity for  $m/z$  <sup>+36</sup> is much greater than that of  $m/z$  <sup>+12</sup>, and the ion peaks for  $m/z$  <sup>+48</sup> & <sup>+60</sup> are also more intense in Mexico City. These characteristics of the EC positive ion type are similar to those seen for diesel emissions and LDVs that emit large amounts of smoke from their tailpipe [Sodeman *et al.*, 2005; Toner *et al.*, 2007b; Toner *et al.*, 2006]. While this could also be an artifact due to “hot spots” and shot-to-shot variability in the LDI laser used for the ATOFMS [Wenzel and Prather, 2004], that is likely not the case due. If the types between the two studies were due to the LDI process, there would be a more random generation of EC pos only types in both studies, and not the majorities seen for each. This is more of an indication of different particle sources (or atmospheric processes) with both locations having the majority of the EC pos only particles being different. Additionally, the vanadium type for Mexico City, shown in Figure 6.8, is very noticeably different than the type shown for Athens in that the vanadium in Mexico City has large peaks due to EC in the positive ions.

The top matched vanadium, aged EC, aged OC, and PAH-containing signatures matched in Mexico City show larger peaks for NO<sub>x</sub> species in the negative ions than for Athens. This is likely due to the vastly larger amount of gas-phase and particulate pollution that is in Mexico City than in Athens. The presence of the NH<sub>4</sub> rich particle type in Mexico City (shown in Figure 6.8) is also a strong indication of the amount of secondary species in the atmosphere there. While this type only accounted for 0.03% (29,381 of the 979,357 detected supermicron particles) of the matched particles in Mexico City, this type was not detected at all for the Athens dataset. This could be an indication that there is either less ammonium containing particles present in the

atmosphere in Athens compared to Mexico City, or more of the ammonium is in the form of pure ammonium sulfate, or nitrate, in Athens which (in its pure form) is not ionized and detected by the mass spectrometer of the ATOFMS. This is typically a simple particle type to check for as it will appear in the ATOFMS data as a lot of scattered particles that do not produce a mass spectrum. This has been referred to as a “missing type” in previous ATOFMS studies [Wenzel *et al.*, 2003]. Unfortunately, the data for scattered particles without mass spectra (or, missed particles) is not available for the Athens dataset to check for this type.

#### **6.4.5 Future implementations**

A major goal of the source library matching approach is to be able to perform on-the-fly (or real-time) apportionment when running the ATOFMS instrument. Experimental modifications to the ATOFMS software have been made to include the particle source library along with a variation of the match-ART-2a algorithm in order to instantly compare the spectra of each particle to the source library as they are detected with the instrument. The results are then displayed in real time along with the other on-screen displays for the instrument. This kind of application of the source library can be particularly useful for mobile experiments or chase studies where the sampling specific sources are desired. Since the analysis would be taking place in real-time, the sampling location could be adjusted accordingly by the user to detect the desired source (or sources).

The results shown in this paper indicate that the source library matching method is accurate when apportioning ATOFMS detected ambient particles. Additionally, the

method is much faster in its analysis than the traditional hand classification of ART-2a results. It can take weeks to months to classify an ATOFMS dataset of a million particles using the traditional ART-2a clustering followed by hand grouping and classification, where the match-ART-2a technique with the source signature library can classify the majority of the particles in same dataset in about 6 hours (using a 3-GHz Pentium processor computer with 4-Gb of RAM). While the current source library only contains seeds for seven specific sources (LDV, HDDV, biomass burning, dust, sea salt, industrial emissions, and meat cooking), these are seven of the largest contributors to ambient PM<sub>2.5</sub> in urban areas [Kim *et al.*, 2005; Kleeman and Cass, 1998; Liu *et al.*, 2003; Noble and Prather, 1996; Park and Kim, 2005; Pastor *et al.*, 2003; Querol *et al.*, 2001; Swietlicki *et al.*, 1996; Ward *et al.*, 2006; Ying and Kleeman, 2006; Zhao and Hopke, 2006]. As more ATOFMS source characterization studies are conducted, new source signatures can be added to the source library to increase its diversity and ability to distinguish individual sources of ambient aerosols. As particles become increasingly aged or agglomerated, identifying their original primary source becomes more difficult. In this case, the particles will be classified as secondary (or aged) particles since their signatures are now dominated by secondary species. As many recent studies have shown that SOA can make up 75 – 90 % of the submicron OC particles [Buzcu-Guven *et al.*, 2007; Kleinman *et al.*, 2007; Volkamer *et al.*, 2006; Weber *et al.*, 2007; Williams *et al.*, 2007; Zhang *et al.*, 2005b], it is important to be able to distinguish between primary and secondary particles. This is why the more general (non-source specific) seeds (EC pos only, aged OC, aged EC, amines, PAH's, vanadium containing, and NH<sub>4</sub> containing) are included in the library. Future ATOFMS studies where the particles from specific

sources are put under controlled aging environments, such as in smog chamber or flow tube experiments, will help resolve the origin of these types of particles and help reduce the amount of unclassified particles when using the source library matching method. In addition, such experiments could yield the signatures for the aged version of the source particles and could allow for the determination of how much secondary species are on the primary particles.

## **6.5 Acknowledgements**

The authors thank Laura Shields, Sharon Qin, Thomas Rebotier, and Kerri Denkenberger for their help and input with testing the source signature library. Funding for the development of the source library was provided by the California Air Resources Board (CARB).

Chapter 6 is in preparation for submission to Atmospheric Environment in 2007. Toner, S.M., Moffet, R.C., Dall'Osto, M., Harrison, R.M., and K.A. Prather, Source apportionment of PM<sub>2.5</sub> in Athens (Greece) and Mexico City using an ATOFMS derived mass spectral source library. Copyright 2007, Elsevier.

## 6.6 References

- Allen, J.O., Software toolkit to analyze single-particle mass spectral data - <http://www.yaada.org>, 2006.
- Ault, A.P., H. Furutani, G. Dominguez, M.H. Thiemens, and K.A. Prather, A mass spectral fingerprint of ship emission particles by aerosol time-of-flight mass spectrometry and applications for source apportionment, *In Preparation*, 2007.
- Baumgardner, D., G.B. Raga, G. Kok, J. Ogren, I. Rosas, A. Baez, and T. Novakov, On the evolution of aerosol properties at a mountain site above Mexico City, *Journal of Geophysical Research-Atmospheres*, 105 (D17), 22243-22253, 2000.
- Bein, K.J., Y. Zhao, N.J. Pekney, C.I. Davidson, M.V. Johnston, and A.S. Wexler, Identification of sources of atmospheric PM at the Pittsburgh Supersite-Part II: Quantitative comparisons of single particle, particle number, and particle mass measurements, *Atmospheric Environment*, 40 (Suppl. 2), S424-S444, 2006.
- Bhave, P.V., D.P. Fergenson, K.A. Prather, and G.R. Cass, Source apportionment of fine particulate matter by clustering single-particle data: tests of receptor model accuracy, *Environmental Science and Technology*, 35 (10), 2060-2072, 2001.
- Buzcu-Guven, B., G. Brown Steven, A. Frankel, R. Hafner Hilary, and T. Roberts Paul, Analysis and apportionment of organic carbon and fine particulate matter sources at multiple sites in the midwestern United States, *Journal of the Air & Waste Management Association*, 57 (5), 606-619, 2007.
- Cass, G.R., L.A. Hughes, P. Bhave, M.J. Kleeman, J.O. Allen, and L.G. Salmon, The chemical composition of atmospheric ultrafine particles, *Philosophical Transactions of the Royal Society of London, Series A: Mathematical, Physical and Engineering Sciences*, 358 (1775), 2581-2592, 2000.
- Chow, J.C., J.G. Watson, D. Crow, D.H. Lowenthal, and T. Merrifield, Comparison of IMPROVE and NIOSH carbon measurements, *Aerosol Science & Technology*, 34 (1), 23-34, 2001.
- Chow, J.C., J.G. Watson, S.A. Edgerton, and E. Vega, Chemical composition of PM<sub>2.5</sub> and PM<sub>10</sub> in Mexico City during winter 1997, *Science of the Total Environment*, 287 (3), 177-201, 2002.
- Chung, C.E., V. Ramanathan, D. Kim, and I.A. Podgorny, Global anthropogenic aerosol direct forcing derived from satellite and ground-based observations, *Journal of Geophysical Research-Atmospheres*, 110 (D24), 2005.

- Dall'Osto, M., and R.M. Harrison, Chemical characterisation of single airborne particles in Athens (Greece) by ATOFMS, *Atmospheric Environment*, 40 (39), 7614-7631, 2006.
- Doran, J.C., J.C. Barnard, W.P. Arnott, R. Cary, R. Coulter, J.D. Fast, E.I. Kassianov, L. Kleinman, N.S. Laulainen, T. Martin, G. Paredes-Miranda, M.S. Pekour, W.J. Shaw, D.F. Smith, S.R. Springston, and X.Y. Yu, The T1-T2 study: evolution of aerosol properties downwind of Mexico City, *Atmospheric Chemistry and Physics*, 7 (6), 1585-1598, 2007.
- Eleftheriadis, K., D. Balis, I.C. Ziomas, I. Colebeck, and N. Manalis, Atmospheric aerosol and gaseous species in Athens, Greece, *Atmospheric Environment*, 32 (12), 2183-2191, 1998.
- Fast, J.D., B. de Foy, F.A. Rosas, E. Caetano, G. Carmichael, L. Emmons, D. McKenna, M. Mena, W. Skamarock, X. Tie, R.L. Coulter, J.C. Barnard, C. Wiedinmyer, and S. Madronich, A meteorological overview of the MILAGRO field campaigns, *Atmospheric Chemistry and Physics*, 7 (9), 2233-2257, 2007.
- Formenti, P., W. Elbert, W. Maenhaut, J. Haywood, and M.O. Andr  ae, Chemical composition of mineral dust aerosol during the Saharan Dust Experiment (SHADE) airborne campaign in the Cape Verde region, September 2000, *Journal of Geophysical Research, [Atmospheres]*, 108 (D18), SAH 3/1-SAH 3/15, 2003.
- Fraser, M.P., M.J. Kleeman, J.J. Schauer, and G.R. Cass, Modeling the atmospheric concentrations of individual gas-phase and particle-phase organic compounds, *Environmental Science and Technology*, 34 (7), 1302-1312, 2000.
- Ganor, E., The composition of clay minerals transported to Israel as indicators of Saharan dust emission, *Atmospheric Environment, Part A: General Topics*, 25A (12), 2657-64, 1991.
- Gard, E., J.E. Mayer, B.D. Morrical, T. Dienes, D.P. Fergenson, and K.A. Prather, Real-time analysis of individual atmospheric aerosol particles: Design and performance of a portable ATOFMS, *Analytical Chemistry*, 69 (20), 4083-4091, 1997.
- Griffin, R.J., D. Dabdub, M.J. Kleeman, M.P. Fraser, G.R. Cass, and J.H. Seinfeld, Secondary organic aerosol 3. Urban/regional scale model of size- and composition-resolved aerosols, *Journal of Geophysical Research, [Atmospheres]*, 107 (D17), AAC5/1-AAC5/14, 2002.
- Guazzotti, S.A., D.T. Suess, K.R. Coffee, P.K. Quinn, T.S. Bates, A. Wisthaler, A. Hansel, W.P. Ball, R.R. Dickerson, C. Neususs, P.J. Crutzen, and K.A. Prather, Characterization of carbonaceous aerosols outflow from India and Arabia:

- biomass/biofuel burning and fossil fuel combustion, *Journal of Geophysical Research, [Atmospheres]*, 108 (D15), ACL13/1-ACL13/14, 2003.
- Guazzotti, S.A., J.R. Whiteaker, D. Suess, K.R. Coffee, and K.A. Prather, Real-time measurements of the chemical composition of size-resolved particles during a Santa Ana wind episode, California USA, *Atmospheric Environment*, 35 (19), 3229-3240, 2001.
- Hodzic, A., S. Madronich, B. Bohn, S. Massie, L. Menut, and C. Wiedinmyer, Wildfire particulate matter in Europe during summer 2003: meso-scale modeling of smoke emissions, transport and radiative effects, *Atmospheric Chemistry and Physics*, 7 (15), 4043-4064, 2007.
- Hsieh, Y.M., and M.S. Tsai, Physical and chemical analyses of unburned carbon from oil-fired fly ash, *Carbon*, 41 (12), 2317-2324, 2003.
- Hu, C.-W., M.-R. Chao, K.-Y. Wu, G.-P. Chang-Chien, W.-J. Lee, L.W. Chang, and W.-S. Lee, Characterization of multiple airborne particulate metals in the surroundings of a municipal waste incinerator in Taiwan, *Atmospheric Environment*, 37 (20), 2845-2852, 2003.
- Imhof, D., E. Weingartner, C. Ordonez, R. Gehrig, M. Hill, B. Buchmann, and U. Baltensperger, Real-world emission factors of fine and ultrafine aerosol particles for different traffic situations in Switzerland, *Environmental Science and Technology*, 39 (21), 8341-8350, 2005.
- Kanias, G.D., L.G. Viras, and A.P. Grimanis, Source identification of trace elements emitted into Athens atmosphere, *Journal of Radioanalytical and Nuclear Chemistry*, 260 (3), 509-518, 2004.
- Karageorgos, E.T., and S. Rapsomanikis, Chemical characterization of the inorganic fraction of aerosols and mechanisms of the neutralization of atmospheric acidity in Athens, Greece, *Atmospheric Chemistry and Physics*, 7 (11), 3015-3033, 2007.
- Kim, E., P.K. Hopke, D.M. Kenski, and M. Koerber, Sources of Fine Particles in a Rural Midwestern U.S. Area, *Environmental Science and Technology*, 39 (13), 4953-4960, 2005.
- Kittelson, D.B., W.F. Watts, J.P. Johnson, J.J. Schauer, and D.R. Lawson, On-road and laboratory evaluation of combustion aerosols-Part 2: Summary of spark ignition engine results, *Journal of Aerosol Science*, 37 (8), 931-949, 2006.
- Kleeman, M.J., and G.R. Cass, Source contributions to the size and composition distribution of urban particulate air pollution, *Atmospheric Environment*, 32 (16), 2803-2816, 1998.



- Kleeman, M.J., J.J. Schauer, and G.R. Cass, Size and composition distribution of fine particulate matter emitted from motor vehicles, *Environmental Science and Technology*, 34 (7), 1132-1142, 2000.
- Kleinman, L.I., P.H. Daum, Y.-N. Lee, G.I. Senum, S.R. Springston, J. Wang, C. Berkowitz, J. Hubbe, R.A. Zaveri, F.J. Brechtel, J. Jayne, T.B. Onasch, and D. Worsnop, Aircraft observations of aerosol composition and ageing in New England and Mid-Atlantic States during the summer 2002 New England Air Quality Study field campaign, *Journal of Geophysical Research, [Atmospheres]*, 112 (D9), D09310/1-D09310/18, 2007.
- Lance, G.N., and W.T. Williams, A General Theory of Classificatory Sorting Strategies .1. Hierarchical Systems, *Computer Journal*, 9 (4), 373, 1967.
- Lehmann, U., M. Mohr, T. Schweizer, and J. Rutter, Number size distribution of particulate emissions of heavy-duty engines in real world test cycles, *Atmospheric Environment*, 37 (37), 5247-5259, 2003.
- Liu, D.Y., R.J. Wenzel, and K.A. Prather, Aerosol time-of-flight mass spectrometry during the Atlanta Supersite experiment: 1. Measurements, *Journal of Geophysical Research-Atmospheres*, 108 (D7), 8426, 2003.
- Metzger, S., N. Mihalopoulos, and J. Lelieveld, Importance of mineral cations and organics in gas-aerosol partitioning of reactive nitrogen compounds: case study based on MINOS results, *Atmospheric Chemistry and Physics*, 6 (9), 2549-2567, 2006.
- Moffet, R.C., B. de Foy, L.T. Molina, M.J. Molina, and K.A. Prather, Characterization of ambient aerosols in northern Mexico City by single particle mass spectrometry, *Atmospheric Chemistry and Physics Discussion*, 7, 6413-6457, 2007.
- Moya, M., M. Grutter, and A. Baez, Diurnal variability of size-differentiated inorganic aerosols and their gas-phase precursors during January and February of 2003 near downtown Mexico City, *Atmospheric Environment*, 38 (33), 5651-5661, 2004.
- Murphy, D.M., A.M. Middlebrook, and M. Warshawsky, Cluster analysis of data from the particle analysis by laser mass spectrometry (PALMS) instrument, *Aerosol Science and Technology*, 37 (4), 382-391, 2003.
- Noble, C.A., and K.A. Prather, Real-time measurement of correlated size and composition profiles of individual atmospheric aerosol particles, *Environmental Science and Technology*, 30 (9), 2667-2680, 1996.
- Owega, S., G.J. Evans, R.E. Jervis, M. Fila, R. D'Souza, and B.-U.-Z. Khan, Long-range sources of Toronto particulate matter (PM<sub>2.5</sub>) identified by Aerosol Laser

- Ablation Mass Spectrometry (LAMs), *Atmospheric Environment*, 38 (33), 5545-5553, 2004.
- Papayannis, A., D. Balis, V. Amiridis, G. Chourdakis, G. Tsaknakis, C. Zerefos, A.D.A. Castanho, S. Nickovic, S. Kazadzis, and J. Grabowski, Measurements of saharan dust aerosols over the Eastern Mediterranean using elastic backscatter-Raman lidar, spectrophotometric and satellite observations in the frame of the EARLINET project, *Atmospheric Chemistry and Physics*, 5 (8), 2065-2079, 2005.
- Park, S.S., and Y.J. Kim, Source contributions to fine particulate matter in an urban atmosphere, *Chemosphere*, 59 (2), 217-226, 2005.
- Pastor, S.H., J.O. Allen, L.S. Hughes, P. Bhawe, G.R. Cass, and K.A. Prather, Ambient single particle analysis in Riverside, California by aerosol time-of-flight mass spectrometry during the SCOS97-NARSTO, *Atmospheric Environment*, 37 (Suppl. 2), 239-258, 2003.
- Phares, D.J., K.P. Rhoads, A.S. Wexler, D.B. Kane, and M.V. Johnston, Application of the ART-2a algorithm to laser ablation aerosol mass spectrometry of particle standards, *Analytical Chemistry*, 73 (10), 2338-2344, 2001.
- Qin, X., and K.A. Prather, Impact of biomass emissions on particle chemistry during the California Regional Particulate Air Quality Study, *International Journal of Mass Spectrometry*, 258 (1-3), 142-150, 2006.
- Querol, X., A. Alastuey, S. Rodriguez, F. Plana, C.R. Ruiz, N. Cots, G. Massague, and O. Puig, PM10 and PM2.5 source apportionment in the Barcelona Metropolitan area, Catalonia, Spain, *Atmospheric Environment*, 35 (36), 6407-6419, 2001.
- Ramana, M.V., and V. Ramanathan, Abrupt transition from natural to anthropogenic aerosol radiative forcing: Observations at the ABC-Maldives Climate Observatory, *Journal of Geophysical Research-Atmospheres*, 111 (D20), 2006.
- Ramanathan, V., and P.J. Crutzen, New directions: Atmospheric brown "Clouds", *Atmospheric Environment*, 37 (28), 4033-4035, 2003.
- Rebotier, T.P., and K.A. Prather, Aerosol time-of-flight mass spectrometry data analysis: A benchmark of clustering algorithms, *Analytica Chimica Acta*, 585 (1), 38-54, 2007.
- Reilly, P.T.A., R.A. Gieray, W.B. Whitten, and J.M. Ramsey, Real-time characterization of the organic composition and size of individual diesel engine smoke particles, *Environmental Science and Technology*, 32 (18), 2672-2679, 1998.

- Robinson, A.L., R. Subramanian, N.M. Donahue, A. Bernardo-Bricker, and W.F. Rogge, Source apportionment of molecular markers and organic aerosol. 3. Food cooking emissions, *Environmental Science & Technology*, 40 (24), 7820-7827, 2006.
- Rogge, W.F., L.M. Hildemann, M.A. Mazurek, G.R. Cass, and B.R.T. Simoneit, Sources of fine organic aerosol. 1. Charbroilers and meat cooking operations, *Environmental Science and Technology*, 25 (6), 1112-25, 1991.
- Salcedo, D., T.B. Onasch, K. Dzepina, M.R. Canagaratna, Q. Zhang, J.A. Huffman, P.F. DeCarlo, J.T. Jayne, P. Mortimer, D.R. Worsnop, C.E. Kolb, K.S. Johnson, B. Zuberi, L.C. Marr, R. Volkamer, L.T. Molina, M.J. Molina, B. Cardenas, R.M. Bernabe, C. Marquez, J.S. Gaffney, N.A. Marley, A. Laskin, V. Shutthanandan, Y. Xie, W. Brune, R. Leshner, T. Shirley, and J.L. Jimenez, Characterization of ambient aerosols in Mexico City during the MCMA-2003 campaign with aerosol mass spectrometry: results from the CENICA Supersite, *Atmospheric Chemistry and Physics*, 6 (4), 925-946, 2006.
- San Martini, F.M., E.J. Dunlea, R. Volkamer, T.B. Onasch, J.T. Jayne, M.R. Canagaratna, D.R. Worsnop, C.E. Kolb, J.H. Shorter, S.C. Herndon, M.S. Zahniser, D. Salcedo, K. Dzepina, J.L. Jimenez, J.M. Ortega, K.S. Johnson, G.J. McRae, L.T. Molina, and M.J. Molina, Implementation of a Markov Chain Monte Carlo method to inorganic aerosol modeling of observations from the MCMA-2003 campaign - Part II: model application to the CENICA, Pedregal and Santa Ana sites, *Atmospheric Chemistry and Physics*, 6 (12, Pt. 3), 4889-4904, 2007.
- Scheff, P.A., and C. Valiozis, Characterization and source identification of respirable particulate matter in Athens, Greece, *Atmospheric Environment, Part A: General Topics*, 24A (1), 203-11, 1990.
- Shields, L.G., D.T. Suess, and K.A. Prather, Determination of single particle mass spectral signatures from heavy duty diesel vehicle emissions for PM<sub>2.5</sub> source apportionment, *Atmospheric Environment*, 41 (18), 3841-3852, 2007.
- Silva, P.J., R.A. Carlin, and K.A. Prather, Single particle analysis of suspended soil dust from Southern California, *Atmospheric Environment*, 34 (11), 1811-1820, 2000.
- Silva, P.J., D.Y. Liu, C.A. Noble, and K.A. Prather, Size and chemical characterization of individual particles resulting from biomass burning of local Southern California species, *Environmental Science & Technology*, 33 (18), 3068-3076, 1999.
- Sodeman, D.A., S.M. Toner, and K.A. Prather, Determination of single particle mass spectral signatures from light duty vehicle emissions, *Environmental Science & Technology*, 39 (12), 4569-4580, 2005.

- Song, X.H., N.M. Faber, P.K. Hopke, D.T. Suess, K.A. Prather, J.J. Schauer, and G.R. Cass, Source apportionment of gasoline and diesel by multivariate calibration based on single particle mass spectral data, *Analytica Chimica Acta*, 446 (1-2), 329-343, 2001.
- Song, X.H., P.K. Hopke, D.P. Fergenson, and K.A. Prather, Classification of single particles analyzed by ATOFMS using an artificial neural network, ART-2A, *Analytical Chemistry*, 71(4), 860-865, 1999.
- Su, Y., M.F. Sipin, H. Furutani, and K.A. Prather, Development and characterization of an aerosol time-of-flight mass spectrometer with increased detection efficiency, *Analytical Chemistry*, 76 (3), 712-719, 2004.
- Suarez, A.E., and J.M. Ondov, Ambient aerosol concentrations of elements resolved by size and by source: Contributions of some cytokine-active metals from coal- and oil-fired power plants, *Energy & Fuels*, 16 (3), 562-568, 2002.
- Swietlicki, E., S. Puri, H.-C. Hansson, and H. Edner, Urban air pollution source apportionment using a combination of aerosol and gas monitoring techniques, *Atmospheric Environment*, 30 (15), 2795-2809, 1996.
- Tan, P.V., O. Malpica, G.J. Evans, S. Owega, and M.S. Fila, Chemically-assigned classification of aerosol mass spectra, *Journal of the American Society for Mass Spectrometry*, 13 (7), 826-38, 2002.
- Tolocka, M.P., D.A. Lake, M.V. Johnston, and A.S. Wexler, Number concentrations of fine and ultrafine particles containing metals, *Atmospheric Environment*, 38 (20), 3263-3273, 2004.
- Toner, S.M., L.G. Shields, and K.A. Prather, Source apportionment of freeway-side PM<sub>2.5</sub> using ATOFMS, *Atmospheric Environment*, submitted for publication, 2007a.
- Toner, S.M., L.G. Shields, D.A. Sodeman, and K.A. Prather, Using mass spectral source signatures to apportion exhaust particles from gasoline and diesel powered vehicles in a freeway study using UF-ATOFMS., *Atmospheric Environment*, doi:10.1016/j.atmosenv.2007.08.005, 2007b.
- Toner, S.M., D.A. Sodeman, and K.A. Prather, Single particle characterization of ultrafine and accumulation mode particles from heavy duty diesel vehicles using aerosol time-of-flight mass spectrometry, *Environmental Science & Technology*, 40 (12), 3912-3921, 2006.
- Valavanidis, A., K. Fiotakis, T. Vlahogianni, E.B. Bakeas, S. Triantafillaki, V. Paraskevopoulou, and M. Dassenakis, Characterization of atmospheric

- particulates, particle-bound transition metals and polycyclic aromatic hydrocarbons of urban air in the center of Athens (Greece), *Chemosphere*, 65 (5), 760-768, 2006.
- Vassilakos, C., D. Veros, J. Michopoulos, T. Maggos, and C.M. O'Connor, Estimation of selected heavy metals and arsenic in PM10 aerosols in the ambient air of the Greater Athens Area, Greece, *Journal of Hazardous Materials*, 140 (1-2), 389-398, 2007.
- Vega, E., V. Mugica, E. Reyes, G. Sanchez, J.C. Chow, and J.G. Watson, Chemical composition of fugitive dust emitters in Mexico City, *Atmospheric Environment*, 35 (23), 4033-4039, 2001.
- Volkamer, R., J.L. Jimenez, F. San Martini, K. Dzepina, Q. Zhang, D. Salcedo, L.T. Molina, D.R. Worsnop, and M.J. Molina, Secondary organic aerosol formation from anthropogenic air pollution: rapid and higher than expected, *Geophysical Research Letters*, 33 (17), L17811/1-L17811/4, 2006.
- Ward, J.H., Hierarchical grouping to optimize an objective function, *Journal of the American Statistical Association*, 58 (301), 236, 1963.
- Ward, T., L. Rinehart, and T. Lange, The 2003/2004 Libby, Montana PM<sub>2.5</sub> source apportionment research study, *Aerosol Science and Technology*, 40 (3), 166-177, 2006.
- Weber, R.J., A.P. Sullivan, R.E. Peltier, A. Russell, B. Yan, M. Zheng, J. de Gouw, C. Warneke, C. Brock, J.S. Holloway, E.L. Atlas, and E. Edgerton, A study of secondary organic aerosol formation in the anthropogenic-influenced Southeastern United States, *Journal of Geophysical Research*, [Atmospheres], 112 (D13), D13302/1-D13302/13, 2007.
- Wenzel, R.J., D.-Y. Liu, E.S. Edgerton, and K.A. Prather, Aerosol time-of-flight mass spectrometry during the Atlanta Supersite Experiment: 2. Scaling procedures, *Journal of Geophysical Research*, [Atmospheres], 108 (D7), SOS 15/1-SOS 15/8, 2003.
- Wenzel, R.J., and K.A. Prather, Improvements in ion signal reproducibility obtained using a homogeneous laser beam for on-line laser desorption/ionization of single particles, *Rapid Communications in Mass Spectrometry*, 18 (13), 1525-1533, 2004.
- Williams, B.J., A.H. Goldstein, D.B. Millet, R. Holzinger, N.M. Kreisberg, S.V. Hering, A.B. White, D.R. Worsnop, J.D. Allan, and J.L. Jimenez, Chemical speciation of organic aerosol during the International Consortium for Atmospheric Research on

- Transport and Transformation 2004: results from in situ measurements, *Journal of Geophysical Research, [Atmospheres]*, 112 (D10), D10S26/1-D10S26/14, 2007.
- Ying, Q., and M.J. Kleeman, Source contributions to the regional distribution of secondary particulate matter in California, *Atmospheric Environment*, 40 (4), 736-752, 2006.
- Zavala, M., S.C. Herndon, R.S. Slott, E.J. Dunlea, L.C. Marr, J.H. Shorter, M. Zahniser, W.B. Knighton, T.M. Rogers, C.E. Kolb, L.T. Molina, and M.J. Molina, Characterization of on-road vehicle emissions in the Mexico City Metropolitan Area using a mobile laboratory in chase and fleet average measurement modes during the MCMA-2003 field campaign, *Atmospheric Chemistry and Physics*, 6, 5129-5142, 2006.
- Zhang, K.M., A.S. Wexler, D.A. Niemeier, Y.F. Zhu, W.C. Hinds, and C. Sioutas, Evolution of particle number distribution near roadways. Part III: Traffic analysis and on-road size resolved particulate emission factors, *Atmospheric Environment*, 39 (22), 4155-4166, 2005a.
- Zhang, Q., D.R. Worsnop, M.R. Canagaratna, and J.L. Jimenez, Hydrocarbon-like and oxygenated organic aerosols in Pittsburgh: Insights into sources and processes of organic aerosols, *Atmospheric Chemistry and Physics*, 5 (12), 3289-3311, 2005b.
- Zhao, W., and P.K. Hopke, Source apportionment for ambient particles in the San Gorgonio wilderness, *Atmospheric Environment*, 38 (35), 5901-5910, 2004.
- Zhao, W., and P.K. Hopke, Source identification for fine aerosols in Mammoth Cave National Park, *Atmospheric Research*, 80 (4), 309-322, 2006.

# 7 Conclusion and Future Directions

## 7.1 Conclusion

Methods of measuring the chemical and physical properties of aerosols as well as proper source apportionment of ambient particles are necessary to provide insight as to the roles they play in the environment and their impact on human health. In addition, the ability to apportion ambient particles quickly and accurately will be very helpful for environmental and health agencies and for monitoring and enforcing emission standards by allowing such agencies to determine the primary source of aerosols in their monitoring areas. The goal of this dissertation research was to provide a new approach for aerosol source apportionment using aerosol time-of-flight mass spectrometry (ATOFMS) single particle data. This objective was accomplished by determining unique mass spectral source signatures for specific aerosol sources and by developing these signatures into a source signature library in which ambient ATOFMS data can be matched and apportioned. Based on the low error of apportionment determined for the initial testing of the source signature library on the freeway study data (Chapter 4) as well as the comparable apportionment results to the classification studies for the Athens and Mexico City studies (Chapter 6), it has been shown that the source signature library matching method developed in this research is an accurate and viable means of aerosol source apportionment. Additionally, the development of the source signature library and matching method has provided a monumental step towards real-time source apportionment for ATOFMS single particle data.

In Chapter 2, particle source signatures for solid fueled rocket motors (SRM) used to launch payloads into outer space were determined by sampling and characterizing the exhaust wake of a statically fired SRM using ultrafine ATOFMS (UF-ATOFMS) and standard ATOFMS. The goal of this work was not only to obtain mass spectral signatures for SRMs but to test the ability of the ART-2a algorithm in distinguishing inorganic particle types with similar mass spectral signatures. This Chapter represents the first attempt at apportioning chemically similar particle types from two distinct sources with ATOFMS. Determining SRM signatures is important because SRMs have been shown to release several tons of alumina and reactive chlorine species into the stratosphere [*Brady et al.*, 1994; *Cofer et al.*, 1989]. While such particles have a very short lifetime in the troposphere, the lifetime, transport, and extent of reaction with the ozone layer in the stratosphere are yet to be fully determined. Using these chemical signatures along with A-ATOFMS studies using aircraft that can sample in the stratosphere may help to shed further light on the degree of damage SRM wake particles have on the upper atmosphere.

In Chapter 3, particle source signatures (50 - 300 nm) for heavy duty diesel vehicles (HDDVs) were determined by sampling the exhaust emissions of HDDVs operating on a dynamometer using UF-ATOFMS. These signatures were found to compliment those obtained in a previous HDDV emission study with standard ATOFMS for larger sized particles (150 – 3000 nm) [*Shields et al.*, 2007]. This work was done in part of a series of dynamometer studies for gasoline powered light duty vehicles (LDV) and HDDV aerosol emissions for the expressed purpose of determining unique chemical signatures and distinguishing between the two vehicle types [*Shields et al.*, 2007;



*Sodeman et al.*, 2005; *Toner et al.*, 2006]. The particle types detected in the HDDV emissions were compared to those detected in the LDV emissions in order to find unique markers that can be used for distinguishing the exhaust particles of the two vehicle types. Comparing the source signatures for LDVs obtained in *Sodeman et al.*, 2005 versus those obtained for HDDV with UF-ATOFMS has shown that the particles from these sources are distinguishable from one another as was discussed in Chapter 3 and Chapter 4. As found in previous HDDV emission studies, the particles from HDDVs are from lubrication oil combustion and primarily contain elemental carbon as well as calcium and phosphate [*Canagaratna et al.*, 2004; *Gautam et al.*, 1999; *Harrison et al.*, 2003; *Shields et al.*, 2007; *Spencer et al.*, 2006].

Chapter 4 discussed the process of creating a source signature library for HDDV and LDV emissions and the ability of the library matching method to properly apportion between the two sources on ambient ATOFMS data collected next to a major freeway. It was shown that, while there are similarities between the two exhaust types, there are features that can be used to distinguish HDDV particles from LDV. Some features that can be used to distinguish HDDV from LDV are more intense peaks for calcium and phosphate and that the intensity of the peak at  $^{36}\text{C}_3^+$  is greater than that of  $^{12}\text{C}_1^+$  in EC particles emitted from HDDV particles. The results presented in Chapter 4 represent the first step in using mass spectral source signatures acquired in LDV and HDDV dynamometer source characterization studies for ambient source apportionment and demonstrated that the two sources are readily distinguishable in a fresh emission environment, verifying the matching method as a valid means for apportioning single particle ATOFMS data. Additionally, after validating the matching method, the overall

contribution to the total ambient aerosol at the freeway location by HDDV and LDV emissions was determined.

Chapter 5 is a continuation of the apportionment work presented in Chapter 4. The source signature library was extended for multiple specific sources (HDDV, LDV, dust, sea salt, biomass, and meat cooking) and for non-source specific particles (aged organic carbon, aged elemental carbon, amine containing particles, PAHs, ammonium rich particles, vanadium particles, and elemental carbon particles) and was used to apportion particles detected alongside the same freeway dataset as in Chapter 4. In addition, the steps involved in data quality assurance were discussed as well as how particle size measurements and gas phase instrumentation contribute to proper aerosol source apportionment. This work showed that the source matching method is able to accurately distinguish different particle sources and that there can be a large contribution from sources other than vehicles near a major freeway.

Finally, Chapter 6 investigated the feasibility of using the ATOFMS mass spectral source library matching method on a global scale and in more polluted environments. This assessment was done by using the matching technique on ATOFMS data collected at two major global cities (Athens, Greece and Mexico City) and comparing the results to those from general classification studies of the same datasets [*Dall'Osto and Harrison, 2006; Moffet et al., 2007*]. In addition to showing that this apportionment technique is viable for apportionment of ATOFMS data collected around the world, it also showed that the library matching technique could work for data collected with ATOFMS instruments from different research groups. This chapter also discussed how fast using the library matching technique is for apportioning ATOFMS particles, where a million

single particle spectra can be classified in six hours. This can be extremely helpful for environmental agencies to quickly determine the sources of aerosol pollution in sampled regions and enforce regulations on a faster timescale.

## 7.2 Future Directions

The work presented in this thesis is just the beginning for the development of the ATOFMS mass spectral source library. While the current source library only contains seeds for seven specific sources (LDV, HDDV, biomass burning, dust, sea salt, industrial emissions, and meat cooking), these are seven of the largest contributors to ambient  $PM_{2.5}$  in urban areas [Kim *et al.*, 2005; Kleeman and Cass, 1998; Liu *et al.*, 2003; Noble and Prather, 1996; Park and Kim, 2005; Pastor *et al.*, 2003; Querol *et al.*, 2001; Swietlicki *et al.*, 1996; Toner *et al.*, 2007; Ward *et al.*, 2006; Ying and Kleeman, 2006; Zhao and Hopke, 2006]. Depending on the location being sampled, these sources can represent 80 – 90 % of the primary  $PM_{2.5}$ . As more ATOFMS source characterization studies are conducted, new source signatures can be added to the source library to increase its diversity and ability to distinguish individual sources of ambient aerosols. Likewise, specific source spectra can be removed from the library if they are found to interfere with proper apportionment. Particle aging, coating, agglomeration, and water uptake will play important roles in affecting particle source apportionment in other studies using this source library technique. Studies have shown that 10 – 35 % of the organic aerosols found in urban atmospheres is due to secondary organic aerosols (SOA) [Schauer *et al.*, 2002; Schauer *et al.*, 1996]. However, more recent studies propose an even higher number than that, and stating that up to 75 – 90 % of submicron OC particles

are from SOA [Buzcu-Guven *et al.*, 2007; Kleeman *et al.*, 2007; Kleinman *et al.*, 2007; Plaza *et al.*, 2006; Tsigaridis and Kanakidou, 2007; Volkamer *et al.*, 2006; Weber *et al.*, 2007; Williams *et al.*, 2007; Zhang *et al.*, 2007; Zhang *et al.*, 2005]. These changes will, undoubtedly, make matching to source signatures more challenging, particularly at locations further from the source. This is why the more general non-source specific seeds (EC pos only, aged OC, aged EC, amines, PAH's, vanadium containing, and NH<sub>4</sub> containing) are currently included in the library. While these generically named classes do not directly denote a source, the trends in their detection can be examined with other particle types, as well as peripheral instrumentation, in order to better understand their origin. Future ATOFMS studies where the particles from specific sources are put under controlled aging environments, such as in smog and reaction chamber experiments, may help resolve the origin of these types of particles and help reduce the amount of unclassified particles when using the source library matching method. Some of the sources, such as biomass, sea salt, and dust, are readily distinguishable whether or not the particles are aged. The biggest challenge with aging will be with differentiating LDV and HDDV exhaust particles from one another.

Additional methods to validate the source signature matching method also need to be considered. As was discussed for Chapter 4, impactor samples run by the Kleeman research group from UC-Davis were acquired alongside the ATOFMS instruments during the freeway-side study. When the data from the impactor samples is made available, their results can be compared to the single particle source apportionment results. The single particle measurements will hopefully be able to distinguish unique source signatures superimposed on high ambient background concentrations that may not be

apparent in the MOUDI mass concentrations where only slight changes are due to vehicle emissions (at least for the accumulation mode). Also, once the data are available, the source percentage predictions made with the source library matching method on the ATOFMS data can be compared with organic tracer MOUDI and impactor based method results from the freeway study obtained by the Kleeman research group. Additionally, future analysis using different clustering algorithms, such as Hierarchical clustering and Positive Matrix Factorization (PMF), can be used in comparison to the results found in this thesis. PMF is a technique used to group data based on their temporal time-series correlations [Chueinta *et al.*, 2000; Jaeckels *et al.*, 2007; Lanz *et al.*, 2007; Lee *et al.*, 1999; Paatero and Tapper, 1993]. This comparison could be done by using the standard ART-2a cluster results from the freeway data (or Athens, or Mexico City) as the input for PMF analysis. Upon determining the correct number of sources (factors) based on the PMF output, the temporal trends and the particles assigned to the PMF sources could then be compared to those apportioned with the source signature matching method. If similar results are obtained, this would be a valuable confirmation for the accuracy of the source signature matching method. If the results do not agree, then further analysis would have to be carried through to determine why the results vary and which method would be considered more correct.

### **7.3 Final Thought**

Hopefully the work presented in this dissertation reflects the passion I have had for advancing the process of ATOFMS source apportionment. It is my sincere hope that

this technique becomes an invaluable tool for atmospheric scientists, or at the very least, a starting point to inspire an even better method for aerosol source apportionment.

## 7.4 References

- Brady, B.B., E.W. Fournier, L.R. Martin, and R.B. Cohen, Stratospheric ozone reactive chemicals generated by space launches worldwide, pp. 34 pp., Technology Operations, Aerospace Corp., El Segundo, CA. USA., 1994.
- Buzcu-Guven, B., G. Brown Steven, A. Frankel, R. Hafner Hilary, and T. Roberts Paul, Analysis and apportionment of organic carbon and fine particulate matter sources at multiple sites in the midwestern United States, *Journal of the Air & Waste Management Association*, 57 (5), 606-619, 2007.
- Canagaratna, M.R., J.T. Jayne, D.A. Ghertner, S. Herndon, Q. Shi, J.L. Jimenez, P.J. Silva, P. Williams, T. Lanni, F. Drewnick, K.L. Demerjian, C.E. Kolb, and D.R. Worsnop, Chase studies of particulate emissions from in-use New York City vehicles, *Aerosol Science & Technology*, 38 (6), 555-573, 2004.
- Chueinta, W., P.K. Hopke, and P. Paatero, Investigation of sources of atmospheric aerosol at urban and suburban residential areas in Thailand by positive matrix factorization, *Atmospheric Environment*, 34 (20), 3319-3329, 2000.
- Cofer, W.R., III, E.L. Winstead, and L.E. Key, Surface composition of solid-rocket exhausted aluminum oxide particles, *Journal of Propulsion and Power*, 5 (6), 674-7, 1989.
- Dall'Osto, M., and R.M. Harrison, Chemical characterisation of single airborne particles in Athens (Greece) by ATOFMS, *Atmospheric Environment*, 40 (39), 7614-7631, 2006.
- Gautam, M., K. Chitoor, M. Durbha, and J.C. Summers, Effect of diesel soot contaminated oil on engine wear - investigation of novel oil formulations, *Tribology International*, 32 (12), 687-699, 1999.
- Harrison, R.M., R. Tilling, M.S.C. Romero, S. Harrad, and K. Jarvis, A study of trace metals and polycyclic aromatic hydrocarbons in the roadside environment, *Atmospheric Environment*, 37 (17), 2391-2402, 2003.
- Jaekels, J.M., M.-S. Bae, and J.J. Schauer, Positive Matrix Factorization (PMF) Analysis of Molecular Marker Measurements to Quantify the Sources of Organic Aerosols, *Environmental Science & Technology*, 41 (16), 5763-5769, 2007.

- Kim, E., P.K. Hopke, D.M. Kenski, and M. Koerber, Sources of Fine Particles in a Rural Midwestern U.S. Area, *Environmental Science and Technology*, 39 (13), 4953-4960, 2005.
- Kleeman, M.J., and G.R. Cass, Source contributions to the size and composition distribution of urban particulate air pollution, *Atmospheric Environment*, 32 (16), 2803-2816, 1998.
- Kleeman, M.J., Q. Ying, J. Lu, M.J. Mysliwiec, R.J. Griffin, J. Chen, and S. Clegg, Source apportionment of secondary organic aerosol during a severe photochemical smog episode, *Atmospheric Environment*, 41 (3), 576-591, 2007.
- Kleinman, L.I., P.H. Daum, Y.-N. Lee, G.I. Senum, S.R. Springston, J. Wang, C. Berkowitz, J. Hubbe, R.A. Zaveri, F.J. Brechtel, J. Jayne, T.B. Onasch, and D. Worsnop, Aircraft observations of aerosol composition and ageing in New England and Mid-Atlantic States during the summer 2002 New England Air Quality Study field campaign, *Journal of Geophysical Research, [Atmospheres]*, 112 (D9), D09310/1-D09310/18, 2007.
- Lanz, V.A., M.R. Alfarra, U. Baltensperger, B. Buchmann, C. Hueglin, and A.S.H. Prevot, Source apportionment of submicron organic aerosols at an urban site by factor analytical modelling of aerosol mass spectra, *Atmospheric Chemistry and Physics*, 7 (6), 1503-1522, 2007.
- Lee, E., C.K. Chan, and P. Paatero, Application of positive matrix factorization in source apportionment of particulate pollutants in Hong Kong, *Atmospheric Environment*, 33 (19), 3201-3212, 1999.
- Liu, D.Y., R.J. Wenzel, and K.A. Prather, Aerosol time-of-flight mass spectrometry during the Atlanta Supersite experiment: 1. Measurements, *Journal of Geophysical Research-Atmospheres*, 108 (D7), 8426, 2003.
- Moffet, R.C., B. de Foy, L.T. Molina, M.J. Molina, and K.A. Prather, Characterization of ambient aerosols in northern Mexico City by single particle mass spectrometry, *Atmospheric Chemistry and Physics Discussion*, 7, 6413-6457, 2007.
- Noble, C.A., and K.A. Prather, Real-time measurement of correlated size and composition profiles of individual atmospheric aerosol particles, *Environmental Science and Technology*, 30 (9), 2667-2680, 1996.
- Paatero, P., and U. Tapper, Analysis of different modes of factor analysis as least squares fit problems, *Chemometrics and Intelligent Laboratory Systems*, 18 (2), 183-94, 1993.

- Park, S.S., and Y.J. Kim, Source contributions to fine particulate matter in an urban atmosphere, *Chemosphere*, 59 (2), 217-226, 2005.
- Pastor, S.H., J.O. Allen, L.S. Hughes, P. Bhawe, G.R. Cass, and K.A. Prather, Ambient single particle analysis in Riverside, California by aerosol time-of-flight mass spectrometry during the SCOS97-NARSTO, *Atmospheric Environment*, 37 (Suppl. 2), 239-258, 2003.
- Plaza, J., F.J. Gomez-Moreno, L. Nunez, M. Pujadas, and B. Artinano, Estimation of secondary organic aerosol formation from semi-continuous OC-EC measurements in a Madrid suburban area, *Atmospheric Environment*, 40 (6), 1134-1147, 2006.
- Querol, X., A. Alastuey, S. Rodriguez, F. Plana, C.R. Ruiz, N. Cots, G. Massague, and O. Puig, PM10 and PM2.5 source apportionment in the Barcelona Metropolitan area, Catalonia, Spain, *Atmospheric Environment*, 35 (36), 6407-6419, 2001.
- Schauer, J.J., M.P. Fraser, G.R. Cass, and B.R.T. Simoneit, Source Reconciliation of Atmospheric Gas-Phase and Particle-Phase Pollutants during a Severe Photochemical Smog Episode, *Environmental Science and Technology*, 36 (17), 3806-3814, 2002.
- Schauer, J.J., W.F. Rogge, L.M. Hildemann, M.A. Mazurek, and G.R. Cass, Source apportionment of airborne particulate matter using organic compounds as tracers, *Atmospheric Environment*, 30 (22), 3837-3855, 1996.
- Shields, L.G., D.T. Suess, and K.A. Prather, Determination of single particle mass spectral signatures from heavy duty diesel vehicle emissions for PM<sub>2.5</sub> source apportionment, *Atmospheric Environment*, 41 (18), 3841-3852, 2007.
- Sodeman, D.A., S.M. Toner, and K.A. Prather, Determination of single particle mass spectral signatures from light duty vehicle emissions, *Environmental Science & Technology*, 39 (12), 4569-4580, 2005.
- Spencer, M.T., L.G. Shields, S.M. Toner, D.A. Sodeman, and K.A. Prather, Comparison of oil and fuel particle chemical signatures with particle emissions from heavy and light duty vehicles, *Atmospheric Environment*, 40 (27), 5224-5235, 2006.
- Swietlicki, E., S. Puri, H.-C. Hansson, and H. Edner, Urban air pollution source apportionment using a combination of aerosol and gas monitoring techniques, *Atmospheric Environment*, 30 (15), 2795-2809, 1996.
- Toner, S.M., L.G. Shields, D.A. Sodeman, and K.A. Prather, Using mass spectral source signatures to apportion exhaust particles from gasoline and diesel powered vehicles in a freeway study using UF-ATOFMS., *Atmospheric Environment*, doi:10.1016/j.atmosenv.2007.08.005, 2007.



- Toner, S.M., D.A. Sodeman, and K.A. Prather, Single particle characterization of ultrafine and accumulation mode particles from heavy duty diesel vehicles using aerosol time-of-flight mass spectrometry, *Environmental Science & Technology*, 40 (12), 3912-3921, 2006.
- Tsigaridis, K., and M. Kanakidou, Secondary organic aerosol importance in the future atmosphere, *Atmospheric Environment*, 41 (22), 4682-4692, 2007.
- Volkamer, R., J.L. Jimenez, F. San Martini, K. Dzepina, Q. Zhang, D. Salcedo, L.T. Molina, D.R. Worsnop, and M.J. Molina, Secondary organic aerosol formation from anthropogenic air pollution: rapid and higher than expected, *Geophysical Research Letters*, 33 (17), L17811/1-L17811/4, 2006.
- Ward, T., L. Rinehart, and T. Lange, The 2003/2004 Libby, Montana PM<sub>2.5</sub> source apportionment research study, *Aerosol Science and Technology*, 40 (3), 166-177, 2006.
- Weber, R.J., A.P. Sullivan, R.E. Peltier, A. Russell, B. Yan, M. Zheng, J. de Gouw, C. Warneke, C. Brock, J.S. Holloway, E.L. Atlas, and E. Edgerton, A study of secondary organic aerosol formation in the anthropogenic-influenced Southeastern United States, *Journal of Geophysical Research, [Atmospheres]*, 112 (D13), D13302/1-D13302/13, 2007.
- Williams, B.J., A.H. Goldstein, D.B. Millet, R. Holzinger, N.M. Kreisberg, S.V. Hering, A.B. White, D.R. Worsnop, J.D. Allan, and J.L. Jimenez, Chemical speciation of organic aerosol during the International Consortium for Atmospheric Research on Transport and Transformation 2004: results from in situ measurements, *Journal of Geophysical Research, [Atmospheres]*, 112 (D10), D10S26/1-D10S26/14, 2007.
- Ying, Q., and M.J. Kleeman, Source contributions to the regional distribution of secondary particulate matter in California, *Atmospheric Environment*, 40 (4), 736-752, 2006.
- Zhang, Q., J.L. Jimenez, D.R. Worsnop, and M. Canagaratna, A Case Study of Urban Particle Acidity and Its Influence on Secondary Organic Aerosol, *Environmental Science & Technology*, 41 (9), 3213-3219, 2007.
- Zhang, Q., D.R. Worsnop, M.R. Canagaratna, and J.L. Jimenez, Hydrocarbon-like and oxygenated organic aerosols in Pittsburgh: Insights into sources and processes of organic aerosols, *Atmospheric Chemistry and Physics*, 5 (12), 3289-3311, 2005.
- Zhao, W., and P.K. Hopke, Source identification for fine aerosols in Mammoth Cave National Park, *Atmospheric Research*, 80 (4), 309-322, 2006.

### A1 Development of an ATOFMS Mass Spectral Source

#### Signature Library

##### A1.1 Synopsis

The development of the mass spectral source signature library involved using the aerosol time-of-flight mass spectrometry (ATOFMS) single particle ion spectra data from several studies. This appendix describes the development of the source signature library to provide supporting information for Chapters 4 and 5.

##### A1.2 Heavy Duty & Light Duty Vehicle Signatures

The assembly of an ATOFMS mass spectral source signature library began with characterizing the particles from three vehicle studies. These studies consisted of two heavy duty diesel vehicle (HDDV) studies and another on gasoline powered light duty vehicles (LDV) [Shields *et al.*, 2007b; Sodeman *et al.*, 2005; Toner *et al.*, 2006]. The first HDDV study was conducted in 2001 using the West Virginia portable HDDV dynamometer [Clark *et al.*, 1995] in Riverside, Ca. In this study, a standard inlet aerosol time-of-flight mass spectrometer (ATOFMS) [Gard *et al.*, 1997] that was tuned to characterize particles from 100 to 2500 nm was utilized. The second HDDV study was conducted in 2003 using a modified West Virginia portable HDDV dynamometer in Riverside, Ca. For the second HDDV study, an ultrafine aerosol time-of-flight mass spectrometer (UF-ATOFMS) [Su *et al.*, 2004] and a standard inlet ATOFMS were used

to characterize HDDV particles with a combined size range from 50 to 2500 nm. The LDV study was conducted in 2002 at the California Air Resources Board Haagen-Smit dynamometer facility in El Monte, Ca. The LDV study also used both the UF-ATOFMS and ATOFMS instruments for characterization of particles from 50 to 2500 nm.

The particles detected from each of these studies were separately imported into Matlab and analyzed with the ART-2a clustering algorithm [Song *et al.*, 1999] using a vigilance factor (VF) of 0.85, learning rate of 0.05, and 20 iterations. Since ART-2a does not converge, it can create chemically similar clusters during its initial clustering process for each particle data set. To combine similar clusters, a secondary regrouping function is run on the ART-2a particle clusters to group clusters together within the original vigilance factor. For the purpose of communicating the general particle types for each dynamometer study in their respective manuscripts, the regrouped clusters were further hand grouped into more general classes that represented the particle clusters that each contained. However, for the purpose of building an ATOFMS mass spectral library for source apportionment, the minor differences in clusters that went into each general class are now far more valuable. Hence, the clusters that resulted from the initial ART-2a run were added to the library as well as the clusters that resulted from the ART-2a regrouping technique.

To test the effectiveness of these HDDV and LDV mass spectral signatures, they were tested on an ambient data set where the UF-ATOFMS and ATOFMS instruments sampled along side a major freeway (Interstate 5) in San Diego, Ca. in 2004 [Toner *et al.*, 2007b]. This sampling site was located in a relatively clean, costal environment where the major contribution of particles was from freeway traffic exhaust. In addition, the

vehicle particles detected at this site have undergone very little aging, which make them more comparable to the vehicle source library.

Particles detected with the ATOFMS instruments were matched to the signatures in the source library using a matching function version of the ART-2a algorithm. The match-ART-2a function (YAADA v.1.20 – <http://www.yaada.org>) uses existing ART-2a clusters as source “seeds” for the purpose of determining whether other particles match those seeds. In this case, ART-2a runs normal with prescribed particle clusters unable to be changed by the addition of new particles to each cluster. Since the clusters do not change as particles are matched to them, this function allows the clusters/seeds to stay “true” to the original source signatures. Particles being considered in the matching are either matched exclusively to a particular cluster (above a set VF) or not at all. If a particle matches above the threshold for two or more clusters, it will be added to the one which yields the highest dot product. The VF used for match-ART-2a is the same as that used for the source studies ( $VF = 0.85$ ).

Various combinations of the vehicle source library were created and tested in order to optimize their matching on the particles detected from the freeway-side study. These combinations ranged from using just the top 10 – 20 ART-2a clusters to using all the resulting clusters from ART-2a for each vehicle study. Many combinations in between these extremes were also attempted in the effort to maximize the amount of freeway-side vehicle related ambient particles matched and with the highest accuracy possible. The initial optimization was done by matching particle detected by the UF-ATOFMS. The majority of the particles detected with this instrument are in the ultrafine (50 – 100 nm) and low accumulation mode (100 – 400 nm) size ranges and are

considered “fresher” particles emitted by the vehicle traffic, and thus, more comparable to the source seeds.

As was discussed in Chapter 4, the top ART-2a clusters that account for about 90% of the particles from each vehicle study were used for the signature matching process. These studies consisted of UF-ATOFMS characterization of HDDV particles (HDDV03) [Toner *et al.*, 2006], ATOFMS characterization of HDDV particles (HDDV01) [Shields *et al.*, 2007b], and UF-ATOFMS characterization of LDV particles (LDV02) [Sodeman *et al.*, 2005]. The seeds were then separated by size, where ultrafine (50 – 100 nm) and accumulation mode (100 – 140 nm & 140 – 1000 nm) mass spectral libraries have been created for each source. The reason the accumulation mode was split into two libraries (for this study) was because of the regional background EC and vanadium types discussed in Chapters 4 and 5 which were found to influence the accumulation mode above 140 nm [Toner *et al.*, 2007b]. The data from the UF-ATOFMS (HDDV03 and LDV02) was used to generate the ultrafine (UF) seeds to make 36 HDDV seeds and 24 LDV seeds, each set representing about 90% of their respective source study particles. The data from the UF-ATOFMS (HDDV03 & LDV02) and the ATOFMS (HDDV01) were used to create the seeds for the smaller accumulation mode (SAM) (100 – 140 nm) and the larger accumulation mode (LAM) (140 – 1000 nm). The SAM seeds consist of 61 HDDV (31 HDDV03 and 30 HDDV01) and 28 LDV seeds, while the LAM seeds consist of 61 HDDV (31 HDDV03 and 30 HDDV01) and 31 LDV seeds. Once again, these seeds represent about 90% of the particles for each study in their respective size ranges.

In addition to the vehicle source seeds, clusters generated by running ART-2a on the UF-ATOFMS freeway detected particles were also incorporated into the source seed library. This was done for two reasons: The first is because there were detector noise peaks in the vehicle study (labeled as “cross-talk” in their manuscripts) that either weren’t in the freeway spectra, or were located at a different mass-to-charge. These peaks are generally caused by a very large ion signal from the positive spectrum interfering with the negative ion spectrum. The freeway data has particle spectra that are identical to the top particle types from the vehicle studies, but weren’t matching the source seeds due to these differences in the “cross-talk” peaks. Therefore, seeds were made from those freeway particle types and incorporated into the library. The majority of these clusters were attributed to HDDVs, as their spectra matched best to the HDDV library source seeds than to the LDV seeds. The second reason certain ambient freeway types were incorporated into the vehicle source library was to have particles in the library that represented more aged vehicle particle types due to the increased uptake of nitrate and/or sulfate. These seeds were only generated for types representing top vehicle particle types and that have high enough correlations with specific vehicle seeds as to properly label them HDDV or LDV. After incorporating the ambient seeds into the vehicle source seed library, the SAM vehicle library contains 76 HDDV seeds and 30 LDV seeds, and the LAM vehicle library contains 82 HDDV seeds and 31 LDV seeds. No ambient seeds were incorporated into the UF vehicle library since the ambient UF particles have undergone very little aging and the library seeds appear very representative of the UF ambient particles (due to the high percentage of UF matching).

While there are more HDDV than LDV seeds in each vehicle library size range, this does not appear to be the reason for why the freeway side apportionment yields more HDDV matched particles than LDV. Figure A1.1 shows a statistical breakdown of how many particles matched to each seed within each size-mode library. What is very apparent from this figure is that, while HDDV seeds match more particles than the LDV seeds, a higher fraction of the LDV seeds match the ambient particles than do the HDDV seeds. For the UF particles, 83% of the LDV seeds match particles, while only 61% of the HDDV seeds match. For the SAM particles, 84% of the LDV seeds and 70% of the HDDV seeds match particles. Lastly, for the LAM particles, 87% of the LDV seeds and 68% of the HDDV seeds match particles. This is a good indication that the majority of the seeds in the LDV libraries are very representative of the LDV particles near the freeway.

For the SAM and LAM libraries, the majority of the seeds that don't match any particles are the types that have large "cross-talk" peaks in the negative ion spectra that were discussed earlier. Seeds 62 – 76 in the SAM and 62 – 82 in the LAM libraries are the HDDV seeds created from ambient freeway data. Since these types are representative of the top HDDV source types, just without the "cross-talk", or with secondary species on them from aging, they match a higher percentage of the ambient particles. There was very little detector "cross-talk" in the data from the LDV vehicle study, which is why it wasn't necessary to create ambient seeds to compensate for that in the LDV seeds. Also, the seeds within the LDV library have corresponding particle types with and without secondary species (nitrate and sulfate) which is also why there weren't ambient seeds created to represent those types for this study. Only two LDV seeds were created from

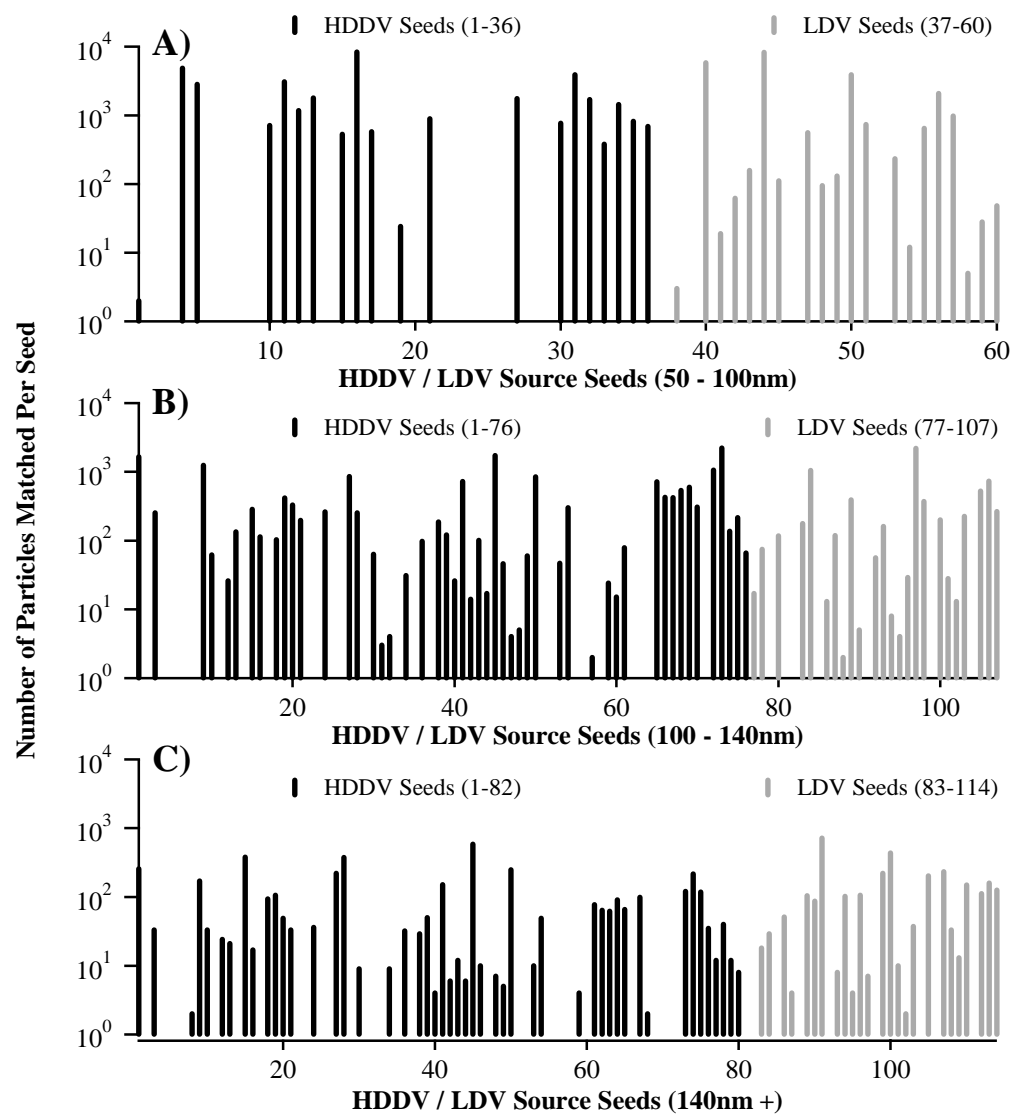


**Figure A1.1** Number of particles matched to each HDDV and LDV source seed for A) Ultrafine particles (50-100 nm); B) Smaller accumulation mode (SAM) particles (100-140 nm); C) Larger accumulation mode (LAM) particles > 140 nm.



ambient data (for the SAM library) that are representative of the top LDV source type, but with a larger sulfate ( $m/z$  -97) peak.

Another note to make about the “cross-talk” peaks is that they may be an additional indicator of HDDV emission (for EC-Ca containing particles discussed in Chapters 3 and 4) as they absorb the 266nm laser light used to desorb and ionize the particles more strongly than most other particle types. The larger absorption of the LDI radiation will produce a much larger number of positive ions and thus a much more intense positive ion signal. The much more intense positive ion signals are most likely responsible for creating the “cross-talk” interference seen in the negative ion signal, but further work is necessary to confirm this. If this is indeed the cause of the “cross-talk” peaks in the negative ions, then it is an issue that will not be of concern in newer models of the ATOFMS instrument due to improvements in the detector technology used [Denkenberger *et al.*, 2007; Holecek *et al.*, 2007a]. Since these improvements eliminate the “cross-talk” issue, such peaks will no longer be appropriate for the apportionment of HDDV particles. This is yet further justification for using the equivalent ambient seeds that do not contain "cross-talk" peaks to perform ambient source apportionment.

For the UF vehicle library, seeds 30 – 36 represent the top HDDV seeds (as seen in Figure 4.4 of Chapter 4), which is why they match a large portion of the HDDV detected particles. As previously discussed, many of the clusters that didn’t match particles in the HDDV UF seeds are clusters with “cross-talk” peaks in the negative ions that aren’t seen in the freeway study. Also, as seen in the SAM and LAM size ranges, while more particles match to the HDDV seeds, a much larger fraction of the LDV seeds match to the freeway-side ambient particles.

### A1.3 Additional Source Signatures

Since the source signature matching method was proven to be a viable technique for apportioning HDDV and LDV particles (which are chemically similar), the next step was to add other source signatures to the library. Certain specific sources, such as sea salt, dust, biomass burning, meat cooking, and industrial emissions have proven to be readily distinguishable in previous ATOFMS ambient characterization measurements [Gard *et al.*, 1998; Guazzotti *et al.*, 2003; Liu *et al.*, 2003; Moffet *et al.*, 2007; Silva *et al.*, 2000; Silva *et al.*, 1999; Sodeman *et al.*, 2005; Suess, 2002]. Representative weight matrices for each of these sources were generated from ART-2a results from several different ambient and lab studies and incorporated into the source signature library. Such studies include the freeway 2004 (FWY) study [Toner *et al.*, 2007a; Toner *et al.*, 2007b], the study of organic aerosols in Riverside, CA (SOAR 1 & 2) studies [Qin *et al.*, 2007; Shields *et al.*, 2007a], the Cloud Indirect Effects Experiment in Trinidad Head, CA (CIFEX) study [Holecek *et al.*, 2007b; Wilcox *et al.*, 2006], the ABC Post Monsoonal Experiment in Hanimaadhoo, Republic of Maldives (APMEX) study [Spencer *et al.*, 2007], and the Megacity Initiative: Local and Global Research Observations in Mexico City, Mexico (MILAGRO) study [Moffet *et al.*, 2007]. These additional sources, along with seven non-source specific signature types (elemental carbon (positive ion only), aged elemental carbon, aged organic carbon, amines, PAH's, vanadium rich, and NH<sub>4</sub> rich) were added accordingly to the three different size range libraries that were constructed for the vehicle signatures and are listed in Table A1.1 for the ultrafine mode, Table A1.2 for the SAM, and Table A1.3 for the SAM & above particles. The notations

**Table A1.1** Structure of the Mass Spectral Source Signature Library for Ultrafine (50 – 100 nm) Particle Matching.

Source	Study Generated From	Instrument	Amount of Seeds
HDDV	HDDV 2003	UF-ATOFMS	36
LDV	LDV 2002	UF-ATOFMS	24
Sea Salt	CIFEX	ATOFMS - LVN	9
Biomass	CIFEX	ATOFMS - LVN	5
Biomass	FWY Study	UF-ATOFMS	8
Sea Salt	APMEX	ATOFMS - LVN	11
Dust	APMEX	ATOFMS - LVN	1
Dust	CIFEX	ATOFMS - LVN	3
Dust	Lab resuspended samples	ATOFMS - LVN & ELD	101
Biomass	FWY Study	ATOFMS - LVN	2
Sea Salt	FWY Study	ATOFMS - LVN	2
Dust	SOAR 2	ATOFMS - LVN	21
Sea Salt	SOAR 2	ATOFMS - LVN	4
Amine	SOAR 1	ATOFMS - LVN	4
NH <sub>4</sub> Rich	SOAR 1	ATOFMS - LVN	2
Vanadium Rich	SOAR 1	ATOFMS - LVN	3
Aged EC	SOAR 1	ATOFMS - LVN	2
Aged OC	SOAR 1	ATOFMS - LVN	5
Biomass	SOAR 1	ATOFMS - LVN	5
Vanadium Rich	SOAR 2	ATOFMS - LVN	14
Vanadium Rich	FWY Study (upwind)	ATOFMS - ELD	10
Sea Salt	FWY Study (upwind)	ATOFMS - ELD	24
Dust	FWY Study (upwind)	ATOFMS - ELD	7
Amine	FWY Study (upwind)	ATOFMS - ELD	13
Meat Cooking	MILAGRO - 2006 & FWY - 2004 (upwind)	ATOFMS - LVN & ELD	16

**Table A1.2** Structure of the Mass Spectral Source Signature Library for Smaller Accumulation Mode (SAM: 100 – 140 nm) Particle Matching.

Source	Study Generated From	Instrument	Amount of Seeds
HDDV	HDDV 2003 dynamometer (warmed-up engines)	UF-ATOFMS	31
HDDV	HDDV 2001 dynamometer (warmed-up engines)	ATOFMS - ELD	30
HDDV	FWY Study	ATOFMS - LVN	3
HDDV	FWY Study	UF-ATOFMS	7
LDV	LDV 2002 dynamometer (warmed-up engines)	UF-ATOFMS	29
Sea Salt	CIFEX	ATOFMS - LVN	9
Biomass	CIFEX	ATOFMS - LVN	5
Biomass	FWY Study	UF-ATOFMS	8
Sea Salt	APMEX	ATOFMS - LVN	11
Dust	APMEX	ATOFMS - LVN	1
Dust	CIFEX	ATOFMS - LVN	3
Dust	Lab resuspended samples	ATOFMS - LVN & ELD	101
Biomass	FWY Study	ATOFMS - LVN	2
Sea Salt	FWY Study	ATOFMS - LVN	2
Dust	SOAR 2	ATOFMS - LVN	21
Sea Salt	SOAR 2	ATOFMS - LVN	4
Amine	SOAR 1	ATOFMS - LVN	4
NH <sub>4</sub> Rich	SOAR 1	ATOFMS - LVN	2
Vanadium Rich	SOAR 1	ATOFMS - LVN	3
Aged EC	SOAR 1	ATOFMS - LVN	2
Aged OC	SOAR 1	ATOFMS - LVN	5
Aged OC	FWY Study	UF-ATOFMS	1
Aged OC	FWY Study	ATOFMS - LVN	1
Biomass	SOAR 1	ATOFMS - LVN	5
Vanadium Rich	SOAR 2	ATOFMS - LVN	14
Vanadium Rich	FWY Study (upwind)	ATOFMS - ELD	10
Sea Salt	FWY Study (upwind)	ATOFMS - ELD	24
Dust	FWY Study (upwind)	ATOFMS - ELD	7
Amine	FWY Study (upwind)	ATOFMS - ELD	13
Sea Salt	FWY Study	ATOFMS - LVN	4
Meat Cooking	MILAGRO - 2006 & FWY - 2004 (upwind)	ATOFMS - LVN & ELD	16

**Table A1.3** Structure of the Mass Spectral Source Signature Library for Larger Accumulation Mode (LAM: 140 – 1000 nm) & Supermicron (1000 nm +) Particle Matching.

Source	Study Generated From	Instrument	Amount of Seeds
HDDV	HDDV 2003 dynamometer (warmed-up engines)	UF-ATOFMS	31
HDDV	HDDV 2001 dynamometer (warmed-up engines)	ATOFMS - ELD	30
HDDV	FWY Study - 2004	ATOFMS - LVN	3
HDDV	FWY Study - 2004	UF-ATOFMS	16
HDDV	FWY Study - 2004	ATOFMS - ELD	3
LDV	LDV 2002 dynamometer (warmed-up engines)	UF-ATOFMS	27
LDV	FWY Study - 2004	UF-ATOFMS	2
EC Pos Only	FWY Study - 2004	UF-ATOFMS	2
Sea Salt	CIFEX - 2004	ATOFMS - LVN	9
Biomass	CIFEX - 2004	ATOFMS - LVN	5
Biomass	FWY Study - 2004	UF-ATOFMS	8
Sea Salt	APMEX	ATOFMS - LVN	11
Dust	APMEX	ATOFMS - LVN	1
Dust	CIFEX - 2004	ATOFMS - LVN	3
Dust	Lab resuspended samples	ATOFMS - LVN & ELD	101
Biomass	FWY Study - 2004	ATOFMS - LVN	2
Sea Salt	FWY Study - 2004	ATOFMS - LVN	2
Dust	SOAR 2 - Fall 2005	ATOFMS - LVN	21
Sea Salt	SOAR 2 - Fall 2005	ATOFMS - LVN	4
Amine	SOAR 1 - Summer 2005	ATOFMS - LVN	4
Amine	FWY Study - 2004 (upwind)	ATOFMS - ELD	1
NH <sub>4</sub> Rich	SOAR 1 - Summer 2005	ATOFMS - LVN	2
Vanadium Rich	SOAR 1 - Summer 2005	ATOFMS - LVN	3
Aged EC	SOAR 1 - Summer 2005	ATOFMS - LVN	2
Aged EC	FWY Study - 2004 (upwind)	ATOFMS - ELD	1
Aged OC	SOAR 1 - Summer 2005	ATOFMS - LVN	5
Aged OC	FWY Study - 2004	UF-ATOFMS	1
Aged OC	FWY Study - 2004	ATOFMS - LVN	2
Biomass	SOAR 1 - Summer 2005	ATOFMS - LVN	5
Vanadium Rich	SOAR 2 - Fall 2005	ATOFMS - LVN	14
Vanadium Rich	FWY Study - 2004 (upwind)	ATOFMS - ELD	10
Sea Salt	FWY Study - 2004 (upwind)	ATOFMS - ELD	24
Dust	FWY Study - 2004 (upwind)	ATOFMS - ELD	7
Amine	FWY Study - 2004 (upwind)	ATOFMS - ELD	13
Vanadium (Ship)	FWY Study - 2004	ATOFMS - LVN & ELD	28
EC Pos Only	FWY Study - 2004	ATOFMS - LVN	7
EC Pos Only	FWY Study - 2004 (upwind)	ATOFMS - ELD	1
Sea Salt	FWY Study - 2004	ATOFMS - LVN	4
Meat Cooking	MILAGRO - 2006 & FWY - 2004 (upwind)	ATOFMS - LVN & ELD	16

LVN and ELD are used to distinguish between two standard-inlet ATOFMS instruments in the tables. The two instruments are the same except that ATOFMS-LVN has some components which use newer technology.

While the ability of the source library to apportion particles in an environment consisting mainly of fresh vehicle emissions has been shown to be very good, the library still needs to be expanded to include seeds representing particles of a more aged nature for each source. This task is still in progress, where additional clusters are being added to the source library by running ART-2a on particles detected in very aged environments. The SOAR 1 and SOAR 2 data sets are excellent sources for aged particles types as the air in Riverside, CA. is extremely polluted. However, in very aged environments, the particles can be so convoluted that they are indistinguishable from any source. For this reason, the non-source specific particle types were added to the signature library. While these generic named classes do not directly denote a source, the trends in their detection can be examined with other particle types, as well as peripheral instrumentation, in order to better understand their origin.

## A1.4 References

- Clark, N.N., M. Gautam, R.M. Bata, W.-G. Wang, J.L. Loth, G.M. Palmer, and D.W. Lyons, Technical Report: Design and operation of a new transportable laboratory for emissions testing of heavy duty trucks and buses, *Int. J. of Vehicle Design*, 2 (3/4), 308-322, 1995.
- Denkenberger, K.A., X. Qin, L.G. Shields, J.C. Holecek, R.C. Moffet, and K.A. Prather, Ground-based field comparison of the A-ATOFMS with the nozzle-inlet ATOFMS and UF-ATOFMS, *In Preparation*, 2007.
- Gard, E., J.E. Mayer, B.D. Morrical, T. Dienes, D.P. Fergenson, and K.A. Prather, Real-time analysis of individual atmospheric aerosol particles: Design and performance of a portable ATOFMS, *Analytical Chemistry*, 69 (20), 4083-4091, 1997.
- Gard, E.E., M.J. Kleeman, D.S. Gross, L.S. Hughes, J.O. Allen, B.D. Morrical, D.P. Fergenson, T. Dienes, M.E. Galli, R.J. Johnson, G.R. Cass, and K.A. Prather, Direct observation of heterogeneous chemistry in the atmosphere, *Science (Washington, D. C.)*, 279 (5354), 1184-1187, 1998.
- Guazzotti, S.A., D.T. Suess, K.R. Coffee, P.K. Quinn, T.S. Bates, A. Wisthaler, A. Hansel, W.P. Ball, R.R. Dickerson, C. Neususs, P.J. Crutzen, and K.A. Prather, Characterization of carbonaceous aerosols outflow from India and Arabia: biomass/biofuel burning and fossil fuel combustion, *Journal of Geophysical Research, [Atmospheres]*, 108 (D15), ACL13/1-ACL13/14, 2003.
- Holecek, J.C., K.A. Denkenberger, J.E. Mayer, R.C. Moffet, G. Poon, R.O. Sanchez, T.P. Rebotier, H. Furutani, Y.X. Su, S.A. Guazzotti, and K.A. Prather, Aircraft-ATOFMS Instrument Development., *In Preparation*, 2007a.
- Holecek, J.C., M.T. Spencer, and K.A. Prather, Single particle analysis of rainwater samples: insoluble particles and direct comparisons with ambient concentrations from the Northeast Pacific and Indian Ocean, *Journal of Geophysical Research - Atmospheres*, *Accepted*, 2007b.
- Liu, D.-Y., R.J. Wenzel, and K.A. Prather, Aerosol time-of-flight mass spectrometry during the Atlanta Supersite Experiment: 1. Measurements, *Journal of Geophysical Research, [Atmospheres]*, 108 (D7), SOS 14/1-SOS 14/16, 2003.
- Moffet, R.C., B. de Foy, L.T. Molina, M.J. Molina, and K.A. Prather, Characterization of ambient aerosols in northern Mexico City by single particle mass spectrometry, *manuscript in preparation*, 2007.

- Qin, X., L.G. Shields, S.M. Toner, and K.A. Prather, Single Particle Characterization in Riverside, CA during the SOAR 2005 Campaign – Part 1: Seasonal Comparisons, *manuscript in preparation*, 2007.
- Shields, L.G., X. Qin, S.M. Toner, and K.A. Prather, Characterization of Trace Metals in Single Urban Particles during the SOAR 2005 Campaign, *manuscript in preparation*, 2007a.
- Shields, L.G., D.T. Suess, and K.A. Prather, Determination of single particle mass spectral signatures from heavy duty diesel vehicle emissions for PM<sub>2.5</sub> source apportionment, *Atmospheric Environment*, 41 (18), 3841-3852, 2007b.
- Silva, P.J., R.A. Carlin, and K.A. Prather, Single particle analysis of suspended soil dust from Southern California, *Atmospheric Environment*, 34 (11), 1811-1820, 2000.
- Silva, P.J., D.-Y. Liu, C.A. Noble, and K.A. Prather, Size and Chemical Characterization of Individual Particles Resulting from Biomass Burning of Local Southern California Species, *Environmental Science and Technology*, 33 (18), 3068-3076, 1999.
- Sodeman, D.A., S.M. Toner, and K.A. Prather, Determination of single particle mass spectral signatures from light duty vehicle emissions, *Environmental Science & Technology*, 39 (12), 4569-4580, 2005.
- Song, X.H., P.K. Hopke, D.P. Fergenson, and K.A. Prather, Classification of single particles analyzed by ATOFMS using an artificial neural network, ART-2A, *Analytical Chemistry*, 71(4), 860-865, 1999.
- Spencer, M.T., J.C. Holecek, C.E. Corrigan, V. Ramanathan, and K.A. Prather, Size-resolved chemical composition of individual particles during a monsoonal transition period in the north Indian Ocean, *Journal of Geophysical Research - Atmospheres*, Submitted, 2007.
- Su, Y., M.F. Sipin, H. Furutani, and K.A. Prather, Development and characterization of an aerosol time-of-flight mass spectrometer with increased detection efficiency, *Analytical Chemistry*, 76 (3), 712-719, 2004.
- Suess, D.T., Single particle mass spectrometry combustion source characterization and atmospheric apportionment of vehicular, coal, and biofuel exhaust emission, Ph.D. thesis, University of California, Riverside, Riverside, 2002.
- Toner, S.M., L.G. Shields, and K.A. Prather, Source apportionment of freeway-side PM<sub>2.5</sub> using ATOFMS, *manuscript in preparation*, 2007a.



- Toner, S.M., L.G. Shields, D.A. Sodeman, and K.A. Prather, Using mass spectral source signatures to apportion exhaust particles from gasoline and diesel powered vehicles in a freeway study using UF-ATOFMS., *Atmospheric Environment*, doi:10.1016/j.atmosenv.2007.08.005, 2007b.
- Toner, S.M., D.A. Sodeman, and K.A. Prather, Single particle characterization of ultrafine and accumulation mode particles from heavy duty diesel vehicles using aerosol time-of-flight mass spectrometry, *Environmental Science & Technology*, 40 (12), 3912-3921, 2006.
- Wilcox, E.M., G. Roberts, and V. Ramanathan, Influence of aerosols on the shortwave cloud radiative forcing from North Pacific oceanic clouds: Results from the Cloud Indirect Forcing Experiment (CIFEX), *Geophysical Research Letters*, 33 (21), 2006.

### A2 Supporting Information for Chapter 4

#### A2.1 Error and Percent Matching as a Function of Vigilance Factor

While the topic of the appropriate ART-2a vigilance factor (VF) that should be used for particle clustering has been discussed [*Phares et al.*, 2001; *Rebotier and Prather*, 2007; *Wenzel and Prather*, 2004; *Zhou et al.*, 2006], the proper VF for match-ART-2a (in Chapters 4) is a new issue to address. When running ART-2a as a standard clustering tool, using a low VF results in less clusters, however, the clusters will have significant variability within them since the particle mass spectra only have to match within a relatively loose degree. On the other hand, using too high of a VF generally results in a large number of clusters, but the clusters have less variability within them since the particles that make them up have to have very similar mass spectra. When using ART-2a in its matching form for source apportionment, changing the VF will change the degree to which particles will match the seeds. If the VF is too high, fewer particles will be matched to the seeds, but the particles that do match will be very similar to the seed they are matched to and thus, have a low matching error. On the other hand, if the VF is too low, particles will still match to the source seed with which they have the highest dot product, but particles may be matched to a source they do not originate from since the dot product threshold needed to be included within source may be too relaxed. This would

**Table A2.1** Percent of particles matched with varying vigilance factor (VF)

VF	Ultrafine (50 - 100nm)		Fine (100 - 300nm)	
	% Matched	% Error	% Matched	% Error
0.95	80.00	1.08	27.83	1.13
0.90	93.70	2.15	54.48	2.83
0.85	95.80	2.89	65.98	4.01
0.80	96.39	4.48	71.69	10.59
0.75	96.74	5.22	75.91	15.59
0.70	96.98	8.61	79.86	19.89
0.65	97.26	14.24	84.28	23.67
0.60	97.45	14.63	87.91	26.71
0.55	97.68	14.95	90.78	29.08
0.50	98.01	15.34	94.12	31.70

make the error for matching higher, as particles may be erroneously matched to source seeds that they do not belong to.

Table A2.1 describes how the percentage of particles detected with the UF-ATOFMS sampling freeway-side match to the vehicle source seeds as VF is changed from high to low ( $VF = 0.95 - 0.50$ ). The error for matching was determined by matching the vehicle seeds to the vehicle source particles at the same VF's as well as the number of non-vehicle freeway particles that started becoming matched to vehicle seeds as the VF was lowered. As can be seen in Table A2.1, as the VF goes down, the percent of particles matched goes up, but so does the error. For the accumulation mode particles, the error remains low (under 5%) from VF of 0.95 to 0.85 until a VF of 0.80 when it more than doubles. For UF particles, the error stays low from VF of 0.95 to 0.75, and then it rises to 8.61% when going from 0.75 to 0.70. It is likely that the error for the UF particles didn't rise as much as that for the accumulation mode particles because the primary source for the UF particles along the freeway was from vehicular emissions. A VF of 0.85 was chosen for matching with this study because it has a relatively high percentage of matching with a low amount of error.

In order to determine if the reason for the error increase corresponds to the VF used to create the original seed clusters, a second library was created where the seeds were made at a  $VF = 0.70$ . These seeds were used to match back to the original dynamometer source particles as well as the particles from the freeway data set using the same method of error analysis. These results are shown in Table A2.2. As can be seen, the error is much higher, even when matching at a  $VF = 0.95$ . The reason for this is because the weight matrices (WM) within the seed clusters are not as representative of

**Table A2.2** Percent of particles matched with varying vigilance factor (VF) for vehicle source seeds made at a VF of 0.70

VF	Ultrafine (50 - 100nm)		Fine (100 - 300nm)	
	% Matched	% Error	% Matched	% Error
0.95	39.27	20.94	24.05	26.40
0.90	64.92	22.84	66.24	31.62
0.85	77.24	23.31	80.20	34.52
0.80	84.57	23.41	86.94	35.97
0.75	89.22	23.63	90.44	36.45
0.70	94.05	24.09	93.60	37.07
0.65	98.41	24.78	97.64	37.98
0.60	98.89	25.52	98.47	38.53
0.55	99.16	25.81	98.86	38.82
0.50	99.43	25.99	99.09	39.08

the dynamometer data as those made with the  $VF = 0.85$ . This is also the reason why the error doesn't increase with the same magnitude as with previous seeds. With the seeds being made at such a loose VF, it causes their WM's have ion peaks that are not reflective of the actual vehicle particle types, and it causes them to match to things they otherwise wouldn't when made at a higher VF. Not only did this cause a lot of matching to non-vehicle particles in the freeway data, but lots of mismatching when matching to the vehicle source particles as well. These results show that a high VF is necessary when creating initial source seeds in order to keep the variability within the seed WM's low as well as the error if used for matching purposes.

## A2.2 References

- Phares, D.J., K.P. Rhoads, A.S. Wexler, D.B. Kane, and M.V. Johnston, Application of the ART-2a algorithm to laser ablation aerosol mass spectrometry of particle standards, *Analytical Chemistry*, 73 (10), 2338-2344, 2001.
- Rebotier, T.P., and K.A. Prather, Aerosol time-of-flight mass spectrometry data analysis: A benchmark of clustering algorithms, *Analytica Chimica Acta*, 585 (1), 38-54, 2007.
- Wenzel, R.J., and K.A. Prather, Improvements in ion signal reproducibility obtained using a homogeneous laser beam for on-line laser desorption/ionization of single particles, *Rapid Communications in Mass Spectrometry*, 18 (13), 1525-1533, 2004.
- Zhou, L., P.K. Hopke, and P. Venkatachari, Cluster analysis of single particle mass spectra measured at Flushing, NY, *Analytica Chimica Acta*, 555 (1), 47-56, 2006.

### A3 Supporting Information for Chapter 6

#### A3.1 Variations in the Source Signature Matching Technique

As was mentioned in Chapter 6, source signature matching was also carried out at a lower vigilance factor ( $VF = 0.75$ ) and with a different technique using only the positive ions for the unclassified particles to see how these parameters affect the matching process. One of the major reasons to lower the VF when matching is to increase the amount of particles matched to the seeds. This can be a necessity when attempting to match to highly aged particles, as many of the source seeds in the library are for fresher emissions. The problem with lowering the VF, as discussed in Chapter 4 and Appendix 2, is that the potential error in source assignment increases as the VF decreases [Toner *et al.*, 2007]. Therefore, careful inspection of the particle assignments must be carried out when lower VF's are used in order determine the validity of their source assignments.

The other matching technique used involved matching just the positive ion spectra from the source seeds to the positive ion spectra from the datasets (at  $VF = 0.85$ ). This was done only on the unclassified particles after performing the regular dual ion matching at a VF of 0.85. The reason for performing the positive ion matching after the initial matching (and not on all the data) is to ensure the lowest amount of matching error possible by removing the particles in the first matching run that can match to the source seeds at  $VF = 0.85$ . This technique is also useful for matching particles in aged environments that contain secondary species in the negative ions that cause the particles

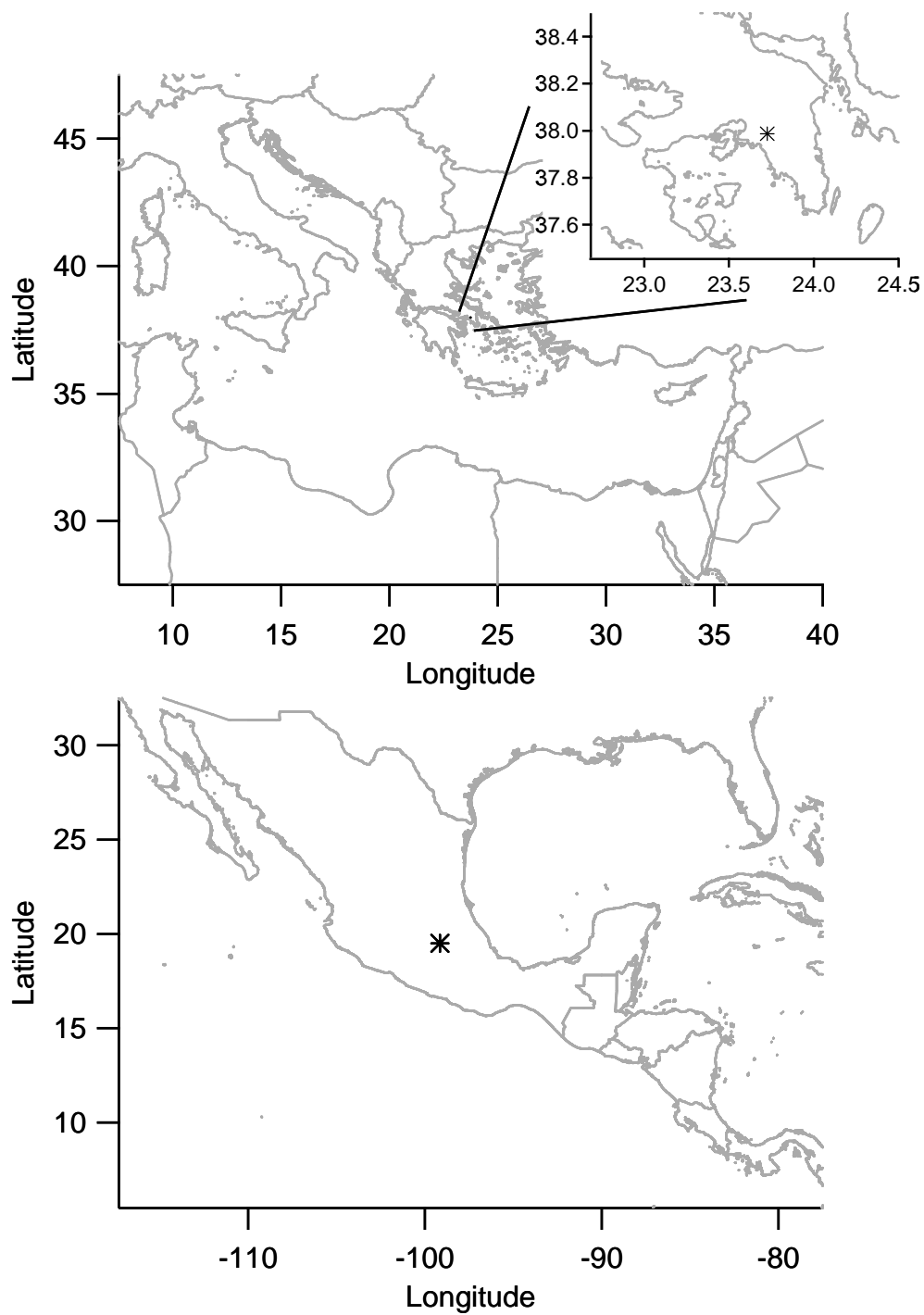


**Figure A3.1** Top) Athens, Greece sampling site location; Bottom) Mexico City sampling site location.



to not match to the dual ion source seeds. Additionally, there are datasets (such as those discussed in this manuscript) where many of the single particle negative ion spectra are miscalibrated, which prevents such particles to match to the source signatures. Therefore, an attempt at matching the unclassified particles from the initial dual ion matching step can be made based on exclusively matching to their positive ions to try and help identify such particles.

These variations in source signature matching were done for both the Athens and Mexico City datasets (locations shown in Figure A3.1) and are compared to the standard dual ion matching at  $VF = 0.85$ . These results are shown in Figures A3.2, A3.3, and A3.4 for Athens, and Figures A3.5, A3.6, and A3.7 for Mexico City. The temporal series figures for each study are separated by submicron (A3.2 for Athens & A3.5 for Mexico City) and supermicron (A3.3 for Athens & A3.6 for Mexico City) size modes. Table A3.1 summarizes the matching percentages with the different techniques for the Athens dataset, while Table A3.2 summarizes the results for Mexico City. Figure A3.4 and A3.8 show the size resolved source apportionment for Athens and Mexico City, respectively.

### **A3.2 Matching Technique Variation Results for Athens, Greece**

When examining the matching results for the submicron Athens, Greece data in Figure A3.2, it can be seen how the amount of unclassified particles decreases when using the positive ion matching (Figure A3.2B) and even more so when matching at  $VF = 0.75$  (Figure A3.2C). As can be seen in this figure, and Table A3.1, the sources that match more particles are dust, biomass, and vehicles. It is only when the  $VF$  is dropped to 0.75 that the aged OC class increases, which is also noticeable in Figure A3.2C. The

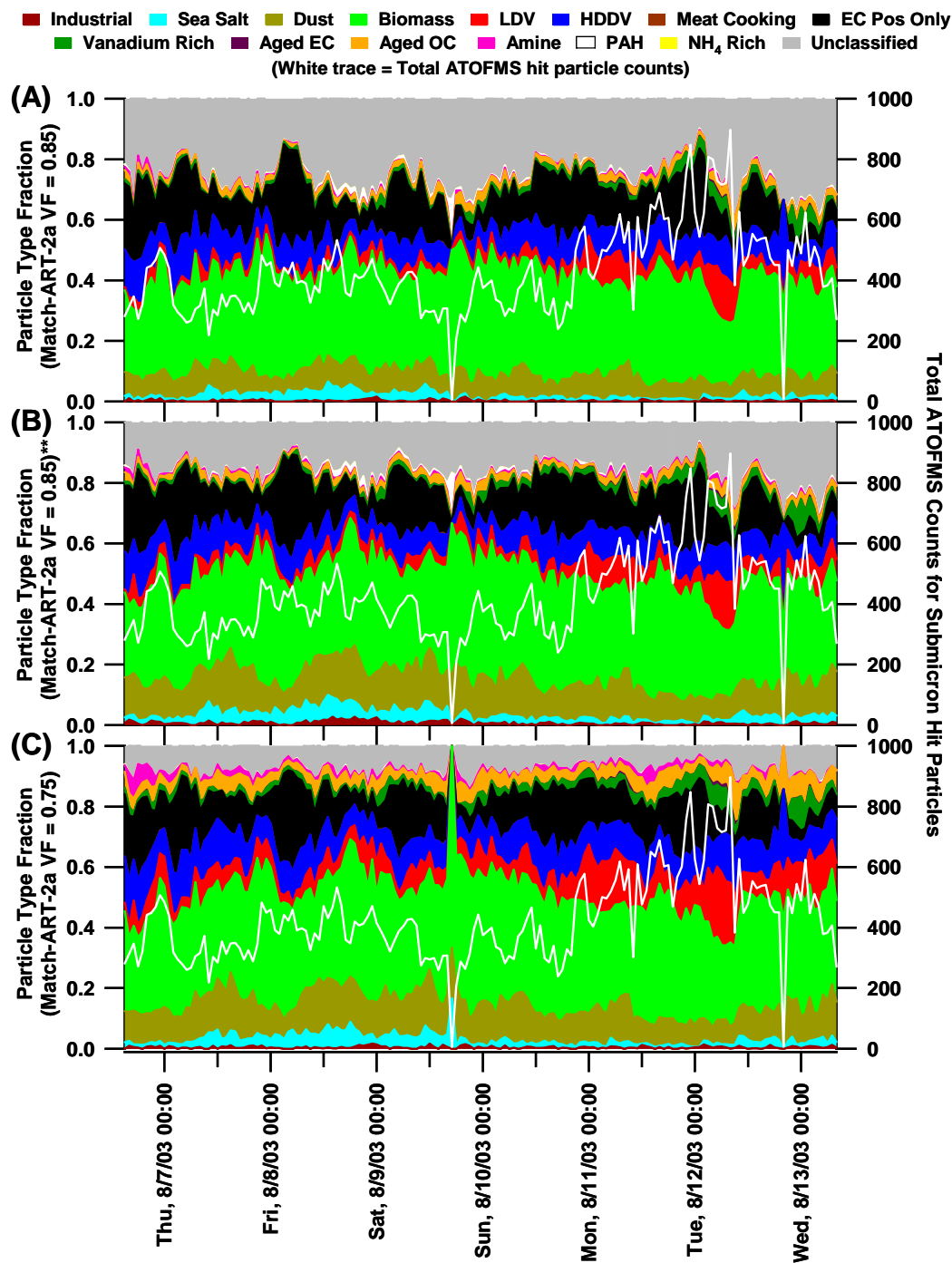


**Figure A3.2** Temporal series of the mass spectral source library matching results for Athens, Greece submicron ATOFMS detected particles at A) Match-ART-2a vigilance factor (VF) = 0.85; B) Match-ART-2a vigilance factor (VF) = 0.85 with the unclassified particles being rematched again based on their positive ions; C) Match-ART-2a vigilance factor (VF) = 0.75.

**Table A3.1** Percent of Athens, Greece particles matched to the mass spectral source library at different match-ART-2a Vigilance Factors (VF).

Particle Source	Matching VF = 0.85		Matching VF = 0.85**		Matching VF = 0.75	
	Sub %	Super %	Sub %	Super %	Sub %	Super %
Industrial	0.29	0.54	0.72	1.37	0.48	1.23
Sea Salt	1.78	10.45	2.77	19.30	2.66	19.36
Dust	7.18	21.09	11.95	38.64	11.62	41.81
Biomass	32.56	5.11	34.41	6.30	36.57	7.06
LDV	4.30	0.12	5.02	0.18	8.33	0.28
HDDV	8.90	1.42	8.90	1.42	10.37	4.27
Meat Cooking	0.01	0.00	0.01	0.00	0.01	0.00
EC (Positive only)	14.03	0.35	14.03	0.35	13.44	0.37
Vanadium Rich	1.82	0.15	2.04	0.26	2.60	0.29
Aged EC	0.07	0.00	0.07	0.00	0.09	0.00
Aged OC	2.34	0.36	2.34	0.36	4.73	1.02
Amine Containing	0.39	0.07	0.60	0.14	1.36	0.14
PAH Containing	0.62	0.07	0.62	0.07	0.06	0.04
NH4 Containing	0.00	0.00	0.00	0.00	0.00	0.00
Unclassified	25.72	60.26	16.51	31.60	7.69	24.13

Sub = Submicron particles (200-1000nm)

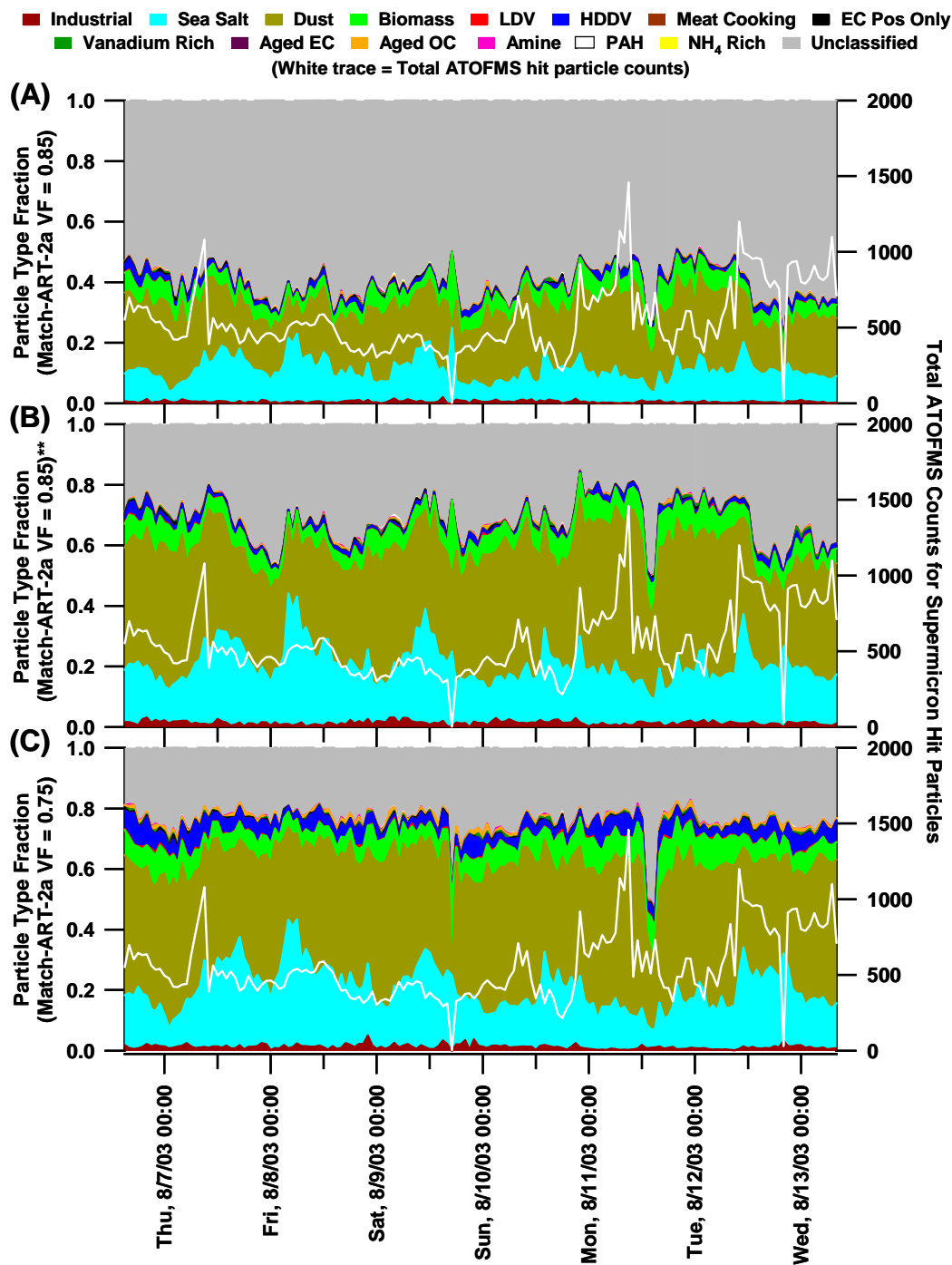
Super = Supermicron particles (1000-3000nm)

\*\* Matching at VF = 0.85 including rematching unclassified particles using positive ion only matching

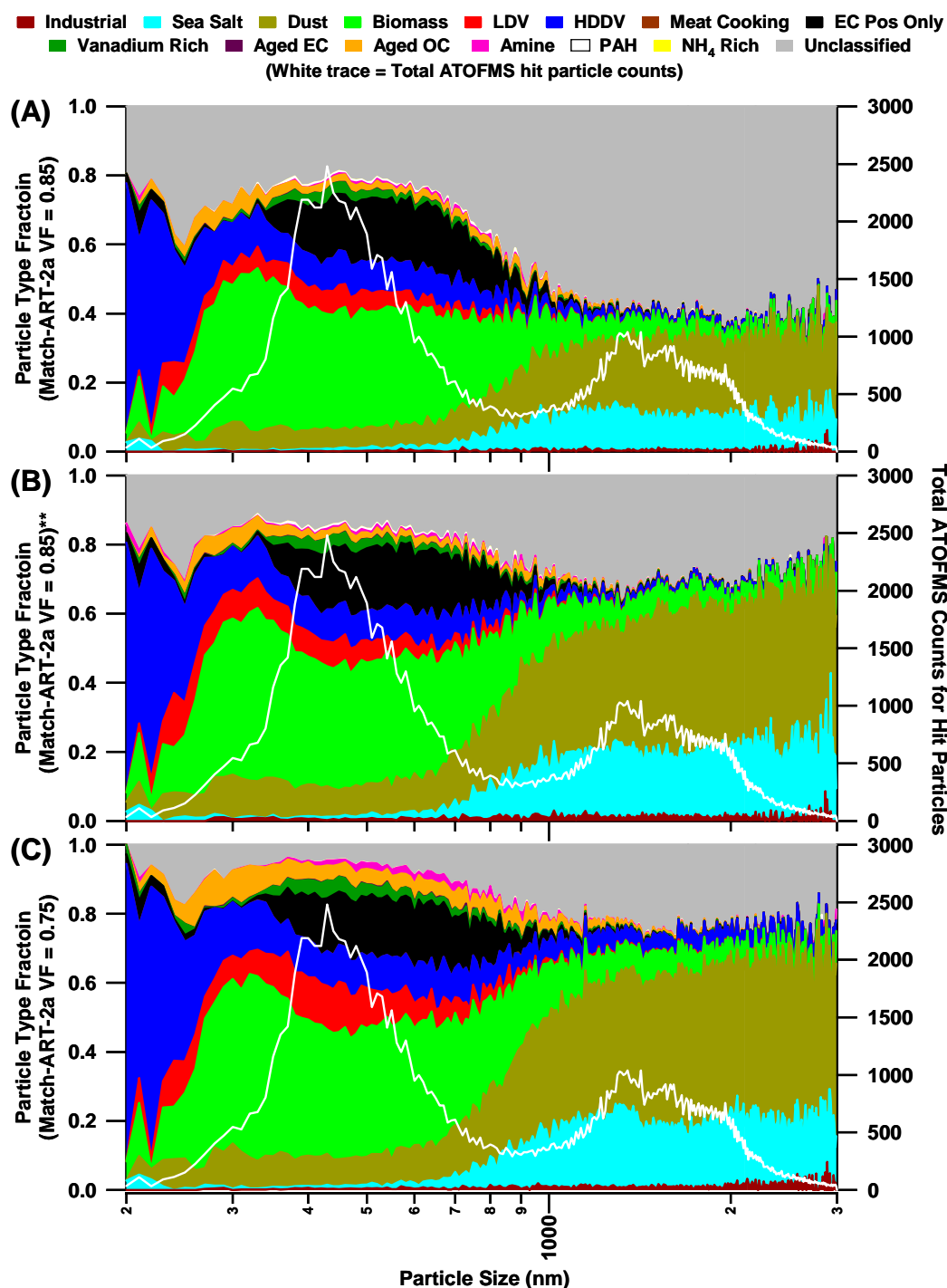
trends between the standard matching at  $VF = 0.85$  (Figure A3.2A) and the additional positive ion matching (Figure A3.2B) are very similar, which was expected since the positive ion matching was performed on the unclassified particles from the initial  $VF = 0.85$  results. The  $VF = 0.75$  matching results (Figure A3.2C) also have a similar trend, but match about 18% more particles than the  $VF = 0.85$  technique.

Figure A3.3 shows the Athens supermicron particle matching results for  $VF = 0.85$  (Figure A3.3A), positive ion matching (Figure A3.3B), and  $VF = 0.75$  (Figure A3.3C). As was discussed in Chapter 6, there were a large amount of supermicron particles left unclassified by matching at  $VF = 0.85$ . The reason for this is because the data collected for this study has many spectra with low signal to noise and a large fraction (~15% in the submicron and over 35% in the supermicron) of spectra with miscalibrated peaks [Dall'Osto and Harrison, 2006]. These noisy and miscalibrated spectra typically do not match to the source library spectra, especially at a high  $VF$  of 0.85, as their ion peaks simply do not match.

As can be seen in Figure A3.3 (and Table A3.1), 60% of the supermicron particles were not classified by the library matching at  $VF = 0.85$ . However, when using the positive ion matching at  $VF = 0.85$  on these unclassified particles, the amount of unclassified particles goes down to 32%, with most of the particles matching to dust and sea salt positive ion source signatures. The amount of unclassified goes down even more, to 24%, when matching at  $VF = 0.75$ , but there is an increase in the apportioned HDDV particles (from 1% at  $VF = 0.85$  to 4% at  $VF = 0.75$ ) which does not seem reasonable. When examining these HDDV particles at  $VF = 0.75$ , it was found that they most closely resemble biomass particles, but had a miscalibrated peak for potassium (which should be



**Figure A3.3** Temporal series of the mass spectral source library matching results for Athens, Greece supermicron ATOFMS detected particles at A) Match-ART-2a vigilance factor (VF) = 0.85; B) Match-ART-2a vigilance factor (VF) = 0.85 with the unclassified particles being rematched again based on their positive ions; C) Match-ART-2a vigilance factor (VF) = 0.75.



**Figure A3.4** Size resolved source apportionment of the ATOFMS detected ambient particles for Athens, Greece at A) Match-ART-2a vigilance factor (VF) = 0.85; B) Match-ART-2a vigilance factor (VF) = 0.85 with the unclassified particles being rematched again based on their positive ions; C) Match-ART-2a vigilance factor (VF) = 0.75.

at  $m/z$  39, but was at  $m/z$  40). This explains why they weren't matched with the positive ion matching, because it is the positive ions themselves for these particles that are miscalibrated. Performing the matching technique at  $VF = 0.85$  kept such particles from being classified improperly, but these particles just met the matching threshold at a  $VF$  of 0.75.

### A3.3 Matching Technique Variation Results for Mexico City

Since the amount of noisy and miscalibrated spectra for the Mexico City dataset was much less than that for Athens, the different matching techniques did not have as dramatic of effect on the results for Mexico City as they did for Athens. Figure A3.5 shows the Mexico City submicron particle matching results for  $VF = 0.85$  (Figure A3.5A), positive ion matching (Figure A3.5B), and  $VF = 0.75$  (Figure A3.5C). As can be seen in Figure A3.5 and Table A3.2, the difference in results for matching at  $VF = 0.85$  and using the positive ion matching is very minimal, and the amount of unclassified particles only goes down by 4%. However, when matching at  $VF = 0.75$ , the amount of unclassified particles goes down by 11%. This is an indication that there is more variation between the positive ions from the Mexico City submicron particles and the source signatures than with the negative ions. The positive ion spectra can be affected by the uptake of organic carbon (OC), which is described as being a dominating type in the submicron mode by Moffet, et al., 2007 [Moffet et al., 2007]. If the particles have a coating of OC on them, then there can be will be more OC peaks in the positive ion spectra, making these particles less similar to the source signatures. The unclassified submicron Mexico City particles can also be different than the source signatures just by

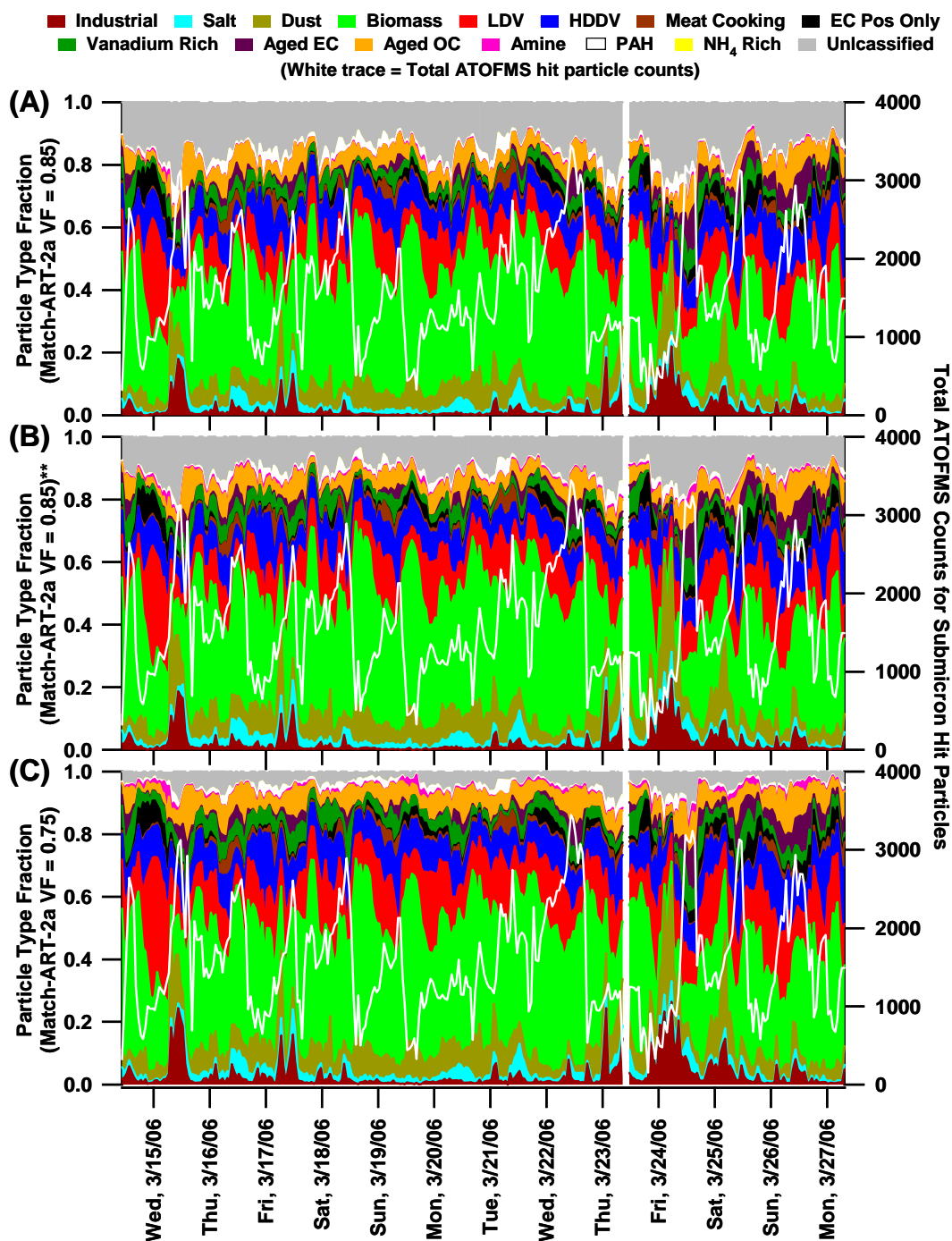


**Figure A3.5** Temporal series of the mass spectral source library matching results for Mexico City submicron ATOFMS detected particles at A) Match-ART-2a vigilance factor (VF) = 0.85; B) Match-ART-2a vigilance factor (VF) = 0.85 with the unclassified particles being rematched again based on their positive ions; C) Match-ART-2a vigilance factor (VF) = 0.75.



**Table A3.2** Percent of Mexico City particles matched to the mass spectral source library at different match-ART-2a Vigilance Factors (VF).

Particle Source	Matching VF = 0.85		Matching VF = 0.85**		Matching VF = 0.75	
	Sub %	Super %	Sub %	Super %	Sub %	Super %
Industrial	2.19	4.56	2.42	4.82	3.23	5.53
Salt	1.99	15.19	2.52	18.16	2.38	17.04
Dust	6.26	34.01	7.63	39.32	7.76	40.20
Biomass	34.07	10.99	35.59	12.02	36.48	12.68
LDV	11.19	0.96	11.71	1.03	14.79	1.65
HDDV	9.84	1.43	9.81	1.42	10.55	2.41
Meat Cooking	1.77	2.17	1.77	2.16	1.74	2.15
EC (Positive only)	2.19	0.21	2.19	0.21	2.26	0.22
Vanadium Rich	4.03	0.69	4.40	0.95	5.00	0.95
Aged EC	2.78	0.30	2.77	0.30	2.84	0.35
Aged OC	5.32	1.00	5.32	1.00	6.25	2.29
Amine Containing	0.37	0.17	0.74	0.42	0.85	0.28
PAH Containing	2.17	3.06	1.57	2.73	1.35	2.43
NH4 Containing	0.00	0.03	0.00	0.03	0.00	0.10
Unclassified	15.83	25.23	11.56	15.44	4.51	11.72

Sub = Submicron particles (180-1000nm)

Super = Supermicron particles (1000-3000nm)

\*\* Matching at VF = 0.85 including rematching unclassified particles using positive ion only matching

having ion intensities for the same particle types being different enough to not allow them to match at  $VF = 0.85$ . Random changes in ATOFMS spectra ion intensity have been shown to occur from using a non-homogeneous laser spot for the laser desorption/ionization process [Wenzel and Prather, 2004]. However, upon lowering the  $VF$  to 0.75, the similarity threshold is lowered and such particles (whether containing extra OC peaks, or different ion intensities) are able to match. As can be seen in Table A3.2, many of the sources increased in matching percentage (by 1 – 2 %) when using  $VF = 0.75$ , indicating that these particles (unmatched at  $VF = 0.85$ ) actually are of those types matched at  $VF = 0.75$ , but have different in ion intensities than the source signature seeds. Visual examination of these particle spectra also confirms this.

Figure A3.6 shows the Mexico City supermicron particle matching results for  $VF = 0.85$  (Figure A3.6A), positive ion matching (Figure A3.6B), and  $VF = 0.75$  (Figure A3.6C). Similar to what was found for the submicron results for Mexico City, there was very little change in the matching between the  $VF$  0.85 and positive ion matching results, as the amount of unclassified particles only went down by 5%. The main sources that did increase in matching were dust, salt, and biomass. When matching at  $VF = 0.75$ , the amount of unclassified particles goes down by 10% for the Mexico City supermicron particles. As can be seen in Figure A3.6C, and Table A3.2, the particles matched to dust seeds increased by the most (from 34% to 40%) while many of the other sources increased by 1 – 2 %. As with the Mexico City submicron particles, this is due to the unclassified particles at  $VF = 0.85$  differing from the source signatures by having ion intensities for the same particle types being different enough to not allow them to match at  $VF = 0.85$ , but will match at  $VF = 0.75$ .

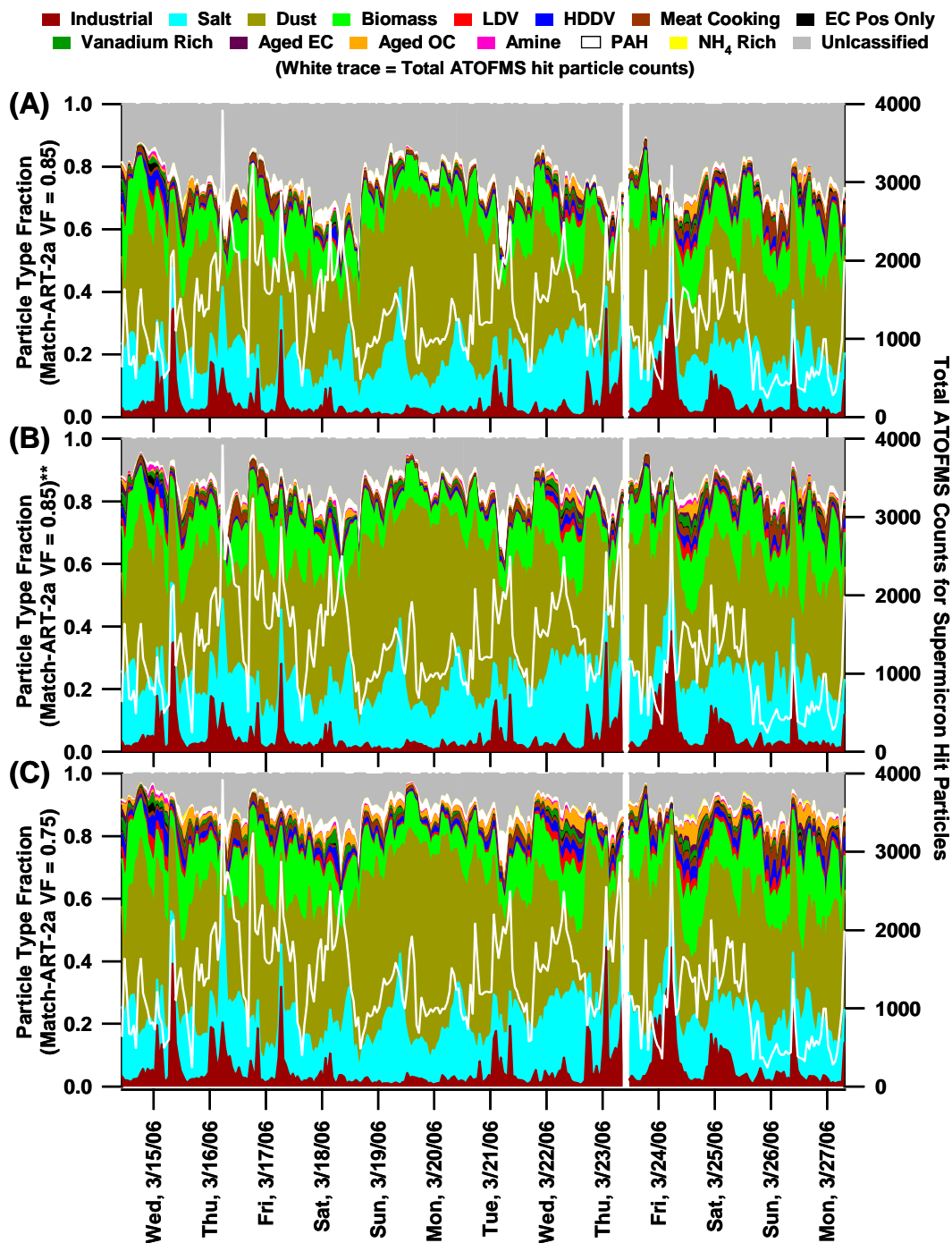


**Figure A3.6** Temporal series of the mass spectral source library matching results for Mexico City supermicron ATOFMS detected particles at A) Match-ART-2a vigilance factor (VF) = 0.85; B) Match-ART-2a vigilance factor (VF) = 0.85 with the unclassified particles being rematched again based on their positive ions; C) Match-ART-2a vigilance factor (VF) = 0.75.

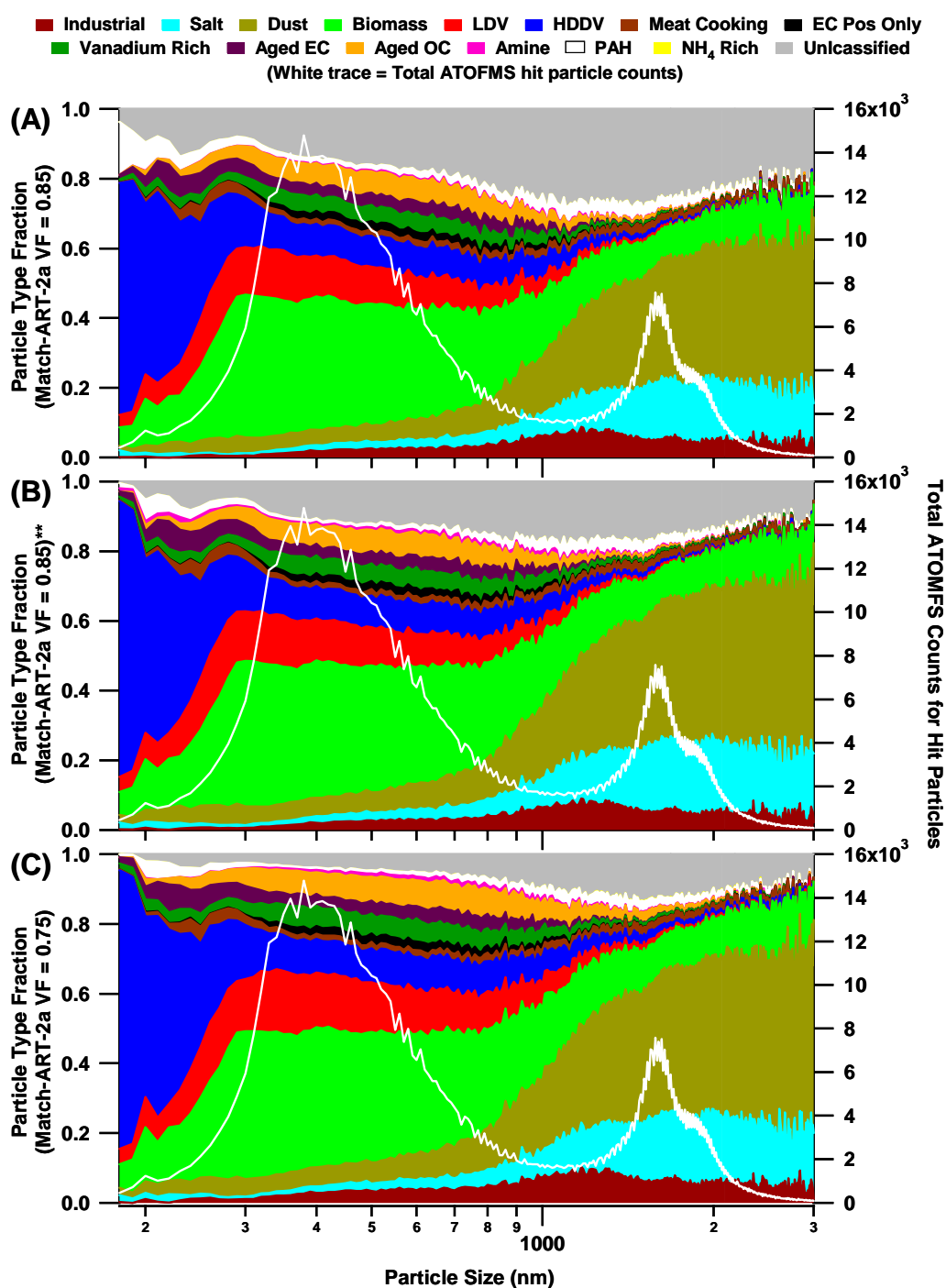


**Figure A3.7** Size resolved source apportionment of the ATOFMS detected ambient particles for Mexico City at A) Match-ART-2a vigilance factor (VF) = 0.85; B) Match-ART-2a vigilance factor (VF) = 0.85 with the unclassified particles being rematched again based on their positive ions; C) Match-ART-2a vigilance factor (VF) = 0.75.

### A3.4 References

- Dall'Osto, M., and R.M. Harrison, Chemical characterisation of single airborne particles in Athens (Greece) by ATOFMS, *Atmospheric Environment*, 40 (39), 7614-7631, 2006.
- Moffet, R.C., B. de Foy, L.T. Molina, M.J. Molina, and K.A. Prather, Characterization of ambient aerosols in northern Mexico City by single particle mass spectrometry, *Atmospheric Chemistry and Physics Discussion*, 7, 6413-6457, 2007.
- Toner, S.M., L.G. Shields, D.A. Sodeman, and K.A. Prather, Using mass spectral source signatures to apportion exhaust particles from gasoline and diesel powered vehicles in a freeway study using UF-ATOFMS., *Atmospheric Environment*, doi:10.1016/j.atmosenv.2007.08.005, 2007.
- Wenzel, R.J., and K.A. Prather, Improvements in ion signal reproducibility obtained using a homogeneous laser beam for on-line laser desorption/ionization of single particles, *Rapid Communications in Mass Spectrometry*, 18 (13), 1525-1533, 2004.

### A4 Source Matching Script

#### A4.1 Introduction

The following Matlab script (Source\_Matching\_Script\_06\_30\_07.m) was created for matching ATOFMS single particle data to the aerosol source signature library. The script and the signatures within it are current to June 30, 2007. The code is copied directly from the Matlab script editor. As a further note, all lines preceded with a percent sign (%) are commented text for informative use. The source signature seeds for each size range correspond to those described in Appendix 1.

#### A4.2 Source\_Matching\_Script\_06\_30\_07

```
% Source_Matching_Script_06_30_07

% need to load file: Source_Seeds_06_30_07

%-----
%-----
totalPID = Your_PID_here; % Enter your PID
%-----

SizeRange = 3; % Choose what size particles your PID contains (1 = UF [50-100nm]; 2 = Fine [100-140nm]; 3 = Fine
& Coarse [140nm and above]);

VF1 = 0.85; % Vigilance Factor for matching to the source seeds

GPR = 0; % Gas phase & noise spectra removal script -- Enter 1 to run, or 0 to skip (Gas Phase Removal)

POM2 = 0; % 1 to run, or 0 to skip; Run's the matching script again on Unmatched particles, but positive ions only
(Positive Only Match)

%-----
%-----
% ***** Don't need to change anything below *****
%-----
%-----
if GPR == 1;
disp(' ')
disp('Searching for Gas Phase & noise spectra before matching')
```

```

disp(' ')
GasP = totalPID;
GasP_dual = run_query(GasP,'Polarity == 1 and Polarity == 0');
GasP_pos = run_query(GasP, 'Polarity == 1');
GasP_negonly = setdiff(GasP, GasP_pos);
GasP_new = setdiff(GasP, GasP_negonly);
GasP_GP = run_query(GasP_new,'sum(Area{1 100}) < 1000'); % can change (raise) area if real spectra are getting
picked in search (originally 1000)
GasP_notGP = run_query(GasP_GP,'sum(Area{100 220}) > 500'); % can change (raise) area if real spectra are
getting picked in search (originally 500)
GasP_GP2 = setdiff(GasP_GP, GasP_notGP);
GasP_new2 = setdiff(GasP_new, GasP_GP2);
GasP_94 = run_query(GasP,'Area{-94} > 200');
GasP_new3 = setdiff(GasP_new2, GasP_94);
totalPID = GasP_new3;
GasP_removed = union(GasP_negonly, GasP_GP2, GasP_94);
clear GasP GasP_dual GasP_neg GasP_pos GasP_negonly GasP_new GasP_GP GasP_notGP GasP_GP2 GasP_new2
GasP_94 GasP_new3 GasP_removed
else
end
%-----

% General search for a marker that shows up for meat cooking (works well for freeway study)
MeatCooking = run_query(totalPID,'Area{178} > 50 or Area{-255} > 50');

%-----
% Matches MeatCooking search to Meat Cooking WM ***
%-----
if length (MeatCooking) < 5000
    [Matchedm] = match_art2a(MeatCooking, Source_Seeds_06_30_07{1}, 2, 0.85, 1); % 1 for exclusive, 0 for non
else
    NumInt = ceil((length (MeatCooking)) / 5000); % ceil: rounds up
    for I = 1:NumInt
        if I == 1
            InPID2 = MeatCooking(1:5000);
        elseif I == NumInt
            InPID2 = MeatCooking((1+5000*(I-1)):length(MeatCooking));
        else
            X = (I-1)*5000 + 1;
            Y = I*5000;
            InPID2 = MeatCooking(X:Y);
        end
        [outPartID] = match_art2a(InPID2, Source_Seeds_06_30_07{1}, 2, 0.85, 1); % 1 for exclusive, 0 for non
        if I == 1
            Matchedm = outPartID;
        else
            for J = 1:size(outPartID,2)
                Matchedm{J} = union(outPartID{J}, Matchedm{J});
            end
        end
    end
end
clear I J NumInt outPartID InPID2 ans X Y GPR
%-----
if length (MeatCooking) > 0
    MeatCooking = Matchedm{1}; % 16 Clusters from Mexico & Freeway ambient meat cooking particles
    for i = 2:16;
        MeatCooking = union(MeatCooking, Matchedm{i});
    end
    totalPID = setdiff(totalPID, MeatCooking);

```

```

else
end
clear i
%-----
%-----
%-----
%-----
%-----
%-----
%-----
%-----
if SizeRange == 1; % (1 = UF [50-100nm])
%-----
%-----
%-----
%-----
% Matches totalPIDs to WM ***
%-----
disp(' ')
disp('***** Matching your PID to the Source Seeds *****')
disp(' SizeRange == 1 (Ultrafine particles 50-100nm) ')
disp(' ')
if length(totalPID) < 5000
[Matched1] = match_art2a(totalPID, Source_Seeds_06_30_07{2}, 2, VF1, 1); % 1 for exclusive, 0 for non
else
NumInt = ceil((length(totalPID)) / 5000); % ceil: rounds up
for I = 1:NumInt
if I == 1
InPID2 = totalPID(1:5000);
elseif I == NumInt
InPID2 = totalPID((1+5000*(I-1)):length(totalPID));
else
X = (I-1)*5000 + 1;
Y = I*5000;
InPID2 = totalPID(X:Y);
end
[outPartID] = match_art2a(InPID2, Source_Seeds_06_30_07{2}, 2, VF1, 1); % 1 for exclusive, 0 for non
if I == 1
Matched1 = outPartID;
else
for J = 1:size(outPartID,2)
Matched1{J} = union(outPartID{J}, Matched1{J});
end
end
end
end
clear I J NumInt outPartID InPID2 ans X Y
%-----

hdv1 = Matched1{1}; % 1-30 are from hdv 2003 jke top 30 clusters from hot particles per truck
for i = 2:30;
hdv1 = union(hdv1, Matched1{i});
end

ldv1 = Matched1{31}; % from ldv 2002 jke top 30 clusters hot particles for (LEV, TWC, TWC-truck (no suzuki
samari or dodge caravan))
for i = 32:60;
ldv1 = union(ldv1, Matched1{i});
end

```



```

hdv2 = union(Matched1{35}, Matched1{41}, Matched1{42}, Matched1{45}, Matched1{47}, Matched1{58});
ldv1 = setdiff(ldv1, hdv2);
% -----
HDDV = union(hdv1, hdv2);
LDV = ldv1;
first_matched = union(HDDV, LDV);
Other = setdiff(totalPID, first_matched);

clear vehicle
clear i hdv1 hdv2 first_matched

% -----

SeaSalt1 = Matched1{61}; % 9 clusters
for i = 62:69;
    SeaSalt1 = union(SeaSalt1, Matched1{i});
end
biomass2a = union(Matched1{61}, Matched1{63}, Matched1{64}, Matched1{65}, Matched1{66});
SeaSalt1 = setdiff(SeaSalt1, biomass2a); % "corrected" SeaSalt1 5/15/06

Biomass1 = Matched1{70}; % 8 clusters
for i = 71:77;
    Biomass1 = union(Biomass1, Matched1{i});
end

SeaSalt2 = Matched1{78}; % 11 clusters
for i = 79:88;
    SeaSalt2 = union(SeaSalt2, Matched1{i});
end
dust3a = Matched1{84};
SeaSalt2 = setdiff(SeaSalt2, dust3a); % "corrected" SeaSalt2 5/15/06

Dust1 = Matched1{89}; % 3 clusters
for i = 90:91;
    Dust1 = union(Dust1, Matched1{i});
end

Dust2 = Matched1{92}; % 101 clusters from lab resuspended dust samples (derived from ReSoilAM)
for i = 93:192;
    Dust2 = union(Dust2, Matched1{i});
end

Biomass2 = union(Matched1{193}, Matched1{194});
SeaSalt3 = union(Matched1{195}, Matched1{196});

Dust3 = Matched1{197}; % 21 clusters from LVN at SOAR2
for i = 198:217;
    Dust3 = union(Dust3, Matched1{i});
end
seasalt3a = union(Matched1{210}, Matched1{211}, Matched1{212}, Matched1{213});
Dust3 = setdiff(Dust3, seasalt3a);

Amine2 = union(Matched1{218}, Matched1{219}, Matched1{220}, Matched1{221}); % 4 clusters from LVN at SOAR

NH4rich = union(Matched1{222}, Matched1{223}); % 2 clusters from LVN at SOAR

Vrich1 = union(Matched1{224}, Matched1{225}, Matched1{226}); % 3 clusters from LVN at SOAR

AgedEC = union(Matched1{227}, Matched1{228}); % 2 clusters from LVN at SOAR

```

```

AgedOC2 = union(Matched1{229}, Matched1{230}, Matched1{231}, Matched1{232}, Matched1{233}); % 5
clusters from LVN at SOAR

Biomass3 = union(Matched1{234}, Matched1{235}, Matched1{236}, Matched1{237}, Matched1{238}); % 5
clusters from LVN at SOAR

Vrich2 = Matched1{239}; % 14 clusters from LVN at SOAR2
for i = 240:252;
    Vrich2 = union(Vrich2, Matched1{i});
end

Vrich3 = Matched1{253}; % 10 clusters from ELD FWY added 5/22/06
for i = 254:262;
    Vrich3 = union(Vrich3, Matched1{i});
end

SeaSalt4 = Matched1{263}; % 24 clusters from ELD FWY added 5/22/06
for i = 264:286;
    SeaSalt4 = union(SeaSalt4, Matched1{i});
end

Dust4 = Matched1{287}; % 7 clusters from ELD FWY added 5/22/06
for i = 288:293;
    Dust4 = union(Dust4, Matched1{i});
end

Amine3 = Matched1{294}; % 13 clusters from ELD FWY added 5/22/06
for i = 295:306;
    Amine3 = union(Amine3, Matched1{i});
end

%-----

matched_other = union(Biomass1, SeaSalt1, SeaSalt2, Dust1, Dust2, Biomass2, SeaSalt3, Dust3, Amine2, NH4rich,
Vrich1, AgedEC, AgedOC2, Biomass3, Vrich2, Vrich3, SeaSalt4, Dust4, Amine3, biomass2a, dust3a, seasalt3a);
Other = setdiff(Other, matched_other);
Vrich = union(Vrich1, Vrich2, Vrich3);
Amine = union(Amine2, Amine3);
AgedOC = AgedOC2;
Biomass = union(Biomass1, Biomass2, Biomass3, biomass2a);
SeaSalt = union(SeaSalt1, SeaSalt2, SeaSalt3, SeaSalt4, seasalt3a);
Dust = union(Dust1, Dust2, Dust3, Dust4, dust3a);
clear matched_other
clear SeaSalt1 SeaSalt2 SeaSalt3 SeaSalt4 Biomass1 Biomass2 Biomass3 Dust1 Dust2 Dust3 Dust4 biomass1b
SeaSalt1a Dust1a Amine1 Amine2 Amine3 AgedOC1 AgedOC2 Vrich1 Vrich2 Vrich3 V_ship
clear i hdv1 ldv1 biomass1a biomass2a seasalt1a totalPID vanadium1a dust1a dust2a dust3a seasalt2a seasalt3a

% -----

Sources{1} = HDDV;
Sources{2} = LDV;
Sources{3} = Dust;
Sources{4} = SeaSalt;
Sources{5} = Biomass;
Sources{6} = AgedEC;
Sources{7} = AgedOC;
Sources{8} = Amine;
Sources{9} = NH4rich;

```

```

Sources{10} = Vrich;
Sources{11} = MeatCooking;
Sources{12} = Other;

clear HDDV LDV Dust SeaSalt Biomass AgedEC AgedOC Amine NH4rich Vrich EC_pos MeatCooking Other

% -----
% -----
% -----
% -----
if POM2 == 1;
totalPID = Sources{12};
%-----
% Matches Unmatched from first round to the same WM's, but positive only matching ***
%-----
disp(' ')
disp('Commencing with optional matching to the positive ion source seeds')
disp(' ')
if length(totalPID) < 5000
    [Matched2] = match_art2a(totalPID, Source_Seeds_06_30_07{3}, 1, VF1, 1); % 1 for exclusive, 0 for non
else
    NumInt = ceil((length(totalPID)) / 5000); % ceil: rounds up
    for I = 1:NumInt
        if I == 1
            InPID2 = totalPID(1:5000);
        elseif I == NumInt
            InPID2 = totalPID((1+5000*(I-1)):length(totalPID));
        else
            X = (I-1)*5000 + 1;
            Y = I*5000;
            InPID2 = totalPID(X:Y);
        end
        [outPartID] = match_art2a(InPID2, Source_Seeds_06_30_07{3}, 1, VF1, 1); % 1 for exclusive, 0 for non
        if I == 1
            Matched2 = outPartID;
        else
            for J = 1:size(outPartID,2)
                Matched2{J} = union(outPartID{J}, Matched2{J});
            end
        end
    end
end
clear I J NumInt outPartID InPID2 ans X Y
%-----

hdv1 = Matched2{1}; % 1-30 are from hdv 2003 jke top 30 clusters from hot particles per truck
for i = 2:30;
    hdv1 = union(hdv1, Matched2{i});
end

ldv1 = Matched2{31}; % from ldv 2002 jke top 30 clusters hot particles for (LEV, TWC, TWC-truck (no suzuki
samari or dodge caravan))
for i = 32:60;
    ldv1 = union(ldv1, Matched2{i});
end
hdv2 = union(Matched2{35}, Matched2{39}, Matched2{41}, Matched2{42}, Matched2{45}, Matched2{47},
Matched2{50}, Matched2{55}, Matched2{56}, Matched2{58}); % 49 has 36>12, but a huge Ca
[union(Matched2{35}, Matched2{39}, Matched2{41}, Matched2{42}, Matched2{45}, Matched2{47}, Matched2{49},
Matched2{50}, Matched2{55}, Matched2{56}, Matched2{58});]
ldv1 = setdiff(ldv1, hdv2);

```

```

% -----
HDDV = union(hdv1, hdv2);
LDV = ldv1;
first_matched = union(HDDV, LDV);
Other = setdiff(totalPID, first_matched);

clear vehicle
clear i hdv1 hdv2 first_matched

% -----

SeaSalt1 = Matched2{61}; % 9 clusters
for i = 62:69;
    SeaSalt1 = union(SeaSalt1, Matched2{i});
end
biomass2a = union(Matched2{61}, Matched2{63}, Matched2{64}, Matched2{65}, Matched2{66});
SeaSalt1 = setdiff(SeaSalt1, biomass2a); % "corrected" SeaSalt1 5/15/06

Biomass1 = Matched2{70}; % 8 clusters
for i = 71:77;
    Biomass1 = union(Biomass1, Matched2{i});
end

SeaSalt2 = Matched2{78}; % 11 clusters
for i = 79:88;
    SeaSalt2 = union(SeaSalt2, Matched2{i});
end
dust3a = Matched2{84};
SeaSalt2 = setdiff(SeaSalt2, dust3a); % "corrected" SeaSalt2 5/15/06

Dust1 = Matched2{89}; % 3 clusters
for i = 90:91;
    Dust1 = union(Dust1, Matched2{i});
end

Dust2 = Matched2{92}; % 101 clusters from lab resuspended dust samples (derived from ReSoilAM)
for i = 93:192;
    Dust2 = union(Dust2, Matched2{i});
end

Biomass2 = union(Matched2{193}, Matched2{194});
SeaSalt3 = union(Matched2{195}, Matched2{196});

Dust3 = Matched2{197}; % 21 clusters from LVN at SOAR2
for i = 198:217;
    Dust3 = union(Dust3, Matched2{i});
end
seasalt3a = union(Matched2{210}, Matched2{211}, Matched2{212}, Matched2{213});
Dust3 = setdiff(Dust3, seasalt3a);

Amine2 = union(Matched2{218}, Matched2{219}, Matched2{220}, Matched2{221}); % 4 clusters from LVN at SOAR

NH4rich = union(Matched2{222}, Matched2{223}); % 2 clusters from LVN at SOAR

Vrich1 = union(Matched2{224}, Matched2{225}, Matched2{226}); % 3 clusters from LVN at SOAR

AgedEC = union(Matched2{227}, Matched2{228}); % 2 clusters from LVN at SOAR

```

```

AgedOC2 = union(Matched2{229}, Matched2{230}, Matched2{231}, Matched2{232}, Matched2{233}); % 5
clusters from LVN at SOAR

Biomass3 = union(Matched2{234}, Matched2{235}, Matched2{236}, Matched2{237}, Matched2{238}); % 5
clusters from LVN at SOAR

Vrich2 = Matched2{239}; % 14 clusters from LVN at SOAR2
for i = 240:252;
    Vrich2 = union(Vrich2, Matched2{i});
end

Vrich3 = Matched2{253}; % 10 clusters from ELD FWY added 5/22/06
for i = 254:262;
    Vrich3 = union(Vrich3, Matched2{i});
end

SeaSalt4 = Matched2{263}; % 24 clusters from ELD FWY added 5/22/06
for i = 264:286;
    SeaSalt4 = union(SeaSalt4, Matched2{i});
end

Dust4 = Matched2{287}; % 7 clusters from ELD FWY added 5/22/06
for i = 288:293;
    Dust4 = union(Dust4, Matched2{i});
end

Amine3 = Matched2{294}; % 13 clusters from ELD FWY added 5/22/06
for i = 295:306;
    Amine3 = union(Amine3, Matched2{i});
end

%-----

matched_other = union(Biomass1, SeaSalt1, SeaSalt2, Dust1, Dust2, Biomass2, SeaSalt3, Dust3, Amine2, NH4rich,
Vrich1, AgedEC, AgedOC2, Biomass3, Vrich2, Vrich3, SeaSalt4, Dust4, Amine3, biomass2a, dust3a, seasalt3a);
Other = setdiff(Other, matched_other);
Vrich = union(Vrich1, Vrich2, Vrich3);
Amine = union(Amine2, Amine3);
AgedOC = AgedOC2;
Biomass = union(Biomass1, Biomass2, Biomass3, biomass2a);
SeaSalt = union(SeaSalt1, SeaSalt2, SeaSalt3, SeaSalt4, seasalt3a);
Dust = union(Dust1, Dust2, Dust3, Dust4, dust3a);
clear matched_other
clear SeaSalt1 SeaSalt2 SeaSalt3 SeaSalt4 Biomass1 Biomass2 Biomass3 Dust1 Dust2 Dust3 Dust4 biomass1b
SeaSalt1a Dust1a Amine1 Amine2 Amine3 AgedOC1 AgedOC2 Vrich1 Vrich2 Vrich3 V_ship
clear i hdv1 ldv1 biomass1a biomass2a seasalt1a totalPID vanadium1a dust1a dust2a dust3a seasalt2a seasalt3a

% -----

Sources2{1} = HDDV;
Sources2{2} = LDV;
Sources2{3} = Dust;
Sources2{4} = SeaSalt;
Sources2{5} = Biomass;
Sources2{6} = AgedEC;
Sources2{7} = AgedOC;
Sources2{8} = Amine;
Sources2{9} = NH4rich;
Sources2{10} = Vrich;

```

```
Sources2{11} = Sources{11};
Sources2{12} = Other;
```

```
clear HDDV LDV Dust SeaSalt Biomass AgedEC AgedOC Amine NH4rich Vrich EC_pos MeatCooking Other
% -----
Sources{1} = union(Sources{1}, Sources2{1});
Sources{2} = union(Sources{2}, Sources2{2});
Sources{3} = union(Sources{3}, Sources2{3});
Sources{4} = union(Sources{4}, Sources2{4});
Sources{5} = union(Sources{5}, Sources2{5});
Sources{6} = union(Sources{6}, Sources2{6});
Sources{7} = union(Sources{7}, Sources2{7});
Sources{8} = union(Sources{8}, Sources2{8});
Sources{9} = union(Sources{9}, Sources2{9});
Sources{10} = union(Sources{10}, Sources2{10});
Sources{11} = union(Sources{11}, Sources2{11});
Sources{12} = Sources2{12};

clear Sources2
else
end
% -----
% -----
% -----
% -----
disp(' ')
disp('Search for PAH type particles that did not match to source seeds')
disp(' ')
other = Sources{12};
PAH = run_query(other, '(sum(Area{212 250}) > 1000) or (sum(Area{186 202}) > 800)');
other2 = setdiff(other, PAH);
Sources{12} = PAH;
Sources{13} = other2;
clear other PAH other2

%-----
% To clean up some issues in the "other" category
%-----
disp(' ')
disp('Searching for issue/noise and gas phase spectra in the unmatched particles')
disp(' ')
other = Sources{13};
other_dual = run_query(other, 'Polarity == 1 and Polarity == 0');
other_pos = run_query(other, 'Polarity == 1');
other_neg = run_query(other, 'Polarity == 0');
other_negonly = setdiff(other, other_pos);
other_new = setdiff(other, other_negonly);
other_GP = run_query(other_new, 'sum(Area{1 100}) < 1500');
other_notGP = run_query(other_GP, 'sum(Area{100 220}) > 1000');
other_GP2 = setdiff(other_GP, other_notGP);
other_new2 = setdiff(other_new, other_GP2);
other_94 = run_query(other, 'Area{-94} > 200');
other_new3 = setdiff(other_new2, other_94);
Sources{13} = other_new3;
other_removed = union(other_negonly, other_GP2, other_94);
clear other other_dual other_neg other_pos other_negonly other_new other_GP other_notGP other_GP2 other_new2
other_94 other_new3
%-----

Sources_Matched_UF = Sources;
```

```

clear Sources VF1 POM2
clear other_removed

disp(' ')
disp('***** Finished Matching Data *****')

disp(' ')
disp('~~~~~')
disp('*** A matrix called "Sources_Matched_UF" has been created in your workspace ***')
disp('The order that the Sources appear in the matrix are:')
disp(' ')
disp('1)HDDV 2)LDV 3)Dust 4)SeaSalt 5)Biomass 6)AgedEC 7)AgedOC 8)Amine')
disp('9)NH4rich 10)Vrich 11)MeatCooking 12)PAH 13)Other')
cellsize(Sources_Matched_UF)
disp('~~~~~')

else
end

%-----
%-----
%-----
%-----
%-----
%-----
%-----
%-----
if SizeRange == 2; % (2 = Fine [100-140nm])
%-----
%-----
%-----
%-----
% Matches totalPIDs to WM ***
%-----
disp(' ')
disp('***** Matching your PID to the Source Seeds *****')
disp(' SizeRange == 2 (Fine particles 100-140nm) ')
disp(' ')
if length(totalPID) < 5000
    [Matched1] = match_art2a(totalPID, Source_Seeds_06_30_07{4}, 2, VF1, 1); % 1 for exclusive, 0 for non
else
    NumInt = ceil((length(totalPID)) / 5000); % ceil: rounds up
    for I = 1:NumInt
        if I == 1
            InPID2 = totalPID(1:5000);
        elseif I == NumInt
            InPID2 = totalPID((1+5000*(I-1)):length(totalPID));
        else
            X = (I-1)*5000 + 1;
            Y = I*5000;
            InPID2 = totalPID(X:Y);
        end
        [outPartID] = match_art2a(InPID2, Source_Seeds_06_30_07{4}, 2, VF1, 1); % 1 for exclusive, 0 for non
        if I == 1
            Matched1 = outPartID;
        else

```

```

        for J = 1:size(outPartID,2)
            Matched1{J} = union(outPartID{J}, Matched1{J});
        end
    end
end
clear I J NumInt outPartID InPID2 ans X Y
%-----

hdv1 = Matched1{1}; % 1-30 are from hdv 2003 jke top 30 clusters from hot particles per truck
for i = 2:60; % 31-60 are from hdv 2001 top 30 particle types
    hdv1 = union(hdv1, Matched1{i});
end
hdv2 = union(Matched1{337}, Matched1{338}, Matched1{339}, Matched1{344}, Matched1{345}, Matched1{346},
Matched1{347}, Matched1{348}, Matched1{349}, Matched1{350}); % 3 clusters from LVN fwy ambient; 7 clusters
from JKE 100-150nm fwy ambient

ldv1 = Matched1{61}; % from ldv 2002 jke top 30 clusters hot particles for (LEV, TWC, TWC-truck (no suzuki
samari or dodge caravan))
for i = 62:90;
    ldv1 = union(ldv1, Matched1{i});
end
hdv3 = Matched1{68};
ldv1 = setdiff(ldv1, hdv3);

% -----
HDDV = union(hdv1, hdv2, hdv3);
LDV = ldv1;
first_matched = union(HDDV, LDV);
Other = setdiff(totalPID, first_matched);

clear vehicle
clear i hdv1 hdv2 hdv3 first_matched

% -----

SeaSalt1 = Matched1{91}; % 9 clusters
for i = 92:99;
    SeaSalt1 = union(SeaSalt1, Matched1{i});
end
biomass2a = union(Matched1{91}, Matched1{93}, Matched1{94}, Matched1{95}, Matched1{96});
SeaSalt1 = setdiff(SeaSalt1, biomass2a); % "corrected" SeaSalt1 5/15/06

Biomass1 = Matched1{100}; % 8 clusters
for i = 101:107;
    Biomass1 = union(Biomass1, Matched1{i});
end

SeaSalt2 = Matched1{108}; % 11 clusters
for i = 109:118;
    SeaSalt2 = union(SeaSalt2, Matched1{i});
end
dust3a = Matched1{114};
SeaSalt2 = setdiff(SeaSalt2, dust3a); % "corrected" SeaSalt2 5/15/06

Dust1 = Matched1{119}; % 3 clusters
for i = 120:121;
    Dust1 = union(Dust1, Matched1{i});
end

```



```

Dust2 = Matched1{122}; % 101 clusters from lab resuspended dust samples (derrived from ReSoilAM)
for i = 123:222;
    Dust2 = union(Dust2, Matched1{i});
end

Biomass2 = union(Matched1{223}, Matched1{224});
SeaSalt3 = union(Matched1{225}, Matched1{226});

Dust3 = Matched1{227}; % 21 clusters from LVN at SOAR2
for i = 228:247;
    Dust3 = union(Dust3, Matched1{i});
end
seasalt3a = union(Matched1{240}, Matched1{241}, Matched1{242}, Matched1{243});
Dust3 = setdiff(Dust3, seasalt3a);

Amine2 = union(Matched1{248}, Matched1{249}, Matched1{250}, Matched1{251}); % 4 clusters from LVN at SOAR

NH4rich = union(Matched1{252}, Matched1{253}); % 2 clusters from LVN at SOAR

Vrich1 = union(Matched1{254}, Matched1{255}, Matched1{256}); % 3 clusters from LVN at SOAR

AgedEC = union(Matched1{257}, Matched1{258}); % 2 clusters from LVN at SOAR

AgedOC2 = union(Matched1{259}, Matched1{260}, Matched1{261}, Matched1{262}, Matched1{263},
    Matched1{351}, Matched1{352}, Matched1{353}); % 5 clusters from LVN at SOAR one from Freeway (from LVN J27), one from freeway JKE unmatched 140nmup, one more from Freeway (from LVN J27)

Biomass3 = union(Matched1{264}, Matched1{265}, Matched1{266}, Matched1{267}, Matched1{268}); % 5 clusters from LVN at SOAR

Vrich2 = Matched1{269}; % 14 clusters from LVN at SOAR2
for i = 270:282;
    Vrich2 = union(Vrich2, Matched1{i});
end

Vrich3 = Matched1{283}; % 10 clusters from ELD FWY added 5/22/06
for i = 284:292;
    Vrich3 = union(Vrich3, Matched1{i});
end

SeaSalt4 = Matched1{293}; % 24 clusters from ELD FWY added 5/22/06
for i = 294:316;
    SeaSalt4 = union(SeaSalt4, Matched1{i});
end

Dust4 = Matched1{317}; % 7 clusters from ELD FWY added 5/22/06
for i = 318:323;
    Dust4 = union(Dust4, Matched1{i});
end

Amine3 = Matched1{324}; % 13 clusters from ELD FWY added 5/22/06
for i = 325:336;
    Amine3 = union(Amine3, Matched1{i});
end

SeaSalt5 = union(Matched1{340}, Matched1{341}, Matched1{342}, Matched1{343});

%-----

```

```

matched_other = union(Biomass1, SeaSalt1, SeaSalt2, Dust1, Dust2, Biomass2, SeaSalt3, Dust3, Amine2, NH4rich,
Vrich1, AgedEC, AgedOC2, Biomass3, Vrich2, Vrich3, SeaSalt4, Dust4, Amine3, biomass2a, dust3a, seasalt3a,
SeaSalt5);
Other = setdiff(Other, matched_other);
Vrich = union(Vrich1, Vrich2, Vrich3);
Amine = union(Amine2, Amine3);
AgedOC = AgedOC2;
Biomass = union(Biomass1, Biomass2, Biomass3, biomass2a);
SeaSalt = union(SeaSalt1, SeaSalt2, SeaSalt3, SeaSalt4, seasalt3a, SeaSalt5);
Dust = union(Dust1, Dust2, Dust3, Dust4, dust3a);
clear matched_other
clear SeaSalt1 SeaSalt2 SeaSalt3 SeaSalt4 Biomass1 Biomass2 Biomass3 Dust1 Dust2 Dust3 Dust4 biomass1b
SeaSalt1a Dust1a Amine1 Amine2 Amine3 AgedOC1 AgedOC2 Vrich1 Vrich2 Vrich3 V_ship
clear i hdv1 ldv1 biomass1a biomass2a seasalt1a totalPID vanadium1a dust1a dust2a dust3a seasalt2a seasalt3a
SeaSalt5

% -----

Sources{1} = HDDV;
Sources{2} = LDV;
Sources{3} = Dust;
Sources{4} = SeaSalt;
Sources{5} = Biomass;
Sources{6} = AgedEC;
Sources{7} = AgedOC;
Sources{8} = Amine;
Sources{9} = NH4rich;
Sources{10} = Vrich;
Sources{11} = MeatCooking;
Sources{12} = Other;

clear HDDV LDV Dust SeaSalt Biomass AgedEC AgedOC Amine NH4rich Vrich EC_pos MeatCooking Other

% -----
% -----
% -----
% -----

if POM2 == 1;
totalPID = Sources{12};
%-----
% Matches Unmatched from first round to the same WM's, but positive only matching ***
%-----

disp(' ')
disp('Commencing with optional matching to the positive ion source seeds')
if length(totalPID) < 5000
[Matched2] = match_art2a(totalPID, Source_Seeds_06_30_07{5}, 1, VF1, 1); % 1 for exclusive, 0 for non
else
NumInt = ceil((length(totalPID)) / 5000); % ceil: rounds up
for I = 1:NumInt
if I == 1
InPID2 = totalPID(1:5000);
elseif I == NumInt
InPID2 = totalPID((1+5000*(I-1)):length(totalPID));
else
X = (I-1)*5000 + 1;
Y = I*5000;
InPID2 = totalPID(X:Y);
end
[outPartID] = match_art2a(InPID2, Source_Seeds_06_30_07{5}, 1, VF1, 1); % 1 for exclusive, 0 for non
if I == 1

```

```

        Matched2 = outPartID;
    else
        for J = 1:size(outPartID,2)
            Matched2{J} = union(outPartID{J}, Matched2{J});
        end
    end
end
end
clear I J NumInt outPartID InPID2 ans X Y
%-----

hdv1 = Matched2{1};    % 1-30 are from hdv 2003 jke top 30 clusters from hot particles per truck
for i = 2:60;          % 31-60 are from hdv 2001 top 30 particle types
    hdv1 = union(hdv1, Matched2{i});
end

ldv1 = Matched2{61};   % from ldv 2002 jke top 30 clusters hot particles for (LEV, TWC, TWC-truck (no suzuki
                        % samari or dodge caravan))
for i = 62:90;
    ldv1 = union(ldv1, Matched2{i});
end

% -----
HDDV = hdv1;
LDV = ldv1;
first_matched = union(HDDV, LDV);
Other = setdiff(totalPID, first_matched);

clear vehicle
clear i hdv1 first_matched

% -----

SeaSalt1 = Matched2{91}; % 9 clusters
for i = 92:99;
    SeaSalt1 = union(SeaSalt1, Matched2{i});
end
biomass2a = union(Matched2{91}, Matched2{93}, Matched2{94}, Matched2{95}, Matched2{96});
SeaSalt1 = setdiff(SeaSalt1, biomass2a); % "corrected" SeaSalt1 5/15/06

Biomass1 = Matched2{100}; % 8 clusters
for i = 101:107;
    Biomass1 = union(Biomass1, Matched2{i});
end

SeaSalt2 = Matched2{108}; % 11 clusters
for i = 109:118;
    SeaSalt2 = union(SeaSalt2, Matched2{i});
end
dust3a = Matched2{114};
SeaSalt2 = setdiff(SeaSalt2, dust3a); % "corrected" SeaSalt2 5/15/06

Dust1 = Matched2{119}; % 3 clusters
for i = 120:121;
    Dust1 = union(Dust1, Matched2{i});
end

Dust2 = Matched2{122}; % 101 clusters from lab resuspended dust samples (derrived from ReSoilAM)
for i = 123:222;
    Dust2 = union(Dust2, Matched2{i});
end

```

```

end

Biomass2 = union(Matched2{223}, Matched2{224});
SeaSalt3 = union(Matched2{225}, Matched2{226});

Dust3 = Matched2{227}; % 21 clusters from LVN at SOAR2
for i = 228:247;
    Dust3 = union(Dust3, Matched2{i});
end
seasalt3a = union(Matched2{240}, Matched2{241}, Matched2{242}, Matched2{243});
Dust3 = setdiff(Dust3, seasalt3a);

Amine2 = union(Matched2{248}, Matched2{249}, Matched2{250}, Matched2{251}); % 4 clusters from LVN at SOAR

NH4rich = union(Matched2{252}, Matched2{253}); % 2 clusters from LVN at SOAR

Vrich1 = union(Matched2{254}, Matched2{255}, Matched2{256}); % 3 clusters from LVN at SOAR

AgedEC = union(Matched2{257}, Matched2{258}); % 2 clusters from LVN at SOAR

AgedOC2 = union(Matched2{259}, Matched2{260}, Matched2{261}, Matched2{262}, Matched2{263}); % 5 clusters from LVN at SOAR

Biomass3 = union(Matched2{264}, Matched2{265}, Matched2{266}, Matched2{267}, Matched2{268}); % 5 clusters from LVN at SOAR

Vrich2 = Matched2{269}; % 14 clusters from LVN at SOAR2
for i = 270:282;
    Vrich2 = union(Vrich2, Matched2{i});
end

Vrich3 = Matched2{283}; % 10 clusters from ELD FWY added 5/22/06
for i = 284:292;
    Vrich3 = union(Vrich3, Matched2{i});
end

SeaSalt4 = Matched2{293}; % 24 clusters from ELD FWY added 5/22/06
for i = 294:316;
    SeaSalt4 = union(SeaSalt4, Matched2{i});
end

Dust4 = Matched2{317}; % 7 clusters from ELD FWY added 5/22/06
for i = 318:323;
    Dust4 = union(Dust4, Matched2{i});
end

Amine3 = Matched2{324}; % 13 clusters from ELD FWY added 5/22/06
for i = 325:336;
    Amine3 = union(Amine3, Matched2{i});
end

V_ship = Matched2{337}; % 28 clusters from FWY Vanadium background, added 4/15/07
for i = 338:364;
    V_ship = union(V_ship, Matched2{i});
end

%-----

```

```

matched_other = union(Biomass1, SeaSalt1, SeaSalt2, Dust1, Dust2, Biomass2, SeaSalt3, Dust3, Amine2, NH4rich,
Vrich1, AgedEC, AgedOC2, Biomass3, Vrich2, Vrich3, SeaSalt4, Dust4, Amine3, biomass2a, dust3a, seasalt3a,
V_ship);
Other = setdiff(Other, matched_other);
Vrich = union(Vrich1, Vrich2, Vrich3, V_ship);
Amine = union(Amine2, Amine3);
AgedOC = AgedOC2;
Biomass = union(Biomass1, Biomass2, Biomass3, biomass2a);
SeaSalt = union(SeaSalt1, SeaSalt2, SeaSalt3, SeaSalt4, seasalt3a);
Dust = union(Dust1, Dust2, Dust3, Dust4, dust3a);
clear matched_other
clear SeaSalt1 SeaSalt2 SeaSalt3 SeaSalt4 Biomass1 Biomass2 Biomass3 Dust1 Dust2 Dust3 Dust4 biomass1b
SeaSalt1a Dust1a Amine1 Amine2 Amine3 AgedOC1 AgedOC2 Vrich1 Vrich2 Vrich3 V_ship
clear i hdv1 ldv1 biomass1a biomass2a seasalt1a totalPID vanadium1a dust1a dust2a dust3a seasalt2a seasalt3a

% -----

Sources2{1} = HDDV;
Sources2{2} = LDV;
Sources2{3} = Dust;
Sources2{4} = SeaSalt;
Sources2{5} = Biomass;
Sources2{6} = AgedEC;
Sources2{7} = AgedOC;
Sources2{8} = Amine;
Sources2{9} = NH4rich;
Sources2{10} = Vrich;
Sources2{11} = Sources{11};
Sources2{12} = Other;

clear HDDV LDV Dust SeaSalt Biomass AgedEC AgedOC Amine NH4rich Vrich EC_pos MeatCooking Other
% -----
Sources{1} = union(Sources{1}, Sources2{1});
Sources{2} = union(Sources{2}, Sources2{2});
Sources{3} = union(Sources{3}, Sources2{3});
Sources{4} = union(Sources{4}, Sources2{4});
Sources{5} = union(Sources{5}, Sources2{5});
Sources{6} = union(Sources{6}, Sources2{6});
Sources{7} = union(Sources{7}, Sources2{7});
Sources{8} = union(Sources{8}, Sources2{8});
Sources{9} = union(Sources{9}, Sources2{9});
Sources{10} = union(Sources{10}, Sources2{10});
Sources{11} = union(Sources{11}, Sources2{11});
Sources{12} = Sources2{12};

clear Sources2
else
end
% -----
% -----
% -----
% -----

%-----
% Matches Unmatched from first round to ambient seeds ***
%-----
totalPID = Sources{12};

if length(totalPID) < 5000
    [Matched3] = match_art2a(totalPID, Source_Seeds_06_30_07{6}, 2, VF1, 1); % 1 for exclusive, 0 for non

```

```

else
    NumInt = ceil((length (totalPID)) / 5000); % ceil: rounds up
    for I = 1:NumInt
        if I == 1
            InPID2 = totalPID(1:5000);
        elseif I == NumInt
            InPID2 = totalPID((1+5000*(I-1)):length(totalPID));
        else
            X = (I-1)*5000 + 1;
            Y = I*5000;
            InPID2 = totalPID(X:Y);
        end
        [outPartID] = match_art2a(InPID2, Source_Seeds_06_30_07{6}, 2, VF1, 1); % 1 for exclusive, 0 for non
        if I == 1
            Matched3 = outPartID;
        else
            for J = 1:size(outPartID,2)
                Matched3{J} = union(outPartID{J}, Matched3{J});
            end
        end
    end
end
clear I J NumInt outPartID InPID2 ans X Y
%-----

HDDV = union(Matched3{1}, Matched3{2}, Matched3{3}, Matched3{4}, Matched3{5}); % from JKE freeway
ambient (RG art2a on unmatched particles)
LDV = union(Matched3{6}, Matched3{7}); % from JKE freeway ambient (RG art2a on unmatched particles)
EC_pos = union(Matched3{8}, Matched3{9}); % from JKE freeway ambient (RG art2a on unmatched particles)

matched_other = union(HDDV, LDV, EC_pos);
Other = setdiff(totalPID, matched_other);

Sources3{1} = HDDV;
Sources3{2} = LDV;
Sources3{3} = Sources{3};
Sources3{4} = Sources{4};
Sources3{5} = Sources{5};
Sources3{6} = Sources{6};
Sources3{7} = Sources{7};
Sources3{8} = Sources{8};
Sources3{9} = Sources{9};
Sources3{10} = Sources{10};
Sources3{11} = EC_pos;
Sources3{12} = Sources{11}; % Meat Cooking
Sources3{13} = Other;

clear HDDV LDV EC_pos Other totalPID matched_other
% -----
Sources{1} = union(Sources{1}, Sources3{1});
Sources{2} = union(Sources{2}, Sources3{2});
Sources{3} = Sources3{3};
Sources{4} = Sources3{4};
Sources{5} = Sources3{5};
Sources{6} = Sources3{6};
Sources{7} = Sources3{7};
Sources{8} = Sources3{8};
Sources{9} = Sources3{9};
Sources{10} = Sources3{10};
Sources{11} = Sources3{11};

```

```

Sources{12} = Sources3{12};
Sources{13} = Sources3{13};

clear Sources3

% -----
% -----
% -----
% -----
disp(' ')
disp('Search for PAH type particles that did not match to source seeds')
disp(' ')
other = Sources{13};
PAH = run_query(other,'(sum(Area{212 250}) > 1000) or (sum(Area{186 202}) > 800)');
other2 = setdiff(other, PAH);
Sources{13} = PAH;
Sources{14} = other2;
clear other PAH other2

%-----
% To clean up some issues in the "other" category
%-----
disp(' ')
disp('Searching for issue/noise and gas phase spectra in the unmatched particles')
disp(' ')
other = Sources{14};
other_dual = run_query(other,'Polarity == 1 and Polarity == 0');
other_pos = run_query(other, 'Polarity == 1');
other_neg = run_query(other,'Polarity == 0');
other_negonly = setdiff(other, other_pos);
other_new = setdiff(other, other_negonly);
other_GP = run_query(other_new,'sum(Area{1 100}) < 1500');
other_notGP = run_query(other_GP,'sum(Area{100 220}) > 1000');
other_GP2 = setdiff(other_GP, other_notGP);
other_new2 = setdiff(other_new, other_GP2);
other_94 = run_query(other,'Area{-94} > 200');
other_new3 = setdiff(other_new2, other_94);
Sources{14} = other_new3;
other_removed = union(other_negonly, other_GP2, other_94);
clear other other_dual other_neg other_pos other_negonly other_new other_GP other_notGP other_GP2 other_new2
other_94 other_new3
%-----

Sources_Matched_100to140nm = Sources;
clear Sources VF1 POM2
clear other_removed

disp(' ')
disp('***** How long it took to match your data *****')
toc

disp(' ')
disp('~~~~~')
disp('*** A matrix called "Sources_Matched_100to140nm" has been created in your workspace ***')
disp('The order that the Sources appear in the matrix are:')
disp(' ')
disp('1)HDDV 2)LDV 3)Dust 4)SeaSalt 5)Biomass 6)AgedEC 7)AgedOC 8)Amine')
disp('9)NH4rich 10)Vrich 11)EC Pos Only 12)MeatCooking 13)PAH 14)Other')
cellsize(Sources_Matched_100to140nm)
disp('~~~~~')

```

```

else
end

```

```

%-----
%-----
%-----
%-----
%-----
%-----
%-----
%-----
if SizeRange == 3; % (3 = Fine & Coarse [140nm and above])
%-----
%-----
%-----
%-----
% Matches totalPIDs to WM ***
%-----
disp(' ')
disp('***** Matching your PID to the Source Seeds *****')
disp(' SizeRange == 3 (Fine & Coarse particles above 140nm) ')
disp(' ')
if length (totalPID) < 5000
    [Matched1] = match_art2a(totalPID, Source_Seeds_06_30_07{7}, 2, VF1, 1); % 1 for exclusive, 0 for non
else
    NumInt = ceil((length (totalPID)) / 5000); % ceil: rounds up
    for I = 1:NumInt
        if I == 1
            InPID2 = totalPID(1:5000);
        elseif I == NumInt
            InPID2 = totalPID((1+5000*(I-1)):length(totalPID));
        else
            X = (I-1)*5000 + 1;
            Y = I*5000;
            InPID2 = totalPID(X:Y);
        end
        [outPartID] = match_art2a(InPID2, Source_Seeds_06_30_07{7}, 2, VF1, 1); % 1 for exclusive, 0 for non
        if I == 1
            Matched1 = outPartID;
        else
            for J = 1:size(outPartID,2)
                Matched1{J} = union(outPartID{J}, Matched1{J});
            end
        end
    end
end
clear I J NumInt outPartID InPID2 ans X Y
%-----

hdv1 = Matched1{1}; % 1-30 are from hdv 2003 jke top 30 clusters from hot particles per truck
for i = 2:60; % 31-60 are from hdv 2001 top 30 particle types
    hdv1 = union(hdv1, Matched1{i});
end
hdv2 = union(Matched1{369}, Matched1{370}, Matched1{371}, Matched1{372}, Matched1{373}, Matched1{375},
Matched1{376}, Matched1{377}, Matched1{378}, Matched1{384}, Matched1{385}, Matched1{386},

```



Matched1{391}, Matched1{392}, Matched1{393}, Matched1{394}, Matched1{397}, Matched1{398}, Matched1{399}, Matched1{402}, Matched1{403}, Matched1{404}); % 5 clusters from ambient fwy data (then 4 more from ambient that didn't match jke first time through), 3 more from lvn unmatched fwy ambient; 7 more from jke unmatched fwy 140nmup; 3 more from eld unmatched fwy

ldv1 = Matched1{61}; % from ldv 2002 jke top 30 clusters hot particles for (LEV, TWC, TWC-truck (no suzuki samari or dodge caravan))

for i = 62:90;

ldv1 = union(ldv1, Matched1{i});

end

hdv3 = Matched1{68};

ldv1 = setdiff(ldv1, hdv3);

EC\_PO1 = union(Matched1{66}, Matched1{82});

ldv1 = setdiff(ldv1, EC\_PO1);

ldv2 = union(Matched1{395}, Matched1{396});

% -----

HDDV = union(hdv1, hdv2, hdv3);

LDV = union(ldv1, ldv2);

first\_matched = union(HDDV, LDV, EC\_PO1);

Other = setdiff(totalPID, first\_matched);

clear vehicle

clear i hdv1 hdv2 hdv3 ldv2 first\_matched

% -----

SeaSalt1 = Matched1{91}; % 9 clusters

for i = 92:99;

SeaSalt1 = union(SeaSalt1, Matched1{i});

end

biomass2a = union(Matched1{91}, Matched1{93}, Matched1{94}, Matched1{95}, Matched1{96});

SeaSalt1 = setdiff(SeaSalt1, biomass2a); % "corrected" SeaSalt1 5/15/06

Biomass1 = Matched1{100}; % 8 clusters

for i = 101:107;

Biomass1 = union(Biomass1, Matched1{i});

end

SeaSalt2 = Matched1{108}; % 11 clusters

for i = 109:118;

SeaSalt2 = union(SeaSalt2, Matched1{i});

end

dust3a = Matched1{114};

SeaSalt2 = setdiff(SeaSalt2, dust3a); % "corrected" SeaSalt2 5/15/06

Dust1 = Matched1{119}; % 3 clusters

for i = 120:121;

Dust1 = union(Dust1, Matched1{i});

end

Dust2 = Matched1{122}; % 101 clusters from lab resuspended dust samples (derrived from ReSoilAM)

for i = 123:222;

Dust2 = union(Dust2, Matched1{i});

end

Biomass2 = union(Matched1{223}, Matched1{224});

SeaSalt3 = union(Matched1{225}, Matched1{226});

Dust3 = Matched1{227}; % 21 clusters from LVN at SOAR2

```

for i = 228:247;
    Dust3 = union(Dust3, Matched1{i});
end
seasalt3a = union(Matched1{240}, Matched1{241}, Matched1{242}, Matched1{243});
Dust3 = setdiff(Dust3, seasalt3a);

Amine2 = union(Matched1{248}, Matched1{249}, Matched1{250}, Matched1{251}, Matched1{407}); % 4 clusters
from LVN at SOAR; 1 from ELD fwy study

NH4rich = union(Matched1{252}, Matched1{253}); % 2 clusters from LVN at SOAR

Vrich1 = union(Matched1{254}, Matched1{255}, Matched1{256}); % 3 clusters from LVN at SOAR

AgedEC = union(Matched1{257}, Matched1{258}, Matched1{406}); % 2 clusters from LVN at SOAR; 1 from ELD
fwy study

AgedOC2 = union(Matched1{259}, Matched1{260}, Matched1{261}, Matched1{262}, Matched1{263},
Matched1{383}, Matched1{400}, Matched1{401}); % 5 clusters from LVN at SOAR, one from Freeway (from LVN
J27), one from freeway JKE unmatched 140nmup, one more from Freeway (from LVN J27)

Biomass3 = union(Matched1{264}, Matched1{265}, Matched1{266}, Matched1{267}, Matched1{268}); % 5
clusters from LVN at SOAR

Vrich2 = Matched1{269}; % 14 clusters from LVN at SOAR2
for i = 270:282;
    Vrich2 = union(Vrich2, Matched1{i});
end

Vrich3 = Matched1{283}; % 10 clusters from ELD FWY added 5/22/06
for i = 284:292;
    Vrich3 = union(Vrich3, Matched1{i});
end

SeaSalt4 = Matched1{293}; % 24 clusters from ELD FWY added 5/22/06
for i = 294:316;
    SeaSalt4 = union(SeaSalt4, Matched1{i});
end

Dust4 = Matched1{317}; % 7 clusters from ELD FWY added 5/22/06
for i = 318:323;
    Dust4 = union(Dust4, Matched1{i});
end

Amine3 = Matched1{324}; % 13 clusters from ELD FWY added 5/22/06
for i = 325:336;
    Amine3 = union(Amine3, Matched1{i});
end

V_ship = Matched1{337}; % 28 clusters from FWY Vanadium background, added 4/15/07
for i = 338:364;
    V_ship = union(V_ship, Matched1{i});
end
Vrich4 = union(Matched1{379}, Matched1{380}); % from ambient fwy particles that didn't match the first time
through

EC_pos = union(Matched1{365}, Matched1{366}, Matched1{367}, Matched1{368}, Matched1{374},
Matched1{381}, Matched1{382}, Matched1{405}); % 4 clusters from FWY EC positive only background, added
4/15/07 -- 3 cluster from fwy fine particles that didn't match the first time through; 1 from eld fwy (has CT in negs,
but would be PO if not for that)

```

```

SeaSalt5 = union(Matched1{387}, Matched1{388}, Matched1{389}, Matched1{390}); % From fwy ambient
%-----

matched_other = union(Biomass1, SeaSalt1, SeaSalt2, Dust1, Dust2, Biomass2, SeaSalt3, Dust3, Amine2, NH4rich,
Vrich1, AgedEC, AgedOC2, Biomass3, Vrich2, Vrich3, SeaSalt4, Dust4, Amine3, biomass2a, dust3a, seasalt3a,
V_ship, EC_pos, EC_PO1, Vrich4, SeaSalt5);
Other = setdiff(Other, matched_other);
Vrich = union(Vrich1, Vrich2, Vrich3, V_ship, Vrich4);
Amine = union(Amine2, Amine3);
AgedOC = AgedOC2;
Biomass = union(Biomass1, Biomass2, Biomass3, biomass2a);
SeaSalt = union(SeaSalt1, SeaSalt2, SeaSalt3, SeaSalt4, seasalt3a, SeaSalt5);
Dust = union(Dust1, Dust2, Dust3, Dust4, dust3a);
EC_pos = union(EC_pos, EC_PO1);
clear matched_other
clear SeaSalt1 SeaSalt2 SeaSalt3 SeaSalt4 Biomass1 Biomass2 Biomass3 Dust1 Dust2 Dust3 Dust4 biomass1b
SeaSalt1a Dust1a Amine1 Amine2 Amine3 AgedOC1 AgedOC2 Vrich1 Vrich2 Vrich3 V_ship Vrich4
clear i hdv1 ldv1 biomass1a biomass2a seasalt1a totalPID vanadium1a dust1a dust2a dust3a seasalt2a seasalt3a
EC_PO1 SeaSalt5

% -----

Sources{1} = HDDV;
Sources{2} = LDV;
Sources{3} = Dust;
Sources{4} = SeaSalt;
Sources{5} = Biomass;
Sources{6} = AgedEC;
Sources{7} = AgedOC;
Sources{8} = Amine;
Sources{9} = NH4rich;
Sources{10} = Vrich;
Sources{11} = EC_pos;
Sources{12} = MeatCooking;
Sources{13} = Other;

clear HDDV LDV Dust SeaSalt Biomass AgedEC AgedOC Amine NH4rich Vrich EC_pos MeatCooking Other

% -----
% -----
% -----
% -----

if POM2 == 1;
totalPID = Sources{13};
%-----
% Matches Unmatched from first round to the same WM's, but positive only matching ***
%-----
disp(' ')
disp('Commencing with optional matching to the positive ion source seeds')
if length(totalPID) < 5000
[Matched2] = match_art2a(totalPID, Source_Seeds_06_30_07{8}, 1, VF1, 1); % 1 for exclusive, 0 for non
else
NumInt = ceil((length(totalPID)) / 5000); % ceil: rounds up
for I = 1:NumInt
if I == 1
InPID2 = totalPID(1:5000);
elseif I == NumInt
InPID2 = totalPID((1+5000*(I-1)):length(totalPID));
else
X = (I-1)*5000 + 1;

```

```

        Y = I*5000;
        InPID2 = totalPID(X:Y);
    end
    [outPartID] = match_art2a(InPID2, Source_Seeds_06_30_07{8}, 1, VF1, 1); % 1 for exclusive, 0 for non
    if I == 1
        Matched2 = outPartID;
    else
        for J = 1:size(outPartID,2)
            Matched2{J} = union(outPartID{J}, Matched2{J});
        end
    end
end
end
clear I J NumInt outPartID InPID2 ans X Y
%-----

hdv1 = Matched2{1}; % 1-30 are from hdv 2003 jke top 30 clusters from hot particles per truck
for i = 2:60; % 31-60 are from hdv 2001 top 30 particle types
    hdv1 = union(hdv1, Matched2{i});
end
hdv2 = union(Matched2{365}, Matched2{366}, Matched2{367}, Matched2{368}, Matched2{369}, Matched2{370},
    Matched2{371}, Matched2{372}, Matched2{373}); % 5 clusters from ambient fwy data (then 4 more from ambient
    that didn't match first time through)

ldv1 = Matched2{61}; % from ldv 2002 jke top 30 clusters hot particles for (LEV, TWC, TWC-truck (no suzuki
    samari or dodge caravan))
for i = 62:90;
    ldv1 = union(ldv1, Matched2{i});
end
hdv3 = Matched2{68};
ldv1 = setdiff(ldv1, hdv3);

% -----
HDDV = union(hdv1, hdv2, hdv3);
LDV = ldv1;
first_matched = union(HDDV, LDV);
Other = setdiff(totalPID, first_matched);

clear vehicle
clear i hdv1 hdv2 hdv3 first_matched

% -----

SeaSalt1 = Matched2{91}; % 9 clusters
for i = 92:99;
    SeaSalt1 = union(SeaSalt1, Matched2{i});
end
biomass2a = union(Matched2{91}, Matched2{93}, Matched2{94}, Matched2{95}, Matched2{96});
SeaSalt1 = setdiff(SeaSalt1, biomass2a); % "corrected" SeaSalt1 5/15/06

Biomass1 = Matched2{100}; % 8 clusters
for i = 101:107;
    Biomass1 = union(Biomass1, Matched2{i});
end

SeaSalt2 = Matched2{108}; % 11 clusters
for i = 109:118;
    SeaSalt2 = union(SeaSalt2, Matched2{i});
end
dust3a = Matched2{114};

```

```

SeaSalt2 = setdiff(SeaSalt2, dust3a); % "corrected" SeaSalt2 5/15/06

Dust1 = Matched2{119}; % 3 clusters
for i = 120:121;
    Dust1 = union(Dust1, Matched2{i});
end

Dust2 = Matched2{122}; % 101 clusters from lab resuspended dust samples (derrived from ReSoilAM)
for i = 123:222;
    Dust2 = union(Dust2, Matched2{i});
end

Biomass2 = union(Matched2{223}, Matched2{224});
SeaSalt3 = union(Matched2{225}, Matched2{226});

Dust3 = Matched2{227}; % 21 clusters from LVN at SOAR2
for i = 228:247;
    Dust3 = union(Dust3, Matched2{i});
end
seasalt3a = union(Matched2{240}, Matched2{241}, Matched2{242}, Matched2{243});
Dust3 = setdiff(Dust3, seasalt3a);

Amine2 = union(Matched2{248}, Matched2{249}, Matched2{250}, Matched2{251}); % 4 clusters from LVN at SOAR

NH4rich = union(Matched2{252}, Matched2{253}); % 2 clusters from LVN at SOAR

Vrich1 = union(Matched2{254}, Matched2{255}, Matched2{256}); % 3 clusters from LVN at SOAR

AgedEC = union(Matched2{257}, Matched2{258}); % 2 clusters from LVN at SOAR

AgedOC2 = union(Matched2{259}, Matched2{260}, Matched2{261}, Matched2{262}, Matched2{263},
    Matched2{374}, Matched2{375}); % 5 clusters from LVN at SOAR, one from Freeway (from LVN J27), one from
    freeway JKE unmatched 140nmup

Biomass3 = union(Matched2{264}, Matched2{265}, Matched2{266}, Matched2{267}, Matched2{268}); % 5
clusters from LVN at SOAR

Vrich2 = Matched2{269}; % 14 clusters from LVN at SOAR2
for i = 270:282;
    Vrich2 = union(Vrich2, Matched2{i});
end

Vrich3 = Matched2{283}; % 10 clusters from ELD FWY added 5/22/06
for i = 284:292;
    Vrich3 = union(Vrich3, Matched2{i});
end

SeaSalt4 = Matched2{293}; % 24 clusters from ELD FWY added 5/22/06
for i = 294:316;
    SeaSalt4 = union(SeaSalt4, Matched2{i});
end

Dust4 = Matched2{317}; % 7 clusters from ELD FWY added 5/22/06
for i = 318:323;
    Dust4 = union(Dust4, Matched2{i});
end

Amine3 = Matched2{324}; % 13 clusters from ELD FWY added 5/22/06
for i = 325:336;

```

```

    Amine3 = union(Amine3, Matched2{i});
end

V_ship = Matched2{337}; % 28 clusters from FWY Vanadium background, added 4/15/07
for i = 338:364;
    V_ship = union(V_ship, Matched2{i});
end

Vrich4 = union(Matched2{376}, Matched2{377}); % from ambient fwy particles that didn't match the first time
through

SeaSalt5 = union(Matched2{378}, Matched2{379}, Matched2{380}, Matched2{381}); % From fwy ambient

%-----

matched_other = union(Biomass1, SeaSalt1, SeaSalt2, Dust1, Dust2, Biomass2, SeaSalt3, Dust3, Amine2, NH4rich,
Vrich1, AgedEC, AgedOC2, Biomass3, Vrich2, Vrich3, SeaSalt4, Dust4, Amine3, biomass2a, dust3a, seasalt3a,
V_ship, Vrich4, SeaSalt5);
Other = setdiff(Other, matched_other);
Vrich = union(Vrich1, Vrich2, Vrich3, V_ship, Vrich4);
Amine = union(Amine2, Amine3);
AgedOC = AgedOC2;
Biomass = union(Biomass1, Biomass2, Biomass3, biomass2a);
SeaSalt = union(SeaSalt1, SeaSalt2, SeaSalt3, SeaSalt4, seasalt3a, SeaSalt5);
Dust = union(Dust1, Dust2, Dust3, Dust4, dust3a);
clear matched_other
clear SeaSalt1 SeaSalt2 SeaSalt3 SeaSalt4 Biomass1 Biomass2 Biomass3 Dust1 Dust2 Dust3 Dust4 biomass1b
SeaSalt1a Dust1a Amine1 Amine2 Amine3 AgedOC1 AgedOC2 Vrich1 Vrich2 Vrich3 V_ship Vrich4
clear i hdv1 ldv1 biomass1a biomass2a seasalt1a totalPID vanadium1a dust1a dust2a dust3a seasalt2a seasalt3a
SeaSalt5

% -----

Sources2{1} = HDDV;
Sources2{2} = LDV;
Sources2{3} = Dust;
Sources2{4} = SeaSalt;
Sources2{5} = Biomass;
Sources2{6} = AgedEC;
Sources2{7} = AgedOC;
Sources2{8} = Amine;
Sources2{9} = NH4rich;
Sources2{10} = Vrich;
Sources2{11} = Sources{11};
Sources2{12} = Sources{12};
Sources2{13} = Other;

clear HDDV LDV Dust SeaSalt Biomass AgedEC AgedOC Amine NH4rich Vrich EC_pos MeatCooking Other
% -----
Sources{1} = union(Sources{1}, Sources2{1});
Sources{2} = union(Sources{2}, Sources2{2});
Sources{3} = union(Sources{3}, Sources2{3});
Sources{4} = union(Sources{4}, Sources2{4});
Sources{5} = union(Sources{5}, Sources2{5});
Sources{6} = union(Sources{6}, Sources2{6});
Sources{7} = union(Sources{7}, Sources2{7});
Sources{8} = union(Sources{8}, Sources2{8});
Sources{9} = union(Sources{9}, Sources2{9});
Sources{10} = union(Sources{10}, Sources2{10});
Sources{11} = union(Sources{11}, Sources2{11});

```

```

Sources{12} = union(Sources{12}, Sources2{12});
Sources{13} = Sources2{13};

clear Sources2
else
end
% -----
% -----
% -----
% -----
disp(' ')
disp('Search for PAH type particles that did not match to source seeds')
disp(' ')
other = Sources{13};
PAH = run_query(other, '(sum(Area{212 250}) > 1000) or (sum(Area{186 202}) > 800)');
other2 = setdiff(other, PAH);
Sources{13} = PAH;
Sources{14} = other2;
clear other PAH other2

%-----
% To clean up some issues in the "other" category
%-----
disp(' ')
disp('Searching for issue/noise and gas phase spectra in the unmatched particles')
disp(' ')
other = Sources{14};
other_dual = run_query(other, 'Polarity == 1 and Polarity == 0');
other_pos = run_query(other, 'Polarity == 1');
other_neg = run_query(other, 'Polarity == 0');
other_negonly = setdiff(other, other_pos);
other_new = setdiff(other, other_negonly);
other_GP = run_query(other_new, 'sum(Area{1 100}) < 1500');
other_notGP = run_query(other_GP, 'sum(Area{100 220}) > 1000');
other_GP2 = setdiff(other_GP, other_notGP);
other_new2 = setdiff(other_new, other_GP2);
other_94 = run_query(other, 'Area{-94} > 200');
other_new3 = setdiff(other_new2, other_94);
Sources{14} = other_new3;
other_removed = union(other_negonly, other_GP2, other_94);
clear other other_dual other_neg other_pos other_negonly other_new other_GP other_notGP other_GP2 other_new2
other_94 other_new3
%-----

Sources_Matched = Sources;
clear Sources VF1 POM2
clear other_removed

disp(' ')
disp('***** How long it took to match your data *****')
toc

disp(' ')
disp('~~~~~')
disp('*** A matrix called "Sources_Matched" has been created in your workspace ***')
disp('The order that the Sources appear in the matrix are:')
disp(' ')
disp('1)HDDV 2)LDV 3)Dust 4)SeaSalt 5)Biomass 6)AgedEC 7)AgedOC 8)Amine')
disp('9)NH4rich 10)Vrich 11)EC_PosOnly 12)MeatCooking 13)PAH 14)Other')
cellsize(Sources_Matched)

```

```
disp('~~~~~')  
else  
end  
clear SizeRange
```